UNIVERSITAT DE BARCELONA

Unraveling the neuro-immunological implications of the Ikaros family in schizophrenia and neuroinflammation

Iván Ballasch

UNIVERSITAT DE BARCELONA

Unraveling the neuro-immunological implications of the Ikaros family in schizophrenia and neuroinflammation

Desxifrant les implicacions neuroimmunològiques de la família Ikaros en l'esquizofrènia i la neuroinflamació

PhD degree of Biomedicine in the Faculty of Medicine of the University of Barcelona

Dissertation submitted by:

Iván Ballasch

This work was performed at the Department of Biomedicine of the Faculty of Medicine of the University of Barcelona under the supervision of Dr. Albert Giralt Torroella and Dr. Jordi Alberch Vié.

Iván Ballasch Albert Giralt Torroella Jordi Alberch Vié

Programa de Doctorat de Biomedicina

From the very bottom of my heart, thanks to everyone.

It's been a ride, a long ride...

Table of content

Abbreviations

APCs	Antigen-presenting cells
BBB	Brain-blood-barrier
BDNF	Brain-derived neurotropic factor
BLA	Basolateral amygdala
CA	Cornu Ammonis
CDR3	Complementarity determining region-3
CLPs	Common Lymphoid Progenitors
CMPs	Common Myeloid Progenitors
CNS	Central nervous system
DA	Dopamine
DAMPs	Damage-associated molecular patterns
DNA	Deoxyribonucleic acid
EPs	Erythroyd Progenitors
GABA	Gamma-aminobutyric acid
GLU	Glutamate
GMPs	Granulo-Monocytic Progenitors
GPs	Granulocytic Progenitors
GWAS	Genome-wide association studies
HLA	Human leukocyte antigen
HSCs	Hematopoietic stem cells
IFN- α	Interferon- α
IFN-γ	Interferon- γ
Ikzf	Ikaros zinc finger proteins
Ikzf1	Ikaros
Ikzf2	Helios
Ikzf3	Aiolos
Ikzf4	Eos
Ikzf5	Pegasus
IL	Interleuking
Ip-10	Interferon gamma-induced protein 10
KO	Knock-out
LPS	Lipopolysaccharide
LTP	Long-term potentiation
MEPs	Megakaryocytic-Erythroid Progenitors
MkPs	Megakaryocytic Progenitors

MoNNet	Modular Neuronal Network
MPs	Monocytic Progenitors
NF-k β	Nuclear factor kappa β
NK	Natural Killer
NMDAR	N-methyl-D-aspartate receptor
NORT	Novel object recognition test
PAMPs	Pathogen-associated molecular patterns
PBMCs	Peripheral blood mononuclear cells
PFC	Pre frontal cortex
PNS	Peripheral nervous system
Pro-B	Progenitors for B cells
Pro-DC	Progenitors for Dendritic Cells
Pro-NK	Progenitors for Natural Killer Cells
Pro-T	Progenitors for T cells
PRRs	Pattern-recognition receptors
pTreg	peripherally-induced Treg
PV	Parvalbumin
SN	Substancia nigra
SNPs	Single nucleotide polymorphisms
SST	Somatostatin
Tc	T cytotoxic
TCR	T cell receptor
TGF-β	Transforming growth factor- β
Th	T-helper
Th1	T-helper 1
Th2	T-helper 2
TLR	Toll-like receptor
TNF-α	Tumor necrosis factor-α
Treg	T-regulatory
VTA	Ventral tegmental area
WT	Wild type
ZF	Zinc fingers

I. Abstract

1. Abstract

The Ikaros family of transcription factors has been largely described in the context of immune system function and immune system cells development. In the last years, some of its members were found in neural cells, particularly during perinatal life, associated with CNS development and proper function of some brain regions, such as the hippocampus. Dysregulations of the Ikaros family members have been linked to a wide range of immune-related disorders. However, the implication of the Ikaros family in brain-related disorders remains a widely underexplored area.

Schizophrenia is a psychiatric condition affecting around 21 million people worldwide with an annual associated cost of around 16.500€ per patient in Europe. Schizophrenia symptoms are classified into three broad categories: Positive (e.g. hallucinations, delusions and thought disorder), Negative (e.g. withdrawal and lack of motivation) and Cognitive (e.g. deficiencies in executive functions and working memory). Some of the key-affected brain regions in schizophrenia are the pre-frontal cortex and the hippocampus. Genetic and environmental factors play a role in the risk of developing this condition and, in many cases, these factors act through the immune system. Indeed, one of the most prominent discoveries in schizophrenia research in the last years has been the association of immune dysfunction with its pathogenesis, proposing an aberrant neuro-immune crosstalk in this condition. In that context, two major ways the immune system is proposed to contribute to the appearance of schizophrenia are: neuroinflammation and T cells dysfunction.

Microglia cells are one of the main populations orchestrating neuroinflammation processes within the brain. In schizophrenia, microglia density and cell number have been shown to be generally increased while alterations in density and number of other glia cells seem to be minor. Besides, many pro-inflammatory cytokines, such as IL-6 or TNF-α, have been found to be increased in schizophrenia patients' post-mortem brains. On the other side, T cell mediated immunity dysregulations have also been proposed in schizophrenia, with abnormal invasion of T cells within patients' brains and possibly alterations of dopamine-T cells crosstalk. Therefore, T cells population could be considered as a candidate mediating the aberrant neuro-immune crosstalk in schizophrenia possibly involving neurotoxic effects and contributing to neuroinflammation.

Previous studies have shown that Ikaros and Helios are essential for the proper function of some immune cell types. On the other hand, SPNs of *IKAROS* gene have been found to be related to the age of onset of schizophrenia and Helios protein deficiency have been shown to alter molecular pathways which are also altered in schizophrenia. Furthermore, preliminary data from our lab indicated that Ikaros and Helios are dysregulated in immune cells of schizophrenia patients. Consequently, we aimed to evaluate the potential involvement of Ikaros and Helios in the pathophysiology of schizophrenia.

In the first article, we have found downregulated levels of Ikaros and Helios in PBMCs of schizophrenia patients while their levels were not different from controls in post-mortem brain samples. A doble mutant animal model mimicking the double downregulation of Ikaros and Helios also showed schizophrenia-like behavior in the three categories of symptoms. Using the secretome of the PBMCs from schizophrenia patients, we induced

several schizophrenia-like phenotypes in *in-vitro* and *in-vivo* translational models. We have characterized the molecular profile of the PBMCs secretome and we identified IL-4 and CXCL10 as possible candidates mediating its effects.
In the second article, we have identified Ikaros as a factor involved in microglia homeostasis, particularly in inflammation-associated conditions. Using an Ikaros total *Knockout* model we identified deficiencies linked to a hippocampal-dependent task. Thereafter, we focused on the hippocampus. The Ikaros KO model presented microglial morphological changes associated to inflammatory conditions such as elevated expression of TNFα and NF-kβ and long-term potentiation defects. Besides, we tested the level of Ikaros in other conditions of neuroinflammation and we found augmented levels of Ikaros in all of them. Correspondingly, microglia phagocytic activity was also disrupted under the modulation of Ikaros in vitro. The elevated levels of some inflammasome members and alterations in the acetylation-methylation ratios found in the KO model give some ideas about the mechanisms by which Ikaros could modulate microglia function.
The final model about how the downregulation of Ikaros and Helios in PBMCs of schizophrenia patients could be contributing to the pathogenesis of the condition could be summarized as follows: The combination of the downregulations of Ikaros and Helios in different PBMCs subsets possibly generates elevated levels of IFN-γ and reduced immune suppression capacity of Treg cells. IFN-γ is priming microglia cells that upon second immune stimuli generate oversimplified and neurotoxic inflammatory responses over years deteriorating the nervous tissue until the manifestation of the first psychotic episode. A possibility is that Ikaros dysregulation within microglia is exacerbating this circuit.

Keywords: Ikaros, Helios, Schizophrenia, PBMC, T cells, Microglia, IL-4

2. Resum

La família de factors de transcripció Ikaros ha estat àmpliament estudiada en el context de la funció i el desenvolupament de les cèl·lules del sistema immunitari. En els darrers anys, alguns dels seus membres s'han trobat en cèl·lules neuronals, particularment durant la vida perinatal, associats al desenvolupament del SNC i al funcionament adequat d'algunes regions cerebrals, com l'hipocamp. Les desregulacions dels membres de la família Ikaros s'han relacionat amb una àmplia gamma de trastorns relacionats amb el sistema immunitari. No obstant això, la implicació de la família Ikaros en trastorns relacionats amb el cervell segueix sent un àrea àmpliament inexplorada.
L'esquizofrènia és una afecció psiquiàtrica que afecta aproximadament 21 milions de persones a tot el món, amb un cost anual associat de 16.500 € per pacient a Europa. Els símptomes de l'esquizofrènia es classifiquen en tres grans categories: positius (per exemple, al·lucinacions, deliris i trastorn del pensament), negatius (com la retracció i la manca de motivació) i cognitius (com les deficiències en les funcions executives i la memòria de treball). Algunes de les regions cerebrals més afectades en l'esquizofrènia són el còrtex prefrontal i l'hipocamp. Els factors genètics i ambientals juguen un paper en el risc de desenvolupar aquesta afecció i, en molts casos, aquests factors actuen a través del sistema immunitari. De fet, un dels descobriments més destacats en la investigació

de l'esquizofrènia en els darrers anys ha estat l'associació de la disfunció immunitària amb la seva patogènesi, proposant una interacció neuroimmunitària aberrant en aquesta afecció. En aquest context, dues maneres principals en què es proposa que el sistema immunitari contribueixi a l'aparició de l'esquizofrènia són: la neuroinflamació i la disfunció de les cèl·lules T.

Les cèl·lules microglials són una de les principals poblacions que orquestren els processos de neuroinflamació dins del cervell. En l'esquizofrènia, s'ha demostrat un augment general en la densitat i el nombre de cèl·lules microglials, mentre que en altres cèl·lules glials aquestes alteracions semblen ser menors. A més, s'ha trobat que moltes citocines proinflamatòries, com ara la IL-6 o la TNF-α, augmenten en els cervells post-mortem de pacients amb esquizofrènia. D'altra banda, també s'han proposat desregulacions de la immunitat mediada per cèl·lules T en l'esquizofrènia, amb una invasió anormal de cèl·lules T dins dels cervells dels pacients i possiblement alteracions de la interacció dopamina-cèl·lules T. Per tant, la població de cèl·lules T es podria considerar com una candidata que media la interacció neuroimmunitària aberrant en l'esquizofrènia, possiblement involucrant efectes neurotòxics i contribuint a la neuroinflamació.

Estudis previs han demostrat que Ikaros i Helios són essencials per al funcionament correcte d'alguns tipus de cèl·lules immunitàries. D'altra banda, els SPN d'IKAROS s'han trobat relacionats amb l'edat d'inici de l'esquizofrènia i la deficiència d'Helios ha demostrat modificar els nivells d'una de les proteïnes normalment alterada en l'esquizofrènia. A més, dades preliminars del nostre laboratori van assenyalar nivells desregulats tant d'Ikaros com d'Helios en cèl·lules immunitàries de pacients amb esquizofrènia. En conseqüència, ens vam plantejar com a objectiu avaluar la possible implicació d'Ikaros i Helios en la patogènesi i els processos patològics associats a l'esquizofrènia.

En el primer article, van trobar nivells disminuïts d'Ikaros i Helios en PBMC de pacients amb esquizofrènia, mentre que els seus nivells no diferien dels controls en mostres de cervell post-mortem. A més, un model animal de doble mutant que imita la doble disminució d'Ikaros i Helios va mostrar un comportament semblant a l'esquizofrènia en les tres categories de símptomes. Utilitzant el secretoma dels PBMC dels pacients amb esquizofrènia, vam induir diversos fenotips semblants a l'esquizofrènia en models de traducció in vitro i in vivo. Finalment, vam caracteritzar el perfil molecular del secretoma dels PBMC i vam identificar IL-4 i CXCL10 com a possibles candidats que medien els seus efectes.

En el segon article, vam identificar Ikaros com a factor implicat en l'homeòstasi de la microglia, particularment en condicions associades a la inflamació. Utilitzant un model de knockout (KO) total d'Ikaros, vam observar deficiències relacionades amb una tasca dependent de l'hipocamp. A partir d'aquests resultats, ens vam centrar en l'hipocamp. El model KO d'Ikaros va mostrar canvis morfològics microglials associats a condicions inflamatòries, com ara una expressió elevada de TNFα i NF-κβ i defectes de potenciació a llarg termini. A més, vam examinar els nivells d'Ikaros en altres condicions de neuroinflamació i vam observar un augment dels nivells d'Ikaros en totes elles. Conseqüentment, l'activitat fagocítica de la microglia també es va veure alterada sota la modulació d'Ikaros in vitro. Els nivells elevats d'alguns membres de l'inflammasoma i les

alteracions en les ràtios d'acetilació-metilació observades en el model KO ofereixen pistes sobre els mecanismes pels quals Ikaros podria modular la funció de la microglia.
El model final sobre com la disminució d'Ikaros i Helios en PBMC de pacients amb esquizofrènia podria contribuir a la patogènesi de la condició es podria resumir de la següent manera: La combinació de les disminucions d'Ikaros i Helios en diferents subconjunts de PBMC probablement genera nivells elevats d'IFN-γ i una capacitat de supressió immunitària reduïda de les cèl·lules Treg. L'IFN-γ prepara les cèl·lules microglials que, davant d'estímuls immunitaris secundaris, generen respostes inflamatòries sobresimplificades i neurotòxiques durant anys, deteriorant el teixit nerviós fins a la manifestació del primer episodi psicòtic. Una possible explicació és que la desregulació d'Ikaros dins de la microglia estigui exacerbant aquest circuit.

Keywords: Ikaros, Helios, Esquizofrènia, PBMC, cèl·lules T, Micròglia, IL-4

II. Introduction

1. Ikaros family

Ikaros (Ikzf1) is a zinc finger transcription factor and the founder member of the family "Ikaros zinc finger proteins" (Ikzf). It was identified for the first time in 1992 displaying involvement in lymphocyte development[1]. Over the next two decades, other four members were identified, Helios (Ikzf2), Aiolos (Ikzf3), Eos (Ikzf4), and Pegasus (Ikzf5). Phylogenetically, Ikaros-related proteins are found across different species from most non-vertebrate animals to jawed vertebrates[2]. The Ikzf family members play a crucial role in the development and function of various immune cell types and are also known for their involvement in maintaining the balance between proliferation and differentiation of hematopoietic cells[3]. Through alternative splicing, the *Ikzf* genes can produce many protein isoforms and interactions among isoforms and across family members can generate several numbers of complexes that can act during transcription processes[4].

In most of the Ikzf isoforms is present a highly conserved pair of C2H2 zinc-fingers at the C-terminal that allows dimerization with the members of the family, as well as to interact with other transcriptional regulators. N-terminal domains with up to four zinc-finger motifs are another common property shared by Ikzf family members, these N-terminal are responsible for mediating direct interactions with DNA (Figure 1). Through alternative splicing, the number of N-terminal fingers can vary from one isoform to another one, affecting their capacity to be involved in transcriptional activation.[4] The isoforms that cannot bind DNA but maintain their capacity to dimerize are considered to act in a dominant-negative manner[5]. Ikaros members can also modulate gene transcription indirectly by acting as histone deacetylases activity regulators[4], [6]. Another feature of these family members is that they can be post-transcriptionally modified. For instance, Aiolos can be phosphorylated after IL-2 stimulation, which induces its translocation from the cytoplasm to the nucleus of the cell[7].

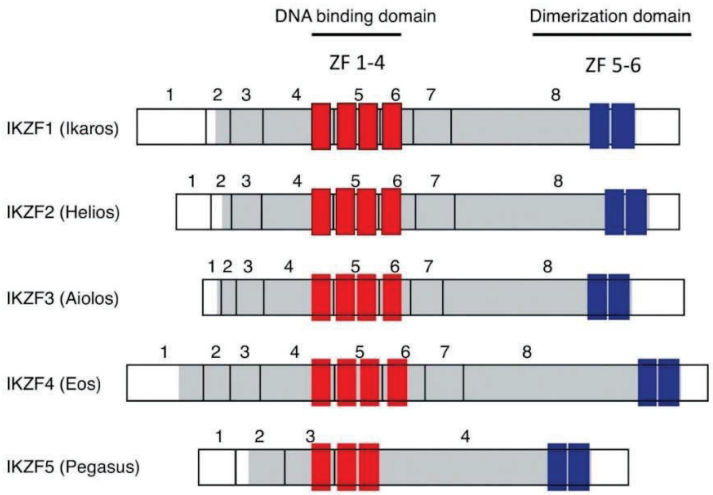

***Figure 1**. Adapted from[8]. Illustration of IKZF family structure. Numbers 1-8 represent exons, in gray coding regions and in white no-coding regions. Zinc fingers (ZF) in red correspond to DNA binding domain and ZF in blue correspond to Dimerization domain.*

1.1 Ikaros family in hematopoiesis and immunity

Ikaros, Helios and Aiolos are known for being related to the development processes of lymphocyte lineages. Besides, Ikaros, Helios and Eos are also present in megakaryocytic-erythroid progenitors, and Ikaros alone in myeloid progenitors and granulo-monocytic progenitors. On the other side, the presence of Eos and Pegasus is restricted to the myeloid lineage, such as granulocytic progenitor and megakaryocytic-erythroid progenitors and Eos alone is also found in erythroid progenitors[9], [10] (see Figure 2).

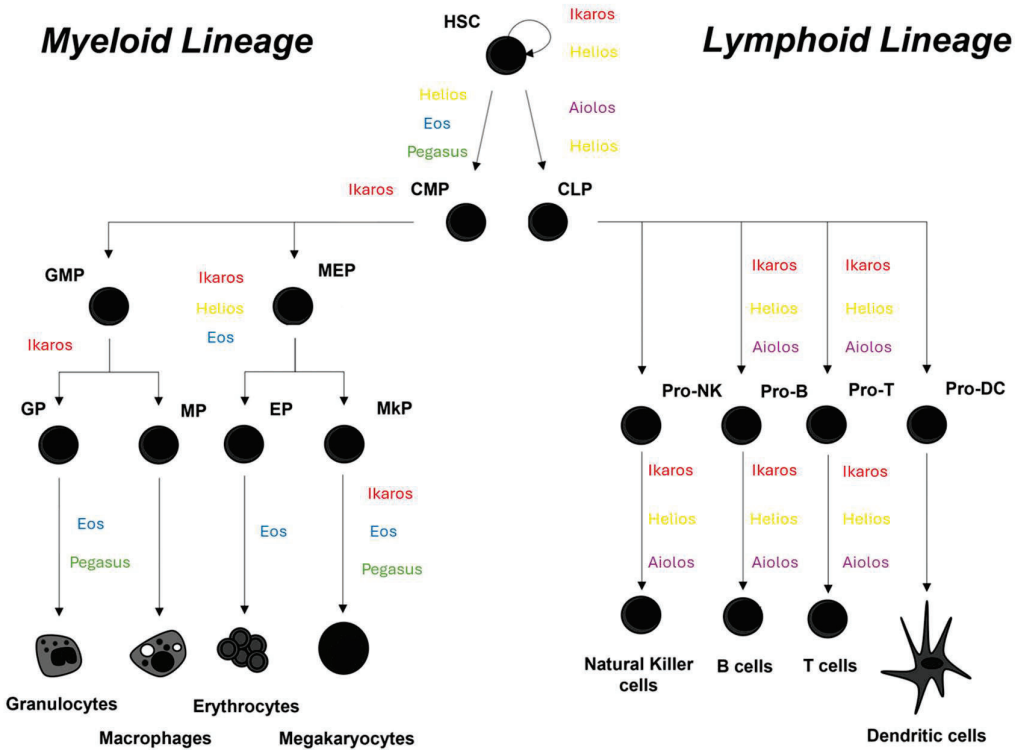

***Figure 2**. Adapted from [9]. Schematic representation of the participation Ikzf family members in cell differentiation and/or maintenance. Hematopoietic stem cells (HSCs), Common Myeloid Progenitors (CMPs), Common Lymphoid Progenitors (CLPs), Granulo-Monocytic Progenitors (GMPs), Megakaryocytic-Erythroid Progenitor (MEPs), Granulocytic Progenitor (GP), Monocytic Progenitor (MP), Erythroid Progenitors (EP), Megakaryocytic Progenitors (MkP), Progenitors for Natural Killer Cells (Pro-NK), Progenitors for B cells (Pro-B), Progenitors for T cells (Pro-T) and Progenitors for Dendritic Cells (Pro-DC).*

1.1.1 Ikaros

The functions associated with Ikaros were initially confined to early stages of lymphoid cells development, as the absence of functional Ikaros was observed to lead to severe alterations of T, B, and NK cell lineages[1], [11]. For example, total knock out (KO) models of Ikaros displayed an absence of B cells and their precursors, accompanied by a lack of fetal but not post-partum T cells[12]. Also, deficiencies in dendritic cells and NK cells were found in this model[13].

Later, studies including conditional knockout models of Ikaros have expanded the understanding of the implication of this factor in transcriptional processes mediated by this family [14], [15]. For instance, a model expressing a dominant-negative form Ikaros displayed a total absence of T cells after birth[16] as well as a severe reduction of long-term repopulation of Hematopoietic stem cells[17] indicating that Ikaros promotes progenitor self-renewal. Another mutant model, where a substitution in the zinc finger 3 inactivates DNA binding but preserves some scaffold function, presented decreased levels of erythroid cells in all developmental stages caused by a reduction of growth and differentiation of erythroblasts[18]. Furthermore, these animals displayed augmented quantity of megakaryocytes and platelets[19]. Finally, using a conditional genetic inactivation model, Ikaros was shown to be essential for normal NK cell lymphopoiesis and its deletion resulted in total loss of peripheral NK cells[20]. Altogether, this showed that Ikaros is capital for a balanced production of immune and blood cells, affecting processes like; cell growing, cell differentiation and precursor self-renewal.

Ikaros has also been shown to be implicated in the regulation of cytokines expressions. For example, Ikaros has been reported to directly associate with the promoters to repress IL-2, IL-12 and Interferon-gamma (IFN-γ) expression in a subset of T-helper cells (Th1)[21]. In other T-helper cells subset (Th2), Ikaros positively promotes the expression of some cytokines, including IL-4, IL-5, and IL-13. In the absence of Ikaros, there is reduced expression of these Th2 cytokines and an increase in IFN-γ production. Therefore, Ikaros can act as a positive regulator of some cytokines and as negative regulator for others[5].

1.1.2 Helios

The functions linked to Helios were initially related to developmental stages of T cells, with Ikaros-Helios complexes specifically localizing at centromeric regions within the nuclei of immature T cells[22]. The fact that only a fraction of Ikaros associated with Helios in T cell nuclei suggested that Helios was involved in regulatory processes within these cells acting as a rate-limiting factor of Ikaros function. Later, T cells differentiation and activation processes were shown to be altered by overexpression of wild-type or dominant-negative isoforms of Helios[23], suggesting a role of Helios in T cells development and homeostasis. Although, the differentiation process and effector functions of T cells were shown not to be altered after inactivation of the *Helios* gene by homologous recombination[24], suggesting that Helios is not fundamental for T cells and that its absence could be compensated by other members of the family.

In the last years, Helios' functions in mature T cell populations have been primarily described within the context of T-regulatory (Treg) cell populations. It has been proposed as marker to differentiate the thymus-derived Treg cells from peripherally-induced Treg (pTreg) cells [25]. Nevertheless, pTreg cells may exhibit Helios expression and whether Helios should be considered or not a specific marker of thymus-derived Treg cells is still under debate[26]. The level of Helios expression positively correlates with the suppressive function of Treg cells[27] and Helios is needed for the stable inhibitory role of both Treg cell populations[28]. Moreover, ablation of Helios in fetal cells has been shown to hinder

their differentiation into pTreg cells following T cell receptor (TCR) stimulation, showing that Helios plays a role in this peripheral differentiation process. Furthermore, this model also indicated that the loss of Helios is associated with impaired immunosuppressive gene expression and a shift towards a pro-inflammatory phenotype[28].

Like Ikaros, Helios has also been shown to be implicated in the modulation of cytokines expressions. For instance, by forming complexes with other proteins Helios has been implicated in the repression of IL-2 and IL-17 expression in Treg cells[29], [30]. In addition, in the absence of Helios there is a rise in the expression of pro-inflammatory cytokines such as IFN-γ and Tumor necrosis factor-α (TNF-α)[28]. Hence, in T reg cells, the role of Helios in modulating cytokines expression seems to be as a negative regulator.

1.2 Ikaros family in the brain

Very little is known about the implication of the Ikaros family in the brain. One of the first reports was during a research of transcription factors that control the expression of enkephalin gene during developmental stages[31]. It was found that Ikaros-1 and Ikaros-2 isoforms are expressed in the embryonic striatum and that, through DNA binding, participate in enkephalin gene expression and enkephalinergic differentiation. A bit later, another study [32] described a role for Ikaros-1 in the generation of late-born striatal neurons, particularly implicated in the second wave of striatal neurogenesis. Congruently, Ikaros null mice displayed less striatal projecting neurons including enkephalin-positive neurons. Furthermore, Ikaros was also shown to promote early-born neuronal fates in the cerebral cortex[33]. In this study, it was described a high expression of Ikaros in progenitor cells during early stages of neurogenesis that thereafter declines over time. Consistently, a transgenic model with sustained Ikaros expression in cortical progenitor cells and neurons displayed developmental anomalies, including the displacement of progenitor cells within the cortical plate, heightened early neural differentiation, and disrupted cortical lamination. These results showed that Ikaros plays a modulating role in the development of different brain cell populations and that its presence tends to decrease over time in the brain.

On the other hand, Helios has been shown to be pivotal for the proper development of striatal medium spiny neurons. Helios, through its expression in neural progenitor cells, was displayed as a regulator of the second wave of striatal neurogenesis resulting in the generation of striatopallidal neurons. Correspondingly, Helios total KO mice exhibited a reduction in the number of dorso-medial striatal medium spiny neurons in adult stages[34]. Another study[35], focused on the expression of Helios during brain development, showed that throughout embryonic development Helios is expressed by many brain regions, including: the olfactory bulb, the hippocampus, the lateral ganglionic eminence and the cingulated, insular and retrosplenial cortices. Further, during postnatal cerebellar development, Helios expression was also detected in Purkinje cells. This study also reported that Helios has an expression peak at E18,5 in the lateral ganglionic eminence and that, thereafter, completely disappears during postnatal development. In addition, it has also been shown that Helios is involved in the maturation and function of

the hippocampal subpopulation Calbindin-positive CA1 pyramidal neurons[36]. Here, the total genetic removal of Helios, which is specifically expressed in the developing hippocampal calbindin-positive CA1 pyramidal neurons, generated alterations in spine density and morphology, as well as deficiencies in spatial memory and synaptic plasticity. As described for Ikaros, these results also indicate that Helios has a role modulating the development and maturation of diverse brain regions and that its presence tends to disappear after perinatal life.

1.3 Ikaros family and related disorders

The members of the Ikaros family seem to be capital for proper function of the immune system. They have been found to act as inhibitors in various forms of lymphoma or leukemia[8], [37] while being excessively expressed in other malignancies, such as malignant plasma cells, monoclonal gammopathy of undetermined significance, and multiple myeloma, where they support the proliferation and survival of cancer cells[38]. However, Ikaros family deficiency is considered to be associated with a range of immune-related disorders including immune thrombocytopenia, autoimmune hepatitis, systemic lupus erythematosus, asthma, Hashimoto thyroiditis, systemic sclerosis, rheumatoid arthritis, Graves' disease and Parkinson disease, among others[39]. Also, the development of other types of cancers, such as, pediatric B-cell precursor acute lymphoblastic leukemia[40], lung cancer[41], among others, are associated with aberrant expression levels of Ikaros family proteins.

1.3.1 Ikaros family and brain-related disorders

When it comes to brain-related disorders, the involvement of the Ikaros family in these conditions remains a relatively understudied area. There is one case study[42] of a patient with intellectual disability (IQ: 64), cognitive dysfunction, and obsessive-compulsive behavior. The patient displayed a compound heterozygous missense mutation in the Ikaros gene, leading to common variable immunodeficiency characterized by recurrent infections, hypogammaglobulinemia, and severe B cell deficiency. The study suggests a potential link between Ikaros mutation and cognitive impairment, highlighting the need to consider the impact of immune-related alterations on cognitive disorders.

Another research[43] proposed that the absence of Helios during neural development induces adult schizophrenia-like behaviors. Using a Helios null model, they found a constant augmentation of *Wdfy1* gene expression in the hippocampus and the striatum, that are key-affected brain regions in schizophrenia. Parallelly, they also observed increased Wdfy1 protein levels in the hippocampus and the dorsolateral prefrontal cortex of schizophrenia patients but not in the hippocampus of a cohort of Alzheimer's disease patients with an associated psychotic disorder. Congruently, mice lacking the *Helios* gene exhibited various schizophrenia-like behaviors, which were associated with impairments in the striatum and hippocampus. Finally, the study suggests that changes in the molecular pathway Helios-Wdfy1 within neurons during the maturation of these crucial

brain regions may have implications for the development of neuropsychiatric conditions like schizophrenia.

Despite the critical role of the Ikaros family in immune regulation and neural development, its implication in brain-related disorders remains a widely underexplored domain. This lack of research presents an opportunity for further investigation into the potential implications of the Ikaros family in mental diseases and brain-related altered conditions.

2. Schizophrenia

Schizophrenia is a complex and debilitating psychiatric condition that impacts various aspects of an individual's cognition, perception, and behavior. Its prevalence round around 21 million people worldwide[44] [45]and accounts for an important health care burden with an average of 16.500€ of annual associated costs per patient in Europe [46]. Schizophrenia symptoms are classically organized in three broad categories. Positive symptoms, such as hallucination, delusions and thought disorder, are typically the motive that brings patients to clinical assessment (Figure 3). Although, this condition is also related to negative symptoms, such as social withdrawal and lack of motivation, and cognitive symptoms, comprising deficiencies in executive functions, working memory and processing speed[47]. Despite positive symptomatology is the most prominent feature of schizophrenia, negative and cognitive symptoms utterly contribute to the long-term burden linked to this condition[48]. The first psychotic episode normally appears in early adulthood. However, a prodromal phase often precedes the firsts positive symptoms manifestation (Figure 4) and, in fact, some evidence suggests schizophrenia pathogenesis starts during neurodevelopment[49]. Life expectancy is also affected in people with schizophrenia, with a mean of 15 years less than general population and around 8% more of risk of death by suicide[50].

DSM-5-TR diagnostic criteria for Schizophrenia

A. Two (or more) of the following, each present for a significant portion of time during a 1-month period. At least one of these must be (1), (2), or (3):

1. Delusions.
2. Hallucinations.
3. Disorganized speech (e.g., frequent derailment).
4. Grossly disorganized or catatonic behavior.
5. Negative symptoms (i.e., diminished emotional expression).

B. For a significant portion of the time since the onset of the disturbance, level of functioning in one or more major areas, such as work, interpersonal relations, or self-care, is markedly below the level achieved prior to the onset.

C. Continuous signs of the disturbance persist for at least 6 months. This 6-month period must include at least 1 month of symptoms (or less if successfully treated) that meet Criterion A (i.e., active-phase symptoms) and may include periods of prodromal or residual symptoms. During these prodromal or residual periods, the signs of the disturbance may be manifested by only negative symptoms.

***Figure 3**. Adapted from DSM-5-TR[51]. Summarizing the diagnostic criteria for Schizophrenia. Besides criteria A, B and C the differential diagnosis must be fulfilled to dismiss other possible causes of the symptoms.*

2.1 The neuropathology of schizophrenia

Schizophrenia was described for the first time by Kraepelin more than a hundred years ago as a disease with a progressive cognitive alteration and deterioration[52]. However, as he based his observations in a direct study, the descriptions of the organic brain abnormalities arrived later.

One of the first organic aspects studied about Schizophrenia was the overall brain size. In 1962, 168 out of 278 patients were diagnosed with cerebral atrophy, suggesting the idea of a brain size reduction during the course of schizophrenia[53]. Some years ago, meta-analysis studies reported reductions of 2% in the total brain volume and in the total brain weight[54], [55]. One of the most consistent features described in schizophrenia underlying brain shrinkage is ventricles enlargement, especially lateral ventricles. These enlargements correlate with patients age, diagnosis and illness severity and constantly progress with aging[56], [57]. Another characteristic behind the brain size reduction in schizophrenia is the overall loss of gray matter across the brain and the reduced cortical thickness particularly found in frontotemporal regions[58], [59].

2.1.1 Frontal Cortex

In the Pre frontal cortex (PFC) of Schizophrenia patients, some studies reported a reduction of the neuronal density[60], whereas the opposite have been shown by others[61]. However, the soma volume of the pyramidal cells and the density of Perineuronal nets have been shown to be decreased in this area[62], [63]. Interestingly, the spine density of the pyramidal neurons within the PFC have also been shown to be decreased by some studies[64], [65]. Besides neurons, glia cells are also altered in the PFC in Schizophrenia. A reduction in oligodendrocyte numbers was found in PFC of patients, whereas the density of microglia was found to be augmented[66], [67]. At the cellular level, a core feature of schizophrenia in PFC is the miscommunication of the interneurons with the pyramidal neurons, suggested to be caused by the reduced number of inhibitory interneurons or the deficient transport or release of GABA in these regions[63], [68]. The upregulated number of post synaptic GABA receptors on the PFC pyramidal neurons is considered a compensatory mechanism for this lack of inhibition[68], [69]. Consistently, the levels of GAD67, Somatostatin (SST) and Parvalbumin (PV) are reported to be reduced by around 30% in the PFC of patients. Nevertheless, the number of inhibitory cells expressing the before mentioned markers have been shown no to be altered, while their transcriptional activity seems to be reduced[70], [71], [72]. Glutamate (GLU) concentrations also progressively decrease in PFC of patients and the density of NMDAR and GluN1 are increased [73], [74]. Besides, the activity of signaling cascades downstream of the NMDAR are also reduced[74]. Altogether this summarizes the altered phenotype of the PFC in schizophrenia possibly contributing to cognitive symptoms and the appearance of psychosis[75].

Alike the PFC, the orbitofrontal cortex has also been shown to have a smaller volume in patients than in controls and that particularly the grey matter is reduced[76], [77]. Although, the density and soma size of glial cells and neurons seems not be altered but the spine density on pyramidal neurons has been shown to be considerably decreased [67], [78].

2.1.2 Hippocampus

One of the most prominent traits of the hippocampus in schizophrenia patients is the whole hippocampal decreased volume[79]. The reduction of the hippocampal volume has been shown to be bilateral and it is believed to be a progressive phenomenon[80], [81]. Early studies have shown cell disarray at the CA of the hippocampus of patients, probably raising the first ideas of the neurodevelopmental pathogenesis of schizophrenia[82]. Interestingly, later other studies observed that the hippocampal neuron density remained unaltered in patients compared to controls[83], [84]. The number of pyramidal neurons has been shown to be not particularly different across CA2-4 in schizophrenia. In contrast, the CA1 displays a major reduction of pyramidal cells number of up to a third compared to controls[82], [85], [86]. Besides pyramidal neurons, the number of non-pyramidal neurons has also been shown to be reduced, in particular PV+ and SST+ interneurons[87]. Across CA1-CA4, the soma size of the pyramidal neurons has been

shown to be decreased in patients by some studies[88], [89], whereas another study displays results with no change of cell size in both pyramidal and non-pyramidal neurons[90]. Along neural populations, glia cells are also affected, there is some data reporting reduced numbers of oligodendrocytes in the hippocampus of patients[91], [92]. On the other hand, the quantity of astrocytes does not seem to be altered in the hippocampus in schizophrenia[93] and the density of microglia is significantly enhanced in the temporal area of patients[94].

Increased neuronal activity in the hippocampus is another general feature in the context of schizophrenia[95], [96], [97], [98]. Some reports have related this phenomenon with altered spine density, elevated post-synaptic density proteins and augmented blood flow in the hippocampus of patients[96], [99], [100]. The specific origin of this enhanced neuronal activity is not well understood. However, the dysfunction of inhibitory interneurons and their reduced number in patients' hippocampi have been suggested as contributor factors to this dysregulation. The hypofunction of NMDARs (proposed by the glutamate hypothesis of schizophrenia[101])on inhibitory interneurons would be leading to hyperactivation of pyramidal neurons and increased release of GLU [87], [102], [103], [104]. Consistent with the altered state of inhibitory neurons, several studies have reported elevated levels of GLU in the hippocampus in schizophrenia[105], [106], [107]. Further, it has also been shown that subjects with clinical high risk for psychosis display increased levels of GLU and that in patients this GLU alteration remains even after 6 weeks of treatment with risperidone[108], [109].

2.1.3 Amygdala

The amygdala is broadly divided into the basolateral amygdala (BLA) and corticomedial amygdala, where the BLA is more pronouncedly affected in schizophrenia[104]. The total volume of the amygdala have been shown to be bilaterally reduced and correlated with disease duration in schizophrenia[110], [111]. In the BLA, the total number of neurons have been shown to be reduced whilst the neuron density seems not to change[112]. Furthermore, it has also been reported a reduction of the Perineuronal nets in the BLA in schizophrenia[113]. The activation of the amygdala is as well altered in schizophrenia, some studies have shown enhanced amygdala activity when patients were shown fearful faces and amygdala hypofunction has been related to empathetic deficits in schizophrenic subjects[114], [115].

2.1.4 Striatum

Similarly to other subcortical areas, the striatum is also affected in schizophrenia. The two main regions of the striatum, caudate and putamen, have been shown to have decreased volume in schizophrenia and decreased volume only in the caudate has also been found in first psychotic episode subjects[112], [116]. Besides, this shrinkage is considered to be progressive, along with ventricles enlargement[117], [118]. The total number of neurons is reduced in the striatum, while the spine density is increased. Furthermore, the caudate of patients display altered spines shape and axon atrophy due to myelin sheath

alteration[112], [119]. Overall, these changes are likely having an impact on neuron-neuron and region-region communication, as for example the Nucleus accumbens (NAcc), that is a gate of many inputs and outputs of the striatum.

The Nacc is considered to directly participates in the abnormal increase of dopamine (DA) in schizophrenia[120]. Its size has been reported to be either, augmented, reduced, or with no associated size change by different studies[121], [122], [123]. Although, elevated excitatory inputs to the Nacc have been shown in schizophrenia[124]. This is from particular importance, as the Nacc receives regulatory inputs from the hippocampus and the Ventral tegmental area (VTA) and it indirectly projects to the VTA which, along with the substancia nigra (SN), is an important source of DA[125].

2.1.5 Substancia nigra

The study of the SN in schizophrenia raised as the DA hypothesis of schizophrenia proposed that DA dysfunction in subcortical areas(e.g. striatum) underpins many symptoms, being the SN implicated via the SN-striatal pathway[126]. Correspondingly, the synthesis of DA in the SN has been shown to be enhanced in schizophrenia. Plus, the neural soma size and neural nucleolar volume have been found increased, whereas the density of astrocytes has been found decreased in contrast to controls[127], [128]. Even if the state of the SN is not totally clear in Schizophrenia, its role in DA production and distribution makes it of particular interest in schizophrenia research.

2.1.6 Thalamus

The complexity of the division of the thalamus makes it challenging to summarize its affectation in schizophrenia. The total volume of the thalamus has been shown to be reduced by some studies[129], [130], whilst others found no volume change[131], [132]. Nonetheless, this disparity can be somehow explained by the fact that the thalamus is deformed in schizophrenia[133], [134]. The medial, the lateral and the anterior group of nuclei display a reduction of neurons number, but this reduction is lateralized only in the left side for the lateral group[130], [135]. Moreover, the lateral zone presents a reduction of PV+ thalamocortical projection neurons[136]. Finally, the geniculate nuclei zone also shows total volume reduction but associated with age[137].

2.2 Schizophrenia risk factors

2.2.1 Genetic

Genetic studies in epidemiology have demonstrated that schizophrenia has a strong hereditary component, even though it is more accurately characterized as having a multifaceted root cause with a complex genetic makeup involving multiple genes[138]. Mounting evidence has shown the involvement of both common and rare genetic variants in the genesis of schizophrenia[139]. Through Genome-wide association studies (GWAS), more than 280 genetic risk loci have been significantly associated with

schizophrenia[140], [141], and GWAS advancement has also made it possible to create polygenic risk scores, offering a genetic risk overview of the condition based on an individual's accumulation of risky alleles. Many of the risk loci related to schizophrenia are also related to immunity functions. For example, the Human leukocyte antigen gene complex (HLA), a highly polymorphic locus, encodes proteins associated with regulation of immune-inflammatory processes and is also of particular interest in the study of neuropsychiatric conditions, such as schizophrenia[142]. However, the genetic risk loci are known to exert only a minor influence on the risk of developing schizophrenia[138]. Therefore, schizophrenia is considered a polygenic condition.

Besides, genetic deletions or duplications of DNA sections are associated with a more elevated risk of developing schizophrenia, but they are only found in less than 4% of the cases. For example, the deletion of megabases of DNA at chromosome 22q11.2 is correlated with around 40% lifetime risk of developing schizophrenia[143]. However, many of the genetic variations linked to schizophrenia may also be linked to other psychiatric conditions (e.g autism, major depression disorder[47], [144]) and immune diseases (e.g Crohn`s disease, multiple sclerosis, primary biliary cirrhosis, psoriasis, rheumatoid arthritis, systemic lupus erythematosus, type 1 diabetes[145]), suggesting the existence of shared risk factors and implicated mechanisms among them.

2.2.2 Environmental

Among identical twins, the pairwise concordance for schizophrenia is only around 50%[146]. This highlights the relevance of the environment in the risk of developing schizophrenia. The range of environmental conditions affecting the risk of clinical manifestations includes: early life challenges, substance abuse, minority and ethnic backgrounds, time of birth, urban living conditions, and pregnancy or perinatal issues[147]. For instance, a study reported that prolonged substance use was correlated with elevated rates of positive symptoms expression[148] and that in particular cannabis use is related to increased risk of presenting schizophrenic clinical manifestations[149]. Another study[150], reported that the status of ethnic minority was associated with augmented reality perception alteration and the onset of negative symptoms.

Insults during pregnancy and childhood also correlate with a higher risk of developing schizophrenia. For example, perinatal complications are associated with higher polygenic risk scores, including obstetric complications, starvation during pregnancy, and maternal infections [151], [152]. Furthermore, infections during childhood, including, gastrointestinal-, skin-, genitourinary-, and respiratory infections, septicemia, and viral hepatitis also increase the risk of schizophrenia[153], [154], suggesting that immunological activation underpins, in part, schizophrenia risk caused by environmental factors[155].

2.2.3 Immune factors in schizophrenia

Over the past years, one of the prominent discoveries in schizophrenia research has been the association of immune dysfunction with its pathogenesis. The increased frequency of autoimmune diseases in patients stands for this assumption[156]. Furthermore, immune dysregulations in schizophrenia were reported in many studies[157], [158], [159], [160], and environmental and genetic risk factors of schizophrenia are often linked to immune constructs, rising the importance of the immune system's role in the pathogenesis of this condition. Two major ways the immune system is proposed to contribute with the appearance of schizophrenia are, neuroinflammation and T cells dysfunction [161], [162].

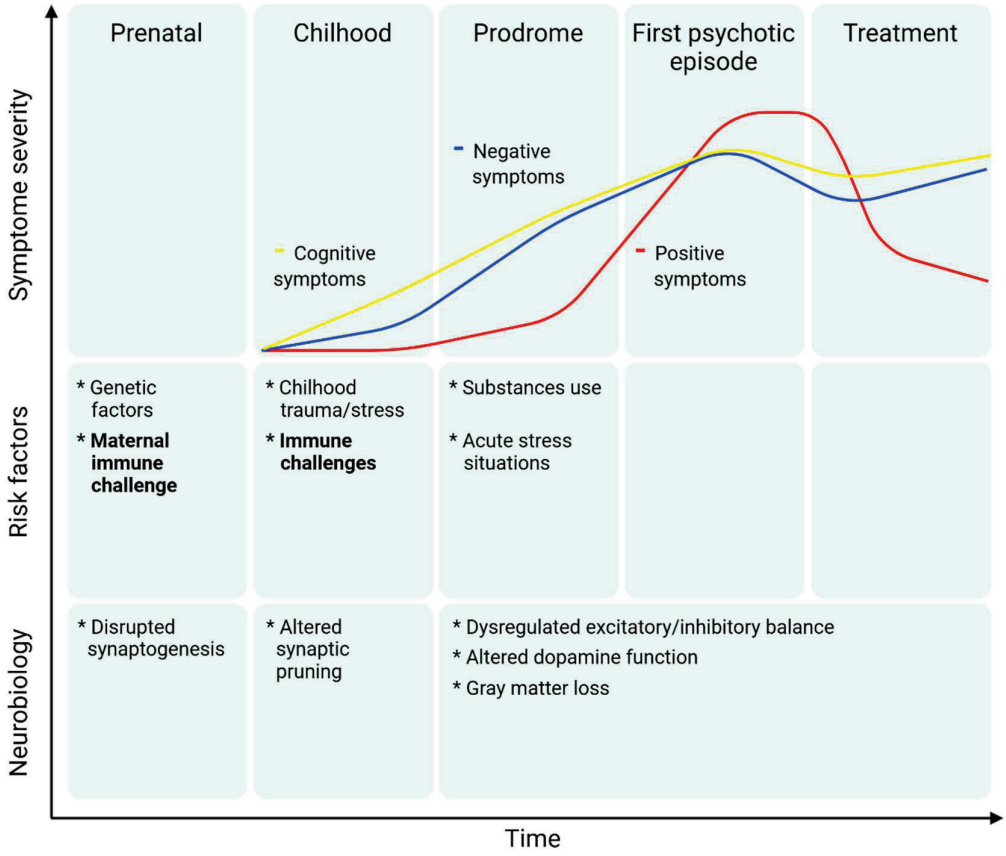

***Figure 4**. Remade based on [47]. People that develop schizophrenia often show minor cognitive and, sometimes, motor difficulties in childhood. During adolescence, negative and cognitive symptoms arise continuing through the prodromal phase. The clinical diagnosis arrives normally with the first psychotic episode. However, prodromal negative and cognitive symptoms are often already debilitating for the patient. Positive symptoms are generally reduced by antipsychotics, but negative and cognitive symptomatology shows less response and can even worsen over time. Genetic and environmental risk factors are also depicted and particularly some immune factors are highlighted. Finally, neurobiological affectations considered to be relevant in schizophrenia are shown.*

3. Neuroinflammation

Neuroinflammation is the body's genuine reaction to potential threats by recruiting immune cells to the affected site within the nervous system[163]. Microglia cells are a non-neuronal population that, among other functions, orchestrate the neuroinflammation process within the brain.

3.1 Microglia

Microglia, which are considered to be the brain parenchyma-resident macrophages, play a crucial role in preserving the environment integrity in the brain and spinal cord[164]. Also, they functionally participate in various central nervous system (CNS) pivotal functions as glio-, vasculo-, neurogenesis, synaptic stripping/remodeling, cell repair processes, and myelination through their process motility, release of soluble factors, and capacity for phagocytosis (Figure 5)[165] [166]. Microglia serve as vigilant monitors of the environment actively scanning for potential threats. In response to stimuli such as pathogens, injury, or neurodegenerative conditions, microglia go through phenotypic changes and present augmented proliferation, changes in protein expression, and the release of immune molecules, including cytokines, chemokines and pro-inflammatory factors[167]. This process is often called microgliosis[168].

During neuroinflammation processes, microgliosis can take place in more than one way, including through damage-associated molecular patterns (DAMPs) and pathogen-associated molecular patterns (PAMPs)[169]. When cell damage occurs, the resulting premature neuronal death triggers DAMPs to alert the immune system about a potential threat. On the other side, in the presence of a foreign microbe, pattern-recognition receptors (PRRs) are activated to sense PAMPs[170]. Ultimately, activated DAMPs/PAMPs induce a signaling cascade that upregulate the transcription of cytokines leading to neuroinflammation[171].

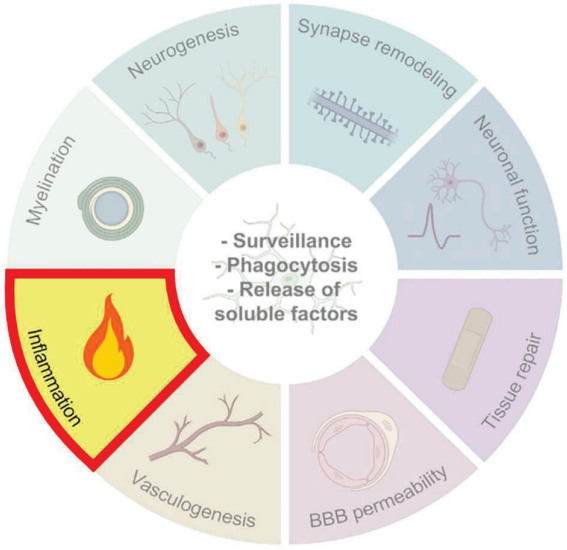

Figure 5. *Adapted from [165]. In the internal circle are depicted main properties of microglia. In the external circle are shown biological functions microglia can participate, in this work we focused mainly on neuroinflammation.*

3.2 Neuroinflammation in schizophrenia

It has been suggested that schizophrenia's early pathology is related to neuroinflammation and that over time develops into neurodegeneration[172]. Neuroinflammation in patients with schizophrenia is often linked to augmented transcription of inflammatory mediators in the CNS, microgliosis, and decreased GLU receptors activity. These factors, in turn, contribute to a reduction in synapse numbers, apoptosis of neurons and reduction of gray matter volume[173].

At the cellular level, microglia density and cell number have been shown to be generally increased across the brain in patients compared to controls[94], [174]. The same result was found when evaluated microglia density according to their morphology in frontal and temporal lobes (e.i ramified microglia and rounded-shape microglia)[175] and also when evaluated according to their location (e.i gray and white matter)[94], [174], [176], the density of microglia seems to be generally elevated in schizophrenia. In contrast, in a meta-analysis[94], no significant differences were found in the density nor in the cell number of macroglia (astrocytes and oligodendrocytes) between patients and controls. Furthermore, a recent study [177] found increased synapse elimination in patient-derived neural cultures and isolated synaptosomes as part of microglia-mediated synapse engulfment process. These results suggest a central role of microglia and other macrophages during neuroinflammation in schizophrenia.

At the molecular level, many cytokines' levels were shown to be altered in the brain of patients. For instance, pro-inflammatory cytokines, such as IL-6, TNF-α, and IL-1β were the most reported increased cytokines[94], [160], [172], [178], and elevated levels of these cytokines were associated with reduced cortical gray matter volumes[179]. Otherwise, some studies found augmented levels of IL-6, IL-12, TGF-β in plasma samples

of patients [94], [172]. Further, a systematic study found that increased levels of C-reactive protein and IL-6 were related with exacerbation of psychotic symptoms[180]. Another systematic review[181], found a constant increase of CCL2 in patients.

Supporting the idea that neuroinflammation has a deleterious effect in schizophrenia patients, a meta-analysis of clinical trials showed that patients diagnosed with schizophrenia displayed a reduction in the severity of mental symptoms when treated with anti-inflammatory drugs[182].

4. T cells

Within the immune system there are two fundamental ways to exert immune responses. Innate responses take place to the same extent, no matter how many times an infectious agent is found. In contrast, adaptative responses improve upon repetitive exposure to an infectious agent. Adaptative Immune responses are carried out by two classes of lymphocytes, B cells and T cells[183].

Two major types of T cells are broadly identified, T helper (Th) and T cytotoxic (Tc), associated with the type of receptors their bear on their membrane, either CD4 or CD8 molecule-based respectively[184]. CD4+ T cells play a pivotal role in orchestrating the cell-mediated immune response. They identify foreign antigens presented by antigen-presenting cells (APCs), and, subsequently, they are activated and produce cytokines to initiate immune responses from other white blood cells/other immune cells of cell-mediated immunity (Figure 6). For instance, they activate macrophages and granulocytes and help to activate B cells[185]. Upon pathogen presentation the CD4+ cells differentiate into different Th cells (Th1, Th2, Th9 Th17, Th22 all differentiated by their cytokine expression profile [186], see Table 1), Treg cells[187], follicular helper T cells[188] and memory T cells over time. Treg cells have the main role to suppress excessive immune response, memory T cells remain in the body for years and can elicit an immediate adaptative immune response to the same antigen under repeated exposure and follicular helper T cells help to enhance B cell activation.

CD4+ subset	Cytokines
Th1	TNF-α, IL2, IFNγ
Th2	IL4, IL5, IL9, IL13, IL25
Th9	IL9, IL21
Th17	IL17, IL21, IL22
Th22	IL-22, IL-13, TNF-α
Treg	IL 35, IL10, TGF-β
Tfh	IL21, IL4

***Table 1**. CD4+ T cell subsets and some of the cytokines they release[189], [190], [191].*

Like CD4+ T cells, CD8+ T cells are also activated after interaction with APCs. Thereafter, Tc cells can migrate and find their antigenic target in infected cells and use their killing functions to eliminate these cells[192]. CD8+ T cells killing functions are mediated by two mechanisms. Through the Fas/Fas Ligand mechanism CD8+ cells induce apoptosis of the target cells. The second method involves the release of granzymes and perforin, similar to the way NK cells do (Figure 6). Granzymes pass through the pores perforins generates on target cell membrane and via caspases activation generates DNA fragmentation and apoptosis[185].

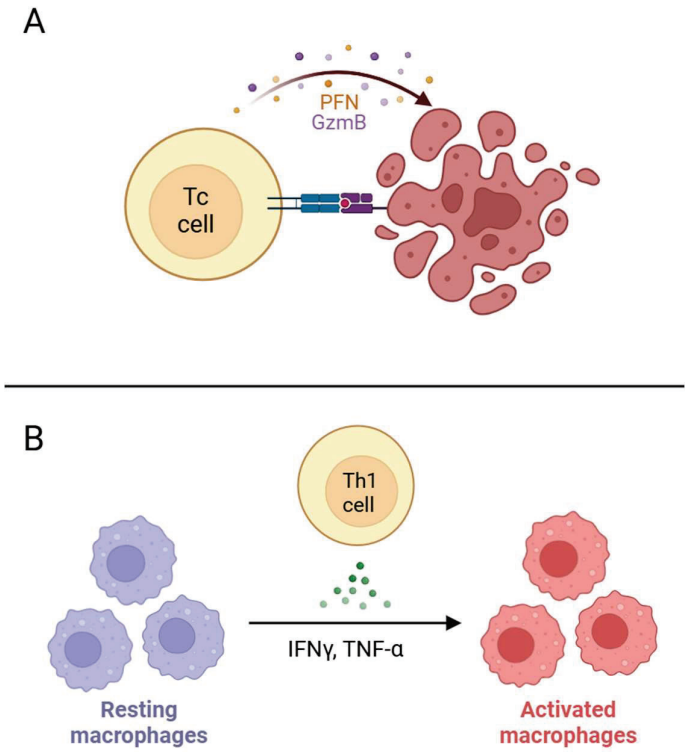

Figure 6. *A- Illustration of a T cytotoxic cell (CD8+) releasing granzymes and perforin to eliminate a cancer cell. B- Illustration of T helper 1 cell (CD4+) releasing cytokines and activating macrophages*

4.1 T cells dysregulation in schizophrenia

Through the last years, mounting evidence has consistently demonstrated T cells mediated immunity alterations in schizophrenia. Some studies have reported reduced numbers of T cells in patients compared to controls [193], [194], whereas other studies have reported elevated percentage of T cells in schizophrenia cases[195], [196]. Furthermore, there is also evidence of no dysregulation of T cells number in schizophrenia patients[197], suggesting that the quantity of T cells can vary among different patients and cannot be taken as a congruent marker in schizophrenia. However, higher densities of T lymphocytes in the hippocampus of schizophrenia patients have also been reported, suggesting an altered infiltration of these cells through the brain-blood-barrier (BBB) into the brain parenchyma[198]. Abnormalities regarding T cell populations have also been

seen in animal models. For example, maternal immune activation in rodents (which is consider a model of schizophrenia) has been shown to contribute to hyperactivated immune response in the adult offspring through preferential development of Th17 cells[199] and increased proliferation of CD4+ cells[200].

The immune repertoire of T cells receptors has also been studied in the context of schizophrenia. For instance, alterations in the distributions of the V segment in the complementarity determining region-3 (CDR3) of T cells receptor-beta chains were found in patients compared to controls[201]. Besides, a pilot study reported an increase in the average length of functional T cell receptor-gamma chains in the CDR3 regions in groups of schizophrenia-specific clonotypes compared with controls[202], suggesting a dysregulation of both T cell receptors -beta and -gamma in patients.

Besides TCRs, DA receptors are also expressed on T cells surface and DA alteration is one of the most prominent and consistent features of schizophrenia[47]. In the last years, it has been shown that dopamine has immunomodulatory effects on T cells playing a role in processes like migration, homing, and proliferation[203], [204]. Many studies have reported the presence of several types of dopaminergic receptors on T cells surface (D1,D2, D3, D4, D5) [205], [206], but the direct effect of DA on T cells are determined by the context, the T cell activation status, the T cell type and subtype, DA concentration and the specific DA receptor subtype that is activated[207]. For example, DA can activate effector functions in resting T cells resulting in proliferation and cytokine release, whereas in already activated T cells DA can act as an inhibitor[206]. Notably, it has also been shown that activation of immune non CNS-resident cells is sufficient to generate alterations in and loss of dopaminergic neurons[208]. Thus, as DA can exert modulatory effects on T cells, the latter can also affect the state of dopaminergic neurons. In schizophrenia, some studies have reported increased mRNA expression of dopaminergic receptors in peripheral lymphocytes[209], [210], while other reports found reduced mRNA levels of these receptors[211]. Interestingly, elevated percentages of CD4 + D4+, CD8 + D4+, and CD8 + D2+ cells were detected in schizophrenia subjects and these increases were shown to be related with schizophrenia severity[212]. Finally, one study focusing in D3 receptors on peripheral lymphocytes found no differences in mRNA levels between patients and controls, but significant variations among schizophrenia subtypes[213]. Overall, these studies suggest a possible impact of the dopamine-T cells crosstalk on the T cell mediated immunity in schizophrenia.

T cell mediated immunity has also been proposed to have both neurotoxic and neuroprotective effects[162]. For instance, in an in vitro study[214], it has been shown that T cells, co-cultured with astrocytes, induced a neuroprotective phenotype in astrocytes, where T cells derived GLU induced the release of thiols (e.g. cysteine, glutathione) and lactate from astrocytes. On the other hand, an expanding body of evidence suggest the implication of T cells-mediated neuroinflammation in degenerative CNS disorders[215], [216], [217]. Cytokines produced by abnormal quantities of T cells have the potential to stimulate the release of pro-inflammatory cytokines, which can trigger microglia activation and subsequently enhance T cell pro inflammatory response.

For example, in an in vitro study[218], IL-1β and IL-23 secreted by microglia stimulated by Toll-like receptor (TLR)-specific ligands induced activation of T cells, leading to the generation of IL-17+ T cells with neurotoxic effects on neurons, and this effect was not found when T cells were activated by other peripheral immune cells. In schizophrenia, increasing evidence points towards a compelling involvement of T cells and microglia together in neuroinflammation[162], [178], [219]. Collectively, with the abnormal levels of T lymphocytes in the brain of schizophrenia subjects this suggest a possible neurotoxic involvement of T cells in the context of schizophrenia[198].

Despite the available data being still insufficient to elucidate the precise role of T cells in the pathogenesis of schizophrenia, an increased body evidence shows T cells dysregulations from different perspectives, and possible T cells implication in neuroinflammation and neurotoxic processes in the context of schizophrenia[162], [193], [194], [195], [196], [202], [207], [212], [217]. This situation places the T cells population as a candidate mediating the abnormal neuro-immune crosstalk in schizophrenia and keeps the door open for further investigation regarding this matter.

III. Hypotheses and Objectives

The primary purpose of this work is to generate fresh insights into the immune factors contributing to the development of schizophrenia. Previous studies have shown that some Ikzf family members are essential for the proper function of some immune cell types[8], [10], [21], [27]. On the other hand, *IKZF1* mutations such as rs116427960 and rs186807222 have been linked to schizophrenia and SNPs of *IKZF1* have been found to be related to the age of onset of schizophrenia[220], [221]. Moreover, Ikzf2 deficiency results in overexpression of WDFY1, an immune scaffold protein commonly elevated in schizophrenia patients and IKZF2 dysregulation has been observed in individuals with autism spectrum disorder, a condition with a prevalence in individuals with schizophrenia of up to 52%[43], [222], [223]. Additionally, preliminary results from our lab indicated that IKZF1 and IKZF2 are dysregulated in immune cells of schizophrenia patients. Altogether, these data led us to think that Ikzf1 and Ikzf2 could be implicated in the pathophysiology of Schizophrenia. Consequently, we aimed to evaluate the potential involvement of Ikzf1 and Ikzf2 in the pathogenesis and associated pathological processes of schizophrenia.

To prosecute our investigation, we proposed the following Hypotheses:

- **Alterations of some members of the Ikzf family contribute to the pathogenesis of Schizophrenia through the neuro-immune crosstalk.**

- **Ikzf1 is implicated in neuroinflammatory processes and the regulation of microglia homeostasis.**

To address our hypotheses, we established the following Objectives:

- **Objective 1: To evaluate the levels of the Ikzf family members in Peripheral blood mononuclear cells (PBMCs) in a cohort of patients diagnosed with schizophrenia.**

- **Objective 2: To mimic the potential alterations of Ikzf family members in patients using animal models.**

- **Objective 3: To perform in-vivo and in-vitro translational approaches (human to mice) to assess the impact of immune cells secretome in the expression of schizophrenia-like phenotypes.**

- **Objective 4: To characterize the molecular profile of the secretome of PBMCs from the cohort of patients diagnosed with schizophrenia.**

- **Objective 5: To assess the role of Ikzf1 within microglia in the context of neuroinflammation.**

IV. Articles

1. Alterations of the *IKZF1-IKZF2* tandem in immune cells of schizophrenia patients regulate associated phenotypes

Ballasch *et al. Journal of Neuroinflammation* (2024) 21:326
https://doi.org/10.1186/s12974-024-03320-3

Journal of Neuroinflammation

RESEARCH Open Access

Alterations of the *IKZF1-IKZF2* tandem in immune cells of schizophrenia patients regulate associated phenotypes

Iván Ballasch[1,2,3†], Laura López-Molina[1,2,3†], Marcos Galán-Ganga[1,2,3], Anna Sancho-Balsells[1,2,3], Irene Rodríguez-Navarro[1,2,3], Sara Borràs-Pernas[1,2,3], M. Angeles Rabadan[4], Wanqi Chen[1,2,3], Carlota Pastó-Pellicer[1,2,3], Francesca Flotta[1,2,3], Wang Maoyu[1,2,3], Joaquín Fernández-Irigoyen[5], Enrique Santamaría[5], Ruth Aguilar[6], Carlota Dobaño[6,7], Natalia Egri[8], Carla Hernandez[10], Miqueu Alfonso[10], Manel Juan[1,8,9], Jordi Alberch[1,2,3,11], Daniel del Toro[1,2,3], Belén Arranz[10], Josep M. Canals[1,2,3,11] and Albert Giralt[1,2,3,11*]

Abstract

Schizophrenia is a complex multifactorial disorder and increasing evidence suggests the involvement of immune dysregulations in its pathogenesis. We observed that *IKZF1* and *IKZF2*, classic immune-related transcription factors (TFs), were both downregulated in patients' peripheral blood mononuclear cells (PBMCs) but not in their brain. We generated a new mutant mouse model with a reduction in *Ikzf1* and *Ikzf2* to study the impact of those changes. Such mice developed deficits in the three dimensions (positive–negative-cognitive) of schizophrenia-like phenotypes associated with alterations in structural synaptic plasticity. We then studied the secretomes of cultured PBMCs obtained from patients and identified potentially secreted molecules, which depended on *IKZF1* and *IKZF2* mRNA levels, and that in turn have an impact on neural synchrony, structural synaptic plasticity and schizophrenia-like symptoms in in vivo and in vitro models. Our results point out that *IKZF1-IKZF2*-dependent immune signals negatively impact on essential neural circuits involved in schizophrenia.

Keywords IL-4, CXCL10, CCL5, Neuronal networks, Ikaros, Helios, Lymphocytes, Mouse models, Cognitive symptoms, Negative symptoms

†Iván Ballasch and Laura López-Molina have contributed equally.

*Correspondence:
Albert Giralt
albertgiralt@ub.edu
[1] Departament de Biomedicina, Facultat de Medicina, Institut de Neurociències, Universitat de Barcelona, 08036 Barcelona, Spain
[2] Institut d'Investigacions Biomèdiques August Pi i Sunyer (IDIBAPS), 08036 Barcelona, Spain
[3] Centro de Investigación Biomédica en Red Sobre Enfermedades Neurodegenerativas (CIBERNED), 28031 Madrid, Spain
[4] ZeClinics SL. and ZeNeuroid SL., Barcelona, Spain
[5] Proteomics Platform, Navarrabiomed, Hospital Universitario de Navarra (HUN), Universidad Pública de Navarra UPNA, IdiSNA, 31008 Pamplona, Spain
[6] ISGlobal, Hospital Clínic – Universitat de Barcelona, Barcelona, Catalonia, Spain
[7] CIBER Enfermedades Infecciosas (CIBERINFEC), Barcelona, Catalonia, Spain
[8] Servei d'Immunologia, Hospital Clinic Barcelona (HCB) - CDB, Fundació Clínic de Recerca Biomèdica - IDIBAPS, Barcelona, Spain
[9] Plataforma d'Immunoteràpia HSJD-HCB, Barcelona, Spain
[10] Parc Sanitari Sant Joan de Déu, CIBERSAM, Barcelona, Spain
[11] Production and Validation Centre of Advanced Therapies (Creatio), Faculty of Medicine and Health Science, University of Barcelona, 08036 Barcelona, Spain

Introduction

Schizophrenia is composed of a myriad of heterogeneous symptoms that challenges a unified description of the disease. This represents a global burden, as schizophrenia ranks within the top 10 causes of disabilities in developed countries, with 24 million people affected worldwide (GHDx). Furthermore, due to its early age of onset of 16–25 years [62, 79], the disease results in more than 12 million disability-adjusted life years annually. Behavioral signatures of schizophrenia are broadly divided into three categories: (1) positive symptoms (delusions and hallucinations); (2) negative symptoms (lack of pleasure, social withdrawal), and (3) cognitive symptoms (impairment of short-term working memory, attention deficit). Current treatments only provide some symptomatic relief for positive symptoms whereas treatments for cognitive and negative symptoms remain elusive [75]. Notably, cognitive and negative symptoms are responsible for a major proportion of the disability associated with schizophrenia and are more constant over time [75, 95]. Also, the current lack of insight into the disease is not only due to the heterogeneity of the symptomatology [74], but also due to the complexity of the causative factors underlying the disease, including genetic and immunological [17]. Therefore, what is urgently needed are novel mechanistic insights into the molecular paths underlying the negative and cognitive symptomatology subtypes of the disorder.

Although schizophrenia has been classically observed as a brain disease, current evidence points towards a multi-system network underlying positive, negative, and cognitive symptoms [12, 99]. In this sense, the communication between the immune and central nervous systems has already been described to be altered in schizophrenia [65]. As illustrative example, it has been shown that lymphocyte invasion is higher in patients with prevalence of negative symptomatology [9] and that levels of inflammatory cytokines (TNF-a and IL-6 or C-reactive protein) correlate with negative and cognitive symptoms in schizophrenia [31, 45, 52]. However, what we know so far is reduced to the description of circulating molecules that probably serve as a molecular bridge between these two systems [77]. Major mechanistic insights are still lacking, especially regarding the regulation of these molecules, their aberrant release, and the specific targeted neural circuits they affect. In this line, a highly promising target as a molecular bridge between the neural and immune system is the Ikaros family of transcription factors (TFs), which include Ikaros zinc finger 1 (*IKZF1* or Ikaros) and Ikaros zinc finger 2 (*IKZF2* or Helios). These TFs have been largely described to be crucial for the normal development of immune cells (T-cells, B-cells, and monocytes) [27] and their function (e.g. production of *mb-1*, *CD3*, *IL2*, *IL4*, and *NFkB* among others [64]. Furthermore, evidence starts to emerge, that they could play an important role in schizophrenia. For instance, specific *IKZF1* single nucleotide polymorphisms (SNPs) such as rs7805803 and rs10276619 have been associated with changes in brain and ventricle volumes [23] and with hippocampal atrophy [69], respectively—neuropathological features heavily implicated in schizophrenia [38]. Additionally, *IKZF1* mutations such as rs116427960 and rs186807222 have been linked to schizophrenia and associated executive function deficits [14, 40]. *IKZF1* levels have also been related with the age of onset of schizophrenia [78]. Regarding *IKZF2*, evidence, although more limited, highlights its relevance. *IKZF2* levels are highly sensitive to treatment with lipopolysaccharides (LPS), a widely used experimental model for schizophrenia [25]. Moreover, Helios deficiency results in overexpression of WDFY1, an immune scaffold protein commonly elevated in schizophrenia patients [81]. Finally, *IKZF2* dysregulation has been observed in individuals with autism spectrum disorder [2, 4], a condition frequently co-occurring with psychosis. Nevertheless, the function of the *IKZF* family in the communication between the immune and neural systems during the development of schizophrenia is practically unexplored.

In the present work, we hypothesized that immune alterations in schizophrenia could be associated with altered mRNA levels (and function) of *IKZF1* and *IKZF2*, and that these potential changes could impact the communication between the immune and central nervous systems during the progression of the disorder. To address this hypothesis, we first confirmed the altered state of the two transcription factors in human samples (brain and circulating immune cells). Subsequently, to validate their specificity and biological relevance, we used genetically modified mice devoid of *Ikzf1*, *Ikzf2*, or both. Finally, to evaluate the aberrant communication between the immune and central nervous systems, we transferred the secretome of human circulating immune cells (PBMCs) into the brains of living mice. In these mice, we evaluated whether schizophrenia-like phenotypes were induced in terms of behavior and histological markers.

Materials and methods

Human post-mortem brain samples

The brain samples from schizophrenia (SCH) patients used in this study were provided by the Sant Joan de Déu Brain Bank (Sant Boi de Llobregat, Barcelona, Spain). The donation and obtention of samples were regulated by the ethics committee of the institution. The sample processing followed the rules of the European Consortium of Nervous Tissues: BrainNet Europe II (BNEII). All the samples were protected in terms of individual donor identification following the BNEII laws. Clinical

diagnosis of SCH in donor subjects was confirmed premortem with DMS-IV (Diagnostic and Statistical Manual of Mental Disorders—4th edition) and ICD-10 (International Statistical Classification of Diseases and Related Health Problems) criteria by clinical examiners. Most donors were hospitalized for more than 40 years and were re-evaluated every 2 years to monitor and update their clinical progression. Case information can be found in Supplementary Table 1. Control samples (hippocampus, putamen, and dorsolateral prefrontal cortex) were obtained from Banc de Teixits Neurològics (Servei Científico-Tècnics, Universitat de Barcelona, Barcelona, Spain) and the sample processing also followed the BNEII rules. Case information can be also found in Supplementary Table 1. All the procedures for the obtention of post-mortem samples followed the ethical guidelines of the Declaration of Helsinki and local ethical committees (Universitat de Barcelona: IRB00003099; Fundació CEIC Sant Joan de Déu: BTN-PSSJD, CER122306).

Immunoblotting

The tissue was lysed by sonication in 250 µl of lysis buffer as described elsewhere [28]. After lysis, samples were centrifuged at 12,000 r.p.m. for 20 min. Supernatant proteins (15 µg) from total brain region extracts were loaded in SDS–PAGE and transferred to nitrocellulose membranes (GE Healthcare, LC, UK). Membranes were blocked in TBS-T (150 mM NaCl, 20 mM Tris–HCl, pH 7.5, 0.5 ml Tween 20) with 50 g l−1 non-fat dry milk and 50 g l−1 BSA. Immunoblots were probed with the following antibodies: anti-Ikzf1 (1:1000, D6N9Y, Cell Signaling Technology, Danvers, MA, USA,#14859), anti-Ikzf2 (1:1000, GeneTex, California. USA, #GTX115630). All blots were incubated with the primary antibody overnight at 4 °C by shaking in PBS with 0.2 g l−1 sodium azide. After three washes in TBS-T, blots were incubated for 1 h at room temperature with the corresponding horseradish peroxidase-conjugated antibody (1:2000; Promega, Madison, WI, USA) and washed again with TBS-T. Immunoreactive bands were visualized using the Western Blotting Luminol Reagent (Santa Cruz Biotechnology, #sc-2048) and quantified by a computer-assisted densitometer (Gel-Pro Analyzer, version 4, Media Cybernetics). For loading control, a mouse monoclonal antibody for actin was used (1:20,000; MP Biochemicals, #0869100-CF).

Recruitment of patients

The sample of this study (NoPI17/00246, PI Belen Arranz) was recruited in the Outpatient clinic located in Cornellà, Barcelona, Spain (Parc Sanitari Sant Joan de Deu). Adult controls and patients with DSM-5 (Diagnostic and Statistical Manual of Mental Disorders) schizophrenia-spectrum disorder at any stage of the disease were included. The inclusion criteria for patients were: (1) adults over 18 years of age; (2) ability to speak Spanish correctly; and (3) signed informed consent. Exclusion criteria were: (1) history of head trauma with loss of consciousness and (2) organic disease with mental repercussions; (3) presence of an acute inflammatory process: (3.1) fever (> 38ºC) or infection in the 2 weeks prior to the baseline interview, or (3.2) have received vaccinations in the past 4 weeks. This study was conducted following the ethical principles of the Declaration of Helsinki and Good Clinical Practice and the Ethics and Research Board from Parc Sanitari Sant Joan de Deu. All participants provided written informed consent prior to their inclusion in the study. Case information can be found in Supplementary Table 2.

Human peripheral blood mononuclear cells (PBMCs) and isolation of CD4 + and CD8 + cells

Human peripheral blood mononuclear cells (PBMCs) were isolated from peripheral blood. The cell fraction corresponding to red blood cells and granulocytes (neutrophils, basophils, and eosinophils) was removed from whole blood by density gradient centrifugation as described elsewhere [47]. For this procedure, 10 ml blood samples were diluted with 10 ml of phosphate-buffered saline (PBS) pH-7.2. Consequently, 10 ml of diluted blood were placed in 15 ml tubes filled with 4 ml of a density gradient medium with $\rho = 1.077$ g/ml (e.g. Ficoll-Paque PLUS) and centrifuged at $500 \times g$ for 35 min at 20 °C without brake. PBMCs were then transferred to 50 ml tubes, the tubes were filled with PBS and centrifuged at $500 \times g$ for 10 min at 20 °C. PBMCs were then lysated for mRNA (see next section) or plated. For PBMCs plating, after elimination of the supernatant, PBMCs were resuspended in X-vivo medium (#BEBP02-055Q Lonza bioscience, Maryland, USA) supplemented with pen/strep 1%/1%, L-glutamine 1% and Hepes 0,02 M. Cells were seeded in 24-well plates (1 ml per well at $4 \cdot 10^6$ cells/ml) and left in an incubator at 37 °C, 5% CO2. After 24 h, PBMCs were treated with PMA (50 ng/ml, #P1585, Sigma-Aldrich Chemical Co., St. Louis, MO, USA) and Ionomycin (1 µM, #I0634 Sigma-Aldrich Chemical Co.) for 6 h, then we centrifuged the cultures to take separately the supernatant and the pellet, both were stored at − 80 °C. For the CD4 + and CD8 + isolation the Pan T Cell Isolation Kit was used to isolate T cells from human PBMC previously obtained through negative selection following manufacturer's instructions (Miltenyi, Cat. #130-096-535). T cells were then subjected to further magnetic labeling and separation to isolate CD4 + and CD8 + cells. First, T cells were incubated with CD8 MicroBeads (Miltenyi, Cat. #130-045-201) for 15 min at

4 °C and cell suspension was applied onto the magnetic columns. The flow-through containing unlabeled cells was collected and considered the CD4+enriched fraction. Then, labeled CD8+cells were removed from the column with buffer. Both fractions were centrifuged at 300 *g*×7 min and the final cellular pellets were lysed with the proper buffer for subsequent RNA extraction.

mRNA extraction and RT-qPCR

PBMCs were homogenized and total RNA was extracted using PureLink RNA Micro Scale kit (#12183-016, Invitrogen) according to manufacturer's recommendations. RNA purity and quantity were determined with Nanodrop 1000 spectrophotometer (Thermo Fisher). 500 ng of purified RNA was reverse transcribed using the High Capacity cDNA Reverse Transcription Kit (Applied Biosystems, Cat. #436814). The cDNA synthesis was performed at 25 °C for 10 min, at 37 °C for 120 min and a final step at 85 °C for 5 min in a final volume of 20 µl as instructed by manufacturer. Then, cDNA was analyzed by quantitative RT-PCR using PrimeTime qPCR Assays (Integrated DNA Technologies, Coralville, Iowa. USA). Human assays: IKZF1 (Hs.PT.58.25575505), IKZF2 (Hs.PT.58.2960172), and 18S (Hs.PT.39a.22214856.g). Mouse assays: IKZF1 (Hs.PT.58.25575505), IKZF2 (Hs.PT.58.2960172) and 18S (Hs.PT.39a.22214856.g). Quantitative PCR was performed in 12 µl of final volume on 96-well plates using the Premix Ex Taq (Takara Biotechnology, #RR037A). Reactions included Segment 1: 1 cycle of 30 s at 95 °C and Segment 2: 40 cycles of 5 s at 95 °C and 20 s at 60 °C. All RT-PCR assays were run in duplicate. To provide negative control and exclude contamination by genomic DNA, the PrimeScript RT enzyme was omitted in the cDNA synthesis step and samples were subjected to the PCR reaction in the same manner with each probe. RT-PCR data were quantified using the comparative quantitation analysis program of 64 MxProTM quantitative PCR software version 3.0 (Stratagene) and 18S gene expression was used as housekeeping gene. To analyze the relative changes in gene expression, the 2(−ΔΔ C(T)) method was used.

Treatments with antipsychotics in mice

Female and male adult (12-week-old) wild type mice (C57BL/6 J strain) were purchased from Jackson Laboratory (Cat. #000664). All mice (male and female, 50% each) were sub-chronically (7 days) or chronically (28 days, only for clozapine) treated (i.p.) with vehicle or paliperidone (0.5 mg/Kg dissolved in PBS, 5% DMSO) or clozapine (1 mg/Kg dissolved in PBS, 5% DMSO). Doses were used following previous literature [57, 94]. One day after the end of the treatments all mice were sacrificed and blood samples were obtained by using a cardiac puncture as previously described [41]. Then, peripheral blood mononuclear cells (PBMCs) were isolated as we did for humans. Blood pools from two mice were used to obtain enough PBMC mRNA concentrations.

Animals

Ikzf1 deficient mice [101] were provided by Professor Katia Georgopoulos whereas Ikzf2 deficient mice were provided by Professor Philippe Kastner [10]. Both lines, with C57BL/6 background, were backcrossed to obtain wild type ($Ik^{+/+}$:$He^{+/+}$), heterozygous for *Ikzf1* ($Ik^{\pm}$:$He^{+/+}$), heterozygous for *Ikzf2* ($Ik^{+/+}$:$He^{\pm}$) and double heterozygous mice ($Ik^{\pm}$:$He^{\pm}$). Adult males and females were used. We also used the Egr1-CreERT2 mice [7]. These mice carry a bacterial artificial chromosome (BAC) including the Egr1 gene in which the coding sequence was replaced by that of CreERT2 fusion protein. They were crossed with R26RCE mice (Gt(ROSA)26Sortm1.1(CAG-EGFP)Fsh/Mmjax, Strain 004077, The Jackson Laboratory), which harbor the R26R CAG-boosted EGFP (RCE) reporter allele with a loxP-flanked STOP cassette upstream of the enhanced green fluorescent protein (EGFP) gene to create the double heterozygous mutant Egr1-CreERT2 x R26RCE mice for the experiments related with characterization of neural populations upon treatment with human secretomes. Single intraperitoneal injections of 4-hydroxytamoxifen (4-HT; #H7904, Sigma-Aldrich Chemical Co.) 50 mg/kg were administered to induce conditional Cre-dependent recombination. The animals were housed with access to food and water ad libitum in a colony room kept at 19–22 °C and 40–60% humidity, under an inverted 12/12 h light/dark cycle (from 8 A.M. to 8 P.M.). All animal procedures were approved by local committees [Universitat de Barcelona, CEEA (136/19); Generalitat de Catalunya (DAAM 10786) following the European Communities Council Directive (86/609/EU).

Behavioral tests

Behavioral phenotyping was performed following widely and previously detailed features of appropriate mouse models of schizophrenia [70] addressing the three dimensions of the symptomatology. First, free exploration and then, evaluation of D-amphetamine-induced hyperlocomotion (D-amphetamine sulfate, 3 mg/kg; TOCRIS 2813), were both evaluated in the open field as described elsewhere [81]. Next, sociability was assessed by using the three-chamber social interaction test as previously described [81]. Finally, object recognition long-term memory was evaluated by performing the novel object recognition test (NORT) as we previously reported [6]. In all behavioral studies animals were tracked and recorded with Smart junior 3.0 software (Panlab).

Golgi staining

Fresh brain hemispheres were submerged and processed following the Golgi-Cox method as described elsewhere [28]. Two hundred microns sections were cut in 70% EtOH on a vibratome (Leica) and washed in water for 5 min. Next, they were reduced in 16% ammonia solution for 1 h before washing in water for 2 min and fixation in Na2S2O3 for 7 min. After a 2-min final wash in water, sections were mounted on superfrost coverslips, dehydrated for 3 min in 50%, then 70, 80 and 100% EtOH, incubated for 5 min in a 2:1 isopropanol:EtOH mixture, followed by 1×5 min in pure isopropanol and 2×5 min in xylol. Bright-field images of Golgi-impregnated stratum radiatum dendrites from hippocampal CA1 pyramidal neurons or from pyramidal neurons of the medial prefrontal cortex (Layer V) or from medium spiny neurons in the striatum, were captured with a Nikon DXM 1200F digital camera attached to a Nikon Eclipse E600 light microscope (×100 oil objective). Only fully impregnated neurons with their soma entirely within the thickness of the section were used. Image z-stacks were taken every 0.2 mm, at 1024×1024-pixel resolution, yielding an image with pixel dimensions of 49.25×49.25 µm. Segments of proximal dendrites were selected for the analysis of spine density. Only spines arising from the lateral surfaces of the dendrites were included in the study. Given that spine density increases as a function of the distance from the soma, reaching a plateau 45 µm away from the soma, we selected dendritic segments of basal dendrites 45 µm away from the cell body. The total number of spines was obtained using the cell counter tool in the ImageJ software.

Quantitative proteomics

Proteins from secretome media were precipitated with acetone, and pellets dissolved in 8 M Urea, 50 mM DTT. Protein quantitation was performed with the Bradford assay kit (Bio-Rad, Hercules, CA, USA). Protein extracts (20 µg) were diluted in Laemmli sample buffer and loaded into a 1,5 mm thick polyacrylamide gel with a 4% stacking gel cast over a 12.5% resolving gel. The run was stopped as soon as the front entered 3 mm into the resolving gel so that the whole proteome became concentrated in the stacking/resolving gel interface. Bands were stained with Coomassie Brilliant Blue, excised from the gel and protein enzymatic cleavage was carried out with trypsin (Promega; 1:20, w/w) at 37 °C for 16 h as previously described [87]. Purification and concentration of peptides were performed using C18 Zip Tip Solid Phase Extraction (Millipore). For LC–MS/MS, dried peptide samples were reconstituted with 2% ACN-0.1% FA (Acetonitrile-Formic acid) and quantified by NanoDropTM spectrophometer (ThermoFisher) before LC–MS/MS analysis using an EASY-1000 nanoLC system coupled to an Exploris 480 mass spectrometer (Thermo Fisher Scientific). Peptides were resolved using a C18 Aurora column (75 µm × 25 cm, 1.6 µm particles; IonOpticks) at a flow rate of 300 nl/min using a 60-min gradient (50 °C): 2% to 5% B in 1 min, 5% to 20% B in 48 min, 20% to 32% B in 12 min, and 32% to 95% B in 1 min (A = FA, 0.1%; B = 100% ACN:0.1% FA). The spray voltage was set at 1.6 kV, and the capillary temperature at 275 °C. Sample data was acquired in a data-independent mode (DIA) with a full MS scan (scan range: 400 to 900 m/z; resolution: 60,000; maximum injection time: 50 ms; normalized AGC target: 100%) and 25 periodical MS/MS segments, applying 20 Th isolation windows (0.5 Th overlap; resolution: 15,000; maximum injection time: 22 ms; normalized AGC target: 3000%). Peptides were fragmented using a normalized HCD collision energy of 30%. Data were acquired in profile and centroid mode for full MS scan and MS/MS, respectively. For data analysis of quantitative proteomics DIA data files were analyzed using Spectronaut (v 17.3, Biognosys) by directDIA analysis (dDIA). Sample raw data was first processed by the Pulsar Spectronaut search engine to generate a spectral library. Pulsar then searched MSMS spectra against Uniprot-Swissprot isoforms Homo Sapiens database. MS1/MS2 calibration and main search tolerance were set to dynamic. The maximum precursor ion charge was set to 4, and fragment selection to intensity-based. Carbamidomethyl (C) was selected as a fixed modification, and Oxidation (M), Acetyl (Protein N-term), Deamidation (N), and Gln- > pyro-Glu as variable modifications (3 maximum modifications per peptide). The enzyme was set to trypsin in a specific mode (two missed cleavages maximum). The target-decoy-based false discovery rate (FDR) filter for PSMs, peptide, and protein groups was set to 1%. Once the Pulsar search was performed, the Spectronaut DIA search engine algorithm initiated the DIA search using the default settings (Proteotypicity filter = Protein group Specific) and filtering the precursors and protein groups by a 1% Q-value. The Perseus software (version 1.6.15.0) [96] was used for statistical analysis and data visualization. Identifications from the reverse database, common contaminants and proteins only identified through a modification peptide were removed. Label-free intensities were then logarithmized (base 2) and the samples were then grouped according to the experimental design. A filter of 70% valid values at least in one group was applied to the resulting matrix followed by a logarithmic transformation (Log2). Then, data were imputated based on the normal distribution and normalized using the "Width adjustment" method. Statistical analysis was performed using "Two-sample tests" for the T-test of two selected experimental groups, based

on permutation-based FDR statistics (250 permutations; FDR 1⁄4 0.07; S0 1⁄4 0.1). The resulting matrixes were exported containing the p-value (-Log) and fold-change (Log2) columns that, after its transformation into linear scale, were filtered by $p < 0.05$ and 30% of significance and fold-change respectively.

Luminex assay

We measured a panel of 30 cytokines, chemokines and growth factors in 14 supernatant samples by Luminex using the Cytokine Human Magnetic 30-Plex Panel LHC6003M from Life Technologies™. Briefly, 25 µl of the sample were tested by applying a modification to the manufacturer's protocol by using half the volume of all reagents including the standards. This modification has been previously tested and showed no difference in assay performance compared to the original protocol and has been used in prior studies [1, 37]. Each plate included 16 serial dilutions (twofold) of a standard sample with known concentrations of each analyte and two blanks. Samples were acquired on a Luminex® 100/200 instrument and analyzed with xPONENT® software 3.1. Concentrations of analytes were obtained by interpolating the median fluorescent intensity (MFI) to a 5-parameter logistic regression curve fitted with the R package (drLumi) [82]. If the algorithm did not converge, a 4-parameter log-logistic model was fitted. Limits of quantification (LOQ) were estimated based on the 30% threshold value for the coefficient of variation (CV) of the standard curve. Molecules outside the LOQ in more than 30% of samples were excluded from the study. For all other markers, observations outside LOQ were imputed. Results were reported as pg/mL. The Luminex assay was performed in the Immune Response and Biomarkers Core Facility at ISGlobal (Barcelona, Spain).

Hippocampal primary cultures and immunocytochemistry

Hippocampal neurons were obtained from E17.5 C57Bl/6 mice. The hippocampus was dissected and mechanically dissociated with a fire-polished Pasteur pipette. Cells were seeded at a density of 50,000 onto 12 mm coverslips placed in 24-well plates. Plates were previously precoated with 0.1 mg/mL poly-D-lysine (Sigma-Aldrich Chemical Co., St. Louis, MO, USA) and neurons were cultured in Neurobasal medium (Gibco-BRL, Renfrewshire, UK) supplemented with 1% Glutamax and 2% B27 (Gibco-BRL). Cultures were maintained at 37 °C in a humidified atmosphere containing 5% CO_2. Primary neurons were fixed with 4% paraformaldehyde solution in PBS for 10 min and blocked in PBS-0.1 M glycine for 10 min. Then, cells were permeabilized in PBS-0.1% saponin 10 min, blocked with PBS-Normal Horse Serum 15% for 30 min, and incubated overnight at 4 °C in the presence of the following primary antibodies: mouse MAP2 (1:500, M1406, Sigma-Aldrich Chemical Co.) and rabbit PSD-95 (1:500, Cell Signaling, Ref: 3450S). Fluorescent secondary antibodies: AlexaFluor 488 goat anti-rabbit (1:100) and/or Cy3 goat anti-mouse (1:100; both from Jackson ImmunoResearch, West Grove, PA, USA) were incubated for 1 h at RT. Nuclei were stained with DAPI-Fluoromount (SouthernBiotech, Birmingham, AL, USA). Immunofluorescence was analyzed using a Leica Confocal SP5-II confocal microscope (Leica Microsystems CMS GmbH, Mannheim, Germany). Images were taken using an HCX PL APO lambda blue 63.0×1.40 OIL objective with a standard pinhole (1 AU), at 1024×1024-pixel resolution, 0.2 µm thick, and 5.0 digital zoom.

Tissue fixation and immunofluorescence

Mice were euthanized by cervical dislocation. Left hemispheres were removed and fixed for 72 h in 4% paraformaldehyde (PFA) in PBS. 40 µm coronal sections were obtained using a Leica vibratome (Leica VT1000S). Next, free-floating sections were washed three times in PBS, treated with NH_4Cl for 30 min, and washed again three times with PBS. Floating sections were permeabilized and blocked with PBS containing 3% Triton X-100, 0.02% Azide, 2% BSA, and 3% NGS (Ab buffer) for 1 h at RT. After three washes in PBS, brain slices were incubated overnight at 4 °C with anti-GFP (1:500, Synaptic Systems, 132006) and anti-Parvalbumin (1:1250, Swant, PV27). Sections were washed three times and incubated for 2 h at RT with fluorescent secondary antibody Alexa Fluor 488 or 647 (1:400; from Jackson Immuno Research, West Grove, PA, USA). Nuclei were stained with DAPI-Fluoromount (SouthernBiotech, Birmingham, AL, USA). Sections were analyzed using a two-photon confocal microscope (Leica SP5). To stain microglia and astrocytes in the hippocampal CA1, anti-Iba1 (1:500, Abcam, #Ab5076) and anti-GFAP (1:500, Synaptic Systems, #132006) were the antibodies employed respectively. Morphometric analysis of GFAP-positive astrocytes and Iba1-positive microglia were performed as described elsewhere [81].

Imaging analysis

To evaluate neuronal morphology by using the Sholl analysis we employed the protocol described elsewhere [18]. For the experiments evaluating PSD-95-positive puncta in primary cultures, we followed the protocol previously described [28]. For quantification of the number of activated neural ensembles and the number of parvalbumin-positive cells in the hippocampal CA1 from Egr1-CreERT2 x R26RCE mice, we used the procedure previously reported by our group [80].

3D Cell culture preparation

Tridimensional neurospheres networks were developed as previously described [72]. Briefly, E18 C57BL/6JOlaHsd pregnant mice were euthanized by cervical dislocation. Hippocampus were dissected in Neurobasal (Gibco) ice-cold media and incubated in 0.25% Trypsin–EDTA (Gibco) at 37 °C for 20 min, followed by 5 min DNAse I (1 µg/ml; Sigma-Aldrich Chemical Co.) incubation at room temperature. Mechanical dissociation of the dissected hippocampus was performed by repeated pipetting with a fire-polished glass Pasteur pipette until a homogenous cell suspension was obtained. Cell viability was determined by Trypan Blue exclusion assay. The cell solution was then centrifuged at 150 g for 10 min, and the supernatant was removed. The resulting cell pellet was resuspended in the culture media containing Neurobasal media, 2% B27, 1% N2, 0.5 mM Glutamate, and 1% Penicillin/Streptomycin (Gibco). Cells were infected with AAV7m8.Syn.GCaMP6s.WPRE.SV40 virus (Unitat de Producció de Vectors, Universitat Autonoma Barcelona) for neuronal GCaMP6s calcium sensor expression. The viral infection was made at 1:1000 dilution at the single-cell suspension stage, just before seeding. For neurospheres network cultures, 5.5×10^4 cells were seeded in poly-dimethylsiloxane (PDMS) customized molds containing an 18 mm^2 square well. PDMS molds were fabricated in UV resin 3D printed cast (Formlab 3 + laser 3D printer) and polymerized overnight at 90 °C. Neurospheres cultures were incubated in culture media at 37 °C and 5% CO_2. Imaging experiments were performed using a wide-field fluorescence microscope (Inverted microscope Zeiss Axio Observer Z1) and ZEN software (Zeiss) was used for image acquisition. Time-lapse videos were recorded at 25 Hz for 5 min at 37 °C and 5% CO_2 in culture media (Neurobasal media, 2% B27, 0.5 mM Glutamate, and 1% Penicillin/Streptomycin (Gibco)). Videos were acquired at DIV28. All computations and visualizations were done using the standard Python-based ecosystems for scientific computing and data visualization (NumPy, SciPy, Seaborn, SciKitLearn, Matplotlib). Statistical significance was plotted using the stat annotations package (https://github.com/trevismd/statannotations). Video data was extracted from.czi files. For neurosphere segmentation was done using the Otsu thresholding technique. A time series of mean intensity values of each neurosphere was extracted. The signal was denoised using a Butterworth filter. After normalization, peaks were detected (prominence (1-mean)/3, height 0.5) and the signal was binarized. Neurospheres without any detected activity were discarded from the subsequent analysis. From the binarized signal the following parameters were computed: mean activity rate, mean peak duration, and average pairwise Pearson correlation of neurospheres. Statistical significance between different conditions was determined at DIV28 by one-way ANOVA and Dunnett's as *post-hoc* test. A subset of neurospheres were fixed and stained against Tuj1 (1:1000, #T8660; Sigma).

Mini-osmotic pumps implantation

Mice were deeply anesthetized with isoflurane (2% induction, 1.5% maintenance) and 2% oxygen and placed in a stereotaxic apparatus for osmotic minipump (model 1004; Alzet, Palo Alto, CA, USA) implantation. A brain infusion kit (#0008663) was also used to deliver into the lateral (left) ventricle (0.1 mm posterior to bregma, ± 0.8 mm lateral to the midline, and − 2.5 mm ventral to the parenchyma surface) 0.11 µl per hour of supernatants obtained from cultured peripheral blood mononuclear cells/PBMC at a protein concentration of 0,2064 µg/µl. Cannulas were fixed on the skull with Loctite 454 (from Alzet). Minipumps, previously equilibrated overnight at 37 °C in PBS, were implanted subcutaneously in the back of the animal. After recovery, the mice were isolated to prevent detachment of the cannulas.

Statistics

All data are expressed as mean ± SEM. Statistical analysis was performed using the unpaired two-sided Student's t test (95% confidence), one-way ANOVA with Tukey's as post hoc tests, or two-way ANOVA with Bonferroni's post hoc test as appropriate and indicated in the figure legends. Values of $p < 0.05$ were considered statistically significant. All experiments in this study were blinded and randomized. All mice bred for the experiments were used for preplanned experiments and randomized to experimental groups. Visibly sick animals were excluded before data collection and analysis. Data were collected, processed, and analyzed randomly. The experimental design and handling of mice were identical across experiments. Littermates were used as controls with multiple litters (3–5) examined per experiment.

Results

IKZF1 and *IKZF2* mRNA expression levels are specifically downregulated in peripheral blood mononuclear cells in patients with schizophrenia

Since we have previously reported that mice full knockout for *Ikzf1* or *Ikzf2* could develop brain-related deficiencies [5, 29, 60, 61], we first aimed to assess *IKZF1* and *IKZF2* mRNA levels by RT-qPCR in different brain regions strongly implicated in the pathophysiology of schizophrenia, namely the hippocampus, dorsolateral prefrontal cortex (DLPFC), and putamen. We evaluated such mRNA levels in post-mortem brain samples from patients with schizophrenia and control patients (Suppl Table 1). We did not detect changes in *IKZF1* and *IKZF2*

mRNA levels in either, the hippocampus (Fig. 1a, b) or the DLPFC (Fig. 1c, d) or putamen (Fig. 1e, f) when comparing samples from schizophrenia patients with samples from control subjects. The same results were observed when protein levels were evaluated by western blot (Suppl. Figure 1). We next hypothesized that, since *IKZF1* and *IKZF2* in adult mammals are both more enriched in circulating immune (lymphocytes) cells than in neural tissues [44] (see also in *The Human Protein Atlas*), it would be conceivable that potential changes could be easier to be detected there rather than in the brain. Thus, we isolated peripheral blood mononuclear cells (PBMCs), which are mostly ~ 70–90% lymphocytes [86], from controls and patients with schizophrenia (Suppl Table 2). A descriptive evaluation of these PBMCs showed no differences in terms of cell density for either, neutrophils or

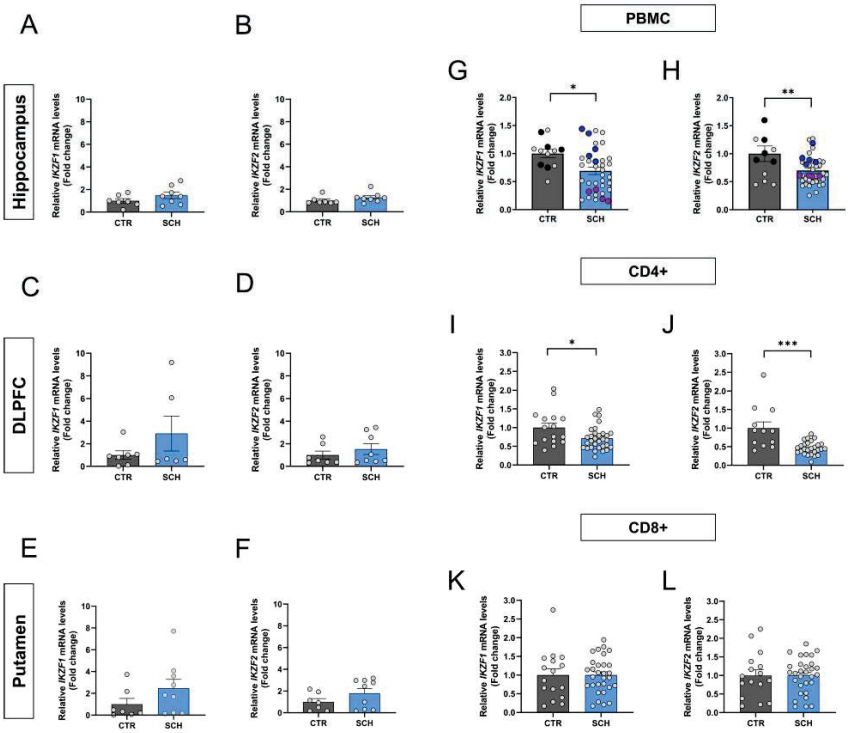

Fig. 1 *IKZF1* and *IKZF2* mRNA levels in the brain and circulating immune cells of patients with schizophrenia. Determination of *IKZF1* and *IKZF2* mRNA levels in different brain regions. Results from RT-qPCR of total *IKZF1* and *IKZF2* mRNA levels in different brain regions namely hippocampus (**a** and **b** respectively), dorso-lateral prefrontal cortex (DLPFC, **c** and **d** respectively) and putamen (**e** and **f** respectively) from patients with schizophrenia (SCH) or matched controls (CTR). Demographics of the samples are displayed in supplementary Table 1. Results from RT-qPCR of total (**g**) *IKZF1* and (**h**) *IKZF2* mRNA levels in peripheral blood mononuclear cells (PBMCs) isolated from patients with schizophrenia (SCH) or matched controls (CTR). Highlighted black, blue and violet dots are the samples selected for the subgroups used in Fig. 4 onwards (CTR, SCH^{Ik+He+} and SCH^{Ik-He-} groups respectively). (**i**) Results from RT-qPCR of total *IKZF1* and (**j**) *IKZF2* mRNA levels in CD4 + cells isolated from PBMCs in **i**-**j**. Results from RT-qPCR of total (**k**) *IKZF1* and (**l**) *IKZF2* mRNA levels in CD8 + cells isolated from PBMCs in **i**-**j**. Demographics of the samples are displayed in supplementary Table 2. Data are means ± SEM and they were analyzed using the two-tailed Student t-test. *$p < 0.05$, **$p < 0.01$ and ***$p < 0.001$ vs CTR

lymphocytes or monocytes when comparing control subjects with patients with schizophrenia (Suppl Table 3). We then extracted their mRNA and evaluated *IKZF1* and *IKZF2* mRNA levels. Interestingly, we detected that *IKZF1* (Fig. 1g) and *IKZF2* (Fig. 1h) were both significantly downregulated in PBMCs mRNA from patients with schizophrenia compared to matched controls. As we did for brain regions, we also confirmed these results at protein levels for IKZF1 but not for IKZF2 (Suppl. Figure 1 and Suppl. Table 4). We then looked at isolated CD4+and CD8+cells from the same PBMCs. We found that *IKZF1* (Fig. 1i) and *IKZF2* (Fig. 1j) mRNA levels were both downregulated in CD4+cells. In contrast, *IKZF1* (Fig. 1k) and *IKZF2* (Fig. 1l) mRNA levels were normal in CD8+cells. Next, to rule out the possibility of unspecific effects mediated by the medications on these changes we decided to sub-chronically treat wild type mice for 7 days with the two most common administered antipsychotics in our cohort of patients; paliperidone and clozapine. We found that *Ikzf1* and *Ikzf2* mRNA levels in mouse PBMCs were not affected by such treatments (Suppl Fig. 2). To further ensure this result we repeated the experiment with a more chronic treatment (28 days) focusing with the most employed antipsychotic in all our cohorts of patients, clozapine. Again, no changes in either *Ikzf1* or *Ikzf2* mRNA levels in mouse PBMCs were found (Suppl. Figure 2). Altogether, these results indicate that the double reduction of *IKZF1* and *IKZF2* mRNA levels in PBMCs is localized in CD4+cells. These alterations could play a role in the dysfunctions described for this cell type in the context of schizophrenia [15].

Mimicking the double *Ikzf1* and *Ikzf2* downregulation in mice results in a myriad of several schizophrenia-like disturbances

Although many different expressed genes (DEGs) and proteins (DEPs) have been identified in patients with schizophrenia, most of them have not been yet characterized or their role in the pathophysiology of the disease remain, at least, controversial [77, 83, 91]. Therefore, we aimed to characterize the relevance of this double reduction by mimicking it in mice. To do so we crossed heterozygous mice for *Ikzf1* ($Ik^{\pm}$:$He^{+/+}$, [61] with heterozygous mice for *Ikzf2* ($Ik^{+/+}$:$He^{\pm}$, [60]) to generate double mutant mice with a double reduction of both, *Ikzf1* and *Ikzf2* ($Ik^{\pm}$:$He^{\pm}$, Fig. 2a). Since both, adult (4–5 months of age) $Ik^{\pm}$:$He^{+/+}$ and $Ik^{+/+}$:$He^{\pm}$ mice displayed only some phenotypes compared to $Ik^{+/+}$:$He^{+/+}$ mice (Suppl. Figure 3), henceforth we focused on the $Ik^{+/+}$:$He^{+/+}$ and $Ik^{\pm}$:$He^{\pm}$ genotypes (a.k.a. Wild type mice and double mutant mice) only. First, the appearance and body weight (Suppl. Figure 4) were indistinguishable between the two groups, thus suggesting a normal health state in male and female $Ik^{\pm}$:$He^{\pm}$ mice. Then, to evaluate the potential schizophrenia-like phenotypes in our mutant mice, we performed a broad behavioral characterization aimed to evaluate positive, negative and cognitive symptomatology as previously established [70]. Regarding the positive-like phenotypes, we first observed that $Ik^{\pm}$:$He^{\pm}$ females (Fig. 2b) and $Ik^{\pm}$:$He^{\pm}$ males (Fig. 2c) displayed increased basal locomotion/agitation in the open field paradigm when compared with their matched $Ik^{+/+}$:$He^{+/+}$ controls. Furthermore, both, $Ik^{\pm}$:$He^{\pm}$ males (Fig. 2d) and females (Fig. 2e) showed an increased sensitivity to the D-Amphetamine in an open field arena. Regarding the negative-like phenotypes, we observed that in the three-chamber social interaction test there was a consistent alteration in sociability showed by both $Ik^{\pm}$:$He^{\pm}$ males (Fig. 2f) and females (Fig. 2g) compared with their matched controls. Finally, long-term declarative memory was also assessed by subjecting the groups of mice to the novel object recognition test (NORT). First, females $Ik^{\pm}$:$He^{\pm}$ were uncapable to recognize the new object with respect the old one when compared to $Ik^{+/+}$:$He^{+/+}$ controls (Fig. 2h). Similarly, $Ik^{+/+}$:$He^{+/+}$ males showed preference for the new object whereas $Ik^{\pm}$:$He^{\pm}$

(See figure on next page.)

Fig. 2 Generation and characterization of the $Ik^{\pm}$:$He^{\pm}$ double mutant mice. **a** Schematic representation of the adult mutant mice generated and used. $Ik^{\pm}$ and $He^{\pm}$ mice were crossed to generate the four genotypes; $Ik^{+/+}$:$He^{+/+}$, $Ik^{+/+}$:$He^{\pm}$, $Ik^{\pm}$:$He^{+/+}$ and $Ik^{\pm}$:$He^{\pm}$. Since the behavioral phenotype in $Ik^{+/+}$:$He^{\pm}$ and $Ik^{\pm}$:$He^{+/+}$ groups of mice were punctual compared to that in $Ik^{+/+}$:$He^{+/+}$ mice (Suppl. Figure 3), we focused on the controls $Ik^{+/+}$:$He^{+/+}$ and the double mutant $Ik^{\pm}$:$He^{\pm}$ mice. Basal locomotor activity was evaluated in the two groups of mice separated into (**b**) females (Genotype effect: $F_{(1, 495)} = 22{,}58$, $p < 0.0001$) and (**c**) males (Genotype effect: $F_{(1, 538)} = 9{,}518$, $p = 0.0021$) in a 15 min testing session of free exploration in an open field. Induced agitation and sensitivity to the psychostimulant D-amphetamine was measured in a 45 min testing session upon injection of 5 mg/Kg of D-amphetamine in (**d**) female (Genotype effect: $F_{(49, 1450)} = 20{,}37$, $p < 0.0001$) and (**e**) male (Genotype effect: $F_{(48, 1668)} = 21{,}28$, $p < 0.0001$) mice from both groups. Sociability was evaluated in the three-chamber social interaction test (TCSIT). Mice from the two groups were subjected to the TCSIT and data were depicted for (**f**) females (Social preference effect: $F_{(1, 6)} = 8{,}456$, $p = 0.0051$) and (**g**) males (Social preference effect: $F_{(1, 64)} = 19{,}36$, $p < 0.0001$). Recognition memory was evaluated in the novel object recognition test (NORT) 24 h after a training session. Mice from two groups were subjected to the NORT and data were depicted for (**h**) females (NORT preference effect: $F_{(1, 54)} = 5{,}415$, $p = 0.0237$) and (**i**) males (NORT preference effect: $F_{(1, 66)} = 18{,}35$, $p < 0.0001$). Data are means ± SEM and they were analyzed using the two-way ANOVA. *$p < 0.05$, ***$p < 0.001$ vs $Ik^{+/+}$:$He^{+/+}$ mice in **b**, **d** and **e**. In **f**, **g**, **h,** and **i** data were analyzed using the two-way ANOVA with Bonferroni's post hoc test; **$p < 0.01$ and ***$p < 0.001$ vs time exploring the stranger or the new object

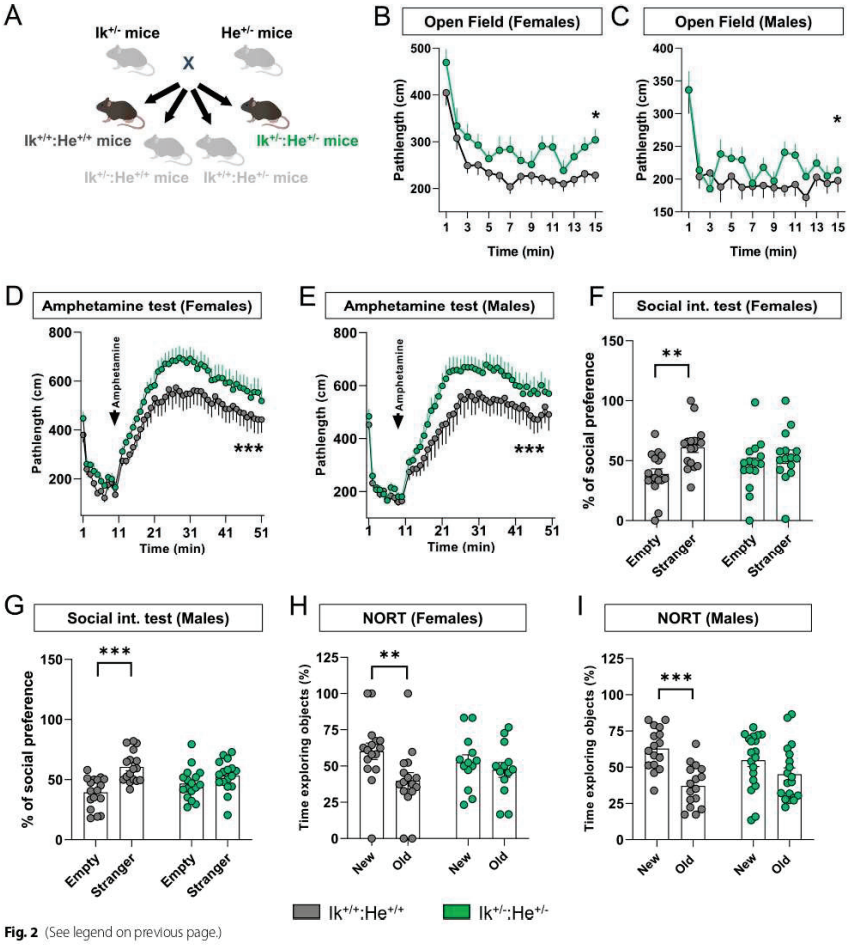

Fig. 2 (See legend on previous page.)

males did not (Fig. 2i), suggesting the presence of detectable cognitive deficits in both $Ik^{\pm}$:$He^{\pm}$ males and females.

To further assess associated schizophrenia-like phenotypes such as dendritic spine loss in several brain regions as described elsewhere in post-mortem samples from patients [30], we quantified spine density in hippocampal CA1 pyramidal neurons, in Medium Spiny Neurons (MSNs) of the dorsal striatum and in pyramidal neurons of the layer V in the medial pre-frontal cortex (mPFC) of $Ik^{+/+}$:$He^{+/+}$ and $Ik^{\pm}$:$He^{\pm}$ mice. First, we identified a significant reduction of dendritic spine density in the MSNs of both, $Ik^{\pm}$:$He^{\pm}$ males (Fig. 3a) and $Ik^{\pm}$:$He^{\pm}$ females (Fig. 3b) compared with their respective $Ik^{+/+}$:$He^{+/+}$ controls. In contrast, alterations in spine density of the

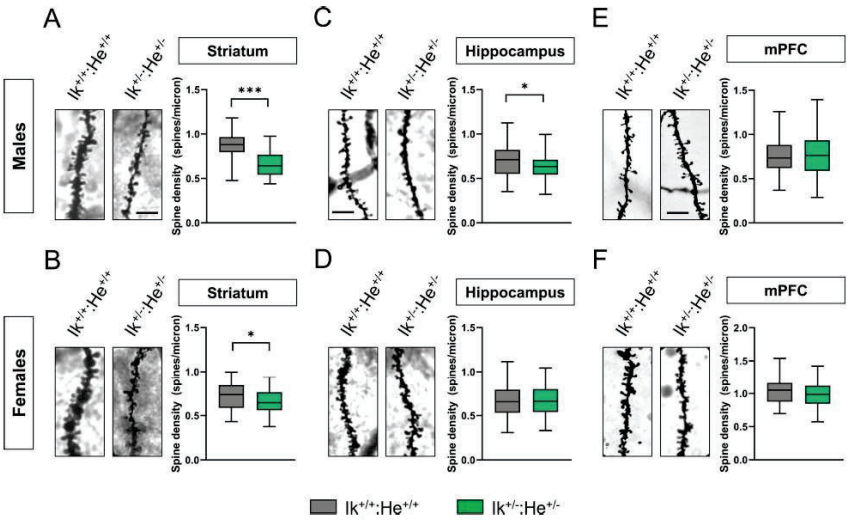

Fig. 3 Characterization of structural synaptic plasticity in the Ik±:He± mice. **a**, **b** Representative images (left panels) and quantification (right panels) of spine density in dendrites from medium spiny neurons (MSNs) of the dorsal striatum labeled with Golgi staining. Images were obtained in a bright-field microscope in adult (**a**) male and (**b**) female $Ik^{+/+}$:$He^{+/+}$ and Ik±:He± mice. Scale bar, 5 µm. **c**, **d** Representative images (left panels) and quantification (right panels) of spine density in secondary apical dendrites from pyramidal neurons of the hippocampal CA1 labeled with Golgi staining. Images were obtained in adult (**c**) male and (**d**) female $Ik^{+/+}$:$He^{+/+}$ and Ik±:He± mice. Scale bar, 5 µm. **e**, **f** Representative images (left panels) and quantification (right panels) of spine density in dendrites from pyramidal neurons of layer V in the frontal cortex labeled with Golgi staining. Images were obtained in adult (**e**) male and (**f**) female $Ik^{+/+}$:$He^{+/+}$ and Ik±:He± mice. Scale bar, 5 µm. Data are means ± SEM and they were analyzed using the two-tailed Student t-test. *$p < 0.05$, ***$p < 0.01$ vs $Ik^{+/+}$:$He^{+/+}$ mice. In **a**, n = 50–54 dendrites/genotype (from 7 mice/genotype). In **b**, n = 54–66 dendrites/genotype (from 7 mice/genotype). In **c**, n = 62–65 dendrites/genotype (from 7 mice/genotype). In **d**, n = 60–68 dendrites/genotype (from 7 mice/genotype). In **e**, n = 89–55 dendrites/genotype (from 7 mice/genotype). In **f**, n = 43–47 dendrites/genotype (from 7 mice/genotype). Scale bar in **a**, 5 µm

CA1 pyramidal cells was only observed in Ik±:He± males (Fig. 3c), but not in Ik±:He± females (Fig. 3d). Finally, regarding to spine density in pyramidal neurons of the mPFC, no changes were observed in any condition (Fig. 3e-f). In conclusion, our newly generated double Ik±:He± mutant mice mimic several features (behavioral and histological) in mice that are also observed in patients with schizophrenia and models.

IKZF1 and *IKZF2* mRNA levels in PBMC regulate the molecular profile of their secretome in patients with schizophrenia

Upon the observation that Ik±:He± mice mimicked schizophrenia-like features, we next aimed to study which is the underlying molecular bridge between the circulating immune system and central nervous system that induces these phenotypes. We hypothesized that altered levels of *IKZF1* and *IKZF2* could impair the transcriptional activity of secreted molecules (secretome) by these circulating immune cells such as cytokines, chemokines, growth factors and other molecules. These impaired secretomes could, in turn, impair neural networks involved with the development of schizophrenia. To address these questions, we opted to use a more translational approach (Suppl. Figure 5a). From patients with schizophrenia studied in Fig. 1g, h, we generated two sub-groups of patients; the first with normal levels of *IKZF1* and *IKZF2* ($SCH^{Ik+:He+}$ group) in PBMC and the second with a double down-regulation of both, *IKZF1* (> 40%) and *IKZF2* (> 40%) in PBMC ($SCH^{Ik-:He-}$ group) compared to control (CTR) patients (Suppl. Figure 5b-c). All groups were matched in terms of number (n = 4–5/group), age (Suppl. Figure 5d), sex, and the PANSS general score (Suppl. Table 5). Also, the number of circulating lymphocytes, neutrophils, platelets, and monocytes were indistinguishable between $SCH^{Ik+:He+}$

and $SCH^{Ik-:He-}$ groups (Suppl. Figure 5e-h). Additionally, based on this criterion of > 40% of reduction, it is worth mentioning the proportion of patients for each condition (Suppl Fig. 2); 6 of 35 patients displayed a double downregulation of both, *IKZF1* and *IKZF2* mRNA levels. 6 of 35 patients showed reduction only in *IKZF1* mRNA levels. Finally, 4 of 35 patients showed reduction only in *IKFZ2* mRNA levels. We then obtained and cultured PBMC from all selected subjects and obtained their supernatants (a.k.a. secretomes; Suppl. Figure 5a) containing the secretome of such cells. We first performed a protein expression screening in these secretomes using a mass spectrometry approach. A principal component analysis (PCA) revealed that the two groups of patients with schizophrenia, $SCH^{Ik+:He+}$ and $SCH^{Ik-:He-}$, were different with respect to the CTR group (Fig. 4a). However, PCA indicated that $SCH^{Ik+:He+}$ and $SCH^{Ik-:He-}$ groups were slightly different between each other (Fig. 4a). Venn diagram representation indicated that 17 and 13 proteins were specifically altered in the $SCH^{Ik+:He+}$ and $SCH^{Ik-:He-}$ groups respectively compared to the CTR group. Also, only changes in 9 proteins were observed to be shared by both $SCH^{Ik+:He+}$ and $SCH^{Ik-:He-}$ groups when compared to CTR subjects (Fig. 4b, c). Proteins changing in this same sense included TUBA8, PFN1, TUBB, and DEFA1 (Fig. 4c, d). In contrast, specific altered proteins in the $SCH^{Ik+:He+}$ group comprised ACTB, COTL1, FLNA, and PRTN3. On the other hand specific altered proteins in the $SCH^{Ik-:He-}$ group involved ACTR3, SH3BGRL, LUZP1, CFL1, CCL5 (RANTES), C1RL and RHOC. To further complement these results from mass spectrometry we also performed a Luminex-based screen of several cytokines and chemokines in the supernatants from the three groups. Results indicated that some proteins were downregulated only in the $SCH^{Ik-:He-}$ group compared to the CTR group such as GMSF and IL-4 (Fig. 4f) or MIP1A (Fig. 4g). Oppositely, CXCL10 was upregulated only in the $SCH^{Ik-:He-}$ group compared to the CTR group (Fig. 4h). Finally, G-CSF and IL-10 were indistinguishable between groups (Fig. 4i). In summary, secretomes from $SCH^{Ik+:He+}$ and $SCH^{Ik-:He-}$ groups were significantly different between them and also compared to CTR secretomes.

IKZF1 and *IKZF2* mRNA levels in PBMCs from patients with schizophrenia modulate neuronal structural plasticity in primary mouse hippocampal neurons

We observed that the secretomes of both, $SCH^{Ik+:He+}$ and $SCH^{Ik-:He-}$ groups, displayed different molecular profiles between each other and also compared to CTR subjects. Next, we aimed to evaluate whether such changes could exert some impact on neuronal functions. To do so, we first set up the safety of using such secretomes from patients in mouse neuronal cultures. We first pooled the secretomes for each group. All three pools (CTR, $SCH^{Ik+:He+}$, and $SCH^{Ik-:He-}$) had a protein concentration of 2,064 µg/µl. We then added two different dilutions, 1:1 and 1:10 from the CTR secretome pool to mouse hippocampal primary neurons at day in vitro 7 (DIV7, Fig. 5a). We also used two additional controls in this experiment, namely a naïve hippocampal primary culture without any treatment and a culture only treated with PBMC media X-Vivo (as a vehicle). We observed that 24 h after treatments, the dilution 1:1 induced neuronal degeneration per se whereas the dilution 1:10 did not affect neuronal morphology as compared with the two other controls (Fig. 5b and d). Thus, we used the 1:10 concentration henceforth for the ulterior experiments using the three secretome pools due to its safety for neuronal viability. Next, we evaluated the effect of these

(See figure on next page.)

Fig. 4 Molecular profile of PBMC secretomes from stratified patients with schizophrenia. From our results in Fig. 1g, h, we selected and stratified patients as follows: Patients with schizophrenia but with unaltered mRNA levels in PBMC of both, *IKZF1* and *IKZF2* respect to CTR subjects ($SCH^{Ik+:He+}$ group; n = 5) and patients with a double reduction (≥ 40%) of *IKZF1* and *IKZF2* mRNA levels in PBMCs ($SCH^{Ik-:He-}$ group; n = 4). These stratified patients were matched to control subjects with normal *IKZF1* and *IKZF2* mRNA levels (CTR group; n = 5). From these stratified patients, supernatants of cultured PBMC were collected and subjected to Mass Spectrometry. **a** Principal component analysis (PCA) for proteomics data from PBMC supernatants. The PCA plot represents the 14 subjects from the three subgroups (CTR in grey, $SCH^{Ik+:He+}$ in blue, and $SCH^{Ik-:He-}$ in violet) that indicates subtle proteomics profile differences between such supernatants. **b** Venn diagram showing the total number of proteins differentially expressed or DEPs in each of the SCH subgroups. The common DEPs (9) comparing both groups ($SCH^{Ik+:He+}$ and $SCH^{Ik-:He-}$) with respect to the CTR group, the specific DEPs (17, blue) comparing $SCH^{Ik+:He+}$ with CTR, and the specific DEPs (13, violet) comparing $SCH^{Ik-:He-}$ with CTR are depicted. **c** Table showing the specific down-regulated (green) and up-regulated (red) DEPs in each comparison extracted from **b**. **d** Volcano plot depicting DEPs when comparing supernatants from the CTR and $SCH^{Ik+:He+}$ groups. Dashed horizontal line shows the p values cutoff, and the two vertical dashed lines indicate down/up regulated proteins. Red points indicate significantly DEPs. Dark points indicate non-significant DEPs. **e** Volcano plot depicting DEPs when comparing supernatants from the CTR and $SCH^{Ik-:He-}$ groups as we did for **d**. Analyte array measured by a Luminex assay depicting the levels in pg/ml of (**f**) FGF, IL-1B, IL-13, IL-12, IL-17, GMCSF, IL-15, HGF, VEGF, IFNg, IFNa, TNFa, IL-17, IL-2R, MIG, IL-4 and (**g**) MIP1A, MIP1B, IL-1RA, IL-8 and (**h**) Eotaxin, CXCL10 and (**i**) G-CSF and IL-10. The analytes are depicted in four (**f**–**i**) different graphs due to their huge variability in terms of the range of concentrations. Data are means ± SEM and they were analyzed using the one-way ANOVA and the Dunnet's post hoc in **f**–**i**. *p < 0.05 vs CTR group

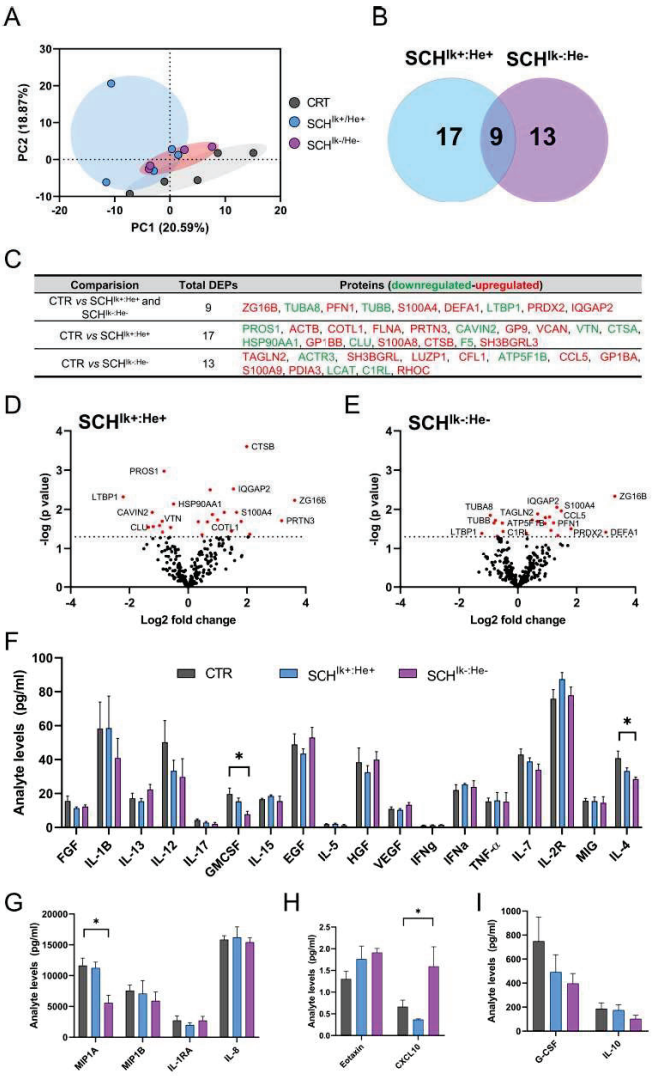

Comparision	Total DEPs	Proteins (downregulated-upregulated)
CTR *vs* SCH$^{lk+:He+}$ and SCH$^{lk-:He-}$	9	ZG16B, TUBA8, PFN1, TUBB, S100A4, DEFA1, LTBP1, PRDX2, IQGAP2
CTR *vs* SCH$^{lk+:He+}$	17	PROS1, ACTB, COTL1, FLNA, PRTN3, CAVIN2, GP9, VCAN, VTN, CTSA, HSP90AA1, GP1BB, CLU, S100A8, CTSB, F5, SH3BGRL3
CTR *vs* SCH$^{lk-:He-}$	13	TAGLN2, ACTR3, SH3BGRL, LUZP1, CFL1, ATP5F1B, CCL5, GP1BA, S100A9, PDIA3, LCAT, C1RL, RHOC

Fig. 4 (See legend on previous page.)

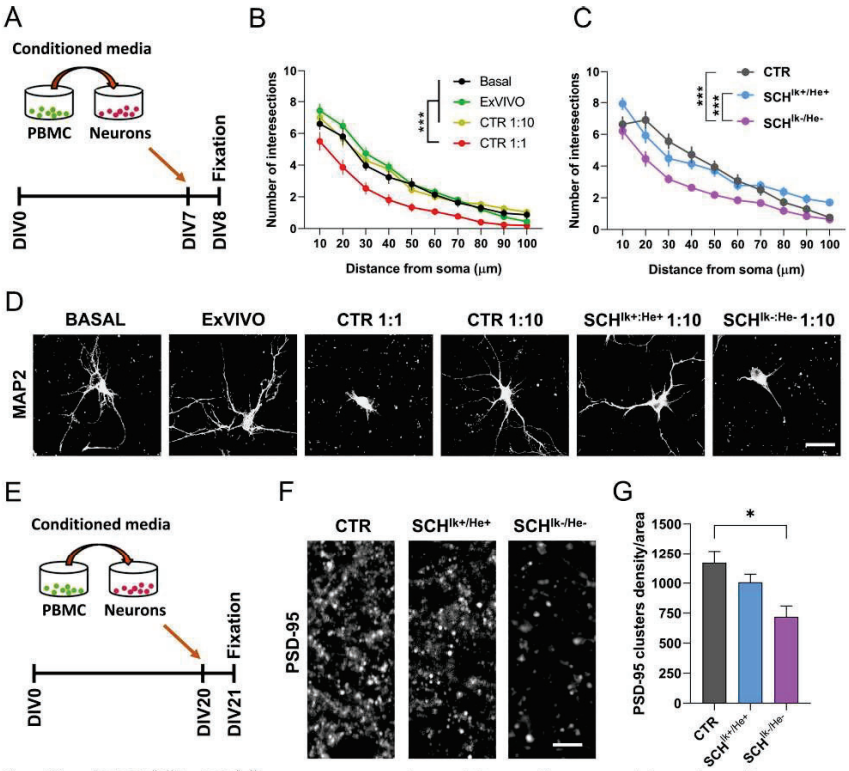

Fig. 5 Effects of CTR, SCH$^{Ik+:He+}$ and SCH$^{Ik-:He-}$ supernatants in neuronal structural plasticity. **a** The experimental design is depicted. Supernatants (a.k.a. conditioned media) from cultured PBMC were added to primary hippocampal neurons at DIV7 and 24 h later, their dendritic morphology was assessed by using the Sholl analysis. **b** and **d** Different concentrations (1:1 and 1:10 supernatants from the CTR pool) and controls (X-Vivo media and naïve primary neurons) were employed (Group effect: $F_{(3, 1166)} = 147{,}1$, $p < 0.0001$). The 1:10 concentration was selected as the one to be used from **c** onwards because of its safety when compared with Basal and X-Vivo control conditions (**b** and **d**). **c** and **d** Effects of CTR, SCH$^{Ik+:He+}$ and SCH$^{Ik-:He-}$ supernatants on neuronal branching in primary hippocampal neurons using the selected (1:10) dose (Group effect: $F_{(2, 890)} = 40{,}97$, $p < 0.0001$). In **b**-**d** MAP2 staining was employed. **e** The experimental design to evaluate synaptic changes is depicted. Supernatants (conditioned media) from cultured PBMC were added to primary hippocampal neurons at DIV20 and 24 h later (**f**) the density of PSD-95 positive puncta per area was assessed in the three groups. **g** Quantification of PSD-95-positive puncta/area from **f** ($F_{(2, 9)} = 6{,}905$, $p = 0.0152$). Data are mean ± SEM. In **b** (n = 30 neurons/group) and **c** (n = 27–33 neurons/group) the two-way ANOVA was applied and Tukey's multiple comparisons test was used as a post hoc. In **g** (n = 4 cultures/group) one-way ANOVA was applied, and Dunnett's multiple comparisons test was used as a post hoc. Scale bar in **d**, 30 μm. Scale bar in **f**, 5 μm

secretomes in neuronal branching by treating neurons at DIV7. While CTR and SCH$^{Ik+:He+}$ secretomes did not induce significant changes on neuronal morphology, the SCH$^{Ik-:He-}$ secretome induced a substantial reduction in the neuronal dendritic complexity (Fig. 5c, d). To further deepen on these effects, we then repeated the experiment but adding the secretomes from the three groups (CTR, SCH$^{Ik+:He+}$ and SCH$^{Ik-:He-}$) to primary hippocampal neuronal cultures at DIV20 (Fig. 5e). Then, 24 h later we quantified the number of PSD-95-positive clusters

(as an excitatory post-synaptic marker) in these cultures. We observed a significant reduction of PSD-95-positive clusters in primary cultures treated with the $SCH^{Ik-:He-}$ secretome but not in primary cultures treated with the $SCH^{Ik+:He+}$ secretomes compared with the CTR group (Fig. 5f, g). We concluded that the different molecular profile displayed by the $SCH^{Ik-:He-}$ PBMC secretome was probably the responsible for these specific effects on structural synaptic plasticity.

The PBMCs secretome of patients with schizophrenia modulate neuronal dynamics: role of *IKZF1* and *IKZF2*

Our previous results indicated that PBMC secretomes from patients with schizophrenia could play a role in structural synaptic plasticity, probably via modulation of synaptic components. To further explore this possibility, we benefit from a new approach called Modular Neuronal Network (MoNNets, [72]) designed to identify neural patterns (based on GcAMP6s-dependent calcium activity) in primary neurons resembling those observed in schizophrenia (Fig. 6a). Thus, MoNNets were generated, transduced with GcAMP6s and treated with CTR, $SCH^{Ik+:He+}$ and $SCH^{Ik-:He-}$ PBMC secretomes at DIV7, DIV14 and DIV21 (Fig. 6b). At DIV28 GcAMP6s-dependent calcium activity was recorded for 5 min in these MoNNets (Fig. 6b-c). Our results showed clear changes in activity in both groups of MoNNets treated with $SCH^{Ik+:He+}$ and $SCH^{Ik-:He-}$ secretomes compared to MoNNets treated with CTR secretome (Fig. 6d). These visual changes in activity in the raster plot were translated to a strong reduction in the average pairwise correlation, a measure of neuronal synchrony [72], in those MoNNets treated with $SCH^{Ik+:He+}$, or $SCH^{Ik-:He-}$ secretomes (Fig. 6e), which mimics what is observed in schizophrenia [97]. Interestingly, we also observed a moderate decrease in activity rate in MoNNets treated with the $SCH^{Ik+:He+}$ secretome, an effect even more robust when MoNNets were treated with the $SCH^{Ik-:He-}$ secretome (Fig. 6f). Finally, only MoNNets treated with the $SCH^{Ik-:He-}$ secretome suffered a reduction in the mean peak duration compared with the CTR condition (Fig. 6g). We concluded that, although both secretomes, the $SCH^{Ik+:He+}$ and the $SCH^{Ik-:He-}$, induced a reduction in MoNNets functional parameters (mainly synchrony) the $SCH^{Ik-:He-}$ was the one that triggered the most severe and global alterations.

IKZF1 and *IKZF2* mRNA levels in PBMCs from patients with schizophrenia modulate schizophrenia-like phenotypes with a specific impact on cognitive function

Our observations in primary neuronal cultures and in MoNNets suggested that neural networks could be influenced by an aberrant molecular profile in the PBMC secretome from patients with schizophrenia. Also, our results indicated that *IKZF1* and *IKZF2* mRNA levels modulate the severity of such impairments. Additionally, since in the double heterozygous $Ik^{\pm}$:$He^{\pm}$ mice (Figs. 2–3) both genes, *Ikzf1* and *Ikzf2*, have been genetically deleted (one allele) also in the brain, it cannot be excluded that this general deletion might have a direct effect on the synaptic plasticity in the hippocampus or other brain regions at any stage of their lifespans. Thus, we aimed to employ a different strategy to address all these points. We used a mouse line that allows a permanent tagging of neurons activated by experience or relevant stimuli: the double mutant mice expressing Egr1-CreERT2 and R26RCE (Fig. 7a) [7, 54, 80]. We permanently and intraventricularly treated these transgenic mice with pooled secretomes from CTR, $SCH^{Ik+:He+}$, and the $SCH^{Ik-:He-}$ subjects using mini-osmotic pumps for 25 days (Fig. 7b, c) at a delivery ratio of 2,5 µl/day to the lateral ventricle. We performed a broad behavioral characterization of these mice assessing the three dimensions of schizophrenia-like phenotypes [70] from day 5 to day 19 of the treatment. On day 20, mice were treated with 4-HT to induce recombination and permanent labeling of activated neural engrams due to the treatments with the secretomes. This design avoided the unspecific labeling of neural engrams due

(See figure on next page.)

Fig. 6 Impact of CTR, $SCH^{Ik+:He+}$, and $SCH^{Ik-:He-}$ supernatants in neuronal activity and synchrony. **a** Schematic overview of MoNNet approach (Left panel). Primary hippocampal cells were infected with AAV7m8.Syn.GCaMP6s.WPRE.SV40, and plated on a PDMS mold for self-organized assembly of MoNNet (a.k.a. neurospheres, Middle panel). Tuj-1 labeled MoNNets (right panel). Scale bar 250 µm. **b** The experimental design is depicted. Pooled supernatants (a.k.a. conditioned media) from each group (CTR, $SCH^{Ik+:He+}$, and $SCH^{Ik-:He-}$) of cultured PBMC were added to primary hippocampal neurons at DIV7, DIV14, and DIV21. At DIV28, their GcAMP6s-based activity was assessed. **c** Maxima projection showing GcAMP6s activity and its subsequent filtering (Gaussian > binarized > and final mask). System-wide cellular-resolution Ca^{2+} imaging was performed at 25 Hz. We analyzed the activity of each neurosphere and compared it with the rest of neurospheres. **d** Representative raster plots from DIV28 recordings in all three groups (CTR, $SCH^{Ik+:He+}$, and $SCH^{Ik-:He-}$). From the binarized signal the following parameters were computed: **e** average pairwise Pearson correlation of MoNNets (one-way ANOVA; $F_{(2, 80)} = 18{,}31$, $p < 0.0001$), (**f**) mean activity rate (one-way ANOVA: $F_{(2, 81)} = 10{,}22$, $p < 0.0001$) and (**g**) mean peak duration (one-way ANOVA: $F_{(2, 108)} = 3{,}893$, $p = 0.023$). In **e**–**g** one-way ANOVA was applied and the Dunnett's multiple comparisons test was used as a post hoc. *$p < 0.05$ and ***$p < 0.001$ vs CTR

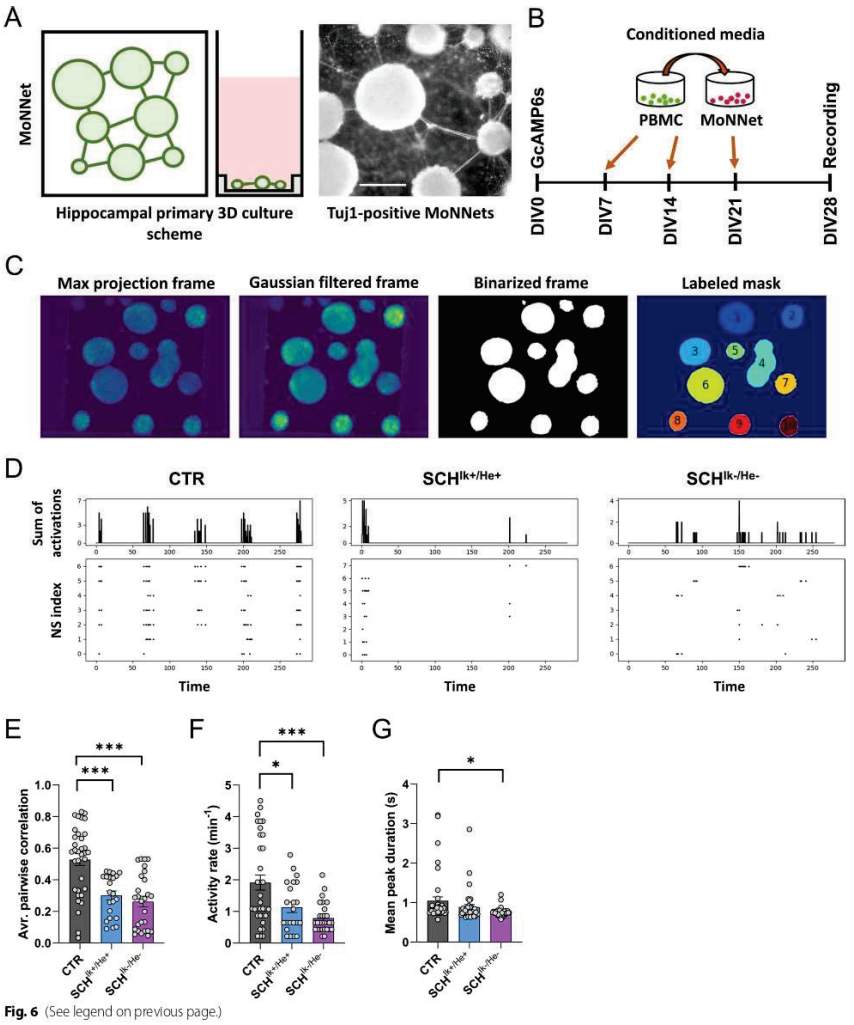

Fig. 6 (See legend on previous page.)

to the extensive behavioral characterization. Finally, brains were processed for histological studies on day 25 of treatment (Fig. 7c). Regarding the results, first, treated mice showed normal body weight (Fig. 7d) and appearance (data not shown) at the end of the study, suggesting that this treatment did not induce sickness-like states. Concerning the behavioral characterization, both $SCH^{Ik+:He+}$ and the $SCH^{Ik-:He-}$ groups showed

no changes in agitation in the open field when compared with the CTR group (Fig. 7e). In contrast, both $SCH^{Ik+:He+}$ and the $SCH^{Ik-:He-}$ groups showed a clear and equal reduction in sociability compared to the CTR group in the three-chamber social interaction test (Fig. 7f). Finally, in the novel object recognition test, the $SCH^{Ik-:He-}$ group but not the $SCH^{Ik+:He+}$ group displayed specific alterations in novel object recognition memory in comparison with the CTR group (Fig. 7g). We then mapped the activation of potential aberrant engrams due to these secretomes in fixed brains from mice of the three groups. Since cognitive alterations seemed to be highly specific to the mice treated with the $SCH^{Ik-:He-}$ secretome, we quantified the number of Egr1-dependent activated neural cells (GFP-positive) in the hippocampal CA1 (Fig. 7h) as suggested to be a core hippocampal sub-region in the physiopathology of schizophrenia [102]. We observed that, although both groups, $SCH^{Ik+:He+}$ and the $SCH^{Ik-:He-}$ displayed an apparent aberrant activation of the Egr1-dependent activated ensembles, only the mice treated with the $SCH^{Ik-:He-}$ secretome suffered a significant increase (Fig. 7h). Interestingly, increases on Egr1 levels have been previously reported in the auditory cortex [43] and in peripheral tissues of schizophrenia patients [11]. We then observed that altered structural synaptic plasticity was only detected in our mice treated with the $SCH^{Ik-:He-}$ secretome. In particular, spine density in the CA1 pyramidal neurons (Fig. 7i) but not in medium spiny neurons of the dorsal striatum (Suppl. Figure 6a) was increased in mice treated with the secretome from $SCH^{Ik-:He-}$ patients compared to the CTR group. These differences, although a trend was observed, were not significant in mice treated with the $SCH^{Ik+:He+}$ secretome. Such aberrantly increased number of Egr1-dependent activated ensembles correlated with a decrease in the number of parvalbumin-positive interneurons mostly observed in the $SCH^{Ik-:He-}$ group, but also in the $SCH^{Ik+:He+}$ group when compared with the CTR group (Fig. 7j). This reduction in parvalbumin interneurons could mediate the Egr1-dependent hyperactivation of CA1 pyramidal cells due to a lack of their inhibition [98]. Finally, because human secretomes have the potential to activate neuroinflammatory processes, we evaluated several morphometric parameters in astroglia and microglia within the same CA1 *stratum radiatum* of the mice. While human secretomes from schizophrenia patients did not alter the overall numbers of hippocampal astrocytes and microglia, they did induce morphometric changes including increased cellular solidity and increased GFAP staining (Suppl. Figure 7). Notably, the $SCH^{Ik-:He-}$ group exhibited more pronounced alterations compared to those observed in the $SCH^{Ik+:He+}$ group (Suppl. Figure 7). These findings suggest that astrocytes and microglia respond to these pathological secretomes. Overall, these results indicate that human secretomes from patients induce schizophrenia-like phenotypes in mice and that *IKZF1* and *IKZF2* levels in PBMC modulate the secretome conformation in a way that specifically impacts hippocampal activated neural ensembles likely through a reduction in parvalbumin interneurons function and ultimately impairing structural plasticity and associated cognitive skills.

(See figure on next page.)

Fig. 7 Schizophrenia-like phenotypes induced by the $SCH^{Ik+:He+}$ and $SCH^{Ik-:He-}$ supernatants when intraventricularly administered in mice. **a** Schematic representation of adult double-heterozygous-mutant Egr1-CreERT2 × R26RCE GFP mice used to label activated neural engrams upon treatment with supernatants. **b** Schematic representation of the intraventricular infusion of CTR, $SCH^{Ik+:He+}$, and $SCH^{Ik-:He-}$ supernatants. Mini-osmotic pumps infused 0,11 µl/h of supernatants at a concentration of 0,206 µg/µl of protein. **c** The experimental design is depicted. After surgical intervention, mice recovered for 4–5 days and then they were subjected to a broad behavioral characterization. At day 19, this behavioral characterization terminated and at day 20 mice were treated with 50 mg/kg of 4-hydroxytamoxifen (4-HT) to induce recombination and labeling (GFP) of activated neural ensembles. At day 25, mice were processed to evaluate neural engrams formation and labeling and to evaluate spine density in the hippocampal CA1. **d** Body weight was monitored on the day of sacrifice. **e** Basal locomotion/agitation was evaluated by using the open field in the three groups of mice (CTR, $SCH^{Ik+:He+}$, and $SCH^{Ik-:He-}$). In the same groups of mice, **f** sociability was measured using the three-chamber social interaction test/TCSIT (Group effect: $F_{(1, 102)} = 18{,}43$, $p < 0.0001$). **g** The same groups of mice were also subjected to the Novel Object Recognition Test/NORT (Group effect: $F_{(1, 106)} = 229{,}3$, $p < 0.0001$) where memory was tested 24 h after a training session. **h** Double fluorescent staining (DAPI in blue, GFP in green) in hippocampal CA1 from mice treated with one of each supernatant (CTR, $SCH^{Ik+:He+}$, and $SCH^{Ik-:He-}$). Graph (right-down) shows quantification of Egr1-dependent activated CA1 pyramidal cells (estimated number of GFP-positive cells/area of 500 µm^2, Group effect: $F_{(2, 22)} = 3{,}926$, $p = 0.034$). Scale bar, 300 µm. **i** Representative images and quantification (right-down panel) of spine density in secondary apical dendrites of the CA1 pyramidal neurons labeled with Golgi staining (n = 72–121 dendrites/group from 7 mice/group). Images were obtained in a bright-field microscope in the three groups of mice treated with CTR, $SCH^{Ik+:He+}$, and $SCH^{Ik-:He-}$ supernatants (Scale bar, 5 µm). **j** Double fluorescent staining (left panels, DAPI in blue, parvalbumin in red) in hippocampal CA1 from the same mice as in **h**. Graph (right) shows quantification of parvalbumin-positive interneurons in the CA1 (estimated number of parvalbumin-positive cells/area of 500 µm^2, Group effect: $F_{(2, 27)} = 33{,}86$, $p < 0.001$). Scale bar, 300 µm. Data are means ± SEM. In **d**, **h** and **I** one-way ANOVA was applied, and Tukey's multiple comparisons test was used as a post hoc. In **e**, **f**, and **g**, two-way ANOVA was applied, and Bonferroni's multiple comparisons test was used as a post hoc. *p < 0.05, vs CTR; ***p < 0.001, vs Empty or vs Old Object. CTR (n = 18); $SCH^{Ik+:He+}$ (n = 20); $SCH^{Ik-:He-}$ (n = 18). In **j** n = 10 in all groups

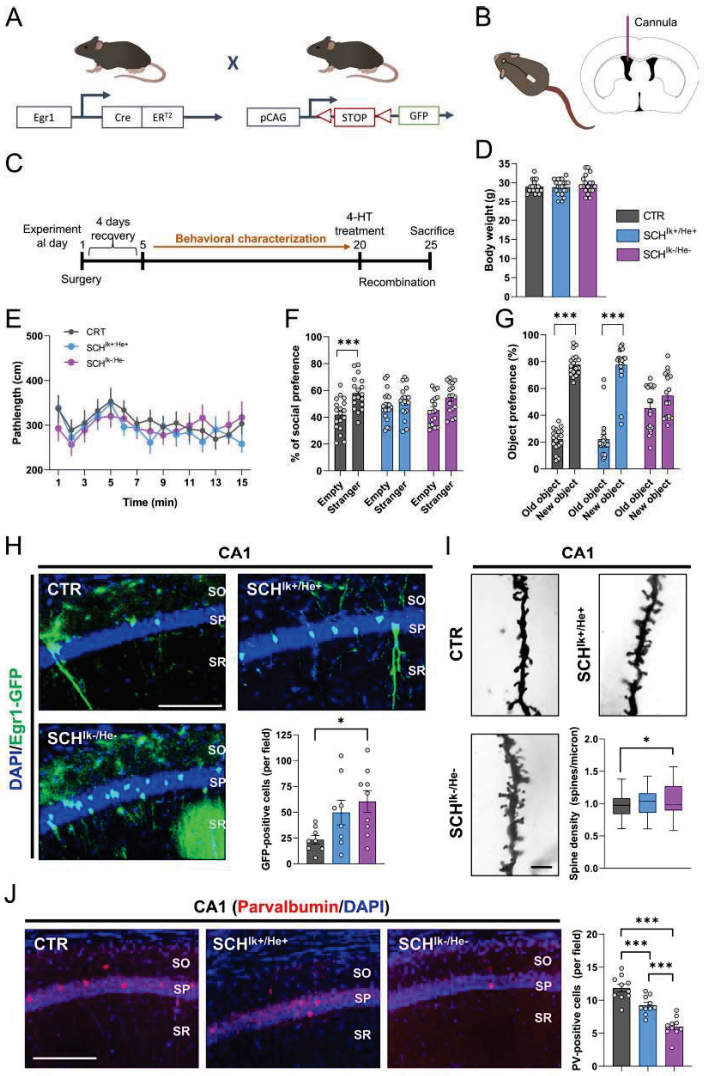

Fig. 7 (See legend on previous page.)

Discussion

In the present work, we show for the first time that both, *IKZF1* and *IKZF2*, are downregulated specifically in immune circulating cells, but not in the brains of patients with schizophrenia. We also observed in mice that a double *Ikzf1* and *Ikzf2* heterozygosis induced schizophrenia-like symptoms in the three dimensions (positive–negative-cognitive) of symptomatology. Exploring the secretome of these circulating immune cells, we observed that high-order cognitive functions are the most susceptible to be affected by the double *IKZF1* and *IKZF2* reduction. Specific and acutely hyperactivated hippocampal engrams, reduced number of parvalbumin interneurons and altered neuronal synchrony were associated with these phenotypes placing molecules such as IL-4 and CXCL10 as potential core signals mediating them.

First, we show that *IKZF1* and *IKZF2* mRNA levels are specifically downregulated in CD4+cells but not in CD8+cells. Such specific double down-regulation could induce changes on numbers of CD4+cells and, in turn, to provoke differences on CD4+/CD8+ratios [16, 90]. Also, a double down-regulation of *IKZF1* and *IKZF2* mRNA levels in CD4 cells could provoke an imbalance between T helper cell type 1 (Th1) and type 2 (Th2) which has been associated with schizophrenia [107]. Interestingly, this imbalance has also been associated to a decrease on IL-4 expression in Th2 cells in schizophrenia patients [68] which is in line with our results on IL-4 levels. This imbalance reinforces the idea about the production of aberrant secretomes by these immune cells (which might be explained, at least in part, by this *IKZF1-IKZF2* double downregulation) and that it would correlate with more severe symptoms and poor therapy outcomes [85] as we observed in our mouse models.

Regarding the impaired secretomes, previous reports have already addressed the molecular profile of PBMCs in patients with schizophrenia [26, 103]. Despite these previous studies and as far as we know, we show for the first time a double down-regulation of *IKZF1* and *IKZF2* mRNA levels. Interestingly, these and other studies have found that WNT signaling is a core pathway affected in these cells and that there is a correlation between WNT signaling and cognitive impairment in schizophrenia [103]. In this line, the WNT family strongly regulates the *IKZF* genes in immune cells [104, 105], being a potential source of this double affectation of *IKZF1* and *IKZF2*. Regarding the cause of this double down-regulation, a plausible possibility is that alterations in *IKZF1* and *IKZF2* mRNA levels are indirectly provoked by other processes, such as immune and/or environmental challenges, as it has been proposed for the disorder [20]. Also, it is noteworthy that secretomes specifically from CD4+, the cell type suffering of the double *IKZF1-IKZF2* downregulation, could be the major source of phenotypes observed in our in vitro and in vivo models. This could be a very promising future line of research.

To demonstrate the relevance of this double downregulation as a potential underlying molecular mechanism explaining the pathophysiology of schizophrenia, we have used both, a genetic and a translational model. In the genetic model, we have observed a highly schizophrenia-like phenotype (with phenotypes in all three dimensions, positive–negative-cognitive) in mice in terms of behavior and neuronal changes. However, although our data support the idea that an *Ikzf1-Ikzf2* double reduction is necessary to display a full three-dimensional schizophrenia-like phenotype, it is worth mentioning that heterozygous $Ik^{\pm}$:$He^{+/+}$ and $Ik^{+/+}$:$He^{\pm}$ mice also display some specific schizophrenia-like phenotypes. This indicates that the observed phenotypes induced by the double reduction are partly synergistic but also partly additive. Besides, in this mouse model, we have explored potential sex differences which were worse in males than in females. Regarding these sex differences, it has been previously reported that in human beings, males and females show differences in terms of pathology and prevalence being worse in males [50]. Concerning cognitive dysfunction, male patients perform worse on measures of executive function, verbal memory and information processing speed than female patients [63] which is in line with our results in our mouse models. Thus, since there are also sex-dependent immune alterations in schizophrenia patients [39, 46, 108], probably the double *IKZF1-IKZF2* double downregulation affects more males than females in terms of some behavioral and neuropathological phenotypes. Regarding the translational model in which we used PBMC secretomes from patients, we concluded that an aberrant immune secretome with a double reduction of *IKZF1* and *IKZF2* from schizophrenia patients is enough to induce negative-like and cognitive-like symptoms. These results are in line with the idea that immune alterations are highly associated with such types of symptoms [32, 58, 76]. Noteworthy, the fact we did not observe differences in agitation in such translational mouse models could be because PBMC' secretomes came from patients under treatment with antipsychotics. Although this statement is just speculative, it is in line with the large evidence stating that antipsychotics target principally positive symptoms whereas negative and cognitive symptoms remain largely unaffected [58]. Shall our hypothesis be true it would reinforce the fact of using agitation in mice as a positive-like phenotype/parameter.

Since our human PBMC secretomes induced so many schizophrenia-like phenotypes in terms of structural synaptic plasticity [66], neuronal synchrony [72], and

schizophrenia-like behaviors [70], we then explored their molecular profile. We first found that levels of RANTES (CCL5), an upregulated cytokine in schizophrenia [19, 22], depended on *IKZF1* and *IKZF2* levels. However, the role of RANTES in schizophrenia is largely unknown. Another promising core molecule is IL-4. IL-4 rises as an interesting molecule coordinating the specific neuronal and cognitive symptoms observed in the induced SCH $^{Ik-/He-}$ in vitro and in vivo models. IL-4 is an attractive candidate since its levels are regulated by both, *IKZF1* and *IKZF2* in circulating immune cells [34, 53, 71, 106]. Second, IL-4 regulates hippocampal-dependent memory [8, 24], and deficiency of its receptor, IL-4R, increased network activity [36] similar to what we observed in the hippocampus of our in vivo induced SCH $^{Ik-/He-}$ mouse model. In the context of schizophrenia, IL-4 has been shown to be significantly decreased in chronic schizophrenia-spectrum [35]. Furthermore, some single nucleotide polymorphisms (SNPs) in IL-4 have been related to the disorder [84]. Additional studies have also shown that IL-4 levels are not related to positive psychotic symptoms [21] but, instead, they correlate with negative symptoms [88]. A third plausible candidate molecule underlying the defects observed in our SCH $^{Ik-/He-}$ mice is CXCL10 (IP10). Supporting this idea previous studies have observed enhanced neural activity accompanied by increased firing rate and excitability and alterations in synaptic network activity after chronic treatment with CXCL10 [13, 67]. These changes were sustained by reduced levels of GABA receptors, augmented levels of glutamate receptors and increased sensitivity of NMDA receptors [13, 67]. All these findings go in line with; the enhanced hippocampal Egr1-dependent activated ensembles in our SCH $^{Ik-/He-}$ mice, the basal hyperexcitability normally seen in schizophrenia patients and the reduced synchronized neural activity present in schizophrenia patients and in our SCH $^{Ik-/He-}$ in vitro MoNNet model. In this line, previous works [33, 89] have already proposed the hyperexcitability of the hippocampus as a core feature contributing to the three categories of symptoms seen in schizophrenia (Suppl Fig. 7a-c). We propose that our $Ik^{\pm}$:$He^{\pm}$ and SCH $^{Ik-/He-}$ models provide key underlying molecular clues, including IL-4 and CXCL10, supporting this model. As it has been reported in patients with schizophrenia [48], we also observed a reduction of parvalbumin-positive interneurons (PV+) in the hippocampal CA1 in our SCH $^{Ik-/He-}$ model. This reduction could be provoked by aberrant levels of IL-4 and CXCL10 from circulating PBMCs with decreased *IKZF1* and *IKZF2* levels. This altered secretome would induce a reduction in PV+cells number and/or function since it has been shown that IL-4 reduces the risk of hyperexcitation [36] and CXCL10 over-expression reduces the levels of GAD65/67 [13] often accompanied of a ferroptosis processes [51]. The reduced function of PV+interneurons would provoke an hyperactivation of pyramidal neurons in the CA1 according to this circuit [98] and ultimately inducing the deficits in structural plasticity and impairments in cognitive function. However, although we provide evidences for this model, we cannot rule out other components allocated in these aberrant secretomes such as small molecules (RNAs) or extracellular vesicles [3, 42]. Future studies could address such possibilities. Finally, although the main effect mediated by the immune secretomes from schizophrenia patients was observed in the parvalbumin interneurons, we also observed some morphological changes in astroglia and microglia suggesting that such changes could also play a role in the synaptic plasticity alterations and associated cognitive and social deficits observed in our intraventricularly injected mice. Indeed, aberrant activation of microglia [59, 100] or astroglia [93] could alter the function of parvalbumin interneurons in the hippocampus.

Our study has important limitations, particularly regarding human samples. First, we focused on mRNA levels in human PBMCs to evaluate *IKZF1* and *IKZF2* expression; however, the protein-level results for *IKZF2* did not fully corroborate the mRNA findings. It is well-established that discrepancies often arise when comparing mRNA and protein levels [49, 73], potentially due to greater variability in protein expression [56]. Therefore, the role of *IKZF2* in our findings should be interpreted with caution. Still with human samples, there is a discrepancy in the number of recruited controls (CTR) and patients with schizophrenia (SCH) in the same experiments using PBMCs, which could introduce bias. Also, patients for the secretome experiments were matched in terms of *IKZF1-IKZF2* mRNA levels but medication was not considered. Finally, we cannot rule out possible effects on neural *IKZF1* and *IKZF2* levels during earlier stages of the disorder since postmortem samples were collected from very old individuals, whereas PBMCs were collected from younger patients. In those same postmortem samples, there were other potential limitations such as differences in the postmortem time intervals and sex discrepancies in terms of proportions in each group. Therefore, although our results are supported by our studies using in vivo and in vitro models, the human data should be interpreted with caution.

Finally, our work fits with the idea that neural identities and probably function are both strongly modulated by peripheral signals and influences [55, 92] as we summarized (Suppl Fig. 8). One of them could be a double down-regulation of *IKZF1* and *IKZF2* mRNA levels in immune cells. In this sense, our results also have potential clinical implications. First, they could contribute to

a better definition and stratification of patients based on their blood mRNA levels of *IKZF1* and *IKZF2*, which could be related to the severity of some symptoms. Additionally, it is tempting to speculate that different types of therapeutic strategies (drugs, RNA probes, Adeno-Associated Virus/AAVs) aimed at increasing mRNA levels of these transcription factors in circulating PBMCs could have positive therapeutic effects in patients with schizophrenia. Therefore, we strongly believe that future research should progress in the study of peripheral signals capable to play a role in the development of symptoms in schizophrenia and, probably, in other psychiatric affectations.

Supplementary Information

The online version contains supplementary material available at https://doi.org/10.1186/s12974-024-03320-3.

Supplementary material 1.

Acknowledgements
We thank María Calvo from the Advanced Microscopy Service (Centres Científics i Tecnològics Universitat de Barcelona) for her help in the acquisition, analysis, and interpretation of the confocal images.

Author contribution
Ivan Ballasch and Laura López-Molina: writing—review & editing, writing—original draft, visualization, validation, methodology, investigation, formal analysis, data curation, conceptualization. Sara Borràs-Pernas, Irene Rodríguez-Navarro, Anna Sancho-Balsells and Marcos Galán-Ganga: methodology, investigation, formal analysis. Angeles Rabadan, Wanqi Chen, Carla Hernández, Miqueu Alfonso, Natalia Egri, Francesca Flotta, Wang Maoyu and Carlota Pastó-Pellicer: investigation, formal analysis. Carlota Dobaño and Ruth Aguilar: resources, formal analysis. Enrique Santamaría and Joaquín Irigoyen: investigation and data curation. Daniel del Toro: resources, writing—review & editing. Jordi Alberch and Manel Juan: supervision, resources. Josep-Maria Canals and Belén Arranz: writing—review & editing, supervision, resources, conceptualization. Albert Giralt: writing—review & editing, visualization, validation, supervision, resources, project administration, funding acquisition, conceptualization.

Funding
This work was supported by grants from Ministerio de Ciencia e Innovación/AEI/https://doi.org/10.13039/501100011033/ and "FEDER" to A.G.: PID2021-122258OB-I00 and to J.A.: PID2020-119386RB-100 and from Instituto de Salud Carlos III (ISCIII): PI17/00246 to B.A. Our technician Ana López, was supported by a María de Maeztu Unit of Excellence (Institute of Neurosciences, University of Barcelona, CEX2021-001159-M, Ministry of Science and Innovation). The project that gave rise to these results received the support of a fellowship from "la Caixa" Foundation (ID 100010434). The fellowship code is LCF/BQ/DR21/11880016 to M.G.-G.

Data availability
No datasets were generated or analysed during the current study.

Declarations

Ethics approval and consent to participate
All the procedures for the obtention of post-mortem samples followed the ethical guidelines of the Declaration of Helsinki and local ethical committees (Universitat de Barcelona: IRB00003099; Fundació CEIC Sant Joan de Déu: BTN-PSSJD). The blood samples of this study (NoPI17/00246, PI Belen Arranz) was recruited in the Outpatient clinic located in Cornellà, Barcelona, Spain (Parc Sanitari Sant Joan de Deu). All animal procedures were approved by local committees [Universitat de Barcelona, CEEA (136/19); Generalitat de Catalunya (DAAM 10786) following the European Communities Council Directive (86/609/EU).

Competing interests
The authors declare no competing interests.

Received: 21 June 2024 Accepted: 6 December 2024
Published online: 18 December 2024

References

1. Aguilar R, Campo JJ, Chicuecue S, Cisteró P, Català A, Luis L, Ubillos I, Galatas B, Aide P, Guinovart C, Moncunill G, Dobaño C. Changing plasma cytokine, chemokine and growth factor profiles upon differing malaria transmission intensities. Malar J. 2019;18:406. https://doi.org/10.1186/s12936-019-3038-x.
2. Ahmad SF, Nadeem A, Ansari MA, Bakheet SA, AL-Ayadhi LY, Attia SM. Downregulation in Helios transcription factor signaling is associated with immune dysfunction in blood leukocytes of autistic children. Prog Neuro-Psychopharmacol Biol Psychiatry. 2018;85:98–104. https://doi.org/10.1016/j.pnpbp.2018.04.011.
3. Alberro A, Iparraguirre L, Fernandes A, Otaegui D. Extracellular vesicles in blood: sources, effects, and applications. Int J Mol Sci. 2021;22:8163. https://doi.org/10.3390/ijms22158163.
4. Alhosaini K, Ansari MA, Nadeem A, Attia SM, Bakheet SA, Al-Ayadhi LY, Mahmood HM, Al-Mazroua HA, Ahmad SF. Dysregulation of Ki-67 expression in T cells of children with autism spectrum disorder. Children. 2021;8:116. https://doi.org/10.3390/children8020116.
5. Alsiö JM, Tarchini B, Cayouette M, Livesey FJ. Ikaros promotes early-born neuronal fates in the cerebral cortex. Proc Natl Acad Sci. 2013. https://doi.org/10.1073/pnas.1215707110.
6. Ballasch I, García-García E, Vila C, Pérez-González A, Sancho-Balsells A, Fernández J, Soto D, Puigdellívol M, Gasull X, Alberch J, Rodríguez MJ, Canals JM, Giralt A. Ikzf1 as a novel regulator of microglial homeostasis in inflammation and neurodegeneration. Brain Behav Immun. 2023;109:144–61. https://doi.org/10.1016/j.bbi.2023.01.016.
7. Brito V, Montalban E, Sancho-Balsells A, Pupak A, Flotta F, Masana M, Ginés S, Alberch J, Martin C, Girault J-A, Giralt A. Hippocampal Egr1-dependent neuronal ensembles negatively regulate motor learning. J Neurosci. 2022;42:5346–60. https://doi.org/10.1523/JNEUROSCI.2258-21.2022.
8. Brombacher TM, Berkiks I, Pillay S, Scibiorek M, Moses BO, Brombacher F. IL-4R alpha deficiency influences hippocampal-BDNF signaling pathway to impair reference memory. Sci Rep. 2020;10:16506. https://doi.org/10.1038/s41598-020-73574-3.
9. Busse S, Busse M, Schiltz K, Bielau H, Gos T, Brisch R, Mawrin C, Schmitt A, Jordan W, Müller UJ, Bernstein H-G, Bogerts B, Steiner J. Different distribution patterns of lymphocytes and microglia in the hippocampus of patients with residual versus paranoid schizophrenia: further evidence for disease course-related immune alterations? Brain Behav Immun. 2012;26:1273–9. https://doi.org/10.1016/j.bbi.2012.08.005.
10. Cai Q, Dierich A, Oulad-Abdelghani M, Chan S, Kastner P. Helios deficiency has minimal impact on T cell development and function. J Immunol. 2009;183:2303–11. https://doi.org/10.4049/jimmunol.0901407.
11. Cattane N, Minelli A, Milanesi E, Maj C, Bignotti S, Bortolomasi M, Chiavetto LB, Gennarelli M. Altered gene expression in schizophrenia: findings from transcriptional signatures in fibroblasts and blood. PLoS ONE. 2015;10: e0116686. https://doi.org/10.1371/journal.pone.0116686.
12. Chaudhry IB, Husain MO, Khoso AB, Husain MI, Buch MH, Kiran T, Fu B, Bassett P, Qurashi I, ur Rahman R, Baig S, Kazmi A, Corsi-Zuelli F, Haddad PM, Deakin B, Husain N. A randomised clinical trial of methotrexate points to possible efficacy and adaptive immune dysfunction in psychosis. Transl Psychiatry. 2020;10:415. https://doi.org/10.1038/s41398-020-01095-8.
13. Cho J, Nelson TE, Bajova H, Gruol DL. Chronic CXCL10 alters neuronal properties in rat hippocampal culture. J Neuroimmunol. 2009;207:92–100. https://doi.org/10.1016/j.jneuroim.2008.12.007.

14. Consortium A.W.G. of T.P.G. Meta-analysis of GWAS of over 16,000 individuals with autism spectrum disorder highlights a novel locus at 10q24.32 and a significant overlap with schizophrenia. Mol Autism. 2017;8:21. https://doi.org/10.1186/s13229-017-0137-9.
15. Corsi-Zuelli F, Deakin B, de Lima MHF, Qureshi O, Barnes NM, Upthegrove R, Louzada-Junior P, Del-Ben CM. T regulatory cells as a potential therapeutic target in psychosis? Current challenges and future perspectives. Brain Behav Immun Heal. 2021;17:100330. https://doi.org/10.1016/j.bbih.2021.100330.
16. Craddock RM, Lockstone HE, Rider DA, Wayland MT, Harris LJW, McKenna PJ, Bahn S. Altered T-cell function in schizophrenia: a cellular model to investigate molecular disease mechanisms. PLoS ONE. 2007;2:e692. https://doi.org/10.1371/journal.pone.0000692.
17. Davis J, Eyre H, Jacka FN, Dodd S, Dean O, McEwen S, Debnath M, McGrath J, Maes M, Amminger P, McGorry PD, Pantelis C, Berk M. A review of vulnerability and risks for schizophrenia: beyond the two hit hypothesis. Neurosci Biobehav Rev. 2016;65:185–94. https://doi.org/10.1016/j.neubiorev.2016.03.017.
18. de Pins B, Cifuentes-Díaz C, Thamila Farah A, López-Molina L, Montalban E, Sancho-Balsells A, López A, Ginés S, Delgado-García JM, Alberch J, Gruart A, Girault J-A, Giralt A. Conditional BDNF delivery from astrocytes rescues memory deficits, spine density and synaptic properties in the 5xFAD mouse model of Alzheimer disease. J Neurosci. 2019. https://doi.org/10.1523/JNEUROSCI.2121-18.2019.
19. Domenici E, Willé DR, Tozzi F, Prokopenko I, Miller S, McKeown A, Brittain C, Rujescu D, Giegling I, Turck CW, Holsboer F, Bullmore ET, Middleton L, Merlo-Pich E, Alexander RC, Muglia P. Plasma protein biomarkers for depression and schizophrenia by multi analyte profiling of case-control collections. PLoS ONE. 2010;5: e9166. https://doi.org/10.1371/journal.pone.0009166.
20. Ermakov EA, Melamud MM, Buneva VN, Ivanova SA. Immune system abnormalities in schizophrenia: an integrative view and translational perspectives. Front Psychiatry. 2022. https://doi.org/10.3389/fpsyt.2022.880568.
21. Fila-Danilow A, Kucia K, Kowalczyk M, Owczarek A, Paul-Samojedny M, Borkowska P, Suchanek R, Kowalski J. Association study of interleukin-4 polymorphisms with paranoid schizophrenia in the Polish population: a critical approach. Mol Biol Rep. 2012;39:7941–7. https://doi.org/10.1007/s11033-012-1639-3.
22. Frydecka D, Krzystek-Korpacka M, Lubeiro A, Stramecki F, Stańczykiewicz B, Beszłej JA, Piotrowski P, Kotowicz K, Szewczuk-Bogusławska M, Pawlak-Adamska E, Misiak B. Profiling inflammatory signatures of schizophrenia: a cross-sectional and meta-analysis study. Brain Behav Immun. 2018;71:28–36. https://doi.org/10.1016/j.bbi.2018.05.002.
23. Furney SJ, Simmons A, Breen G, Pedroso I, Lunnon K, Proitsi P, Hodges A, Powell J, Wahlund L-O, Kloszewska I, Mecocci P, Soininen H, Tsolaki M, Vellas B, Spenger C, Lathrop M, Shen L, Kim S, Saykin AJ, Weiner MW, Lovestone S. Genome-wide association with MRI atrophy measures as a quantitative trait locus for Alzheimer's disease. Mol Psychiatry. 2011;16:1130–8. https://doi.org/10.1038/mp.2010.123.
24. Gadani SP, Cronk JC, Norris GT, Kipnis J. IL-4 in the brain: a cytokine to remember. J Immunol. 2012;189:4213–9. https://doi.org/10.4049/jimmunol.1202246.
25. Gao Y, Li J, Cai G, Wang Y, Yang W, Li Y, Zhao X, Li R, Gao Y, Tuo W, Baldwin RL, Li C, Fang L, Liu GE. Single-cell transcriptomic and chromatin accessibility analyses of dairy cattle peripheral blood mononuclear cells and their responses to lipopolysaccharide. BMC Genom. 2022;23:338. https://doi.org/10.1186/s12864-022-08562-0.
26. Gardiner EJ, Cairns MJ, Liu B, Beveridge NJ, Carr V, Kelly B, Scott RJ, Tooney PA. Gene expression analysis reveals schizophrenia-associated dysregulation of immune pathways in peripheral blood mononuclear cells. J Psychiatr Res. 2013;47:425–37. https://doi.org/10.1016/j.jpsychires.2012.11.007.
27. Georgopoulos K, Winandy S, Avitahl N. The role of the ikaros gene in lymphocyte development and homeostasis. Annu Rev Immunol. 1997;15:155–76. https://doi.org/10.1146/annurev.immunol.15.1.155.
28. Giralt A, Brito V, Chevy Q, Simonnet C, Otsu Y, Cifuentes-Díaz C, de Pins B, Coura R, Alberch J, Ginés S, Poncer J-C, Girault J-A. Pyk2 modulates hippocampal excitatory synapses and contributes to cognitive deficits in a Huntington's disease model. Nat Commun. 2017;8:15592. https://doi.org/10.1038/ncomms15592.
29. Giralt A, Brito V, Pardo M, Rubio SE, Marion-Poll L, Martín-Ibáñez R, Zamora-Moratalla A, Bosch C, Ballesteros JJ, Blasco E, García-Torralba A, Pascual M, Pumarola M, Alberch J, Ginés S, Martín ED, Segovia J, Soriano E, Canals JM. Helios modulates the maturation of a CA1 neuronal subpopulation required for spatial memory formation. Exp Neurol. 2020;323:113095. https://doi.org/10.1016/j.expneurol.2019.113095.
30. Glausier JR, Lewis DA. Dendritic spine pathology in schizophrenia. Neuroscience. 2013;251:90–107. https://doi.org/10.1016/j.neuroscience.2012.04.044.
31. Goldsmith DR, Haroon E, Miller AH, Strauss GP, Buckley PF, Miller BJ. TNF-α and IL-6 are associated with the deficit syndrome and negative symptoms in patients with chronic schizophrenia. Schizophr Res. 2018;199:281–4. https://doi.org/10.1016/j.schres.2018.02.048.
32. Goldsmith DR, Rapaport MH. Inflammation and negative symptoms of schizophrenia: implications for reward processing and motivational deficits. Front Psychiatry. 2020. https://doi.org/10.3389/fpsyt.2020.00046.
33. Grace AA, Gomes FV. The circuitry of dopamine system regulation and its disruption in schizophrenia: insights into treatment and prevention. Schizophr Bull. 2019;45:148–57. https://doi.org/10.1093/schbul/sbx199.
34. Gregory GD. Mast cell IL-4 expression is regulated by Ikaros and influences encephalitogenic Th1 responses in EAE. J Clin Invest. 2006;116:1327–36. https://doi.org/10.1172/JCI27227.
35. Halstead S, Siskind D, Amft M, Wagner E, Yakimov V, Shih-Jung Liu Z, Walder K, Warren N. Alteration patterns of peripheral concentrations of cytokines and associated inflammatory proteins in acute and chronic stages of schizophrenia: a systematic review and network meta-analysis. Lancet Psychiatry. 2023;10:260–71. https://doi.org/10.1016/S2215-0366(23)00025-1.
36. Hanuscheck N, Thalman C, Domingues M, Schmaul S, Muthuraman M, Hetsch F, Ecker M, Endle H, Oshaghi M, Martino G, Kuhlmann T, Bozek K, van Beers T, Bittner S, von Engelhardt J, Vogt J, Vogelaar CF, Zipp F. Interleukin-4 receptor signaling modulates neuronal network activity. J Exp Med. 2022. https://doi.org/10.1084/jem.20211887.
37. Harding BN, Aguilar R, Espinosa A, Castaño-Vinyals G, Papantoniou K, Navarrete JM, Such Faro P, Torrejón A, Dobaño C, Moncunill G, Kogevinas M. Disruption of cellular immune response among male rotating night shift workers in Spain– The HORMONIT study. Front Immunol. 2022. https://doi.org/10.3389/fimmu.2022.776917.
38. Harrison PJ. Neuropathology of schizophrenia. Psychiatry. 2008;7:421–4. https://doi.org/10.1016/j.mppsy.2008.07.013.
39. He J, Wei Y, Li J, Tang Y, Liu J, He Z, Zhou R, He X, Ren H, Liao Y, Gu L, Yuan N, Chen X, Tang J. Sex differences in the association of treatment-resistant schizophrenia and serum interleukin-6 levels. BMC Psychiatry. 2023;23:470. https://doi.org/10.1186/s12888-023-04952-0.
40. Hornann J, Osburg T, Ohlei O, Dobricic V, Deecke L, Bos I, Vandenberghe R, Gabel S, Scheltens P, Teunissen CE, Engelborghs S, Frisoni G, Blin O, Richardson JC, Bordet R, Lleó A, Alcolea D, Popp J, Clark C, Peyratout G, Martinez-Lage P, Tainta M, Dobson RJB, Legido-Quigley C, Sleegers K, Van Broeckhoven C, Wittig M, Franke A, Lill CM, Blennow K, Zetterberg H, Lovestone S, Streffer J, ten Kate M, Vos SJB, Barkhof F, Visser PJ, Bertram L. Genome-wide association study of Alzheimer's disease brain imaging biomarkers and neuropsychological phenotypes in the European medical information framework for Alzheimer's disease multimodal biomarker discovery dataset. Front Aging Neurosci. 2022. https://doi.org/10.3389/fnagi.2022.840651.
41. Houthuys E, Movahedi K, De Baetselier P, Van Ginderachter JA, Brouckaert P. A method for the isolation and purification of mouse peripheral blood monocytes. J Immunol Methods. 2010;359:1–10. https://doi.org/10.1016/j.jim.2010.04.004.
42. Hunter MP, Ismail N, Zhang X, Aguda BD, Lee EJ, Yu L, Xiao T, Schafer J, Lee M-LT, Schmittgen TD, Nana-Sinkam SP, Jarjoura D, Marsh CB. Detection of microRNA expression in human peripheral blood microvesicles. PLoS ONE. 2008;3: e3694. https://doi.org/10.1371/journal.pone.0003694.
43. Iwakura Y, Kawahara-Miki R, Kida S, Sotoyama H, Gabdulkhaev R, Takahashi H, Kunii Y, Hino M, Nagaoka A, Izumi R, Shishido R, Someya T, Yabe H, Kakita A, Nawa H. Elevation of EGR1/zif268, a neural activity marker, in the auditory cortex of patients with schizophrenia and its animal

model. Neurochem Res. 2022;47:2715–27. https://doi.org/10.1007/s11064-022-03599-9.
44. John LB, Ward AC. The ikaros gene family: transcriptional regulators of hematopoiesis and immunity. Mol Immunol. 2011;48:1272–8. https://doi.org/10.1016/j.molimm.2011.03.006.
45. Johnsen E, Fathian F, Kroken RA, Steen VM, Jørgensen HA, Gjestad R, Løberg E-M. The serum level of C-reactive protein (CRP) is associated with cognitive performance in acute phase psychosis. BMC Psychiatry. 2016;16:60. https://doi.org/10.1186/s12888-016-0769-x.
46. Kamitaki N, Sekar A, Handsaker RE, de Rivera H, Tooley K, Morris DL, Taylor KE, Whelan CW, Tombleson P, Loohuis LMO, Boehnke M, Kimberly RP, Kaufman KM, Harley JB, Langefeld CD, Seidman CE, Pato MT, Pato CN, Ophoff RA, Graham RR, Criswell LA, Vyse TJ, McCarroll SA. Complement genes contribute sex-biased vulnerability in diverse disorders. Nature. 2020;582:577–81. https://doi.org/10.1038/s41586-020-2277-x.
47. Kleiveland CR. Peripheral blood mononuclear cells. In: The impact of food bioactives on health. Cham: Springer International Publishing; 2015. p. 161–7. https://doi.org/10.1007/978-3-319-16104-4_15.
48. Konradi C, Yang CK, Zimmerman EI, Lohmann KM, Gresch P, Pantazopoulos H, Berretta S, Heckers S. Hippocampal interneurons are abnormal in schizophrenia. Schizophr Res. 2011;131:165–73. https://doi.org/10.1016/j.schres.2011.06.007.
49. Li J, Han S, Li H, Udeshi ND, Svinkina T, Mani DR, Xu C, Guajardo R, Xie Q, Li T, Luginbuhl DJ, Wu B, McLaughlin CN, Xie A, Kaewsapsak P, Quake SR, Carr SA, Ting AY, Luo L. Cell-surface proteomic profiling in the fly brain uncovers wiring regulators. Cell. 2020;180:373-386.e15. https://doi.org/10.1016/j.cell.2019.12.029.
50. Li X, Zhou W, Yi Z. A glimpse of gender differences in schizophrenia. Gen psychiatry. 2022;35: e100823. https://doi.org/10.1136/gpsych-2022-100823.
51. Liang P, Zhang X, Zhang Y, Wu Y, Song Y, Wang X, Chen T, Liu W, Peng B, Yin J, He F, Fan Y, Han S, He X. Neurotoxic A1 astrocytes promote neuronal ferroptosis via CXCL10/CXCR3 axis in epilepsy. Free Radic Biol Med. 2023;195:329–42. https://doi.org/10.1016/j.freeradbiomed.2023.01.002.
52. Liemburg EJ, Nolte IM, Klein HC, Knegtering H. Relation of inflammatory markers with symptoms of psychotic disorders: a large cohort study. Prog Neuro-Psychopharmacol Biol Psychiatry. 2018;86:89–94. https://doi.org/10.1016/j.pnpbp.2018.04.006.
53. Long Y, Xia C, Xu L, Liu C, Fan C, Bao H, Zhao X, Liu C. The imbalance of circulating follicular helper T cells and follicular regulatory T cells is associated with disease activity in patients with ulcerative colitis. Front Immunol. 2020. https://doi.org/10.3389/fimmu.2020.00104.
54. Longueville S, Nakamura Y, Brami-Cherrier K, Coura R, Hervé D, Girault J. Long-lasting tagging of neurons activated by seizures or cocaine administration in Egr1-CreER T2 transgenic mice. Eur J Neurosci. 2021;53:1450–72. https://doi.org/10.1111/ejn.15060.
55. López M, Tovar S, Vázquez MJ, Williams LM, Diéguez C. Peripheral tissue–brain interactions in the regulation of food intake. Proc Nutr Soc. 2007;66:131–55. https://doi.org/10.1017/S0029665107005368.
56. Luo J, Li L, Niu M, Kong D, Jiang Y, Poudel S, Shieh AW, Cheng L, Giase G, Grennan K, White KP, Chen C, Wang SH, Pinto D, Wang Y, Liu C, Peng J, Wang X. Genetic regulation of human brain proteome reveals proteins implicated in psychiatric disorders. Mol Psychiatry. 2024;29:3330–43. https://doi.org/10.1038/s41380-024-02576-8.
57. MacDowell KS, Munarriz-Cuezva E, Caso JR, Madrigal JLM, Zabala A, Meana JJ, García-Bueno B, Leza JC. Paliperidone reverts Toll-like receptor 3 signaling pathway activation and cognitive deficits in a maternal immune activation mouse model of schizophrenia. Neuropharmacology. 2017;116:196–207. https://doi.org/10.1016/j.neuropharm.2016.12.025.
58. Malashenkova IK, Ushakov VL, Zakharova NV, Krynskiy SA, Ogurtsov DP, Hailov NA, Chekulaeva EI, Ratushnyy AY, Kartashov SI, Kostyuk GP, Didkovsky NA. Neuro-immune aspects of schizophrenia with severe negative symptoms: new diagnostic markers of disease phenotype. Sovrem Tehnol Med. 2021. https://doi.org/10.17691/stm2021.13.6.03.
59. Mao M, Zhou Z, Sun M, Wang C, Sun J. The dysfunction of parvalbumin interneurons mediated by microglia contributes to cognitive impairment induced by lipopolysaccharide challenge. Neurosci Lett. 2021;762:136133. https://doi.org/10.1016/j.neulet.2021.136133.
60. Martín-Ibáñez R, Pardo M, Giralt A, Miguez A, Guardia I, Marion-Poll L, Herranz C, Esgleas M, Barriga GG-D, Edel MJ, Vicario-Abejón C, Alberch J, Girault J-A, Chan S, Kastner P, Canals JM. Helios expression coordinates the development of a subset of striatopallidal medium spiny neurons. Development. 2017. https://doi.org/10.1242/dev.138248.
61. Martín-Ibáñez R, Crespo E, Urbán N, Sergent-Tanguy S, Herranz C, Jaumot M, Valiente M, Long JE, Pineda JR, Andreu C, Rubenstein JLR, Marín Ó, Georgopoulos K, Mengod G, Fariñas I, Bachs O, Alberch J, Canals JM. Ikaros-1 couples cell cycle arrest of late striatal precursors with neurogenesis of enkephalinergic neurons. J Comp Neurol. 2010;518:329–51. https://doi.org/10.1002/cne.22215.
62. McGrath J, Saha S, Chant D, Welham J. Schizophrenia: a concise overview of incidence, prevalence, and mortality. Epidemiol Rev. 2008;30:67–76. https://doi.org/10.1093/epirev/mxn001.
63. Mendrek A, Mancini-Marie A. Sex/gender differences in the brain and cognition in schizophrenia. Neurosci Biobehav Rev. 2016;67:57–78. https://doi.org/10.1016/j.neubiorev.2015.10.013.
64. Molnár A, Georgopoulos K. The Ikaros gene encodes a family of functionally diverse zinc finger DNA-binding proteins. Mol Cell Biol. 1994;14:8292–303. https://doi.org/10.1128/MCB.14.12.8292.
65. Momtazmanesh S, Zare-Shahabadi A, Rezaei N. Cytokine alterations in schizophrenia: an updated review. Front Psychiatry. 2019. https://doi.org/10.3389/fpsyt.2019.00892.
66. Moyer CE, Shelton MA, Sweet RA. Dendritic spine alterations in schizophrenia. Neurosci Lett. 2015;601:46–53. https://doi.org/10.1016/j.neulet.2014.11.042.
67. Nelson TE, Gruol DL. The chemokine CXCL10 modulates excitatory activity and intracellular calcium signaling in cultured hippocampal neurons. J Neuroimmunol. 2004;156:74–87. https://doi.org/10.1016/j.jneuroim.2004.07.009.
68. O'Brien SM, Scully P, Dinan TG. Increased tumor necrosis factor-alpha concentrations with interleukin-4 concentrations in exacerbations of schizophrenia. Psychiatry Res. 2008;160:256–62. https://doi.org/10.1016/j.psychres.2007.11.014.
69. Potkin SG, Guffanti G, Lakatos A, Turner JA, Kruggel F, Fallon JH, Saykin AJ, Orro A, Lupoli S, Salvi E, Weiner M, Macciardi F. Hippocampal atrophy as a quantitative trait in a genome-wide association study identifying novel susceptibility genes for Alzheimer's disease. PLoS ONE. 2009;4:e6501. https://doi.org/10.1371/journal.pone.0006501.
70. Powell CM, Miyakawa T. Schizophrenia-relevant behavioral testing in rodent models: a uniquely human disorder? Biol Psychiatry. 2006;59:1198–207. https://doi.org/10.1016/j.biopsych.2006.05.008.
71. Quirion MR, Gregory GD, Umetsu SE, Winandy S, Brown MA. Cutting edge: ikaros is a regulator of Th2 cell differentiation. J Immunol. 2009;182:741–5. https://doi.org/10.4049/jimmunol.182.2.741.
72. Rabadan MA, De La Cruz ED, Rao SB, Chen Y, Gong C, Crabtree G, Xu B, Markx S, Gogos JA, Yuste R, Tomer R. An in vitro model of neuronal ensembles. Nat Commun. 2022;13:3340. https://doi.org/10.1038/s41467-022-31073-1.
73. Reimegård J, Tarbier M, Danielsson M, Schuster J, Baskaran S, Panagiotou S, Dahl N, Friedländer MR, Gallant CJ. A combined approach for single-cell mRNA and intracellular protein expression analysis. Commun Biol. 2021;4:624. https://doi.org/10.1038/s42003-021-02142-w.
74. Remington G. Book review: the schizophrenia spectrum. Can J Psychiatry. 2018;63:257–257. https://doi.org/10.1177/0706743718758042.
75. Remington G, Foussias G, Fervaha G, Agid O, Takeuchi H, Lee J, Hahn M. Treating negative symptoms in schizophrenia: an update. Curr Treat Options Psychiatry. 2016;3:133–50. https://doi.org/10.1007/s40501-016-0075-8.
76. Ribeiro-Santos R, Lucio Teixeira A, Vinicius Salgado J. Evidence for an immune role on cognition in schizophrenia: a systematic review. Curr Neuropharmacol. 2014;12:273–80. https://doi.org/10.2174/1570159X1203140511160832.
77. Rømer TB, Jeppesen R, Christensen RHB, Benros ME. Biomarkers in the cerebrospinal fluid of patients with psychotic disorders compared to healthy controls: a systematic review and meta-analysis. Mol Psychiatry. 2023;28:2277–90. https://doi.org/10.1038/s41380-023-02059-2.
78. Sada-Fuente E, Aranda S, Papiol S, Heilbronner U, Moltó MD, Aguilar EJ, González-Peñas J, Andreu-Bernabeu Á, Arango C, Crespo-Facorro B, González-Pinto A, Fañanás L, Arias B, Bobes J, Costas J, Martorell L, Schulze TG, Kalman JL, Vilella E, Muntané G. Correction: common

genetic variants contribute to heritability of age at onset of schizophrenia. Transl Psychiatry. 2023;13:369. https://doi.org/10.1038/s41398-023-02651-8.
79. Saha S, Chant D, Welham J, McGrath J. A systematic review of the prevalence of schizophrenia. PLoS Med. 2005;2: e141. https://doi.org/10.1371/journal.pmed.0020141.
80. Sancho-Balsells A, Borràs-Pernas S, Brito V, Alberch J, Girault J-A, Giralt A. Cognitive and emotional symptoms induced by chronic stress are regulated by EGR1 in a subpopulation of hippocampal pyramidal neurons. Int J Mol Sci. 2023;24:3833. https://doi.org/10.3390/ijms24043833.
81. Sancho-Balsells A, Brito V, Fernández B, Pardo M, Straccia M, Ginés S, Alberch J, Hernández I, Arranz B, Canals JM, Giralt A. Lack of helios during neural development induces adult schizophrenia-like behaviors associated with aberrant levels of the TRIF-recruiter protein WDFY1. Front Cell Neurosci. 2020;14:5. https://doi.org/10.3389/fncel.2020.00093.
82. Sanz H, Aponte JJ, Harezlak J, Dong Y, Ayestaran A, Nhabomba A, Mpina M, Maurin OR, Díez-Padrisa N, Aguilar R, Moncunill G, Selidji Todagbe A, Daubenberger C, Dobaño C, Valim C. drLumi: An open-source package to manage data, calibrate, and conduct quality control of multiplex bead-based immunoassays data analysis. PLoS ONE. 2017;12: e0187901. https://doi.org/10.1371/journal.pone.0187901.
83. Schizophrenia Working Group of the Psychiatric Genomics Consortium. Biological insights from 108 schizophrenia-associated genetic loci. Nature. 2014;511:421–7. https://doi.org/10.1038/nature13595.
84. Schwarz MJ, Krönig H, Riedel M, Dehning S, Douhet A, Spellmann I, Ackenheil M, Möller H-J, Müller N. IL-2 and IL-4 polymorphisms as candidate genes in schizophrenia. Eur Arch Psychiatry Clin Neurosci. 2006;256:72–6. https://doi.org/10.1007/s00406-005-0603-9.
85. Schwarz MJ, Müller N, Riedel M, Ackenheil M. The Th2-hypothesis of schizophrenia: a strategy to identify a subgroup of schizophrenia caused by immune mechanisms. Med Hypotheses. 2001;56:483–6. https://doi.org/10.1054/mehy.2000.1203.
86. Sen P, Kemppainen E, Orešič M. Perspectives on systems modeling of human peripheral blood mononuclear cells. Front Mol Biosci. 2018. https://doi.org/10.3389/fmolb.2017.00096.
87. Shevchenko A, Tomas H, Havli J, Olsen JV, Mann M. In-gel digestion for mass spectrometric characterization of proteins and proteomes. Nat Protoc. 2006;1:2856–60. https://doi.org/10.1038/nprot.2006.468.
88. Şimşek Ş, Yıldırım V, Çim A, Kaya S. Serum IL-4 and IL-10 Levels correlate with the symptoms of the drug-naive adolescents with first episode, early onset schizophrenia. J Child Adolesc Psychopharmacol. 2016;26:721–6. https://doi.org/10.1089/cap.2015.0220.
89. Sonnenschein SF, Gomes FV, Grace AA. Dysregulation of midbrain dopamine system and the pathophysiology of schizophrenia. Front Psychiatry. 2020. https://doi.org/10.3389/fpsyt.2020.00613.
90. Spemer-Unterweger B, Whitworth A, Kemmler G, Hilbe W, Thaler J, Weiss G, Fleischhacker WW. T-cell subsets in schizophrenia: a comparison between drug-naive first episode patients and chronic schizophrenic patients. Schizophr Res. 1999;38:61–70. https://doi.org/10.1016/S0920-9964(98)00175-3.
91. Sullivan PF. Questions about DISC1 as a genetic risk factor for schizophrenia. Mol Psychiatry. 2013;18:1050–2. https://doi.org/10.1038/mp.2012.182.
92. Sun Y, Koyama Y, Shimada S. Inflammation from peripheral organs to the brain: how does systemic inflammation cause neuroinflammation? Front Aging Neurosci. 2022. https://doi.org/10.3389/fnagi.2022.903455.
93. Sutley-Koury SN, Taitano-Johnson C, Kulinich AO, Farooq N, Wagner VA, Robles M, Hickmott PW, Santhakumar V, Mirnche PN, Ethell IM. EphB2 signaling is implicated in astrocyte-mediated parvalbumin inhibitory synapse development. J Neurosci. 2024;44: e0154242024. https://doi.org/10.1523/JNEUROSCI.0154-24.2024.
94. Szlachta M, Pabian P, Kuśmider M, Solich J, Kolasa M, Żurawek D, Dziedzicka-Wasylewska M, Faron-Górecka A. Effect of clozapine on ketamine-induced deficits in attentional set shift task in mice. Psychopharmacology. 2017;234:2103–12. https://doi.org/10.1007/s00213-017-4613-x.
95. Tamminga CA, Buchanan RW, Gold JM. The role of negative symptoms and cognitive dysfunction in schizophrenia outcome. Int Clin Psychopharmacol. 1998;13:S21–6. https://doi.org/10.1097/00004850-199803003-00004.
96. Tyanova S, Temu T, Sinitcyn P, Carlson A, Hein MY, Geiger T, Mann M, Cox J. The Perseus computational platform for comprehensive analysis of (prote)omics data. Nat Methods. 2016;13:731–40. https://doi.org/10.1038/nmeth.3901.
97. Uhlhaas PJ, Singer W. Abnormal neural oscillations and synchrony in schizophrenia. Nat Rev Neurosci. 2010;11:100–13. https://doi.org/10.1038/nrn2774.
98. Valero M, de la Prida LM. The hippocampus in depth: a sublayer-specific perspective of entorhinal–hippocampal function. Curr Opin Neurobiol. 2018;52:107–14. https://doi.org/10.1016/j.conb.2018.04.013.
99. van Mierlo HC, Schot A, Boks MPM, de Witte LD. The association between schizophrenia and the immune system: review of the evidence from unbiased 'omic-studies.' Schizophr Res. 2020;217:114–23. https://doi.org/10.1016/j.schres.2019.05.028.
100. Venturino A, Schulz R, De Jesús-Cortés H, Maes ME, Nagy B, Reilly-Andújar F, Colombo G, Cubero RJA, Schoot Uiterkamp FE, Bear MF, Siegert S. Microglia enable mature perineuronal nets disassembly upon anesthetic ketamine exposure or 60-Hz light entrainment in the healthy brain. Cell Rep. 2021;36:109313. https://doi.org/10.1016/j.celrep.2021.109313.
101. Wang J-H, Nichogiannopoulou A, Wu L, Sun L, Sharpe AH, Bigby M, Georgopoulos K. Selective defects in the development of the fetal and adult lymphoid system in mice with an ikaros null mutation. Immunity. 1996;5:537–49. https://doi.org/10.1016/S1074-7613(00)80269-1.
102. Wegrzyn D, Juckel G, Faissner A. Structural and functional deviations of the hippocampus in schizophrenia and schizophrenia animal models. Int J Mol Sci. 2022;23:5482. https://doi.org/10.3390/ijms23105482.
103. Wu JQ, Green MJ, Gardiner EJ, Tooney PA, Scott RJ, Carr VJ, Cairns MJ. Altered neural signaling and immune pathways in peripheral blood mononuclear cells of schizophrenia patients with cognitive impairment: a transcriptome analysis. Brain Behav Immun. 2016;53:194–206. https://doi.org/10.1016/j.bbi.2015.12.010.
104. Wu W, Nelson GM, Koch R, Donovan KA, Nowak RP, Heavican-Foral TB, Nirmal AJ, Liu H, Yang L, Duffy J, Powers F, Stevenson KE, Jones MK, Ng SY, Wu G, Jain S, Xu R, Amaka S, Trevisani C, Donaldson NL, Hagner PR, de Leval L, Gaulard P, Iqbal J, Thakurta A, Fischer ES, Adelman K, Weinstock DM. Overcoming IMiD resistance in T-cell lymphomas through potent degradation of ZFP91 and IKZF1. Blood. 2022;139:2024–37. https://doi.org/10.1182/blood.2021014701.
105. Xiao J, Zhou H, Wu N, Wu L. The non-canonical Wnt pathway negatively regulates dendritic cell differentiation by inhibiting the expansion of Flt3+ lymphocyte-primed multipotent precursors. Cell Mol Immunol. 2016;13:593–604. https://doi.org/10.1038/cmi.2015.39.
106. Xie S, Wei H, Peng A, Xie A, Li J, Fang C, Shi F, Yang Q, Huang H, Xie H, Pan X, Tian X, Huang J. Ikzf2 regulates the development of ICOS+ Th cells to mediate immune response in the spleen of S. japonicum-Infected C57BL/6 Mice. Front Immunol. 2021. https://doi.org/10.3389/fimmu.2021.687919.
107. Zhang T, Zeng J, Wei Y, Ye J, Tang X, Xu L, Hu Y, Cui H, Xie Y, Tang Y, Liu X, Liu H, Chen T, Li C, Wang J. Changes in inflammatory balance correlates with conversion to psychosis among individuals at clinical high-risk: A prospective cohort study. Psychiatry Res. 2022;318:114938. https://doi.org/10.1016/j.psychres.2022.114938.
108. Zhu M, Liu Z, Guo Y, Sultana MS, Wu K, Lang X, Lv Q, Huang X, Yi Z, Li Z. Sex difference in the interrelationship between TNF-α and oxidative stress status in first-episode drug-naïve schizophrenia. J Neuroinflammation. 2021;18:202. https://doi.org/10.1186/s12974-021-02261-5.

Publisher's Note

2. Ikzf1 as a novel regulator of microglial homeostasis in inflammation and neurodegeneration

Brain, Behavior, and Immunity 109 (2023) 144–161

Contents lists available at ScienceDirect

Brain Behavior and Immunity

journal homepage: www.elsevier.com/locate/ybrbi

Ikzf1 as a novel regulator of microglial homeostasis in inflammation and neurodegeneration

Iván Ballasch [a,b,c], Esther García-García [a,b,c], Cristina Vila [b,c,d,e], Anna Pérez-González [a,b,d], Anna Sancho-Balsells [a,b,c], Jéssica Fernández [a,b,c], David Soto [a,b,f], Mar Puigdellívol [a,b,f], Xavier Gasull [a,b,f], Jordi Alberch [a,b,c,e], Manuel J. Rodríguez [a,b,c], Josep M. Canals [b,c,d,e], Albert Giralt [a,b,c,e,*]

[a] Departament de Biomedicina, Facultat de Medicina, Institut de Neurociències, Universitat de Barcelona, Barcelona, Spain
[b] Institut d'Investigacions Biomèdiques August Pi i Sunyer (IDIBAPS), Barcelona, Spain
[c] Centro de Investigación Biomédica en Red sobre Enfermedades Neurodegenerativas (CIBERNED), Spain
[d] Laboratory of Stem Cells and Regenerative Medicine, Department of Biomedicine, University of Barcelona, Barcelona, Spain
[e] Production and Validation Center of Advanced Therapies (Creatio), Faculty of Medicine and Health Science, University of Barcelona, 08036 Barcelona, Spain
[f] Laboratori de Neurofisiologia, Departament de Biomedicina, Facultat de Medicina i Ciències de la Salut, Institut de Neurociències, Universitat de Barcelona, Barcelona, Spain

ARTICLE INFO

Keywords:
Synaptic plasticity
Synaptic engulfment
Learning
Memory
Astrogliosis
Long-term potentiation

ABSTRACT

In the last two decades, microglia have emerged as key contributors to disease progression in many neurological disorders, not only by exerting their classical immunological functions but also as extremely dynamic cells with the ability to modulate synaptic and neural activity. This dynamic behavior, together with their heterogeneous roles and response to diverse perturbations in the brain parenchyma has raised the idea that microglia activation is more diverse than anticipated and that understanding the molecular mechanisms underlying microglial states is essential to unravel their role in health and disease from development to aging. The *Ikzf1* (a.k.a. Ikaros) gene plays crucial roles in modulating the function and maturation of circulating monocytes and lymphocytes, but whether it regulates microglial functions and states is unknown. Using genetic tools, here we describe that Ikzf1 is specifically expressed in the adult microglia in brain regions such as cortex and hippocampus. By characterizing the *Ikzf1* deficient mice, we observed that these mice displayed spatial learning deficits, impaired hippocampal CA3-CA1 long-term potentiation, and decreased spine density in pyramidal neurons of the CA1, which correlates with an increased expression of synaptic markers within microglia. Additionally, these *Ikzf1* deficient microglia exhibited a severe abnormal morphology in the hippocampus, which is accompanied by astrogliosis, an aberrant composition of the inflammasome, and an altered expression of disease-associated microglia molecules. Interestingly, the lack of *Ikzf1* induced changes on histone 3 acetylation and methylation levels in the hippocampus. Since the lack of *Ikzf1* in mice appears to induce the internalization of synaptic markers within microglia, and severe gliosis we then analyzed hippocampal Ikzf1 levels in several models of neurological disorders. Ikzf1 levels were increased in the hippocampus of these neurological models, as well as in postmortem hippocampal samples from Alzheimer's disease patients. Finally, over-expressing *Ikzf1* in cultured microglia made these cells hyporeactive upon treatment with lipopolysaccharide, and less phagocytic compared to control microglia. Altogether, these results suggest that altered Ikzf1 levels in the adult hippocampus are sufficient to induce synaptic plasticity and memory deficits via altering microglial state and function.

1. Introduction

Microglia constitute 5–10 % of total brain cells and are the main CNS parenchymal macrophages (Frost and Schafer, 2016). Microglia play diverse roles in the healthy central nervous system (CNS) (Sierra et al., 2019), including synapse monitoring and pruning, also known as "synaptic survey" (Paolicelli et al., 2011; Schafer et al., 2012), but the functional significance of such microglia–synapse interactions in the

* Correspondence autor at: Departament de Biomedicina, Facultat de Medicina, Institut de Neurociències, Universitat de Barcelona, Barcelona, Spain.
E-mail address: albertgiralt@ub.edu (A. Giralt).

https://doi.org/10.1016/j.bbi.2023.01.016
Received 13 September 2022; Received in revised form 28 December 2022; Accepted 20 January 2023
Available online 23 January 2023

adult brain remains largely unknown. Several studies have demonstrated a direct role of microglia in neurodegenerative and neurological disorders, which are usually accompanied by neuroinflammation, synaptic and neuronal loss, and cognitive decline (Li and Barres, 2018). Currently, microglia-related dysfunctions in neurodegenerative disorders such as Alzheimer's Disease (AD) is understood as the coexistence of multiple altered microglia states in terms of morphology, genetic profile and metabolic changes among others that may vary depending on the disease type, its stage and tissue affected (Paolicelli et al., 2022). For instance, in AD pathology, altered microglial functions have been shown to promote its interaction with amyloid beta, and contribute to an excessive synaptic and neuronal loss (El Hajj et al., 2019; Hong et al., 2016; Puigdellívol et al., 2021; Rajendran and Paolicelli, 2018; Shi et al., 2019; Yeh et al., 2017).

In response to an insult, microglia have the ability to shift into different functional states, modifying its proliferation (Gomez-Nicola et al., 2013), morphology (Cuadros, 1998), phagocytic activity (Sierra et al., 2013), antigen presentation (Jimenez-Ferrer et al., 2017; McGeer et al., 1988) and the release of inflammatory mediators such as cytokines and chemokines (Kettenmann et al., 2011). Traditionally, macrophage and microglial activation have been classified in two different and opposite states: classic (M1 pro-inflammatory) and alternative (M2 tissue repair). However, nowadays a broad array of activation profiles and phenotypes have been described, especially in disease context (De Biase et al., 2017; Keren-Shaul et al., 2017). The latter works suggest that the microglial control of brain homeostasis is a very complex and thinly process. However, the literature addressing the molecular pathways related to intrinsic microglia homeostasis is still scarce.

A highly promising molecular mechanism that could regulate intrinsic microglial homeostasis is Ikzf1 (a.k.a. Ikaros). Ikzf1 is the founding member of a family that was initially identified as an hematopoietic cell type-specific transcription factor (TF) (Georgopoulos, 2002; Yoshida et al., 2006). The family is composed of five members (Ikaros/*IKZF1*, Helios/*IKZF2*, Aiolos/*IKZF3*, Eos/*IKZF4* and Pegasus/*IKZF5*) of TFs. These TFs have also been described to be crucial for the normal development of immune cells (*T*-cells, B-cells and monocytes) (Georgopoulos et al., 1997) and their function (i.e. production of *mb-1*, *CD3*, *IL2* and *NF-kB* among others (Molnár and Georgopoulos, 1994)). Traditionally, it has been suggested that in the brain, Ikzf1 members are only expressed in developing striatal and cortical neurons (Agoston et al., 2007; Alsiö et al., 2013; Martín-Ibáñez et al., 2010), but its expression and function in microglia has never been addressed. More recently, Ikzf1 has been described to be important in coordinating the complex macrophage transcriptional program in response to pathogen challenges (Oh et al., 2018) and regulating epigenetic remodeling in diseased monocytes (Faia et al., 2021) or playing a role in myeloid precursors proliferation (Yagi et al., 2002). Altogether and given that microglia are myeloid in origin, as monocytes and macrophages (Li and Barres, 2018), we hypothesized that Ikzf1 could be expressed and play a relevant role in microglial cells.

Using different tools, in the present work we show that Ikzf1 is specifically expressed in adult cortical and hippocampal microglia. We also showed that Ikzf1 deficient mice show altered spatial learning, hippocampal dendritic spines and long-term potentiation. We also observed that mouse microglia devoid of Ikzf1 exhibit an abnormal morphology concomitant with an increase of synaptic markers staining within microglia, suggesting increased engulfment of synaptic material. Molecular screening indicated that the inflammasome as well as epigenetic alterations accompanied such alterations. Surprisingly, experiments in several models of neurodegeneration and neuroinflammation showed increases of Ikzf1 levels in microglia, suggesting that altered microglial Ikzf1 expression led to dysfunctional microglia. Finally, in order to address whether Ikzf1 is important for microglia homeostasis, we showed that cultured microglia over-expressing Ikzf1 was less reactive to lipopolysaccharide (LPS)-induced inflammation and was less phagocytic than control microglia, indicating that appropriate microglial Ikzf1 expression is essential for microglial homeostasis.

2. Materials & methods

2.1. Animals

In the present study we used the Ikzf1-Cre mice provided by Professor Michelle Cayouette. These mice are a BAC transgenic mouse line expressing Cre recombinase under the regulatory elements of the Ikaros (*Ikzf1*) gene (Tarchini et al., 2012). Ikzf1-Cre mice were used as heterozygous and crossed with R26RCE mice (B6.Cg-Gt(ROSA)26Sortm14 (CAG-tdTomato)Hze/J, Strain 007914, a.k.a. Ai14(RCL-tdT)-D. The Jackson Laboratory, which harbor the R26R CAG-boosted tdTomato reporter allele with a loxP-flanked STOP cassette upstream of the tdTomato gene to create the double heterozygous mutant Ikzf1-Cre × Ai14(RCL-tdT)-D mice (Ikzf1-Cre:tdTomato^{Flox} mice) for the experiments related with characterization of neural populations expressing Ikzf1. Ikzf1 deficient mice (Wang et al., 1996) were provided by Professor Katia Georgopoulos and backcrossed with C57BL/6 mice to obtain hemizygous, heterozygous and wild type mice. In this study, we also used the transgenic mouse line 5xFAD (MMRRC catalog #034840-JAX, RRID:MMRRC_034840-JAX). 5xFAD mice (8 wt mice and 11 5xFAD mice) overexpress the 695-amino acid isoform of the human amyloid precursor protein (APP695) carrying the Swedish, London, and Florida mutations under the control of the murine Thy-1 promoter. In addition, they express human presenilin-1 (PSEN-1) carrying the M146L/L286V mutation, also under the control of the murine Thy-1 promoter (Oakley et al., 2006). Genotypes were determined from an ear biopsy as described elsewhere (Martín-Ibáñez et al., 2010). For genotyping of the Cre transgenes we used standard PCR assays following The Jackson Laboratory manufacturer's instructions. All mice were housed together in numerical birth order in groups of mixed genotypes (three to five mice per cage). The animals were housed with access to food and water ad libitum in a colony room kept at 19–22 °C and 40–60 % humidity, under an inverted 12/12 h light/dark cycle (from 8 A.M. to 8 P.M.). All animal procedures were approved by local committees [Universitat de Barcelona, CEEA (133/10); Generalitat de Catalunya (DAAM 5712); and Animal Care Committee of the University of Paris (APAFIS #15638)], in accordance with the European Communities Council Directive (86/609/EU).

2.2. Chemical mouse models

For this study, we used pups (Postnatal day 5, P5) and adult (10-week-old) C57/BL6 males (MGI catalog #5657800, RRID: MGI:5657800) in experiments related with treatments with lipopolysaccharide (LPS) and pilocarpine, respectively. First, mouse pups at P5 were intraperitoneally injected with 6 mg/kg of LPS (n = 3) or vehicle (n = 3). Twenty-four hours later mice were sacrificed, and brains fixed for histological experiments.

Another cohort of adult (10-weeks-old) mice were subjected to the lithium-pilocarpine model of temporal lobe epilepsy (TLE). Briefly, mice were treated intraperitoneally with lithium (LiCl, 423 mg/kg, ip) 20–23 h prior to administration of scopolamine, an anti-muscarinic molecule (1 mg/kg, ip). 30 min after the administration with methyl-scopolamine, animals (n = 7) were treated with pilocarpine (45 mg/kg, ip). Control animals (n = 6) were injected with saline solution. Status epilepticus (SE) was stopped after approximately 120 min with an intraperitoneal injection of valium (10 mg/kg, ip). Only animals that displayed 120 min of SE, survived and showed the following level of epileptic seizure were selected: mouth and facial movement, tremors, head nodding and forelimb clonus. The later chemical mouse models were approved by local committees (University of Barcelona, 225/17 and Generalitat de Catalunya, 404/18), in accordance with the European Communities Council Directive (86/609/EU).

2.3. Behavioral tests

The animals subjected to behavioural experimentation were housed with access to food and water ad libitum in a specialized room to perform behavioral tests. The room was also kept at 19–22 °C and 40–60 % humidity, under an inverted 12/12 h light/dark cycle (from 8 A.M. to 8P.M.). The timeline of the behavioral experimentation was scheduled following a sequence of less-to-more anxiogenic tests allowing resting days in between tests (Supp. Fig. 1). The light intensity was ~40 lx throughout the arena and the room. The number of mice used were 14 Ikzf1$^{+/+}$, 15 Ikzf1$^{+/-}$ and 9 Ikzf1$^{-/-}$ throughout the behavioral testing.

SHIRPA assessment. To provide detailed general phenotype assessment, mice were tested using a modified version of the primary screen so-called Phenotype Assessment (SHIRPA) protocol (Giralt et al., 2013). Briefly, we measured several parameters such as body weight (g) and body length (cm), body position (curved or normal), tremors (present or not), palpebral closure (eyes visible or visually closed), coat appearance (presence or absence of piloerection), number of whiskers (present or clearly reduced), defecations (presence of defecations or absence), locomotor activity (number of 2.5 cm^2 squares crossed during 30 s), touch escape reflex (animal reacts or not to touching), corneal reflex (presence or not of palpebral closure reflex when touching), biting behavior (animal bites or not a pencil when placing it close to its mouth), vocalization (the mouse screams or not) and muscular strength (animal keeps at least 30 s in a turned wire or not).

Muscular strength: Neuromuscular abnormalities were analyzed by the hanging wire test as described elsewhere (Giralt et al., 2011) in adult mice. A standard wire cage lid was used. To test balance and grip strength, mice were placed on top of a wire cage lid. The lid was shaken slightly to cause the mouse to grip the wires and then turned upside down for 60 *sec*. The number of falls of each mouse was recorded.

Open field: To check spontaneous locomotor activity and parallel index we used the open field. Briefly, the apparatus consisted of a white square arena measuring 40 × 40 × 40 cm in length, width and height respectively. Dim light intensity was 60 lx throughout the arena. Animals were placed on the arena center and allowed to explore freely for 30 min. Spontaneous activity and navigation were measured. At the end of each trial, any defecation was removed, and the apparatus was wiped with 30 % ethanol.

Balance beam: The motor coordination and balance of mice were also assessed by measuring their ability to traverse a narrow beam (Giralt et al., 2011). The beam consisted of a long wooden square (50 cm) with a 50 mm-square cross-section and a 1,5 mm-squared. The beam was placed horizontally, 50 cm above the bench surface, with each end mounted on a narrow support. Animals were allowed to walk for 1 min along the beam, while number of slips and distance covered were measured.

Novel object recognition test: The device consisted in a white square arena with 40 cm depth, 40 cm length and 40 cm high. Mice were first habituated to the arena in the absence of objects (1 days, 15 min/day). On the second day, two similar objects were presented to each mouse during 10 min (A′A″ condition) after which they were returned to their home cage. Twenty-four hours later, the same animals were re-tested for 5 min in the arena with a familiar and a new object (AB condition). The object preference was measured as the time exploring each object × 100/time exploring both objects. The arena was rigorously cleaned between animal trials in order to avoid odors.

Spontaneous alternation in a transparent Y-maze: A Y-maze apparatus, made of clear Perspex, was used (Y-maze dimensions: arms, 35 cm length, 25 cm height, 15 cm width). Mice were placed in the stem arm of the Y and allowed to freely explore for 10 min the three arms. Big and highly perceptible objects were situated surrounding the maze at 20 cm. Number of triads were quantified as previously reported (de Pins et al., 2019). In all behavioral studies animals were tracked and recorded with Smart junior 3.0 software (Panlab).

2.4. Tissue fixation and immunofluorescence

Mice were euthanized by cervical dislocation. Left hemispheres were removed and fixed for 72 h in 4 % paraformaldehyde (PFA) in PBS. 40 µm coronal sections were obtained using a Leica vibratome (Leica VT1000S). Next, free floating sections were washed three times in PBS, treated with NH4Cl for 30 min and washed again three times with PBS. Floating sections were permeabilized and blocked with PBS containing 3 % Triton X-100, 0.02 % Azide, 2 % BSA and 3 % NGS (Ab buffer) for 1 h at RT. After three washes in PBS, brain slices were incubated overnight at 4 °C with anti-NeuN (1:1000, Chemicon, Ref: MAB377); anti-Iba1 (1:500, Synaptic Systems, Ref: 234008), anti-Iba1 (1:500, Wako, Ref: 019-19741), anti-GFAP (1:500, Dako, Ref: Z0334), anti-Asc-tms1 (1:500, Cell Signalling, Ref: D2w8u), TMEM119 (1:100, Synaptic Systems, Ref:400011), anti-CD206 (1:100, Bio-rad, Ref: MCA2235T), anti-IL-1B (1:100, GeneTex, Ref: GTX636887), anti-NF-kB (1:50, Santa Cruz Biotechnology, Ref: sc-372), anti-Ikzf1 (1:100, D6N94Y, Cell Signaling, Ref: 14859), anti-GFAP (1:500, Dako, Ref: GA524), anti-TNFα (1:100, Abcam, Ref: ab1793), anti-Midkine (1:500, Proteintech, Ref: 11009-1-AP) and anti-PSD-95 (1:500, Cell Signaling, Ref: 3450S). Sections were washed three times and incubated for 2 h at RT with fluorescent secondary antibody Alexa Fluor 488 or 647 (1:400; from Jackson Immuno Research, West Grove, PA, USA). Sections were analyzed using a two-photon confocal microscope (Leica SP5).

2.5. Immunohistochemistry

For diaminobenzidine immunohistochemistry experiments, endogenous peroxidases were blocked for 30–45 min in PBS containing 10 % methanol and 3 % H_2O_2. Then, nonspecific protein interactions were blocked with normal serum or bovine serum albumin. Tissue was incubated overnight at 4 °C with the following primary antibodies: anti-NeuN (1:1000; Chemicon, Ref: MAB377), anti-parvalbumin (1:1250; Swant, Ref: PV27) and anti-Calbindin 28 kDa (1:500; Swant, Ref: 300). Sections were washed three times in PBS and incubated with a biotinylated secondary antibody (1:200; Pierce) at room temperature for 2 h. The immunohistochemical reaction was developed using the ABC kit (Pierce) and visualized with diaminobenzidine. No signal was detected in controls in which the primary antibodies were omitted.

2.6. Imaging analysis

For the experiments using the Ikzf1-Cre:tdTomato mice, images (at 1024 × 1024-pixel resolution) in a mosaic format were acquired with a Leica Confocal two-photon SP5 with a × 40 oil-immersion or × 20 normal objectives and standard (1 Airy disk) pinhole (1AU) and frame averaging (three frames per z step) were held constant throughout the study. For cell counting, we analyzed three sections from 4 different mice, spaced 240 µm apart. The areas of analysis were, dorsal hippocampus (Antero-posterior axis: −1.5 to −2.22 from bregma), motor cortex, sensory cortex, and cingulate cortex (Antero-posterior axis: 0 to −0.7 from bregma). Unbiased blind counting of tdTomato-positive cells (Ikzf1 expressing cells) colocalizing with NeuN-positive (neuronal marker) or Iba1-positive (microglia marker) or astrocyte-shaped (tdTomato-positive) cells relative to condition was performed and normalized to the area of counting. In experiments performed in Ikzf1 deficient mice and cultured microglia 1024 × 1024-pixel resolution images were obtained using 40x oil-immersion objectives and standard (1 Airy disc) pinhole (1 AU) and frame averaging (3 frames per z step) were held constant throughout the study. For the morphological studies carried out in microglia *in vivo*, the entire 3D stack of images was obtained using the Z drive. Images were analyzed using the freeware NIH ImageJ by Wayne Rasband (National Institutes of Health, Bethesda, MD). Microglia were defined automatically following the application of the IsoData mask and being selected by the wand tracing tool. Then the shape descriptors already present in the software were applied. For the

colocalization studies the freeware ImageJ was also used. Briefly, for each section, the dendritic spine area (clusters) was delineated based on positive pixels for PSD-95 on the one hand and the number of Iba1-positive pixels inside each PSD-95-positive cluster were determined on the other hand. Total number of PSD-95 positive particles, and the number of double Iba1/PSD-95 positive pixels were quantified.

2.7. Electrophysiology

Mice (8 Ikzf1$^{+/+}$ and 5 Ikzf1$^{-/-}$ mice) were anesthetized using isoflurane and decapitated. Brains were rapidly removed and placed in ice-cold artificial CSF1 (aCSF1, in mM; 206 sucrose, 1.25 NaH_2PO_4, 26 $NaHCO_3$, 1.3 KCl, 1 $CaCl_2$, 10 $MgSO_4$, 11 glucose, purged with 95 % O_2/ 5 %CO_2, pH: 7.35). Coronal slices (380um thick) were then obtained with a vibratome (VT1200 S; Leica Microsystems, Wetzlar, Germany) in the same cold solution. Slices were placed in an incubator beaker containing aCSF2 (in mM, 119 NaCl, 1.25 NaH_2PO_4, 25 $NaHCO_3$, 2.5 KCl, 2.5 $CaCl_2$, 1.5 $MgSO_4$, 11 glucose, purged with 95 % O_2/ 5 % CO_2, pH: 7.35). Slices were kept at 34 °C for 1 h and subsequently at RT for at least 1 h before starting the recordings. Slices were transferred into a measuring chamber continuously perfused with aCSF2 at 27–29 °C for field excitatory post-synaptic potential (fEPSP) recordings. A bipolar stimulation electrode was placed in the Schaffer collateral pathway. The recording electrode filled with aCSF2 was placed in the dendritic branching of the CA1 region. A stimulus isolation unit A385 (WPI, Hertfordshire, UK) was used to elicit stimulation currents between 25 and 155 μA. Before baseline recordings for long-term potentiation (LTP), input–output (IO) curves were recorded for each slice at 0.03 Hz. The stimulation current was then adjusted for each recording to evoke fEPSPs at which the slope was at 50–60 % of maximally evoked fEPSP slope value. After baseline recording for 30 min with 0.03 Hz, LTP was induced by theta-burst stimulation (TBS; 10 theta bursts of four pulses of 100 Hz with an interstimulus interval of 200 ms repeated seven times with 0.03 Hz). After LTP induction, fEPSPs were recorded for 1 additional hour with 0.03 Hz. Paired-pulse fEPSPs were measured directly before LTP induction with 0.03 Hz and an interstimulus interval of 50 and 100 ms. All recordings were amplified and stored using amplifier AxoClamp 2B (Molecular Devices, San Jose, CA). Traces were analyzed using Axon pClamp software (Molecular Devices, version 10.6).

2.8. Golgi staining

Fresh brain hemispheres were submerged and processed following the Golgi-Cox method as described elsewhere (Giralt et al., 2017). Two hundred-microns sections were cut in 70 % EtOH on a vibratome (Leica) and washed in water for 5 min. Next, they were reduced in 16 % ammonia solution for 1 h before washing in water for 2 min and fixation in $Na_2S_2O_3$ for 7 min. After a 2-min final wash in water, sections were mounted on superfrost coverslips, dehydrated for 3 min in 50 %, then 70, 80 and 100 % EtOH, incubated for 5 min in a 2:1 isopropanol:EtOH mixture, followed by 1 × 5 min in pure isopropanol and 2 × 5 min in xylol. Bright-field images of Golgi-impregnated stratum radiatum dendrites from hippocampal CA1 pyramidal neurons were captured with a Nikon DXM 1200F digital camera attached to a Nikon Eclipse E600 light microscope (x 100 oil objective). Only fully impregnated pyramidal neurons with their soma entirely within the thickness of the section were used. Image z-stacks were taken every 0.2 mm, at 1,024 × 1,024-pixel resolution, yielding an image with pixel dimensions of 49.25 × 49.25 μm. Segments of proximal apical dendrites were selected for the analysis of spine density. Only spines arising from the lateral surfaces of the dendrites were included in the study. Given that spine density increases as a function of the distance from the soma, reaching a plateau 45 μm away from the soma, we selected dendritic segments of basal dendrites 45 μm away from the cell body. The total number of spines was obtained using the cell counter tool in the ImageJ software. A total of 84–94 dendrites per group from 4 to 5 animals per genotype were analyzed.

2.9. Immunoblotting

Animals (n = 4–8 per group) were killed by cervical dislocation. The hippocampus was dissected out, frozen using CO_2 pellets and stored at −80 °C until use. Briefly, the tissue was lysed by sonication in 250 ml of lysis buffer as described elsewhere (Giralt et al., 2017). After lysis, samples were centrifuged at 12,000 r.p.m. for 20 min. Supernatant proteins (15 mg) from total brain regions extracts were loaded in SDS–PAGE and transferred to nitrocellulose membranes (GE Healthcare, LC, UK). Membranes were blocked in TBS-T (150 mM NaCl, 20 mM Tris-HCl, pH 7.5, 0.5 ml Tween 20) with 50 g l^{-1} non-fat dry milk and 50 g l^{-1} BSA. Immunoblots were probed with the following antibodies: anti-Ikzf1 (D6N9Y, Cell Signaling Technology, Danvers, MA, USA. Ref: 14859), anti-H3 (1:1000, Abcam, Ref: ab1791), anti-acetyl-H3-L14 (1:1000, Millipore, Ref: 07–353), anti-methyl-H3-K9 (1:1000, Abcam, Ref: ab9045), anti-3-methyl-H3-K9 (1:1000, Abcam, ab8898), anti-Nalp1 (1:1000 Santa Cruz, #sc-166368), anti-TREM2 (1:1000, Santa Cruz Biotechnology, Ref: sc-373828), anti-Clec7a (1:100, Bioss Antibodies, Ref: bs-2455R), anti-CX3CR1 (1:1000, Sigma, E3271-2B11), anti-SIRT1 (1:1000, Cell Signaling, #CST2028S) and anti-phospho-SIRT1-Ser47 (1:1000, Bioss, #BS-3393R). The inflammasome kit (Cell Signalling, #20836) to detect protein levels of Nalp3, ACs/tms1, Aim2, Caspase-1, cleaved Caspase-1 and IL-1B was also used in the same immunoblotting experiments. All blots were incubated with the primary antibody overnight at 4 °C by shaking in PBS with 0.2 g l^{-1} sodium azide. After three washes in TBS-T, blots were incubated for 1 h at room temperature with the corresponding horseradish peroxidase-conjugated antibody (1:2000; Promega, Madison, WI, USA) and washed again with TBS-T. Immunoreactive bands were visualized using the Western Blotting Luminol Reagent (Santa Cruz Biotechnology) and quantified by a computer-assisted densitometer (Gel-Pro Analyzer, version 4, Media Cybernetics). For loading control a mouse monoclonal antibody for actin was used (1:20,000; MP Biochemicals, #0869100-CF).

2.10. Human post-mortem samples

Postmortem hippocampal samples from Alzheimer's disease (n = 9) patients and controls (n = 12) were obtained from Banc de Teixits Neurològics (IDIBAPS, Barcelona, Spain). The donation and obtaining of samples were regulated by the ethics committee of the Universitat de Barcelona. The sample processing followed the rules of the European Consortium of Nervous Tissues: BrainNet Europe II (BNEII). All the samples were protected in terms of individual donor identification following the BNEII laws. Case information can be found in Supplementary Table 1. All the procedures for the obtention of postmortem samples followed the ethical guidelines of the Declaration of Helsinki and local ethical committees (Universitat de Barcelona ethical committee: IRB00003099).

2.11. Microglial cultures

Primary microglial cultures were obtained as previously described (Saura et al., 2003). Briefly, glial hippocampal cultures from 2-day-old C57BL/6 mice (Charles River, France) were obtained by mechanical dissociation. Cell suspensions were seeded in 24-well plates at a density of 78,000 cells/cm^2 with supplemented DMEM (High glucose. Ref: 10-013-CV, GIBCO) containing 10 % fetal bovine serum, 1 % pen-strept and 1:500 Amphotericine B). Media was replaced once per week. At day in vitro 19 (DIV19) microglia were isolated by mild trypsinization (Trypsin/EDTA 1:4) and the floating astroglia was removed. Microglial cells were transfected at DIV20 with a control plasmid (pcDNA3-GFP, (Giralt et al., 2017) or a plasmid to over-express Ikzf1 (pcDNA-IKZF1-V2-V5. Addgene. Ref: 107390) using the Fugene kit (Promega, Ref: E2311) following manufacturer's indications. Transfected microglial cultures at DIV22 were treated with 100 ng/ml of lipopolysaccharides (Sigma-Aldrich. Ref: L2630) and cells at DIV23 were fixed with

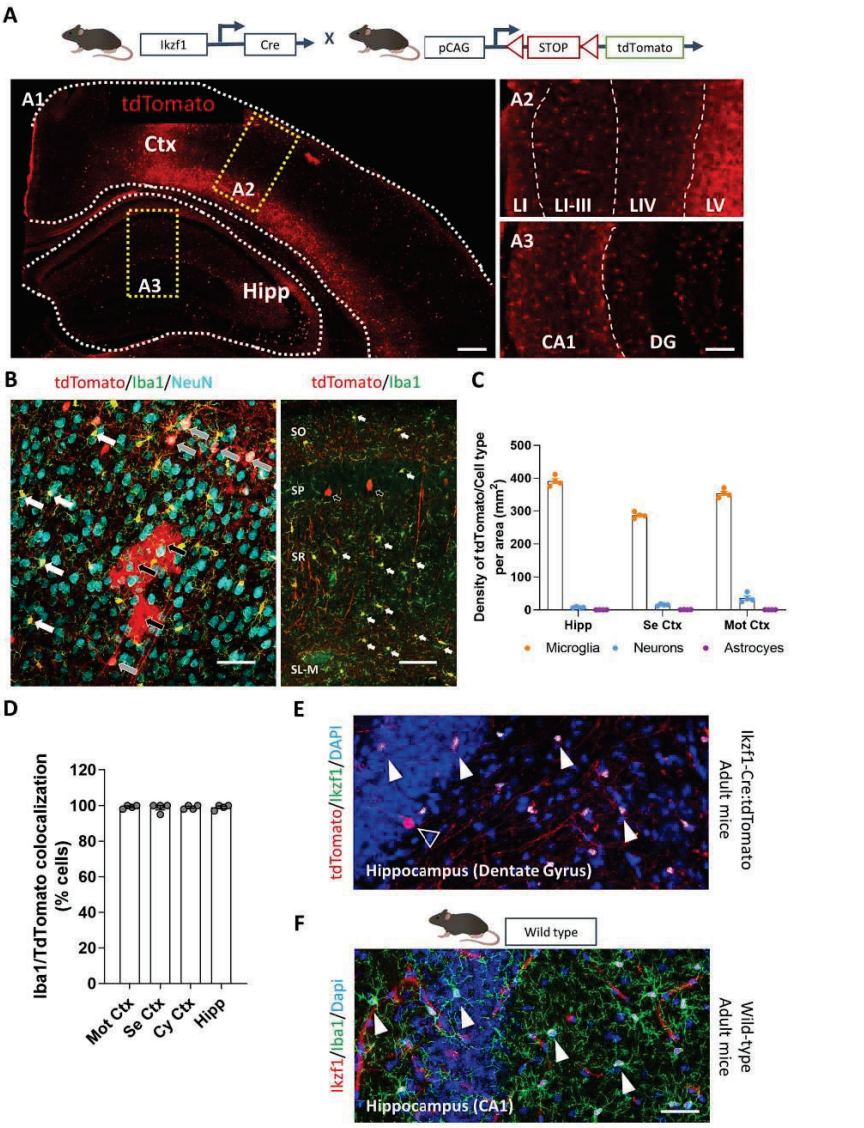

(caption on next page)

Fig. 1. Ikzf1 expressing cells in the adult brain. (A) Upper panel: Schematic representation of double mutant adult Ikzf1-Cre:tdTomato^{Flox} mice used in experiments in B-D and E. Lower panel A1: representative mosaic depicting tdTomato signal in hippocampus and cortical areas from adult Ikzf1-Cre:tdTomato^{Flox} mice. Lower panel A2 and A3: Sensory cortical and hippocampal area insets from A1 depicting tdTomato signal. (B) Left panel, triple staining for microglia (Iba1-positive cells, green), neurons (NeuN-positive cells, turquoise) and all cells that expressed Ikzf1 at some point (tdTomato-positive cells, red) in the mouse sensory cortex. Black arrows are depicting punctual tdTomato-positive astrocytes. Grey arrows are depicting double positive NeuN/tdTomato neurons. White arrows are depicting double positive Iba1/tdTomato microglia. Right panel, double staining labeling microglia (Iba1-positive cells, green), and all cells that expressed Ikzf1 at some point (tdTomato-positive, red) in the hippocampal CA1. White arrows are depicting double positive cells for Iba1 and tdTomato. Black arrows are depicting casual tdTomato-positive cells with a typical shape from pyramidal neurons of the CA1. (C) Cell density quantification in three brain regions (hippocampus or Hipp; sensory cortex or Se Ctx and Cyngulate cortex or Cy Ctx) of the three tdTomato-positive populations: Microglia (Iba1/TdTomato double positive cells), Neurons (NeuN/tdTomato-positive cells) and astrocytes (tdTomato-astocyte-like shaped cells). (D) Percentage of Iba1-positive cells colocalizing with tdTomato labeling. (E) Co-staining of tdTomato (red) with Ikzf1 (green) in the hippocampal CA1. Note Ikzf1 has always a specific nuclear staining. White arrows are depicting double labeled tdTomato/iba1 microglia. Empty arrow is depicting a tdTomato-positive neuron but without Ikzf1 expression which is indicative of having expressed Ikzf1 at some point of its development but not in adulthood. (F) Co-staining of Ikzf1 (red) with Iba1 (green) in the hippocampal CA1. White arrows are depicting double positive Ikzf1/Iba1 cells. Scale bars: In B and E 100 μm.

paraformaldehyde (4 %) for immunofluorescence experiments. On the other hand, another set of transfected microglial cultures at DIV22 were treated with latex beads (see below) as previously described (Lian et al., 2016). Cells at DIV23 were fixed for immunofluorescence experiments. Coverslips were subjected to immunofluorescence as previously described (Rodríguez-Urgellés et al., 2022). Primary antibodies used were anti-V5 (1:500, GeneTex. Ref: GT1078) or anti-GFP FITC-conjugated antibody (1:500, Abcam, ab6662). Secondary antibody used was Alexa Fluor 555 goat anti-mouse (1:400; from Jackson Immuno Research, West Grove, PA, USA). After incubation with secondary antibody, coverslips were mounted with Mowiol and visualized in a SP5 two-photon confocal microscopy (Leica).

2.12. Microglial phagocytosis assay

Microglial phagocytosis assay was performed as previously described (Lian et al., 2016). Briefly, the aqueous orange, fluorescent latex beads (Cat: L9654, Sigma, St. Louis, MI, United States) were pre-opsonize with fetal bovine serum (FBS) for 1 h at 37 °C. The ratio of beads to FBS was 1:5. Then, the bead-containing FBS were diluted with DMEM high glucose (Cat: D5671, Sigma, St. Louis, MI, United States) to reach the final concentrations for beads and FBS in DMEM high glucose of 0.01 % (v/v) and 0.05 % (v/v), respectively. The microglial conditioned culture media were replaced with beads-DMEM and the cultures were then incubated for 1 h at 37 °C. Finally, the cultures were thoroughly washed 5 times with ice-cold PBS and cells were fixed with 4 % PFA for 15 min. Phagocytosis was quantified as the number of beads per cell relativized by their area only in transfected cells.

2.13. Statistics

Analyses were done using Prism version 8.0.2 for Windows (GraphPad Software). Data are expressed as mean ± SEM. Normal distribution was tested with the D'Agostino and Pearson omnibus test. If no difference from normality was detected, statistical analysis was performed using two-tailed Student's *t* test or ANOVA and Tukey's or Dunnett's post hoc tests. If distribution was not normal, nonparametric two-tailed Mann–Whitney test was used. In case of unequal variances in the *t*-test the Welch's correction was applied. Also, the Chi-square ($\chi 2$) test was used in the case of qualitative variables. The $p < 0.05$ was considered as significant.

3. Results

3.1. Ikzf1 is specifically expressed in adult microglia of several brain regions

Ikzf1 protein has been widely studied in the immune system and, to a lesser extent, in the developing CNS (Alsiö et al., 2013; Boast et al., 2021). However, it is unknown whether Ikzf1 is expressed in the adult brain, in which cell type and which is its potential role. In order to address these questions, we first crossed the Ikzf1-Cre mice (Tarchini et al., 2012) with the Ai14(RCL-tdT)-D mice to obtain Ikzf1-Cre:tdTomato^{Flox} mice (Fig. 1A). We then fixed brains from adult (7-weeks-old) Ikzf1-Cre:tdTomato^{Flox} mice (Fig. 1A). With this initial strategy we expected to identify all the neural cells that expressed Ikzf1 at some period of their life. Thus, we then performed colocalization studies to identify colocalization of tdTomato signal (Ikzf1 signal) with markers for neurons and microglia.

We first observed that in the sensory cortex and cingulate cortex tdTomato signal was detected in punctual astrocytes (tdTomato signal in astrocyte-shaped cells), which were GFAP-positive cells (Supp. Fig. 2). TdTomato signal was also found in some neurons (NeuN-positive, Fig. 1B-C). In both cases the frequency was <20 cells / mm^2. In contrast, tdTomato signal was detected in ~290–320 microglial (Iba1-positive) cells / mm^2 (~15 times more in microglia than in neurons). In the hippocampus, this difference was even bigger; almost no tdTomato signal was detected either in neurons (<10 / mm^2) or in tdTomato-positive astrocyte-shaped cells in this brain region (Fig. 1B-C) whereas tdTomato labeling was detected in ~400 microglial cells / mm^2. Indeed, almost 100 % of Iba1-positive microglia colocalized with tdTomato labeling in the motor cortex, sensory cortex, cingulate cortex and in the hippocampus (Fig. 1D). Since with this approach we just quantified the cells that at some point of their lives expressed Ikzf1, we then performed Ikzf1 immunofluorescence in both, adult Ikzf1-Cre:tdTomatoFlox mice (Fig. 1E) and in adult wild type mice (Fig. 1F). The later experiment showed that Ikzf1 was expressed in all adult tdTomato-positive microglia (Fig. 1E) as well as in all Iba1-positive microglia (Fig. 1F) in adult hippocampi. In this line, Iba1-positive microglia highly colocalized with Ikzf1 in several brain regions namely striatum, septum, amygdala, thalamus, hypothalamus and sensory cortical areas (Suppl. Fig. 3). In the hippocampus Ikzf1 also colocalized with TMEM119 (Suppl. Fig. 4A-B), another microglial marker, but, in contrast, Ikzf1 did not colocalize with either, CD68 or CD206 (Supp. Fig. 4C-D), which are considered to be markers for macrophages or monocytes. Interestingly, other neuronal cells did not show Ikzf1 expression in the adult hippocampus from wild type mice (Fig. 1E), supporting the idea that Ikzf1 is expressed in other particular subpopulations of neuronal cells only during their development, but not during adulthood.

3.2. Ikzf1 deficient mice develop specific spatial memory deficits

Since Ikzf1 is specifically expressed in practically all microglia located in several brain regions such as the hippocampus and sensory and motor cortical areas of adult mice, we then decided to evaluate the impact of such expression in high-order cognitive skills. To do so, we used 7-weeks-old Ikzf1$^{-/-}$ mice. As previously described (Martín-Ibáñez et al., 2010), we first observed that these mice were born with low body weight but when they reach adulthood, although still smaller, the appearance was normal (Fig. 2A). To further address the general health state of these mice a SHIRPA characterization was performed comparing Ikzf1$^{-/-}$ mice with their age-matched wild type (Ikzf1$^{+/+}$) control mice

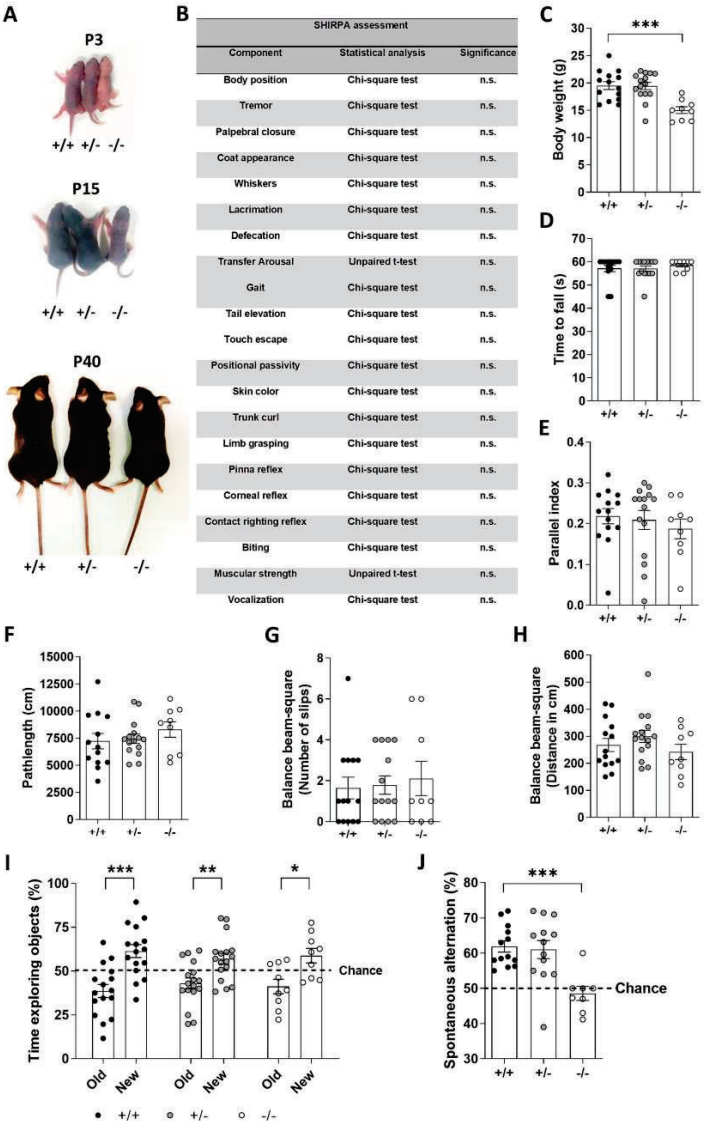

Fig. 2. Behavioral characterization of mice devoid of Ikzf1. (A) Representative images of Ikzf1$^{+/+}$ (+/+), Ikzf1$^{+/-}$ (+/-) and Ikzf1$^{-/-}$ (-/-) mice at postnatal day 3, 15 and 40. (B) SHIRPA characterization of Ikzf1$^{-/-}$ mice compared with Ikzf1$^{+/+}$ mice. Data was analyzed by Student's *t*-test in the case of countable values and by the Chi-square test in the case of uncountable values. (C) Body weight measured in Ikzf1$^{+/+}$, Ikzf1$^{+/-}$ and Ikzf1$^{-/-}$ mice. (C) Muscular strength was measured in Ikzf1$^{+/+}$, Ikzf1$^{+/-}$ and Ikzf1$^{-/-}$ mice with the hanging wire test. Navigation pattern (E) and locomotion/pathlength (F) were measured in Ikzf1$^{+/+}$, Ikzf1$^{+/-}$ and Ikzf1$^{-/-}$ mice with the open field test. Navigation pattern was measured using the parallel index and locomotion using the covered distance (in cm). Motor coordination was measured in Ikzf1$^{+/+}$, Ikzf1$^{+/-}$ and Ikzf1$^{-/-}$ mice by monitoring (G) number of slips and (H) distance traveled in the balance beam test. (I) Long-term recognition memory was assessed in the NORT test. In the NORT, preference for an original object A and a new object B was quantified 24 h after training (old object as *Old*, and new object as *New*). Graphs show the percentage of object preference in Ikzf1$^{+/+}$, Ikzf1$^{+/-}$ and Ikzf1$^{-/-}$ mice. Two-way ANOVA, novelty effect, $F_{(1,\ 70)} = 35.14$, $p < 0.0001$. Group effect, $F_{(2,\ 70)} = 0.5$, $p = 0.999$. (J) In the Y-maze, the spontaneous alternation was measured (as triads) in an 8 min trial in all four genotypes. One-way ANOVA, $F_{(2,\ 31)} = 1.109$, $P = 0.0006$. One-way ANOVA was also performed in C—H. All mice were tested from 6 to 7 weeks of age. Values are means ± SEM. Mice per group; Ikzf1$^{+/+}$ (n = 16), Ikzf1$^{+/-}$ (n = 17) and Ikzf1$^{-/-}$ (n = 9). In I the Tukey's *post hoc* test was used, * $p < 0.05$, ** $p < 0.005$, *** $p < 0.001$ compared with Old. In C and J the Dunnett's *post hoc* test was used *** $p < 0.001$ compared with Ikzf1$^{+/+}$.

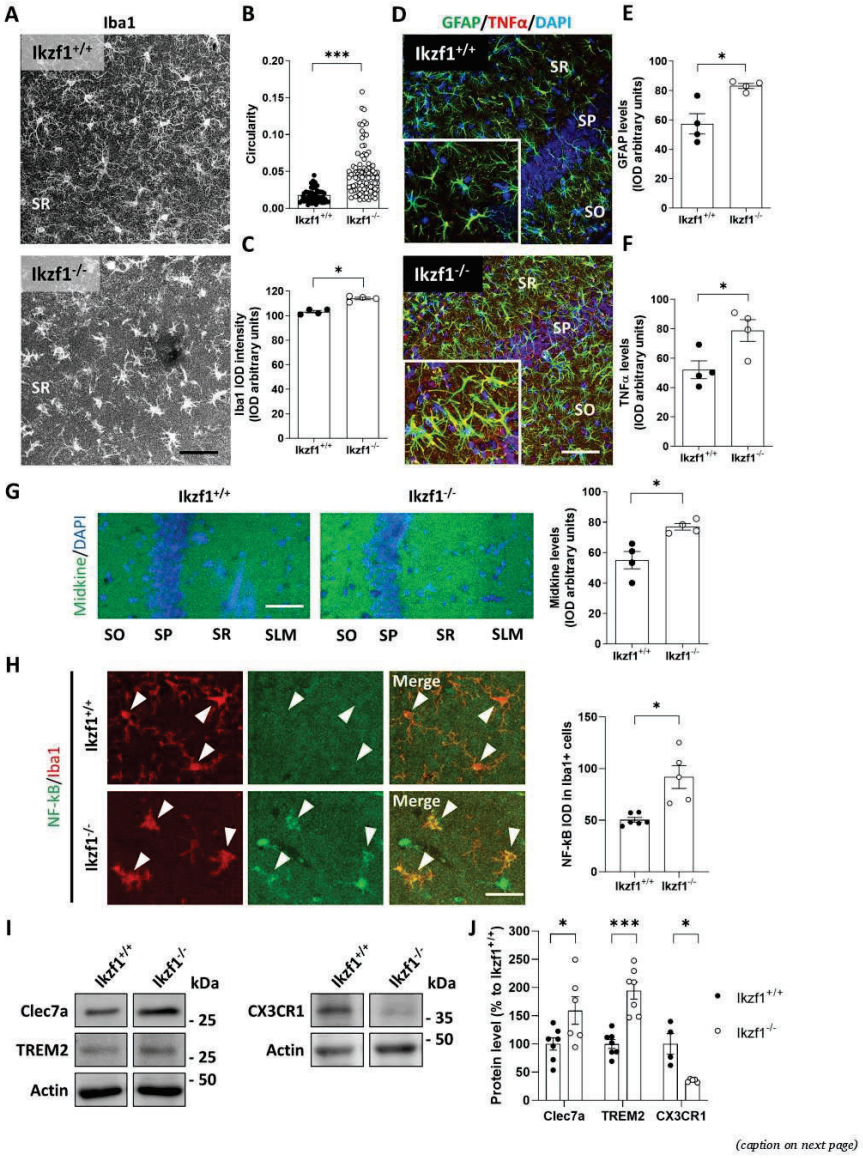

(caption on next page)

Fig. 3. Hippocampal characterization of Ikzf1$^{-/-}$ mice. (A) Representative images of labeled microglia (Iba1) in the CA1 region from Ikzf1$^{+/+}$ and Ikzf1$^{-/-}$ mice. (B) Circularity of Iba1-positive microglia from A was measured in Ikzf1$^{+/+}$ and Ikzf1$^{-/-}$ mice. Mann-Whitney test, U = 565.5, p < 0.0001. (C) Intensity (IOD) of Iba1-positive microglia from A was measured in Ikzf1$^{+/+}$ and Ikzf1$^{-/-}$ mice. Unpaired *t*-test: t = 7,200, df = 6, p = 0.0004. (D) Representative images of stained astrocytes (GFAP, green) co-labeled with TNFα (red) in the CA1 region from Ikzf1$^{+/+}$ and Ikzf1$^{-/-}$ mice. Yellow labelling depicts the GFAP/TNFα colocalization. (E) Intensity (IOD) of GFAP-positive astrocytes from D was measured in Ikzf1$^{+/+}$ and Ikzf1$^{-/-}$ mice. Unpaired *t*-test: t = 3,633, df = 6, p = 0.0109. (F) Intensity (IOD) of TNFα staining in astrocytes from D was measured in Ikzf1$^{+/+}$ and Ikzf1$^{-/-}$ mice. Unpaired *t*-test: t = 2,798, df = 6, p = 0.0301. (G) Left panel, representative images of stained Midkine (green) in the CA1 region from Ikzf1$^{+/+}$ and Ikzf1$^{-/-}$ mice. Right panel, intensity (IOD) of Midkine was measured in Ikzf1$^{+/+}$ and Ikzf1$^{-/-}$ mice. Unpaired *t*-test: t = 3,666, df = 6, p = 0.0105. (H) Left panel, representative images of stained NF-kB (green) and Iba1 (red) in the CA1 region from Ikzf1$^{+/+}$ and Ikzf1$^{-/-}$ mice. Right panel, intensity (IOD) of NF-kB was measured specifically in Iba1-positive microglia from Ikzf1$^{+/+}$ and Ikzf1$^{-/-}$ mice. Unpaired *t*-test: t = 4,023, df = 9, p = 0.0030. (I) Immunoblotting analysis of Clec7a, TREM2 and CX3CR1 and actin as a loading control in 7-weeks-old in Ikzf1$^{+/+}$ and Ikzf1$^{-/-}$ mice. (J) Densitometry quantification of results as in I. Data were normalized to actin for each sample and expressed as percentage of Ikzf1$^{+/+}$. Unpaired *t*-test for Clec7a: t = 2,337, df = 11, p = 0.0394. Unpaired *t*-test for TREM2: t = 5,542, df = 12, p = 0.0001. Unpaired *t*-test for CX3CR1: t = 3,543, df = 7, p = 0.0377. All hippocampal samples were obtained from mice at 6–7 weeks of age. Values are means ± SEM. N = 4–7 mice per group. In A-F three slices containing dorsal hippocampus were used per mouse. Scale bars: In A-D 80 μm, in G 100 μm, in H 25 μm.

(Fig. 2B). No changes in many parameters were detected (Fig. 2B) except for a reduction in the body weight (Fig. 2C) in Ikzf1$^{-/-}$ compared to Ikzf1$^{+/+}$ mice. However, this difference in body weight in Ikzf1$^{-/-}$ mice was not affecting their muscular strength (Fig. 2D). We also evaluated navigation (Fig. 2E) and locomotion (Fig. 2F) in the open field, and no significant differences were detected. Furthermore, gross balance and motor coordination were also similar between groups as assessed by performing the balance beam test (Fig. 2G-H). We then tested higher order cognitive functions such as recognition memory and spatial working memory. We first observed that both, Ikzf1$^{+/+}$ and Ikzf1$^{-/-}$ displayed normal recognition memory in the novel object recognition test (Fig. 2I). However, Ikzf1$^{-/-}$ mice exhibited a significantly impaired spatial working memory in the transparent Y-maze when compared with Ikzf1$^{+/+}$ mice (Fig. 2J). We also noticed that Ikzf1$^{+/-}$ mice were undistinguishable from Ikzf1$^{+/+}$ mice, so we decided to remove this experimental group from the rest of the experiments. Altogether, the results indicated that the major cognitive alteration observed in Ikzf1$^{-/-}$ mice was an impairment in spatial working memory, a function traditionally linked to the hippocampus.

3.3. Specific glial changes in the hippocampus of Ikzf1 deficient mice

We observed that Ikzf1$^{-/-}$ mice show specific impairments on hippocampal-related skills. Thus, we next aimed to characterize the adult hippocampal conformation to detect possible structural deficiencies that could explain such cognitive dysfunction. To rule out the possibility that the loss of neurons in Ikzf1$^{-/-}$ mice is responsible for such cognitive defects, we analyzed neuronal density and observed that neuronal populations such as NeuN-positive neurons (Suppl. Fig. 5A), Parvalbumin-positive neurons (Suppl. Fig. 5B) and Calbindin1-positive neurons (Suppl. Fig. 5C) were unaffected in terms of cell density in the CA1 subarea. Since Ikzf1 is specifically expressed in this cell type in adult brains (Fig. 1F and Supp. Fig. 4B), we then evaluated microglial morphology and their molecular profile in the hippocampus of Ikzf1$^{-/-}$ and Ikzf1$^{+/+}$ mice (Fig. 3A-C). We found that Ikzf1$^{-/-}$ microglia exhibit significantly more rounded shape than Ikzf1$^{+/+}$ microglia (Fig. 3A-B), and Iba1 expression levels analyzed by immunostaining were higher in Ikzf1$^{-/-}$ microglia than in Ikzf1$^{+/+}$ microglia (Fig. 3A and C). We next wanted to test whether these phenotypic changes on Ikzf1$^{-/-}$ microglia were accompanied by changes in other glial cell types such as astroglia, which could indicate a general spreading of neuroinflammation in the brains of Ikzf1$^{-/-}$ mice. Interestingly, we found an increased GFAP immunoreactivity in the CA1 of Ikzf1$^{-/-}$ mice (Fig. 3D-E), concomitant with an increase on TNFα levels in this particular cell type (Fig. 3D and F). Then, we assessed the levels of Midkine (a.k.a. MDK1), a multifunctional cytokine upregulated in neuroinflammation, neurodegeneration and ischemia (Takada et al., 2020). Supporting the results obtained for TNFα, Midkine immunoreactivity was also increased in the CA1 of Ikzf1$^{-/-}$ mice compared with Ikzf1$^{+/+}$ mice (Fig. 3G). These latter results could be indicative of a disease-associated microglia (DAM) signature, which has been related to some neurological disorders (Keren-Shaul et al., 2017; Wang et al., 2022). To further explore this possibility we extended our biochemical studies and observed an upregulation in the expression of NF-kB, a factor that regulates the expression of many genes involved with DAM (Wang et al., 2022), in hippocampal microglia of Ikzf1$^{-/-}$ mice compared with Ikzf1$^{+/+}$ mice (Fig. 3H). Furthermore, we observed an upregulation in Clec7a and TREM2 protein levels, accompanied by downregulated protein levels of CX3CR1 in total hippocampal lysates from Ikzf1$^{-/-}$ mice compared with Ikzf1$^{+/+}$ mice (Fig. 3I-J), supporting the idea that hippocampal microglia devoid of Ikzf1 exhibit a DAM-like profile.

3.4. Ikzf1 deficient mice exhibit impaired hippocampal long-term potentiation, reduced spine density, and increased internalization of synaptic material

Our previous results showed that Ikzf1$^{-/-}$ mice display impaired spatial working memory associated with changes in genes related with DAM (Paolicelli et al., 2022) such as increased Clec7a and TREM2 and reduced CX3CR1 which in turn have been related with neurological disorders such as Alzheimer's disease (Keren-Shaul et al., 2017; Silvin et al., 2022). Therefore, we then tested whether such changes were also related to alterations in structural and functional synaptic plasticity and how impaired microglia could explain such phenomena. First, we found that hippocampal CA3-CA1 long-term potentiation (LTP) was significantly reduced in adult 7-week-old Ikzf1$^{-/-}$ mice when compared with Ikzf1$^{+/+}$ mice (Fig. 4A-B). These alterations were not associated to a presynaptic component since Ikzf1$^{+/+}$ mice showed a normal paired-pulsed facilitation (Fig. 4C), indicating that the post-synaptic component is most likely responsible for such synaptic plasticity alterations. To address this hypothesis, we quantified spine density in apical dendrites of pyramidal neurons in the CA1 in both Ikzf1$^{-/-}$ and Ikzf1$^{+/+}$ mice by performing Golgi staining. We observed that spine density in CA1 pyramidal neurons was reduced in Ikzf1$^{-/-}$ mice compared with Ikzf1$^{+/+}$ mice (Fig. 4D). Given that microglia from Ikzf1$^{-/-}$ mice exhibited a more ameboid morphology than microglia from Ikzf1$^{+/+}$ mice, and such morphology has been linked to highly motile microglia which participate in phagocytosis, we next tested whether the observed synaptic plasticity deficits in Ikzf1$^{-/-}$ mice could be triggered by an increased internalization of synaptic markers. To do so, we performed a double staining for Iba1 and PSD-95 (a post-synaptic marker), and the density of PSD-95-positive clusters as well as its co-localization with Iba1 were analyzed. Co-localization between PSD-95 with Iba1 was increased in the CA1 of Ikzf1$^{-/-}$ mice respect to Ikzf1$^{+/+}$ mice (Fig. 4E-F). Accordingly, we also observed a reduction in the total number of PSD-95-positive clusters in the Ikzf1$^{-/-}$ mice (Fig. 4E and G), suggesting that the lack of microglial Ikzf1 increases microglial phagocytosis of synapses in the hippocampus. In summary, we showed that Ikzf1$^{-/-}$ mice exhibit impaired LTP and reduced spine density in the hippocampus, potentially by increased microglial phagocytosis of synapses.

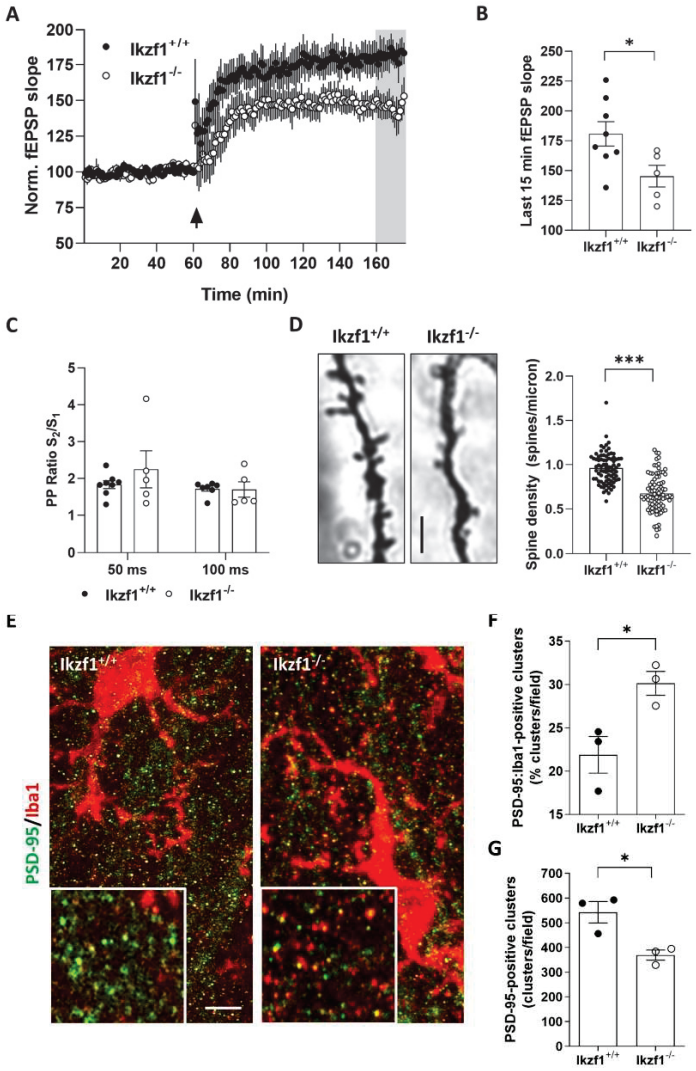

Fig. 4. Characterization of synaptic plasticity in Ikzf1$^{-/-}$ mice. (A) Time course of fEPSP slope (CA3-CA1 LTP) in hippocampal slices from Ikzf1$^{+/+}$ and Ikzf1$^{-/-}$ mice. Arrow indicates theta-burst stimulation (TBS). (B) 15-min average of fEPSP slope 100 min after TBS, normalized to the mean of last 10-min baseline. Unpaired *t*-test: t = 2,381, df = 11, p = 0.0364. (C) Paired-pulse ratio at 50-ms interval and at 100-ms interval at the same synapses. N = 8–5 mice per group (one slice per mouse). (D) Left panel, Golgi-Cox-stained apical dendrites of CA1 *stratum radiatum* pyramidal neurons from Ikzf1$^{+/+}$ and Ikzf1$^{-/-}$ mice. Scale bar, 3 μm. Right panel, quantification of spine density in dendrites as in D. Unpaired *t*-test: t = 9,673, df = 168, p < 0.0001. N = 84–94 dendrites per group from 4 to 5 animals per genotype. (E) Representative images of stained microglia (Iba1, red) co-labeled with PSD-95 (green) in the CA1 region from Ikzf1$^{+/+}$ and Ikzf1$^{-/-}$ mice. Yellow labelling depicts the Iba1/PSD-95 colocalization. (F) Density of double labeled Iba1/PSD-95-positive puncta as in E. Unpaired *t*-test: t = 3,267, df = 4, p = 0.0309. (G) Quantification of single-labeled PSD-95 positive puncta as in D. Unpaired *t*-test: t = 3,608, df = 4, p = 0.0226. All hippocampal samples were obtained from mice at 6–7 weeks of age. Values are means ± SEM. N = 3 mice per group. In E-G three slices containing dorsal hippocampus were used per mouse. Scale bar in E 10 μm.

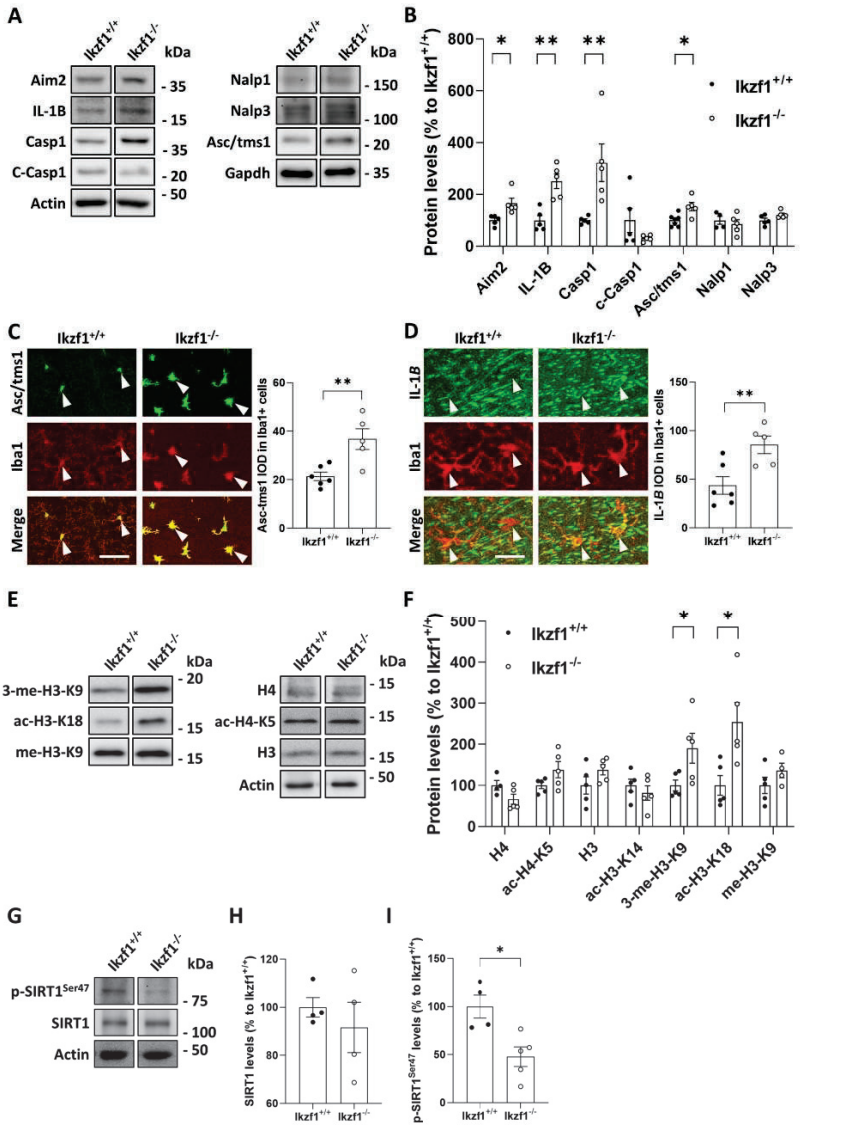

(caption on next page)

Fig. 5. Biochemical characterization of the inflammasome and histone modifications in Ikzf1$^{-/-}$ mice. (A) Immunoblotting analysis of Aim2, IL-1B, Caspase-1 (Casp1), cleaved Caspase-1 (c-Casp1), ASc/tms1, Nalp1 and Nalp3 and actin as a loading control in 7-weeks-old in Ikzf1$^{+/+}$ and Ikzf1$^{-/-}$ mice. (B) Densitometry quantification of results as in A. Data were normalized to actin for each sample and expressed as percentage of wild type. Unpaired *t*-test for Aim2: t = 3,077, df = 8, p = 0.0152. Unpaired *t*-test for IL-1B: t = 4,428, df = 8, p = 0.0022. Unpaired *t*-test for Casp1: t = 3,043, df = 8, p = 0.016. (C) Left panel, representative images of stained Asc-tms1 (green) and Iba1 (red) in the CA1 region from Ikzf1$^{+/+}$ and Ikzf1$^{-/-}$ mice. Right panel, intensity (IOD) of Asc-tms1 was measured in hippocampal microglia (Iba1-positive) from Ikzf1$^{+/+}$ and Ikzf1$^{-/-}$ mice. Unpaired *t*-test: t = 3,548, df = 9, p = 0.0062. (D) Left panel, representative images of stained IL-1B (green) and Iba1 (red) in the CA1 region from Ikzf1$^{+/+}$ and Ikzf1$^{-/-}$ mice. Right panel, intensity (IOD) of IL-1B was measured in hippocampal microglia (Iba1-positive) from Ikzf1$^{+/+}$ and Ikzf1$^{-/-}$ mice. Unpaired *t*-test: t = 3,257, df = 9, p = 0.0099. (E) Immunoblotting analysis of total histone 4 (H4), acetylated H4 in lysine 5 (ac-H4-K5), total histone 3 (H3), acetylated H3 in lysine 14 (ac-H3-K14), three-methylated H3 in lysine 9 (3-me-H3-K9), acetylated H3 in lysine 18 (ac-H3-K18), methylated H3 in lysine 9 (me-H3-K9) and actin as a loading control in 7-weeks-old in Ikzf1$^{+/+}$ and Ikzf1$^{-/-}$ mice. (F) Densitometry quantification of results as in E. Data were normalized to actin for each sample and expressed as percentage of wild type. Unpaired *t*-test for 3-me-H3-K9: t = 2,330, df = 8, p = 0.00482. Unpaired *t*-test for ac-H3-K18: t = 2,913, df = 8, p = 0.0195. (G) Immunoblotting analysis of total SIRT1 levels (SIRT1), phosphorylation levels at Serine 47 in SIRT1 (p-SIRT1^{Ser47}) and actin as a loading control in 7-weeks-old in Ikzf1$^{+/+}$ and Ikzf1$^{-/-}$ mice. (H) Densitometry quantification of results as in G for total SIRT1. (I) Densitometry quantification of results as in G for p-SIRT1^{Ser47}. Data were normalized to actin for each sample and expressed as percentage of wild type. Unpaired *t*-test for p-SIRT1^{Ser47}: t = 3,333, df = 7, p = 0.0125. Values are means ± SEM. N = 5 mice per group. Scale bar in C 40 μm and in D 15 μm.

3.5. Alterations in the inflammasome composition and impaired histone methylation are molecular signatures in the hippocampus of Ikzf1 deficient mice

We have shown that Ikzf1$^{-/-}$ mice exhibited a strong phenotype in the hippocampus. Interestingly, Ikzf1 has been shown to regulate the inflammasome response in stressed macrophages in the liver (Kadono et al., 2022), and regulate epigenetic changes in immune circulating cells through multiple mechanisms (Kim et al., 1999; Koipally and Georgopoulos, 2000). Importantly, inflammasome response is regulated by epigenetic mechanisms involving histones acetylation/methylation rates (Poli et al., 2020). Given the DAM-like signature exhibited by Ikzf1$^{-/-}$ mice, we next asked whether the inflammasome composition could be altered in Ikzf1$^{-/-}$ mice hippocampi and whether epigenetic changes were responsible, at least in part, for such inflammasome activation in microglia.

First, we evaluated several molecular components of the inflammasome by western blot in hippocampal total lysates from adult (7-week-old) Ikzf1$^{+/+}$ and Ikzf1$^{-/-}$ mice. Interestingly, there were changes in different directions. First, Nalp1, Nalp3 and cleaved-Caspase1 protein levels did not change between genotypes (Fig. 5A-B). However, protein levels of Caspase-1, IL-1B, Asc-tms1 and Aim2 were upregulated in Ikzf1$^{-/-}$ mice compared with Ikzf1$^{+/+}$ mice (Fig. 5A-B). We confirmed that these changes were located in hippocampal microglia specifically for Asc-tms1 (Fig. 5C) and IL-1B (Fig. 5D). These results indicated that several alterations in many components of the inflammasome accompanied the microglia phenotype observed in Ikzf1$^{-/-}$ mice.

We then aimed to study whether such inflammasome activation in microglia correlate with epigenetic changes. Thus, we analyzed histone 3 (H3) and 4 (H4) total protein levels and its levels of acetylation and methylation in different residues in hippocampal total lysates from adult (7-week-old) Ikzf1$^{+/+}$ and Ikzf1$^{-/-}$ mice by western blot. We detected similar levels of total H4, total H3 and acetylated H4 in lysine 5 between adult Ikzf1$^{+/+}$ and Ikzf1$^{-/-}$ mice (Fig. 5E, F). Next, we analyzed acetylation levels of H3 in lysine 14, the three-methylation levels of lysine 9, the acetylation levels of lysine 18 and the levels of methylation in lysine 9 (Fig. 5E-F). We found specific increases in the three-methylation levels of lysine 9 and acetylation levels of lysine 18 in Ikzf1$^{-/-}$ mice compared with Ikzf1$^{+/+}$ mice (Fig. 5E-F).

It has been recently shown that Ikzf1 regulates the inflammasome-pyroptosis response in stressed macrophages in a SIRT1-dependent manner (Kadono et al., 2022). Therefore, we evaluated total and phosphorylation levels of SIRT1 in the hippocampi of Ikzf1$^{+/+}$ and Ikzf1$^{-/-}$ mice. We observed that whereas total hippocampal SIRT1 levels were similar in both genotypes (Fig. 5G-H), phosphorylation levels at serine 47 of SIRT1 were reduced in Ikzf1$^{-/-}$ mice compared with Ikzf1$^{+/+}$ mice (Fig. 5G and I). These results suggest that lack of hippocampal Ikzf1 expression is associated with changes in the levels of methylation and acetylation levels of the Histone 3 probably due to an alteration of the SIRT1-Ikzf1 axes.

3.6. Ikzf1 levels are increased during hippocampal-induced inflammation, in temporal lobe epilepsy models and in Alzheimer's disease

Our later results indicated that a lack of Ikzf1 expression in the hippocampus is associated with several processes of neuroinflammation from a reactive microgliosis to an altered composition of the inflammasome. Therefore, we hypothesized that Ikzf1 levels could be altered in disease models with hippocampal dysfunction. First, in order to generate a model of inflammation, we systemically treated wild type (WT) mice at postnatal day 5 (PN5) with LPS (6 mg/kg) and 24 h later their brains were fixed and stained with Iba1 and Ikzf1 antibodies (Fig. 6A-C). We observed that LPS induced a robust increase on Iba1 and Ikzf1 staining in the dorsal hippocampus as well as in their colocalization (Fig. 6A-C) since the majority, but not all, Iba1-positive cells were also Ikzf1-positive. However, the LPS model was not performed in adult mice. Due to this limitation, we then tested the levels of hippocampal Ikzf1 in a model of temporal lobe epilepsy (TLE) induced by pilocarpine (Fig. 6D-E) in adult mice. We observed a strong microgliosis in hippocampi from mice treated with pilocarpine (Fig. 6D), which correlated with increased expression levels of Ikzf1 (Fig. 6E). Then, we evaluated Ikzf1 protein levels in a transgenic mouse model of Alzheimer's disease (AD), the 5xFAD mouse model which is characterized by β-Amyloid accumulation, microgliosis and astrogliosis (Oakley et al., 2006). We found that Ikzf1 levels were also increased in the hippocampus of 8-months-old 5xFAD mice compared with their matched WT controls (Fig. 6F). To further evaluate whether those changes in 5xFAD mice could also be observed in AD patients, we analyzed Ikzf1 levels in post-mortem hippocampal samples from human control and AD individuals. Similar to what we found in animal models, AD patients exhibited increased Ikzf1 levels compared to control individuals (Fig. 6G). Altogether, the present results indicated that models of inflammation and neurodegeneration as well as samples from human subjects with dementia and neurodegeneration display a hippocampal increase of Ikzf1 levels.

3.7. Over-expression of Ikzf1 in cultured microglia reduces their response to LPS and prevents microglial phagocytosis of beads

Our results indicated that Ikzf1 is only expressed in microglia in the adult brain, and that lack of microglial Ikzf1 in mice induce significant changes in microglia morphology and function with several alterations in synaptic plasticity and hippocampal-dependent memory. Also, several models of neurodegeneration show an increase on Ikzf1 levels. Although collectively these data may appear contradictory, we hypothesized that Ikzf1 could act as a regulator of microglia homeostasis. To further support this hypothesis, we performed over-expression experiments in cultured microglia. We predicted that, if Ikzf1 levels are regulating microglia functional homeostasis as stated above, microglia over-expressing Ikzf1 would be unable to respond adequately to different insults. We thus transfected microglia cultures with a plasmid

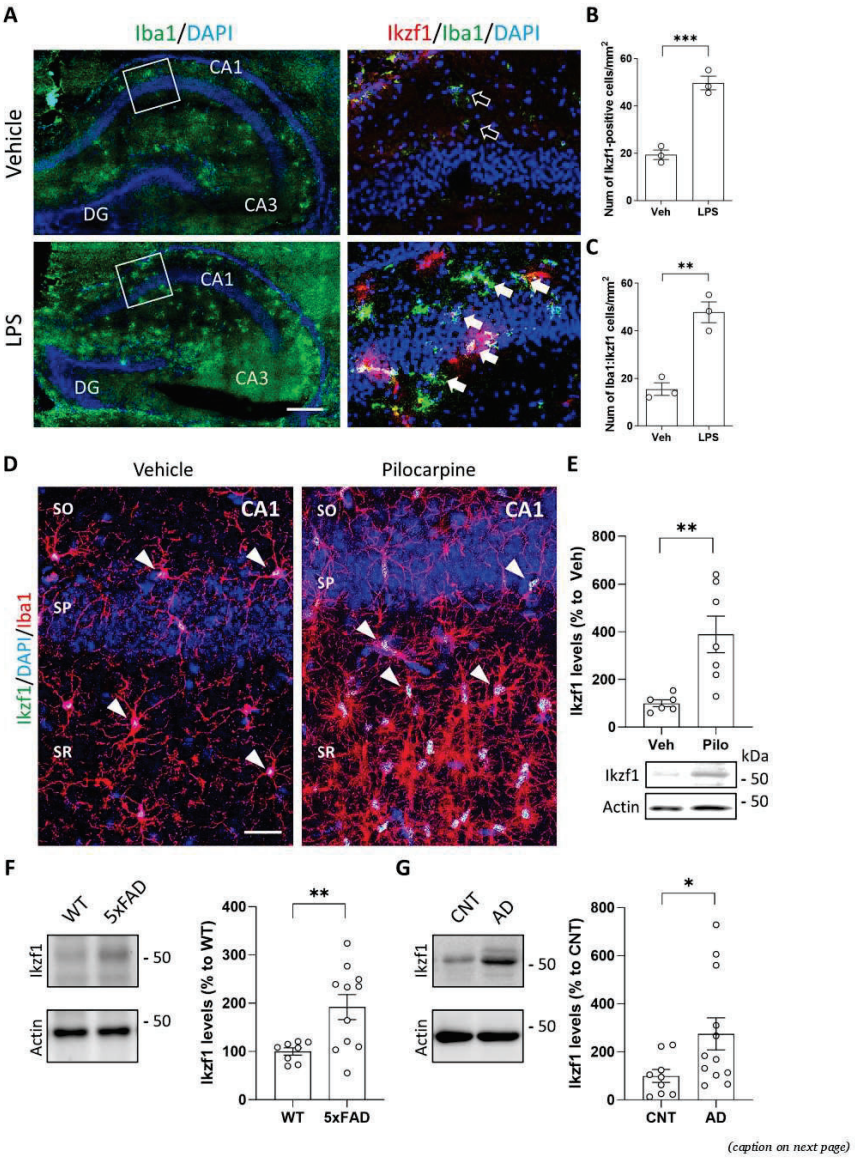

(caption on next page)

Fig. 6. Characterization of Ikzf1 expression in models of neuroinflammation and neurodegeneration. (A) Left panels, representative images of labeled microglia (Iba1) and Ikzf1 (red) in the CA1 region from wild type mouse pups treated with vehicle or lipopolysaccharides (LPS 6 mg/kg). Mice were injected with LPS 6 mg/kg at postnatal day 5 and 24 h later their brains were fixed and processed for immunofluorescence. Right panels, inset from left panel for each condition (vehicle or LPS). Black arrows show Iba1-positive microglia (green) with very low Ikzf1 (red) protein levels. White arrows are depicting high Ikzf1 (red) protein levels in LPS exposed microglia (green). Note Ikzf1 has a specific nuclear staining. (B) Number of Ikzf1-positive cells per area from D was measured in vehicle and LPS treated mouse pups. Unpaired *t*-test: t = 8,663, df = 4, p = 0.0010. (C) Number of double positive Ikzf1/Iba1 cells per area from D was measured in vehicle and LPS treated mouse pups. Unpaired *t*-test: t = 6,314, df = 4, p = 0.0032. (D) Representative images of labeled microglia (Iba1) and Ikzf1 (red) in the CA1 region from adult (12-weeks-old) wild type mice treated with vehicle or pilocarpine. Mice were injected with pilocarpine (45 mg/kg, see methods) at 10,5 weeks of age and 10 days later their brains were fixed and processed for immunofluorescence. (E) Left panel, immunoblotting analysis of hippocampal Ikzf1 and actin as a loading control in wild type mice treated with vehicle or pilocarpine from D. Right panel, densitometry quantification of results as in left panel. Unpaired *t*-test: t = 3,429, df = 11, p = 0.0056. (F) Left panel, immunoblotting analysis of hippocampal Ikzf1 and actin as a loading control in wild type (WT) or in the mouse model of Alzheimer's disease so-called 5xFAD mice. Blots were performed at 8 months of age at an age when these 5xFAD mice display clear cognitive and histopathological phenotypes compared with WT mice. Right panel, densitometry quantification of results as in the left panel. Unpaired *t*-test: t = 2,967, df = 17, p = 0.0086. (G) Left panel, immunoblotting analysis of hippocampal Ikzf1 and actin as a loading control in hippocampal postmortem samples from control patients (CNT) and patients with Alzheimer's Disease (AD). Right panel, densitometry quantification of results as in the left panel. Unpaired *t*-test: t = 2,130, df = 17,54, p = 0.0476. In all blots data were normalized to actin for each sample and expressed as percentage of wild type or control samples. Scale bars: In A 150 μm, in D 50 μm. Values are means ± SEM. Number of samples per group: In B and C n = 3 mice per group, in E n = 6–8, in F n = 8–11, in G n = 9–12.

to over-express Ikzf1. Although microglia are difficult to be transfected, we performed several microglia cultures in order to achieve a satisfactory number of transfected microglia.

Cultured microglia were transfected with a control vector (CNT) or with an Ikzf1 over-expressing vector (Ikzf1). In a first set of experiments, we treated microglia with vehicle (Veh) or 100 ng/ml of LPS and analyzed the area and circularity of such cultured microglia. Interestingly, while LPS-treated control microglia exhibited increase area (Fig. 7A-B) and circularity (Fig. 7A and C), microglia over-expressing Ikzf1 showed no response when treated with LPS either in terms of cell area (Fig. 7A-B) or in terms of circularity (Fig. 7A and C). In a second set of experiments, cultured microglia were subjected to a phagocytosis assay using latex-based nano-beads. Interestingly, we found that microglial phagocytosis of beads was significantly reduced in microglia over-expressing Ikzf1 compared with microglia transfected with the control vector (Fig. 7D-E). Our results point out the possibility that when Ikzf1 is over-expressed in *in vitro* microglia, these cells lose their ability to react in front of distinct perturbations.

4. Discussion

In the present work, we show that Ikzf1 is expressed specifically in hippocampal adult microglia. We found that the lack of Ikzf1 expression in hippocampal microglia of Ikzf1$^{-/-}$ mice triggers a variety of morphological and functional changes in these cells, including a switch to a more ameboid morphology, traditionally associated with higher activity and increased phagocytic capacity. Such changes were accompanied by astrogliosis and variations in several associated-disease markers. Interestingly, hippocampal dendritic spine density and CA3-CA1 long-term-potentiation (LTP) were reduced in Ikzf1$^{-/-}$ mice, probably due to an aberrant microglia-mediated phagocytosis of PSD-95-positive synapses/clusters. At functional level, all these alterations were accompanied with impaired spatial memory in Ikzf1$^{-/-}$ mice. As a potential underlying molecular mechanism, we identified a significant alteration in the inflammasome composition and changes in epigenetic signatures, which could explain the observed phenotype. To study whether altered expression of Ikzf1 could play a role in inflammatory and neurological disorders characterized by neuroinflammation, and synaptic and cognitive dysfunction, we then analyzed Ikzf1 expression in several models of neuroinflammation and neurodegeneration and found that microglial Ikzf1 levels were increased in all of them. Altogether we suggest that Ikzf1 levels and function play a role in the control of microglia homeostasis, and that adequate Ikzf1 expression in microglia is required for the appropriate expression of genes such as NF-kB, IL-1B and Asc-tms1, as well as to maintain its shape and morphology. According to this hypothesis, we showed in *in vitro* assays that microglial responses (i.e. morphological changes) to an inflammatory-like stimulus (i.e. LPS) was abolished when Ikzf1 was overexpressed. Moreover, microglial phagocytosis was found to be compromised when Ikzf1 was overexpressed in cultured microglia.

As far as we know this is the first time demonstrating a specific expression of Ikzf1 in adult microglia, perhaps not surprising given that microglia have a myeloid origin (Li and Barres, 2018) and Ikzf1 is also expressed in circulating monocytes and other macrophages (Faia et al., 2021; Oh et al., 2018; Yagi et al., 2002), all of them sharing a myeloid origin. Importantly, our results change the traditional view in which it was postulated that Ikzf1 is expressed in the brain, only during development and in a particular set of neurons namely medium spiny neurons of the striatum and some pyramidal neurons of the cortex (Agoston et al., 2007; Alsiö et al., 2013; Martín-Ibáñez et al., 2010). Although we have validated such expression using the Ikzf1-Cre:tdTomatoFlox mice, our results demonstrate that the only cells in the adult brain of WT mice that expresses detectable levels of Ikzf1 are microglia.

In order to investigate the possible relevance of Ikzf1 expression in the adult microglia we used the Ikzf1 deficient mice (Ikzf1$^{-/-}$ mice). Microglia morphology in Ikzf1$^{-/-}$ mice acquire a more round-ameboid morphology and exhibit increased expression of Iba1 compared to control mice. Supporting a possible mechanism of 'microglia responsiveness' in these mice, we observed an increased expression of TNFα, NF-kB and MDK1, general markers of neuroinflammation. However, we cannot rule out the participation of reactive astrocytes to such neuroinflammatory signature, as Ikzf1$^{-/-}$ mice also exhibit astrogliosis and both TNFα and MDK1 are also markers of reactive astrocytes (Kumar et al., 2022; Takada et al., 2020; Zahedipour et al., 2022). Nonetheless, our data strongly indicate that the lack of Ikzf1$^{-/-}$ in the adult brain, expressed in microglia but not astrocytes or neurons, lead to neuroinflammation. Thus, we postulated that Ikzf1 could emerge as a modulator of microglial response in neuroinflammation and neurodegeneration. To test this hypothesis, we evaluated Ikzf1 levels in a model of neuroinflammation (lipopolysaccharide or LPS), (Domínguez-Rivas et al., 2021), in a model of temporal lobe epilepsy with associated hippocampal neurodegeneration and sclerosis (Pilocarpine-based model) (Curia et al., 2008), and in a transgenic mouse model of AD (5xFAD mice) (Oakley et al., 2006). Surprisingly, hippocampal Ikzf1 levels were found to be increased in all studied disease-related models, and such increase was also found in hippocampal postmortem samples of AD patients. Therefore, we suggest that, if lack of Ikzf1 induces neuroinflammation and Ikzf1 levels are increased in neurodegenerative diseases, then Ikzf1 could be a potential regulator of microglia homeostasis or even its increased expression levels in such neurological disorders could play a compensatory or neuroprotective role. In this line, we found that overexpression of Ikzf1 in cultured microglia, abolished the response of these cells in artificial paradigms such as LPS or phagocytosis of latex nano-beads, indicating that adequate levels of Ikzf1 are required to maintain appropriate microglial responses. For instance, microglial phagocytosis has multiple beneficial but also

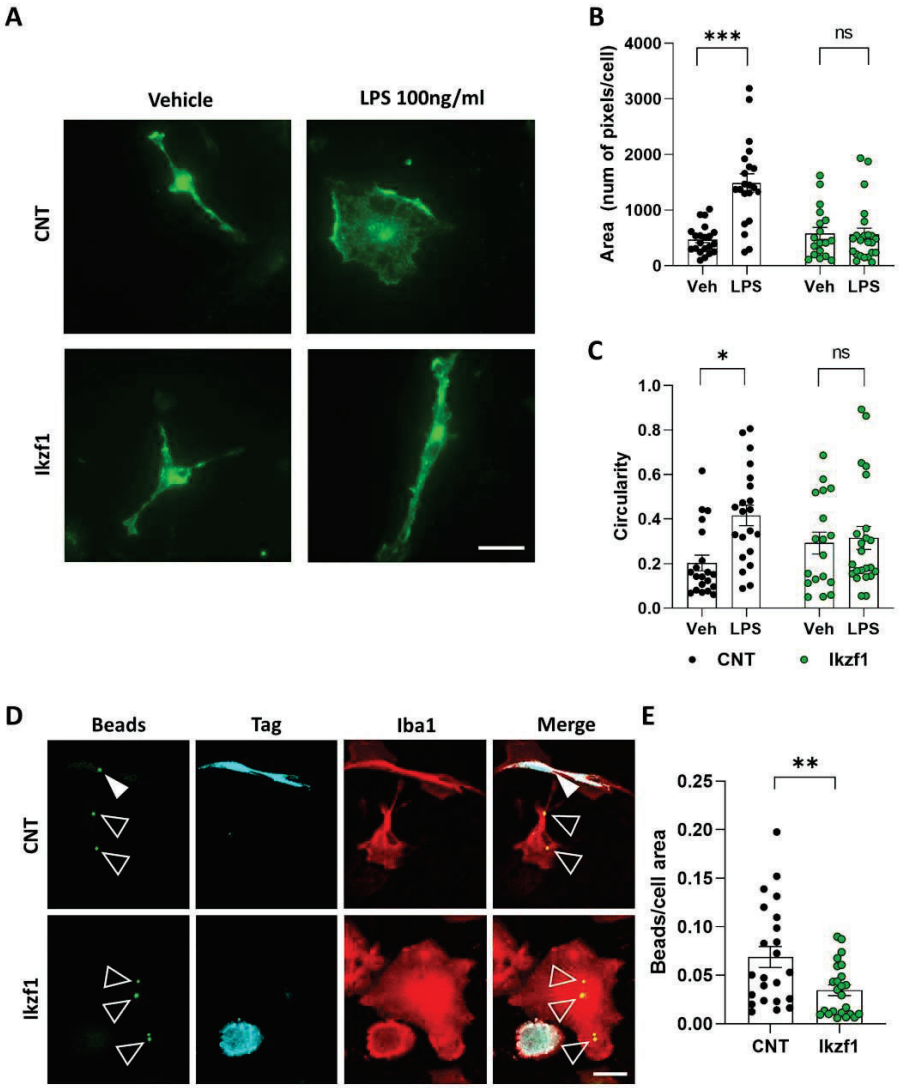

Fig. 7. Characterization of Ikzf1 expression in models of neuroinflammation and neurodegeneration. (A) Representative images of cultured and transfected microglia treated with vehicle or lipopolysaccharides (100 ng/ml) for 24 h. Only microglia transfected with control vector or Ikzf1-overexpressing vector were used for morphological analyses. (B) Cell area was estimated in transfected microglia from A. Two-way ANOVA, interaction effect, $F_{(1, 79)} = 19.34$. Bonferroni's multiple comparisons test was used as a *post hoc* test. (C) Circularity was estimated in transfected microglia from A. Two-way ANOVA, interaction effect, $F_{(1, 78)} = 4.162$. Bonferroni's multiple comparisons test was used as a *post hoc* test. N = 18–23 transfected cells per condition. (D) Representative images of cultured and transfected microglia with control vector or Ikzf1-overexpressing vector. These cells were exposed to a bath application of latex nano-beads (green) and number of "phagocytosed" nano-beads was quantified (E) only in transfected (tag in turquoise) microglia (Iba1-positive in red) and normalized per area and per cell. Unpaired *t*-test: t = 2,859, df = 45, p = 0.0064. N = 18–23 transfected cells per condition. Values are means ± SEM. Scale bars in A and D = 25 μm.

detrimental roles in inflammation and neurodegeneration, and this may also change during disease progression (reviewed in Butler et al., 2021). Thus, our novel results showing that Ikzf1 is specifically expressed in microglia in the adult brain and deregulation of its expression leads to altered phagocytic capacity (both ways, by increasing and abolishing microglial phagocytosis), present Ikzf1 as a novel indicator of microglia homeostasis and a potential molecular target to normalize microglial function (i.e. phagocytic function) in disease context.

By further addressing the relevance of Ikzf1 expression in adult microglia we found that Ikzf1$^{-/-}$ mice displayed impaired spatial memory, decreased spine density in CA1 pyramidal neurons accompanied by reduced PSD-95-positive clusters and reduced long-term-potentiation (LTP) in the same CA3-CA1 circuit. It is broadly accepted that normal hippocampal spine density (Mahmmoud et al., 2015), expression of LTP (Lynch, 2004) and appropriate PSD-95 levels (Caly et al., 2021) are all necessary for adequate spatial memory. Interestingly, recent works have shown that microglia can regulate or influence all of them. Thus, microglia have been shown to regulate spine density and PSD-95 expression in disease conditions (Geloso and D'Ambrosi, 2021; Sellgrenet al., 2019), LTP expression (Zhou et al., 2019), and spatial learning and memory (Cornell et al., 2022). Given that microglia are able to regulate this wide range of processes and that lack of microglial Ikzf1 in mice compromised all of them, our results suggest that Ikzf1 could be a novel core molecule located in microglia capable to regulate all these processes. To further support our hypothesis it has been shown in genome-wide association (GWAS) studies that the *IKZF1* gene has been associated with hippocampal atrophy and Alzheimer's disease (Potkin et al., 2009; Schwartzentruber et al., 2021). However, despite the evidence discussed above, we cannot rule out an indirect neurodevelopmental effect mediated by altered neurons from Ikzf1$^{-/-}$ mice since Ikzf1 is also expressed in some neurons during development (Alsiö et al., 2013; Martín-Ibáñez et al., 2010).

At a molecular level, we investigated how Ikzf1 levels could exert its effects on microglial response and function. First, we investigated the inflammasome composition since its role in microglial function during neuroinflammatory challenges is crucial (Mata-Martínez et al., 2022). We found a significant alteration in several members of this protein macro complex which could in turn induce the aberrant increased microglial responses (Scholz and Eder, 2017) observed in Ikzf1$^{-/-}$ mice. Indeed, microgliosis *per se* is associated to spatial memory deficits in several models (Wadhwa et al., 2017), including AD (Chesworth et al., 2021). Also, alterations in several components of the inflammasome have been linked to compromised spatial memory function (Cheon et al., 2020; Sun et al., 2021). In particular, we found that Ikzf1$^{-/-}$ mice exhibited changes on hippocampal Aim2, involved in the inflammasome assembly (de Rivero Vaccari et al., 2014; Lamkanfi and Dixit, 2014). More importantly, we also found increased caspase-1 and IL-1β in the hippocampus of Ikzf1$^{-/-}$ mice. Since caspase-1 regulates the maturation of pro-inflammatory IL-1β (Mangan et al., 2018), which is also upregulated in Ikzf1$^{-/-}$ mice, those changes could orchestrate a possible initiation of an inflammatory form of cell dysfunction, named pyroptosis (Kayagaki et al., 2011; Mangan et al., 2018; Yi, 2017) which in turn, could lead to hippocampal dysfunction and associated spatial memory deficits observed in Ikzf1$^{-/-}$ mice. Such changes in protein levels of these macro complexes could be due to variations in gene transcription. One way in which Ikzf1 could modulate gene expression is through epigenetic modifications, in particular the regulation of histone methylation/acetylation rates (Song et al., 2016). Indeed, Ikzf1 has been shown to regulate the inflammasome response in stressed macrophages in the liver (Kadono et al., 2022). Also, it is postulated that regulation of histone acetylation/methylation rates plays crucial roles in memory function (Levenson et al., 2004; Maity et al., 2021) and, more recently, in modulating the expression of several components of the inflammasome multiprotein complex (Raneros et al., 2021). In this line, we found a specific increase on hippocampal 3-m-H3-Lys9 levels in Ikzf1$^{-/-}$ mice, which agrees with Ikzf1 ability to increase three-methyl levels of other H3 lysins such as Lys27 (Wang et al., 2016). Furthermore, previous reports support our results by showing that increased 3-m-H3-Lys9 is associated with spatial memory deficits and reduced BDNF levels (Wu et al., 2019). Finally, we also found that the lack of Ikzf1 could alter the SIRT1-Ikzf1 axes which is an important mechanism for the deacetylase activity in histones (Kadono et al., 2022). Also, such alteration in SIRT1 function could provoke an induction of the inflammasome (Li et al., 2017, Li et al., 2016). Thus, hippocampal changes in inflammasome components and increased 3-m-H3-Lys9 levels likely induced by an alteration in the SIRT1-Ikzf1 axes could be contributing to the presence of spatial memory deficits in Ikzf1$^{-/-}$ mice.

It is noteworthy that our study has some limitations. First, the Ikzf1$^{-/-}$ mouse model is a full *knockout* mouse model, so we cannot rule out that the effects observed were also due to different cells other than microglia exclusively since during development Ikzf1 is expressed in other brain cells. Second, although the lack of Ikzf1 correlates with astrogliosis, we do not know whether these neuroinflammatory processes (namely microgliosis and astrogliosis) occur simultaneously or one triggers the other one. Finally, the biggest challenge and limitation of our study is the lack of current methods to appropriately transfect or infect microglia *in vivo* to modulate Ikzf1 levels, without altering microglia state due to methodology.

In summary, we found that Ikzf1 plays a key role in the maintenance of microglial homeostasis and that alterations on its levels or function have an impact in hippocampal neural plasticity and related cognitive function.

Declaration of Competing Interest

The authors declare that they have no known competing financial interests or personal relationships that could have appeared to influence the work reported in this paper.

Data availability

Data will be made available on request.

Acknowledgements

AG is a Ramón y Cajal fellow (RYC-2016-19466). This work is supported by grants PID2021-122258OB-I00 (A.G.), PID2021-125785OA-I00 (M.P.), PID2020-119305RB-I00 (X.G.), PID2020-119386RB-100 (J.A. and MJ.R.), and PID2020-119932GB-I00 (D.S.) funded by MCIN/AEI/ 10.13039/501100011033. This work was also supported by grants from Ministerio de Ciencia e Innovación RTI2018-099001-B-I00 (J.M.C.), by Instituto de Salud Carlos III and European Regional Development Fund (ERDF) (Red de Terapia Celular, RD16/0011/0012), and Generalitat de Catalunya (2017SGR-1408). We also thank Ana López (María de Maeztu Unit of Excellence, Institute of Neurosciences, University of Barcelona, MDM-2017-0729, Ministry of Science, Innovation and Universities) for technical support. We thank María Calvo from the Advanced Microscopy Service (Centres Científics i Tecnològics Universitat de Barcelona) for her help in the acquisition, analysis, and interpretation of the confocal images. We thank Professor Michelle Cayouette for providing the Ikzf1-Cre mice. We also thank Professor Katia Georgopoulos for providing the Ikzf1$^{-/-}$ mice.

Appendix A. Supplementary data

Supplementary data to this article can be found online at https://doi.org/10.1016/j.bbi.2023.01.016.

References

Agoston, D.V., Szemes, M., Dobi, A., Palkovits, M., Georgopoulos, K., Gyorgy, A., Ring, M.A., 2007. Ikaros is expressed in developing striatal neurons and involved in

enkephalinergic differentiation. J. Neurochem. 102, 1805–1816. https://doi.org/10.1111/j.1471-4159.2007.04653.x.
Alsiö, J.M., Tarchini, B., Cayouette, M., Livesey, F.J., 2013. Ikaros promotes early-born neuronal fates in the cerebral cortex. Proc. Natl. Acad. Sci. 110 https://doi.org/10.1073/pnas.1215707110.
Boast, B., de Nunes-Santos, C.J., Kuehn, H.S., Rosenzweig, S.D., 2021. Ikaros-associated diseases: from mice to humans and back again. Front. Pediatr. 9 https://doi.org/10.3389/fped.2021.705497.
Butler, C.A., Popescu, A.S., Kitchener, E.J.A., Allendorf, D.H., Puigdellívol, M., Brown, G. C., 2021. Microglial phagocytosis of neurons in neurodegeneration, and its regulation. J. Neurochem. 158, 621–639. https://doi.org/10.1111/jnc.15327.
Cały, A., Śliwińska, M.A., Ziółkowska, M., Łukasiewicz, K., Pagano, R., Dzik, J.M., Kalita, K., Bernaś, T., Stewart, M.G., Giese, K.P., Radwanska, K., 2021. PSD-95 in CA1 area regulates spatial choice depending on age. J. Neurosci. 41, 2329–2343. https://doi.org/10.1523/JNEUROSCI.1996-20.2020.
Cheon, S.Y., Kim, J., Kim, S.Y., Kim, E.J., Koo, B.-N., 2020. Inflammasome and cognitive symptoms in human diseases: biological evidence from experimental research. Int. J. Mol. Sci. 21, 1103. https://doi.org/10.3390/ijms21031103.
Chesworth, R., Gamage, R., Ullah, F., Sonego, S., Millington, C., Fernandez, A., Liang, H., Karl, T., Münch, G., Niedermayer, G., Gyengesi, E., 2021. Spatial memory and microglia activation in a mouse model of chronic neuroinflammation and the anti-inflammatory effects of apigenin. Front. Neurosci. 15 https://doi.org/10.3389/fnins.2021.699329.
Cornell, J., Salinas, S., Huang, H.-Y., Zhou, M., 2022. Microglia regulation of synaptic plasticity and learning and memory. Neural Regen. Res. 17, 705. https://doi.org/10.4103/1673-5374.322423.
Cuadros, M., 1998. The origin and differentiation of microglial cells during development. Prog. Neurobiol. 56, 173–189. https://doi.org/10.1016/S0301-0082(98)00035-5.
Curia, G., Longo, D., Biagini, G., Jones, R.S.G., Avoli, M., 2008. The pilocarpine model of temporal lobe epilepsy. J. Neurosci. Methods 172, 143–157. https://doi.org/10.1016/j.jneumeth.2008.04.019.
De Biase, L.M., Schuebel, K.E., Fusfeld, Z.H., Jair, K., Hawes, I.A., Cimbro, R., Zhang, H.-Y., Liu, Q.-R., Shen, H., Xi, Z.-X., Goldman, D., Bonci, A., 2017. Local cues establish and maintain region-specific phenotypes of basal ganglia microglia. Neuron 95, 341–356.e6. https://doi.org/10.1016/j.neuron.2017.06.020.
de Pins, B., Cifuentes-Díaz, C., Thamila Farah, A., López-Molina, L., Montalban, E., Sancho-Balsells, A., López, A., Ginés, S., Delgado-García, J.M., Alberch, J., Gruart, A., Girault, J.-A., Giralt, A., 2019. Conditional BDNF delivery from astrocytes rescues memory deficits, spine density and synaptic properties in the 5xFAD mouse model of Alzheimer disease. J. Neurosci. 2121–18 https://doi.org/10.1523/JNEUROSCI.2121-18.2019.
de Rivero Vaccari, J.P., Dietrich, W.D., Keane, R.W., 2014. Activation and regulation of cellular inflammasomes: gaps in our knowledge for central nervous system injury. J. Cereb. Blood Flow Metab. 34, 369–375. https://doi.org/10.1038/jcbfm.2013.227.
Domínguez-Rivas, E., Ávila-Muñoz, E., Schwarzacher, S.W., Zepeda, A., 2021. Adult hippocampal neurogenesis in the context of lipopolysaccharide-induced neuroinflammation: a molecular, cellular and behavioral review. Brain. Behav. Immun. 97, 286–302. https://doi.org/10.1016/j.bbi.2021.06.014.
El Hajj, H., Savage, J.C., Bisht, K., Parent, M., Vallières, L., Rivest, S., Tremblay, M.-È., 2019. Ultrastructural evidence of microglial heterogeneity in Alzheimer's disease amyloid pathology. J. Neuroinflammation 16, 87. https://doi.org/10.1186/s12974-019-1473-9.
Faia, C., Plaisance-Bonstaff, K., Vittori, C., Wyczechowska, D., Lassak, A., Meyaski-Schluter, M., Reiss, K., Peruzzi, F., 2021. Attenuated negative feedback in monocyte-derived macrophages from persons living with HIV: a role for IKAROS. Front. Immunol. 12 https://doi.org/10.3389/fimmu.2021.785905.
Frost, J.L., Schafer, D.P., 2016. Microglia: architects of the developing nervous system. Trends Cell Biol. 26, 587–597. https://doi.org/10.1016/j.tcb.2016.02.006.
Geloso, M.C., D'Ambrosi, N., 2021. Microglial pruning: relevance for synaptic dysfunction in multiple sclerosis and related experimental models. Cells 10, 686. https://doi.org/10.3390/cells10030686.
Georgopoulos, K., 2002. Haematopoietic cell-fate decisions, chromatin regulation and ikaros. Nat. Rev. Immunol. 2, 162–174. https://doi.org/10.1038/nri747.
Georgopoulos, K., Winandy, S., Avitahl, N., 1997. The role of the ikaros gene in lymphocyte development and homeostasis. Annu. Rev. Immunol. 15, 155–176. https://doi.org/10.1146/annurev.immunol.15.1.155.
Giralt, A., Carretón, O., Lao-Peregrin, C., Martín, E.D., Alberch, J., 2011. Conditional BDNF release under pathological conditions improves Huntington's disease pathology by delaying neuronal dysfunction. Mol. Neurodegener. 6, 71. https://doi.org/10.1186/1750-1326-6-71.
Giralt, A., Sanchis, D., Cherubini, M., Ginés, S., Cañas, X., Comella, J.X., Alberch, J., 2013. Neurobehavioral characterization of Endonuclease G knockout mice reveals a new putative molecular player in the regulation of anxiety. Exp. Neurol. 247, 122–129. https://doi.org/10.1016/j.expneurol.2013.03.028.
Giralt, A., Brito, V., Chevy, Q., Simonnet, C., Otsu, Y., Cifuentes-Díaz, C., de Pins, B., Coura, R., Alberch, J., Ginés, S., Poncer, J.-C., Girault, J.-A., 2017. Pyk2 modulates hippocampal excitatory synapses and contributes to cognitive deficits in a Huntington's disease model. Nat. Commun. 8, 15592. https://doi.org/10.1038/ncomms15592.
Gomez-Nicola, D., Fransen, N.L., Suzzi, S., Perry, V.H., 2013. Regulation of microglial proliferation during chronic neurodegeneration. J. Neurosci. 33, 2481–2493. https://doi.org/10.1523/JNEUROSCI.4440-12.2013.
Hong, S., Beja-Glasser, V.F., Nfonoyim, B.M., Frouin, A., Li, S., Ramakrishnan, S., Merry, K.M., Shi, Q., Rosenthal, A., Barres, B.A., Lemere, C.A., Selkoe, D.J., Stevens, B., 2016. Complement and microglia mediate early synapse loss in Alzheimer mouse models. Science 80- 352, 712–716. https://doi.org/10.1126/science.aad8373.
Jimenez-Ferrer, I., Jewett, M., Tontanahal, A., Romero-Ramos, M., Swanberg, M., 2017. Allelic difference in Mhc2ta confers altered microglial activation and susceptibility to α-synuclein-induced dopaminergic neurodegeneration. Neurobiol. Dis. 106, 279–290. https://doi.org/10.1016/j.nbd.2017.07.016.
Kadono, K., Kageyama, S., Nakamura, K., Hirao, H., Ito, T., Kojima, H., Dery, K.J., Li, X., Kupiec-Weglinski, J.W., 2022. Myeloid Ikaros–SIRT1 signaling axis regulates hepatic inflammation and pyroptosis in ischemia-stressed mouse and human liver. J. Hepatol. 76, 896–909. https://doi.org/10.1016/j.jhep.2021.11.026.
Kayagaki, N., Warming, S., Lamkanfi, M., Walle, L.V., Louie, S., Dong, J., Newton, K., Qu, Y., Liu, J., Heldens, S., Zhang, J., Lee, W.P., Roose-Girma, M., Dixit, V.M., 2011. Non-canonical inflammasome activation targets caspase-11. Nature 479, 117–121. https://doi.org/10.1038/nature10558.
Keren-Shaul, H., Spinrad, A., Weiner, A., Matcovitch-Natan, O., Dvir-Szternfeld, R., Ulland, T.K., David, E., Baruch, K., Lara-Astaiso, D., Toth, B., Itzkovitz, S., Colonna, M., Schwartz, M., Amit, I., 2017. A unique microglia type associated with restricting development of Alzheimer's disease. Cell 169, 1276–1290.e17. https://doi.org/10.1016/j.cell.2017.05.018.
Kettenmann, H., Hanisch, U.-K., Noda, M., Verkhratsky, A., 2011. Physiology of microglia. Physiol. Rev. 91, 461–553. https://doi.org/10.1152/physrev.00011.2010.
Kim, J., Sif, S., Jones, B., Jackson, A., Koipally, J., Heller, E., Winandy, S., Viel, A., Sawyer, A., Ikeda, T., Kingston, R., Georgopoulos, K., 1999. Ikaros DNA-binding proteins direct formation of chromatin remodeling complexes in lymphocytes. Immunity 10, 345–355. https://doi.org/10.1016/S1074-7613(00)80034-5.
Koipally, J., Georgopoulos, K., 2000. Ikaros interactions with CtBP reveal a repression mechanism that is independent of histone deacetylase activity. J. Biol. Chem. 275, 19594–19602. https://doi.org/10.1074/jbc.M000254200.
Kumar, A., Fontana, I.C., Nordberg, A., 2022. Reactive astrogliosis: afriend or foe in the pathogenesis of Alzheimer's disease. J. Neurochem. https://doi.org/10.1111/jnc.15565.
Lamkanfi, M., Dixit, V.M., 2014. Mechanisms and functions of inflammasomes. Cell 157, 1013–1022. https://doi.org/10.1016/j.cell.2014.04.007.
Levenson, J.M., O'Riordan, K.J., Brown, K.D., Trinh, M.A., Molfese, D.L., Sweatt, J.D., 2004. Regulation of histone acetylation during memory formation in the hippocampus. J. Biol. Chem. 279, 40545–40559. https://doi.org/10.1074/jbc.M402229200.
Li, Q., Barres, B.A., 2018. Microglia and macrophages in brain homeostasis and disease. Nat. Rev. Immunol. 18, 225–242. https://doi.org/10.1038/nri.2017.125.
Li, Y., Wang, P., Yang, X., Wang, W., Zhang, J., He, Y., Zhang, W., Jing, T., Wang, B., Lin, R., 2016. SIRT1 inhibits inflammatory response partly through regulation of NLRP3 inflammasome in vascular endothelial cells. Mol. Immunol. 77, 148–156. https://doi.org/10.1016/j.molimm.2016.07.018.
Li, Y., Yang, X., He, Y., Wang, W., Zhang, J., Zhang, W., Jing, T., Wang, B., Lin, R., 2017. Negative regulation of NLRP3 inflammasome by SIRT1 in vascular endothelial cells. Immunobiology 222, 552–561. https://doi.org/10.1016/j.imbio.2016.11.002.
Lian, H., Roy, E., Zheng, H., 2016. Microglial phagocytosis assay. BIO-PROTOCOL 6. https://doi.org/10.21769/BioProtoc.1988.
Lynch, M.A., 2004. Long-term potentiation and memory. Physiol. Rev. 84, 87–136. https://doi.org/10.1152/physrev.00014.2003.
Mahmmoud, R.R., Sase, S., Aher, Y.D., Sase, A., Gröger, M., Mokhtar, M., Höger, H., Lubec, G., Chapouthier, G., 2015. Spatial and working memory is linked to spine density and mushroom spines. PLoS One 10 (10), e0139739.
Maity, S., Farrell, K., Navabpour, S., Narayanan, S.N., Jarome, T.J., 2021. Epigenetic mechanisms in memory and cognitive decline associated with aging and Alzheimer's disease. Int. J. Mol. Sci. 22, 12280. https://doi.org/10.3390/ijms222212280.
Mangan, M.S.J., Olhava, E.J., Roush, W.R., Seidel, H.M., Glick, G.D., Latz, E., 2018. Targeting the NLRP3 inflammasome in inflammatory diseases. Nat. Rev. Drug Discov. 17, 588–606. https://doi.org/10.1038/nrd.2018.97.
MartÃ-n-lbÃ¡Ã±ez, R., Crespo, E., UrbÃ¡n, N., Sergent-Tanguy, SolÃne, Herranz, C., Jaumot, M., Valiente, M., Long, J.E., Pineda, J.R., Andreu, C., Rubenstein, J.L.R., MarÃ-n, Ã., Georgopoulos, K., Mengod, G., FariÃ±as, I., Bachs, O., Alberch, J., Canals, J.M., 2010. Ikaros-1 couples cell cycle arrest of late striatal precursors with neurogenesis of enkephalinergic neurons. J. Comp. Neurol. 518 (3), 329–351.
Mata-Martínez, E., Díaz-Muñoz, M., Vázquez-Cuevas, F.G., 2022. Glial cells and brain diseases: inflammasomes as relevant pathological entities. Front. Cell. Neurosci. 16 https://doi.org/10.3389/fncel.2022.929529.
McGeer, P.L., Itagaki, S., Tago, H., McGeer, E.G., 1988. Occurrence of HLA-DR reactive microglia in Alzheimer's Disease. Ann. N. Y. Acad. Sci. 540, 319–323. https://doi.org/10.1111/j.1749-6632.1988.tb27086.x.
Molnár, A., Georgopoulos, K., 1994. The Ikaros gene encodes a family of functionally diverse zinc finger DNA-binding proteins. Mol. Cell. Biol. 14, 8292–8303. https://doi.org/10.1128/MCB.14.12.8292.
Oakley, H., Cole, S.L., Logan, S., Maus, E., Shao, P., Craft, J., Guillozet-Bongaarts, A., Ohno, M., Disterhoft, J., Van Eldik, L., Berry, R., Vassar, R., 2006. Intraneuronal beta-amyloid aggregates, neurodegeneration, and neuron loss in transgenic mice with five familial Alzheimer's disease mutations: potential factors in amyloid plaque formation. J. Neurosci. 26, 10129–10140. https://doi.org/10.1523/JNEUROSCI.1202-06.2006.
Oh, K.-S., Gottschalk, R.A., Lounsbury, N.W., Sun, J., Dorrington, M.G., Baek, S., Sun, G., Wang, Z., Krauss, K.S., Milner, J.D., Dutta, B., Hager, G.L., Sung, M.-H., Fraser, I.D. C., 2018. Dual roles for ikaros in regulation of macrophage chromatin state and inflammatory gene expression. J. Immunol. 201, 757–771. https://doi.org/10.4049/jimmunol.1800158.

Paolicelli, R.C., Bolasco, G., Pagani, F., Maggi, L., Scianni, M., Panzanelli, P., Giustetto, M., Ferreira, T.A., Guiducci, E., Dumas, L., Ragozzino, D., Gross, C.T., 2011. Synaptic pruning by microglia is necessary for normal brain development. Science 80 333, 1456–1458. https://doi.org/10.1126/science.1202529.

Paolicelli, R.C., Sierra, A., Stevens, B., Tremblay, M.-E., Aguzzi, A., Ajami, B., Amit, I., Audinat, E., Bechmann, I., Bennett, M., Bennett, F., Bessis, A., Biber, K., Bilbo, S., Blurton-Jones, M., Boddeke, E., Brites, D., Brône, B., Brown, G.C., Butovsky, O., Carson, M.J., Castellano, B., Colonna, M., Cowley, S.A., Cunningham, C., Davalos, D., De Jager, P.L., de Strooper, B., Denes, A., Eggen, B.J.L., Eyo, U., Galea, E., Garel, S., Ginhoux, F., Glass, C.K., Gokce, O., Gomez-Nicola, D., González, B., Gordon, S., Graeber, M.B., Greenhalgh, A.D., Gressens, P., Greter, M., Gutmann, D.H., Haass, C., Heneka, M.T., Heppner, F.L., Hong, S., Hume, D.A., Jung, S., Kettenmann, H., Kipnis, J., Koyama, R., Lemke, G., Lynch, M., Majewska, A., Malcangio, M., Malm, T., Mancuso, R., Masuda, T., Matteoli, M., McColl, B.W., Miron, V.E., Molofsky, A.V., Monje, M., Mracsko, E., Nadjar, A., Neher, J.J., Neniskyte, U., Neumann, H., Noda, M., Peng, B., Peri, F., Perry, V.H., Popovich, P.G., Pridans, C., Priller, J., Prinz, M., Ragozzino, D., Ransohoff, R.M., Salter, M.W., Schaefer, A., Schafer, D.P., Schwartz, M., Simons, M., Smith, C.J., Streit, W.J., Tay, T.L., Tsai, L.-H., Verkhratsky, A., von Bernhardi, R., Wake, H., Wittamer, V., Wolf, S.A., Wu, L.-J., Wyss-Coray, T., 2022. Microglia states and nomenclature: A field at its crossroads. Neuron 110, 3458–3483. https://doi.org/10.1016/j.neuron.2022.10.020.

Poli, G., Fabi, C., Bellet, M.M., Costantini, C., Nunziangeli, L., Romani, L., Brancorsini, S., 2020. Epigenetic mechanisms of inflammasome regulation. Int. J. Mol. Sci. 21, 5758. https://doi.org/10.3390/ijms21165758.

Potkin, S.G., Guffanti, G., Lakatos, A., Turner, J.A., Kruggel, F., Fallon, J.H., Saykin, A.J., Orro, A., Lupoli, S., Salvi, E., Weiner, M., Macciardi, F., Domschke, K., 2009. Hippocampal atrophy as a quantitative trait in a genome-wide association study identifying novel susceptibility genes for Alzheimer's disease. PLoS One 4 (8), e6501.

Puigdellívol, M., Milde, S., Vilalta, A., Cockram, T.O.J., Allendorf, D.H., Lee, J.Y., Dundee, J.M., Pampuščenko, K., Borutaite, V., Nuthall, H.N., Brelstaff, J.H., Spillantini, M.G., Brown, G.C., 2021. The microglial P2Y6 receptor mediates neuronal loss and memory deficits in neurodegeneration. Cell Rep. 37 (13), 110148.

Rajendran, L., Paolicelli, R.C., 2018. Microglia-mediated synapse loss in Alzheimer's Disease. J. Neurosci. 38, 2911–2919. https://doi.org/10.1523/JNEUROSCI.1136-17.2017.

Raneros, A.B., Bernet, C.R., Flórez, A.B., Suarez-Alvarez, B., 2021. An epigenetic insight into NLRP3 inflammasome activation in inflammation-related processes. Biomedicines 9, 1614. https://doi.org/10.3390/biomedicines9111614.

Rodríguez-Urgellés, E., Sancho-Balsells, A., Chen, W., López-Molina, L., Ballasch, I., del Castillo, I., Avila, C., Alberch, J., Giralt, A., 2022. Meridianins rescue cognitive deficits, spine density and neuroinflammation in the 5xFAD model of Alzheimer's Disease. Front. Pharmacol. 13 https://doi.org/10.3389/fphar.2022.791666.

Saura, J., Tusell, J.M., Serratosa, J., 2003. High-yield isolation of murine microglia by mild trypsinization. Glia 44, 183–189. https://doi.org/10.1002/glia.10274.

Schafer, D.P., Lehrman, E.K., Kautzman, A.G., Koyama, R., Mardinly, A.R., Yamasaki, R., Ransohoff, R.M., Greenberg, M.E., Barres, B.A., Stevens, B., 2012. Microglia sculpt postnatal neural circuits in an activity and complement-dependent manner. Neuron 74, 691–705. https://doi.org/10.1016/j.neuron.2012.03.026.

Scholz, H., Eder, C., 2017. Lysophosphatidylcholine activates caspase-1 in microglia via a novel pathway involving two inflammasomes. J. Neuroimmunol. 310, 107–110. https://doi.org/10.1016/j.jneuroim.2017.07.004.

Schwartzentruber, J., Cooper, S., Liu, J.Z., Barrio-Hernandez, I., Bello, E., Kumasaka, N., Young, A.M.H., Franklin, R.J.M., Johnson, T., Estrada, K., Gaffney, D.J., Beltrao, P., Bassett, A., 2021. Genome-wide meta-analysis, fine-mapping and integrative prioritization implicate new Alzheimer's disease risk genes. Nat. Genet. 53, 392–402. https://doi.org/10.1038/s41588-020-00776-w.

Sellgren, C.M., Gracias, J., Watmuff, B., Biag, J.D., Thanos, J.M., Whittredge, P.B., Fu, T., Worringer, K., Brown, H.E., Wang, J., Kaykas, A., Karmacharya, R., Goold, C.P., Sheridan, S.D., Perlis, R.H., 2019. Increased synapse elimination by microglia in schizophrenia patient-derived models of synaptic pruning. Nat. Neurosci. 22, 374–385. https://doi.org/10.1038/s41593-018-0334-7.

Shi, Y., Manis, M., Long, J., Wang, K., Sullivan, P.M., Remolina Serrano, J., Hoyle, R., Holtzman, D.M., 2019. Microglia drive APOE-dependent neurodegeneration in a tauopathy mouse model. J. Exp. Med. 216, 2546–2561. https://doi.org/10.1084/jem.20190980.

Sierra, A., Abiega, O., Shahraz, A., Neumann, H., 2013. Janus-faced microglia: beneficial and detrimental consequences of microglial phagocytosis. Front. Cell. Neurosci. 7 https://doi.org/10.3389/fncel.2013.00006.

Sierra, A., Paolicelli, R.C., Kettenmann, H., 2019. Cien Años de Microglía: milestones in a century of microglial research. Trends Neurosci. 42, 778–792. https://doi.org/10.1016/j.tins.2019.09.004.

Silvin, A., Uderhardt, S., Piot, C., Da Mesquita, S., Yang, K., Geirsdottir, L., Mulder, K., Eyal, D., Liu, Z., Bridlance, C., Thion, M.S., Zhang, X.M., Kong, W.T., Deloger, M., Fontes, V., Weiner, A., Ee, R., Dress, R., Hang, J.W., Balachander, A., Chakarov, S., Malleret, B., Dunsmore, G., Cexus, O., Chen, J., Garel, S., Dutertre, C.A., Amit, I., Kipnis, J., Ginhoux, F., 2022. Dual ontogeny of disease-associated microglia and disease inflammatory macrophages in aging and neurodegeneration. Immunity 55, 1448–1465.e6. https://doi.org/10.1016/j.immuni.2022.07.004.

Song, C., Pan, X., Ge, Z., Gowda, C., Ding, Y., Li, H., Li, Z., Yochum, G., Muschen, M., Li, Q., Payne, K.J., Dovat, S., 2016. Epigenetic regulation of gene expression by Ikaros, HDAC1 and Casein Kinase II in leukemia. Leukemia 30, 1436–1440. https://doi.org/10.1038/leu.2015.331.

Sun, D., Gao, G., Zhong, B., Zhang, H., Ding, S., Sun, Z., Zhang, Y., Li, W., 2021. NLRP1 inflammasome involves in learning and memory impairments and neuronal damages during aging process in mice. Behav. Brain Funct. 17, 11. https://doi.org/10.1186/s12993-021-00185-x.

Takada, S., Sakakima, H., Matsuyama, T., Otsuka, S., Nakanishi, K., Norimatsu, K., Itashiki, Y., Tani, A., Kikuchi, K., 2020. Disruption of Midkine gene reduces traumatic brain injury through the modulation of neuroinflammation. J. Neuroinflammation 17, 40. https://doi.org/10.1186/s12974-020-1709-8.

Tarchini, B., Jolicoeur, C., Cayouette, M., 2012. In vivo evidence for unbiased ikaros retinal lineages using an ikaros-cre mouse line driving clonal recombination. Dev. Dyn. 241, 1973–1985. https://doi.org/10.1002/dvdy.23881.

Wadhwa, M., Prabhakar, A., Ray, K., Roy, K., Kumari, P., Jha, P.K., Kishore, K., Kumar, S., Panjwani, U., 2017. Inhibiting the microglia activation improves the spatial memory and adult neurogenesis in rat hippocampus during 48 h of sleep deprivation. J. Neuroinflammation 14, 222. https://doi.org/10.1186/s12974-017-0998-z.

Wang, C., Fan, L., Khawaja, R.R., Liu, B., Zhan, L., Kodama, L., Chin, M., Li, Y., Le, D., Zhou, Y., Condello, C., Grinberg, L.T., Seeley, W.W., Miller, B.L., Mok, S.-A., Gestwicki, J.E., Cuervo, A.M., Luo, W., Gan, L., 2022. Microglial NF-κB drives tau spreading and toxicity in a mouse model of tauopathy. Nat. Commun. 13, 1969. https://doi.org/10.1038/s41467-022-29552-6.

Wang, J.-H., Nichogiannopoulou, A., Wu, L., Sun, L., Sharpe, A.H., Bigby, M., Georgopoulos, K., 1996. Selective defects in the development of the fetal and adult lymphoid system in mice with an ikaros null mutation. Immunity 5, 537–549. https://doi.org/10.1016/S1074-7613(00)80269-1.

Wang, H., Song, C., Ding, Y., Pan, X., Ge, Z., Tan, B.-H., Gowda, C., Sachdev, M., Muthusami, S., Ouyang, H., Lai, L., Francis, O.L., Morris, C.L., Abdel-Azim, H., Dorsam, G., Xiang, M., Payne, K.J., Dovat, S., 2016. Transcriptional regulation of JARID1B/KDM5B histone demethylase by ikaros, histone deacetylase 1 (HDAC1), and Casein Kinase 2 (CK2) in B-cell acute lymphoblastic leukemia. J. Biol. Chem. 291, 4004–4018. https://doi.org/10.1074/jbc.M115.679332.

Wu, T., Sun, X.-Y., Yang, X., Liu, L., Tong, K., Gao, Y., Hao, J.-R., Cao, J., Gao, C., 2019. Histone H3K9 trimethylation downregulates the expression of brain-derived neurotrophic factor in the dorsal hippocampus and impairs memory formation during anaesthesia and surgery. Front. Mol. Neurosci. 12 https://doi.org/10.3389/fnmol.2019.00246.

Yagi, T., Hibi, S., Takanashi, M., Kano, G., Tabata, Y., Imamura, T., Inaba, T., Morimoto, A., Todo, S., Imashuku, S., 2002. High frequency of Ikaros isoform 6 expression in acute myelomonocytic and monocytic leukemias: implications for up-regulation of the antiapoptotic protein Bcl-XL in leukemogenesis. Blood 99, 1350–1355. https://doi.org/10.1182/blood.V99.4.1350.

Yeh, F.L., Hansen, D.V., Sheng, M., 2017. TREM2, microglia, and neurodegenerative diseases. Trends Mol. Med. 23, 512–533. https://doi.org/10.1016/j.molmed.2017.03.008.

Yi, Y.-S., 2017. Caspase-11 non-canonical inflammasome: a critical sensor of intracellular lipopolysaccharide in macrophage-mediated inflammatory responses. Immunology 152, 207–217. https://doi.org/10.1111/imm.12787.

Yoshida, T., Yao-Ming Ng, S., Zuniga-Pflucker, J.C., Georgopoulos, K., 2006. Early hematopoietic lineage restrictions directed by Ikaros. Nat. Immunol. 7, 382–391. https://doi.org/10.1038/ni1314.

Zahedipour, F., Hosseini, S., Henney, N., Barreto, G., Sahebkar, A., 2022. Phytochemicals as inhibitors of tumor necrosis factor alpha and neuroinflammatory responses in neurodegenerative diseases. Neural Regen. Res. 17, 1675. https://doi.org/10.4103/1673-5374.332128.

Zhou, L.-J., Peng, J., Xu, Y.-N., Zeng, W.-J., Zhang, J., Wei, X., Mai, C.-L., Lin, Z.-J., Liu, Y., Murugan, M., Eyo, U.B., Umpierre, A.D., Xin, W.-J., Chen, T., Li, M., Wang, H., Richardson, J.R., Tan, Z., Liu, X.-G., Wu, L.-J., 2019. Microglia are indispensable for synaptic plasticity in the spinal dorsal horn and chronic pain. Cell Rep. 27, 3844–3859.e6. https://doi.org/10.1016/j.celrep.2019.05.087.

V. Discussion

Schizophrenia is a complex psychiatric condition with a multifactorial etiology still not totally understood. Even if it is not considered an immune disease, schizophrenia pathogenesis is very sensitive to immune insults as many of the risk factors (genetic and environmental) associated to this condition act trough the immune system[94], [173]. The nervous and the immune systems interact in a myriad of ways and understanding how this interaction is altered in schizophrenia could be very challenging. Neuroinflammation and T cell mediated immunity are affected processes in schizophrenia and core candidates involved in the altered neuro-immune crosstalk in this condition. We have shown that two members of the Ikaros family are dysregulated in T cells in patients suffering of chronic schizophrenia and we have demonstrated that the secretome of these cells can induce several schizophrenia-like phenotypes in in-vivo and in-vitro models. On the other side, we have also shown that one member of the Ikaros family (Ikaros) is involved in microglia homeostasis in inflammation and, consequently, influences neuroinflammatory responses.

1. Ikaros and Helios are downregulated in PBMCs but not in the brain of patients diagnosed with schizophrenia

Ikaros and Helios as well as other members of the Ikaros family are capital for proper development and function of the immune system[4], [19]. Thus, in a condition where deleterious mental outcomes are more susceptible to occur upon immune insults it is not counter intuitive to imagine a possible participation of the Ikaros family. However, even if schizophrenia is widely considered a psychiatric condition, we have found that the levels of both Ikaros and Helios are not dysregulated in brain areas considered key-affected in this condition. On the other hand, we showed for the first time that the level of both were downregulated in PBMCs of patients and that particularly, when analyzing CD4+ cells and CD8+ cells, both were downregulated in CD4+ cells but not in CD8+ cells.

The fact that Ikaros and Helios present altered levels in immune cells but not in brain regions implicated in schizophrenia represents a major point reinforcing the idea of the implication of the immune system in the pathogenesis of this condition and, as previous research proposed[162], dysregulations of T cells (the majority of PBMCs population) is a plausible way the immune system is affecting the nervous system in schizophrenia. Regarding possible causes of the downregulation of Ikaros and Helios, as far as we know, GWAS have not identified any specific genetic variation of the members of the Ikaros family in schizophrenia. Nevertheless, a recent study[221] found that single nucleotide polymorphisms (SNPs) affecting the *IKZF1* gene were related to the age of onset of schizophrenia. Besides, as schizophrenia is considered a polygenic and a multifactorial disorder[224], we cannot rule out the possibility that the levels of Ikaros and Helios are indirectly affected by other processes (e.g. immune or environmental challenges) and ultimately contributing to the prognosis of the condition. For example, a recent study [225] found a Helios active regulon in a transcription factors analysis of PBMCs of cattle in

response to LPS stimulation (mimicking an immune challenge). Another possibility could be the implication of the WNT signaling pathway. It has been shown that the activation of the *WNT* gene influences the levels of Ikaros in T cells [226] and that the WNT signaling pathway is affected in PBMCs of patients and particularly in patients with cognitive decline[227]. These ideas may provide some clues about the source of the dysregulation of these members of the Ikaros family, further research could elucidate these possibilities. The identification of the PBMCs subpopulations with altered levels of Ikaros and Helios is of particular importance to try to clarify the possible effects of the downregulation of Ikaros and Helios in PBMCs. We have identified a double downregulation of Ikaros and Helios in CD4+ cells whereas their levels in CD8+ remain invariable. Even so, we cannot assume a changelessness state in other PBMC subpopulations as we have not evaluated all of them. Classically, CD4+ cells play a major role modulating the immune response by releasing specific cytokines according to their specific T cell subset (see Table 1). In this manner, every T cell subset has different effector functions that affect themselves, other immune cells or even non-immune cells[183], [228].

Regarding the downregulation of Ikaros, one possibility is that this reduction is taking place in the Th1 and Th2 subsets. One of the main effector cytokine of the Th1 cells is IFN-γ and Ikaros has been shown to negatively regulate IFN-γ[21]. Among other functions, IFN-γ promotes the activation of macrophages and microglia which results in augmented phagocytic activity[21]and could lead to inflammatory states. Abnormal expression of IFN-γ is also associated with auto-inflammatory and auto-immune disease[229] and schizophrenia has been linked to increased frequency of autoimmune diseases in patients[156]. Further, the production of IFN-γ by Th1 cells promotes the differentiation of naïve Th cells into Th1 cells and reduce the differentiation into Th2 cells[228]. An important effector cytokine of the Th2 subset is IL-4. IL-4 is one of the cytokines we found to be reduced in the $SCH^{Ik-:He-}$ secretome and this cytokine has been shown to be reduced in chronic schizophrenia [230] (Further potential implications of IL-4 will be discussed below). Consistently, the presence of Ikaros in Th2 represses Th1 differentiation and supports Th2 development by positive regulation of IL-4, as IL-4 act in paracrine and autocrine ways on Th2 cells[21]. Hence, the reduction of Ikaros in Th2 cells could be, on one hand, favorizing Th1 differentiation and, consequently, IFN-γ expression, and, on the other hand, reducing Th2 differentiation and, subsequently, IL-4 expression. The expression of IFN-γ is associated to the presence of viral infections and some bacterial infections where it can inhibit viral replication and exert immunostimulatory and immunomodulatory effects[229]. This is congruent with the fact that maternal immune activation and childhood infections are prominent risk factors in schizophrenia[147] and also somehow supporting the viral theory of schizophrenia[231]. Anyhow, even if the levels of IFN-γ have been shown to be elevated in first psychotic episode subjects[232], many studies have found the opposite results in chronic patients [233], [234], [235], the levels of IFN-γ tend to be reduced. However, as many risk factors in schizophrenia, immune insults happen at some points during life (particularly during early and perinatal life) and their consequences are probably accounting and accumulating for the ulterior pathogenesis of the condition[94]. Thereby, the down regulation of Ikaros could be implicated in the abnormal expression of IFN-γ at specific points of life upon immune challenges causing a

dysregulated immune response, including excessive microgliosis and starting neuroinflammation and the dysregulated levels of IFN-γ are probably compensated later. A plausible way IFN-γ levels could be regulated is through medication. A substantial proportion of the antipsychotics used nowadays are known to reduce IFN-γ levels[236], [237], [238]. Thus, consistent with the idea that IFN-γ dysregulation could be linked to immune insults in early life, the posterior pharmacological treatment after the clinical diagnosis would be accounting for its downregulation. Indeed, these ideas go in line with the fact that we did not find altered levels of IFN-γ in any of the secretomes coming from PBMCs of patients (i.e. $SCH^{Ik-:He-}$ and $SCH^{Ik+:He+}$.) as all the patients were under pharmacological treatment.

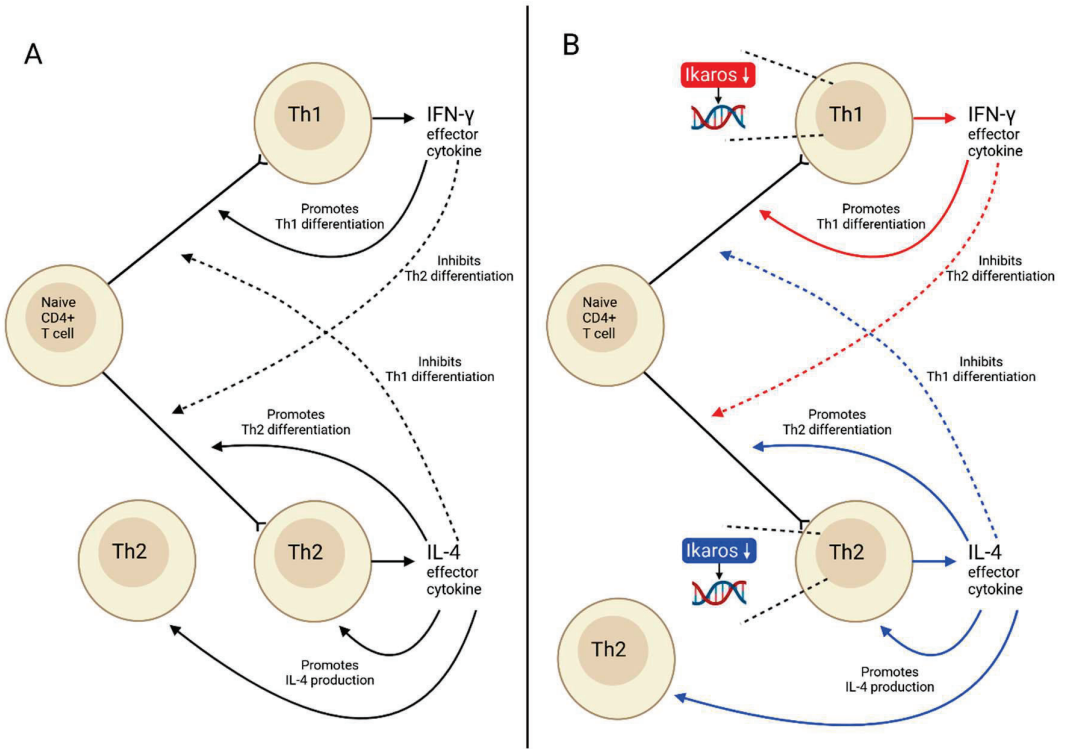

***Figure 6**. A- Simplified illustration of the differentiation of naïve CD4+ cells into either Th1 or Th2 cells and the effects of some cytokines these cells release. B- The impact of the possible downregulation of Ikaros in Th1 and Th2 subsets. Red arrows depict the outcomes that are promoted by the downregulation of Ikaros. Blue arrows depict the outcomes that are reduced or inhibited by the downregulation of Ikaros. Possible cell differentiation is depicted by ⊣.*

Regarding the reduced levels of Helios, more limited knowledge is available about its implication in Th subsets. It has been shown that Helios is markedly expressed in Th2 cells[21]. Nonetheless, unlike Ikaros, Helios seems not to be necessary neither for the expression of Th2-associated cytokines nor for Th2 cells differentiation[21]. Wherefore, the significance of reduced levels of Helios in Th2 cells would be hard to interpret. Notwithstanding, a reduction of Helios in Treg cells could have relevant effects in the context of schizophrenia. Treg cells main function is to regulate the immune system by suppressing or downregulating the activation and reproduction of effector T cells[239]. They also provide tolerance to self-antigens and contribute to prevent local inflammation[239]. Th activated cells release IL-2 which is sensed by Treg cells and activates their suppression functions (e.g production of granzyme B that induces

apoptosis of the effector cells) to maintain immune tolerance and to regulate inflammation. Besides, activated T cells can also peripherally switch to a Treg phenotype(pTreg) upon the presence of IL-2 and TGF-β to prevent inflammation[239]. However, these processes need the presence of Helios. Helios has been shown to be necessary to stabilize the inhibitory role of Treg cells[27], and IL-2 is involved in the differentiation of pTreg cells but maintaining that regulatory phenotype has been linked to the presence of Helios[28]. Furthermore, it has also been shown that in the absence of Helios, Treg cells are prone to swift towards a pro-inflammatory phenotype[28] and can release pro-inflammatory factors such as IFN-γ[28]. Thus, reduced levels of Helios in Treg cells could be, for one side, lowering the downregulation of the effector activity of other T cells and, for the other side, hindering the preservation of pTreg cells regulatory phenotype. Altogether, this probably accounts for the maintenance of the chronic inflammation observed in schizophrenia. Moreover, the quantity of Treg cells has been shown to be increased in patients[240], a fact that could be showing a compensatory mechanism for the dysregulation of Treg cells caused by the lack of Helios. Another important consequence of the Helios-deficient Treg cells in schizophrenia could be the elevated comorbidity of Schizophrenia with autoimmune diseases as preventing their development has been largely described as part of the Treg subset function[30], [239]. Lastly, it is noteworthy that the population of Treg cells is a small percentage(around 5-10%[241]) amongst the CD4+ population, and that Helios downregulation is very probably not an isolated Treg subset associated phenomenon.

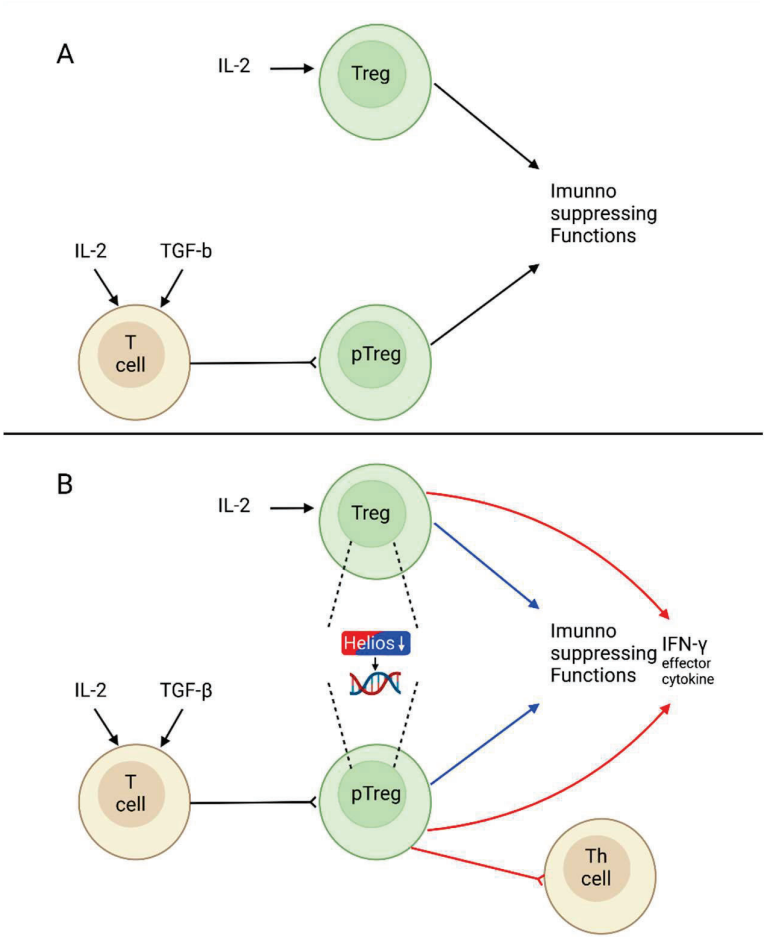

Figure 7. *A- Simplified illustration of how T reg cells engage in immune suppressing functions. B- The impact of the possible downregulation of Helios in the T reg subset. Red arrows depict the outcomes that are promoted by the downregulation of Helios. Blue arrows depict the outcomes that are reduced or inhibited by the downregulation of Helios. Possible cell differentiation is depicted by* ⊣.

The alterations of Ikaros and Helios could also have synergistic effects. For instance, the upregulated differentiation of Th1 cells caused by the lack of Ikaros could be over recruiting Treg cells that, in turn, are releasing IFN-γ (caused by the lack of Helios) and supporting the differentiation of Th1 cells. Thus, the lack of both Ikaros and Helios would be reinforcing this loop and promoting a constant inflammation-prone state. From another point of view, it has been shown that IFN-γ binds to IFN-γR on, amid other immune cells, Treg cells to cause their migration to sites of Th1-associated inflammation[242]. This process is mediated by the expression of CXCR3 on Treg cells after IFN-γ stimulation[239]. CXCR3 is a chemokine receptor that can induce, among other responses, chemotactic migration[243], [244]. One of the major chemokines involved in chemoattraction of CXCR3 is CXCL10[245]. CXCL10 is one of the chemokines we found elevated levels of in the $SCH^{Ik-:He-}$ secretome and the CXCL10-CXCR3 pathway has been linked to perpetuation of inflammation[246] (Further potential implications of CXCL-10 will be discussed below). Considering that a dysregulation of Ikaros in Th1 and Th2 subsets could be promoting inflammation processes and that later IFN-γ levels would be downregulated, as it is reported in schizophrenia[233], the reduced levels of IFN-γ could be diminishing the

migration signaling pathway on Tregs, not allowing them to properly arrive to inflammation sites. On the other hand, possible reduced levels of Helios in Treg cells could be, as mentioned before, hampering the regulatory functions of these cells. Altogether, these phenomena, generated by the synergistic effect of the dysregulations of Ikaros and Helios, could be contributing to the sustained inflammation in Schizophrenia. Although, it is worth mentioning that the release of CXCL10 by immune cells (e.g. CD4+Th1 and CD8+ cells) is generally in response to IFN-γ, and in a lesser degree in response to other IFNs[247], [248]. Therefore, mechanisms related to Ikaros-Helios reduction may account for this elevated level of CXCL10 solely found in the $SCH^{Ik-:He-}$ secretome. Future investigations could address this possibility.

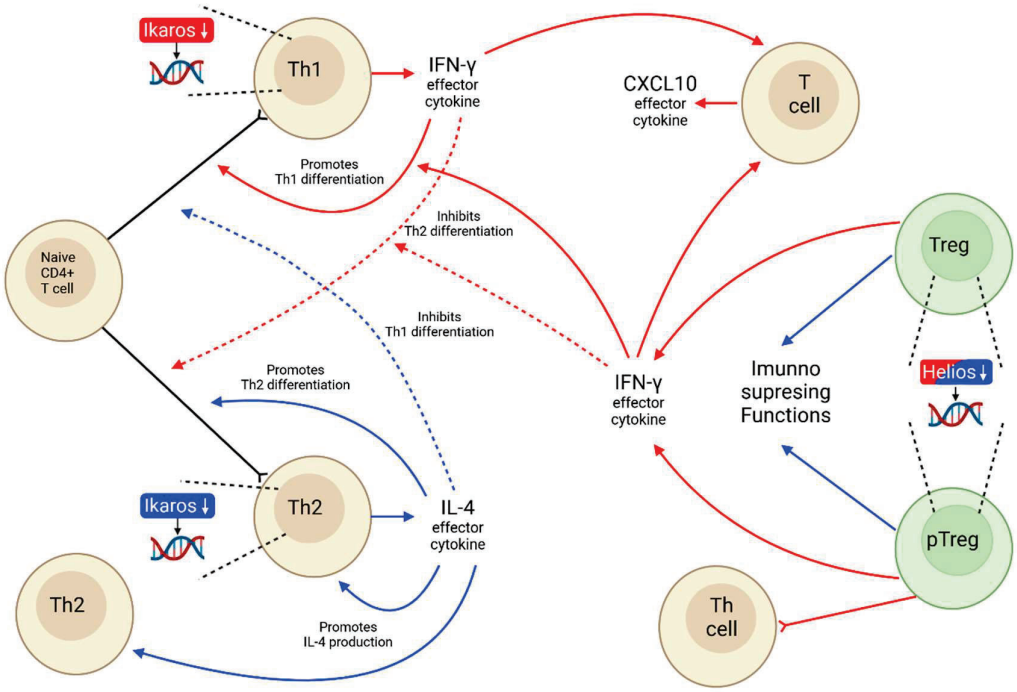

Figure 8. *Representation of the possible joint action effects of the downregulation of Ikaros in Th1 and Th2 cells and Helios in Treg cells. Red arrows depict the outcomes that are promoted by the downregulation of Ikaros and Helios. Blue arrows depict the outcomes that are reduced or inhibited by the downregulation of Ikaros and Helios. Possible cell differentiation is depicted by* ⊣.

Finally, another important point about the downregulation of Ikaros and Helios affecting the brain is how this communication is taking place. It has been shown that most cytokines from the periphery can signal in the CNS, by trespassing the BBB or by alternative ways[249]. Moreover, it has also been shown that under inflammatory conditions the permeability of the BBB barrier can be largely disrupted allowing even more traffic of peripherally secreted peptides and mononuclear cells[250]. On the other hand, there is evidence showing that non CNS-resident immune cells can invade the brain parenchyma, and particularly some studies reported elevated levels of lymphocytes in the brain of subjects diagnosed with schizophrenia[198], [250]. Further, recent studies[251], [252], have characterized a population of brain-resident Treg cells remarking their immunosuppressing function and protecting role during neuropathologies within the brain. Hence, one possibility could be that the immune signaling is coming from the

peripheral T cells and that with time, as the BBB permeability augments, the enhanced traffic of both, T-cells and cytokines, contributes even more to the altered immune state and inflammation in the brain. Otherwise, it could also be possible that, as there are brain-resident Tregs cells and T cells can invade the brain parenchyma, the immune alterations caused by the dysregulation of Ikaros and Helios are at some point ¨moving¨ or mainly taking place in the brain and, therefore, contributing to the genesis of a psychiatric condition such as schizophrenia. Noticeably, the joint action of all possibilities is also a very conceivable case scenario.

2. A murine genetic model **Ik$^{+/-}$: He$^{+/-}$** displays schizophrenia-like symptoms and spine density alterations

The second approach to assess the potential implication of the downregulated levels of Ikaros and Helios we found in PBMCs of patients was through a genetic model with a double heterozygous mutation of both genes *Ikzf1* and *Ikzf2* (Ik$^{+/-}$: He$^{+/-}$). We have observed that these animals displayed behavioral schizophrenia-like phenotypes in the three categories of schizophrenia symptoms (positive, negative and cognitive) and spine density alterations in key-affected brain regions in schizophrenia.

Regarding the behavioral characterization of the double mutant Ik$^{+/-}$: He$^{+/-}$ model, it is important to mention that the animals with heterozygous mutation of only one of the Ikaros family members (e.i. Ik$^{+/+}$: He$^{+/-}$ and Ik$^{+/-}$: He$^{+/+}$) also presented some, but not all, of the schizophrenia-like behavior the **Ik$^{+/-}$: He$^{+/-}$** model displayed. This suggests that a downregulation of one the members, either Ikaros or Helios, can already have a minor effect on the animals' body and that other members of the family are probably not able to compensate it. Nevertheless, the full schizophrenia-like phenotype was only found in the animals with the double downregulation. Suggesting that the effects caused by the alterations of both Ikaros family members are probably synergistic but also additive.

When analyzing the positive-like symptomatology in the Ik$^{+/-}$: He$^{+/-}$ model we found elevated locomotor activity, a parameter of agitation and augmented locomotor activity in response to amphetamine, a parameter of sensitivity to psychotomimetic drugs. Among the main outcomes of the psychoactive effects of Amphetamines are the augmented levels of dopamine by direct induction of dopamine release and by inhibition of dopamine reuptake[253]. In that sense, we found altered spine density in the striatum of the Ik$^{+/-}$: He$^{+/-}$ model, a result that could be underlying the sensitivity to amphetamine. Although, striatal spine density after amphetamine stimulation in patients showed opposite results[254], spine density was augmented whereas we found a reduction. A possible idea to explain this could be that the spine density reduction is the outcome of a chronic altered state of the dopaminergic system in the Ik$^{+/-}$: He$^{+/-}$mutant model.

To evaluate cognitive symptomatology, we used the Novel object recognition test (NORT) as a measure of a general cognitive deficit. We found that the $Ik^{+/-}$: $He^{+/-}$ model had memory deficits that can be considered hippocampal-related. Surprisingly, when we evaluated spine density in the hippocampus, we found alterations in male but not in female mice. Even if it is challenging to relate these facts, the altered spine density state detected in male mice could be somehow in accordance with the fact that male patients can present a more pronounced cognitive decline than female patients [255] and that, possibly, the NORT could not reflect that in mice.

A finally important remark about the $Ik^{+/-}$: $He^{+/-}$ model is that, as every other full KO model, the genetic alterations are not specific for a region or a cell population. Consequently, we cannot rule out the possibility that alterations of *Ikaros* and *Helios* in other cells of the body (e.g. CNS cells) are playing a role in the deficiencies this model displayed. To address this and further characterize the impact of the secretome of PBMCs with downregulated levels of Ikaros and Helios we used translational models.

3. PBMCs secretome from schizophrenia patients induced schizophrenia-like behaviors in an *in-vivo* model and alterations in neuronal synaptic plasticity and neuronal dynamics in *in-vitro* models

To evaluate how PBMCs secretome could be affecting the brain and contributing to the pathogenesis of schizophrenia we relied on human-to-mice translational models. In that line, to test the effect of the PBMCs secretome on neural circuits at the cellular level we used some *in vitro* approaches. We treated cultured hippocampal WT cells with PBMCs secretome to evaluate potential differences in neuronal branching and in synaptic markers. Plus, we also evaluated neuronal activity/synchroneity using calcium imaging with a 3D culture set up (a.k.a. MoNNet)[256]. When evaluating the neuronal branching, we found that only the cultures treated with the $SCH^{Ik-:He-}$ supernatant showed reduced arborization compared to the controls. This result is in line with other studies also reporting reduced arborization in animal models of schizophrenia and with the dendritic pathology associated to schizophrenia[257], [258]. Furthermore, when evaluating post-synaptic density clusters, the results were similar, we found a reduction of PSD-95 positive clusters only in the cultures treated with the $SCH^{Ik-:He-}$ secretome. This result is also congruent with other research with similar results in animal models of schizophrenia and with some studies reporting reduced PSD95 levels in the brain of patients[258], [259]. Besides, dysregulations of PSD95 have been shown to interfere with synaptic function and, in schizophrenia, the molecular abnormalities of PSD95 in the CA1 have been proposed to underly the cognitive dysfunction[260], [261]. Beyond the single-cellular level, the MoNNets experiment shed light in the dysregulations at the synchroneity level the PBMCs secretome induced, we found that the treatment with the PBMCs secretome of patients generated reduced neuronal activity and reduced synchronized activity. The reduced synchronized activity is congruent with the general desynchronized activity and

altered gamma and theta oscillations seen in patients[262], [263], [264] and the reduced activity rate could be contributing to it. However, even if the reduced neural activity could seem contradictory in the context of schizophrenia, some studies have reported that some deficiencies in schizophrenia are sustained by neuronal activity decrease[265]. Anyhow, these possibilities remain beyond the scope of this minimalist in-vitro experiment. As a whole, these results point out the potential of the PBMCs secretome to regulate very fundamental neural processes, such as neuronal branching, synaptic plasticity, neural working synchroneity and in particular emphasize the influence of Ikaros and Helios in the appearance of schizophrenia-like phenotypes as most of the results were only associated to the $SCH^{Ik-:He-}$ condition.

To assess the potential implications of the PBMCs secretome in vivo we directly injected the secretome into mice brains. As a first step, we evaluated the possible consequences in mice behavior, and we observed that the injection of the secretome coming from PBMCs with downregulated levels of Ikaros and Helios was sufficient to induce schizophrenia-phenotypes at the behavioral level. We found decreased place preference for a caged peer conspecific, depicting social withdrawal (negative symptom) and memory deficits in the NORT, depicting a general cognitive deficit (cognitive symptom). These results are may in line with previous studies that related cognitive deficits and the appearance of negative symptoms (in the context of schizophrenia) with different immune alterations such as altered peripheral immune cells numbers[266] and differences in peripheral immune cell markers[267]. This reinforces the idea that dysregulations of T-cells are a plausible way the immune system is contributing to the appearance of schizophrenia. Although, the same animals did not display schizophrenia-like behavior in the positive domain. This was perhaps an unexpected outcome, as positive symptoms are the most prominent symptoms of schizophrenia, but it is may worth noticing that the secretome the animals were treated with came from PBMCs from patients under treatment with anti-psychotics and anti-psychotics are known to mostly alleviate the positive symptoms in patients whilst negative and cognitive symptoms remain generally unaffected. Furthermore, in the cohort of patients we used, the majority was under treatment with clozapine and there is evidence associating dysregulated numbers of dopaminergic receptors on immune cells with cognitive and negative symptoms in patients treated with clozapine[266]. Altogether, this makes some room to think that the dopaminergic cross-talk of T cells with the CNS could be mechanistically involved in the manner T cells are implicated in schizophrenia.

Considering that alterations in the cognitive domain were the most closely linked to the $SCH^{Ik-:He-}$ secretome and that the hippocampus, and particularly the CA1, are crucial brain areas implicated in the pathophysiology of schizophrenia[104], in the next step we focused particularly in the CA1. The fact that the $SCH^{Ik-:He-}$ group showed elevated Egr1-dependent pyramidal neuronal activation in the CA1 suggest, that those mice presented a similar state to the one normally found in the hippocampus of patients, often referred as “an hypermetabolic state”[268]. Further, when analyzing the spine density, the results seem to be in the same line as only de $SCH^{Ik-:He-}$ group displayed increased spine density and, particularly, in the same neuronal population. These results are also congruent with

the previous results in vitro, especially with the reduced levels of PSD95. The elevated spine density could be associated with the augmented activity of the pyramidal neurons, but at the same time could be an indicator of aberrant synapses formation (e.g. excess of immature synapses) caused in patients by the dysregulation of PSD95[269], [270]. Alterations of PSD95 levels have been linked to erratic synapse plasticity, dysregulated dendritic spine formation, and have been proposed to contribute to the cognitive impairments in schizophrenia[261], [269]. Regardless of all possibilities, all these results strongly suggest the implication of Ikaros and Helios in the generation of these phenotypes as they were only associated with the $SCH^{Ik-:He-}$secretome.

Within the context of schizophrenia, the heightened excitability observed in the hippocampus is postulated to stem, at least partially, from the malfunction or scarcity of inhibitory interneurons[98], [125], [271]. Correspondingly, we observed comparable findings in the CA1 of the animals injected with patient-derived secretomes. The lack of PV+ interneurons might explain the hyperactive state in the CA1 of the animals treated with the secretome, aligning with previous research indicating decreased levels of PV+ interneurons in the hippocampus in schizophrenia[87]. Nevertheless, reductions of STT+ interneurons have also been reported in the same region in schizophrenia[87]. Thus, we cannot dismiss the potential implication of different interneurons others than the PV+ ones in this context. Another possibility could be that, along with the reduced number of these interneurons, their internal activity is also reduced. For instance, it has been reported that in the PFC of patients the densities of SST+ and PV+ are not altered but rather their transcript activity is[71].

4. The levels of Ikaros and Helios differentially affect the molecular profile of the PBMCs secretome

Considering all the schizophrenia-like phenotypes induced by the patients-derived $SCH^{Ik-:He-}$ secretome from different perspectives (*in-vivo* and *in-vitro*), we next analyzed their molecular profile. One of the proteins we found altered is C1RL. C1RL is a complement protein involved in immune defense against infection, it is also generally considered a marker of gliobastoma[272]. Interestingly, in a longitudinal study[273], its alteration in peripheral blood at the age of 12 was related with a posterior psychotic event at the age of 18. Moreover, the involvement of the classical complement pathway has already been suggested in the context of schizophrenia[274]. Altogether this suggests that C1RL could be considered as an immune marker of schizophrenia.

Another interesting protein is S100A9. This protein can regulate myeloid-origine cell functions by binding to TLR4[275]. Some of its functions are related to inflammation regulation and leukocyte recruitment[276]. Notably, a study [277]found augmented levels of S100A9 in the hippocampus of patients and, the same study, suggested that this immune activation was affecting the PV+ interneurons and consequently contributing to the cognitive deficits in schizophrenia.

A third protein with an interesting profile is CCL5 (a.k.a. RANTES). CCL5 is a chemokine involved in processes like, migration, proliferation and cytokines release[278]. Akin to our results, its levels have been found to be upregulated in plasma of patients and its expression can be regulated by Ikaros[279], [280]. Even if its implication in schizophrenia is still poorly understood, it has been shown that it can have neurotrophic functions and, notably, it could be involved in hippocampal synapses and memory formation[281]. Alterations of CCL5 let to impairments in learning memory and cognition in an animal model, and these deficiencies were correlated with reduced hippocampal long-term potentiation and defects in synapse structure[281]. Besides, alterations of CCL5 have also been linked to Alzheimer's disease in humans[282]. Altogether, this makes CCL5 an Ikzf1-regulated candidate that could be contributing to the hippocampal pathology and the appearance of cognitive symptoms in schizophrenia.

We also identified dysregulations of growth factors. For example, GM-CSF is a white blood cell growth factor that functions as a cytokine[283]. Amid its functions, it is strongly associated with inflammation modulation and it has been previously linked to schizophrenia pathogenesis[284]. Supporting our results, in a recent study[285], its levels were found to be decreased in patients who relapsed. Furthermore, in an investigation using and *in-situ* protocol [286], it has been shown that through microglia modulation, GM-CSF had the potential to induce neuronal network dysfunction, suggesting that its alteration could be participating in the cognitive decline and the neural oscillations desynchrony in schizophrenia.

Another promising molecule we found downregulated is IL-4. The levels of IL-4 in circulating immune cells can be regulated by both, Ikaros and Helios[21], [287]. Similar to our results, IL-4 levels have been shown to be decreased in schizophrenia[230]. Further, SNPs of the *IL-4* gene have been associated to the risk of developing the condition[288]. Besides of its immune functions, it has also been described that IL-4 exerts roles linked to high cognitive functions, such as regulating hippocampal-dependent memory[289]. In that line, a study showed that alterations of IL-4R in an animal model, can lead to augmented neural activity in the hippocampus[290]. All this, is consistent with the cognitive deficiency and the enhanced hippocampal activity observed in our $SCH^{Ik-:He-}$ model and correlates, at least in part, with the hippocampal hyperactive state in patients[104]. An additional feature of IL-4 in schizophrenia is that its levels have been correlated with negative symptoms and patients with enduring negative symptoms have been shown to be cognitively worsen compared to other schizophrenia patients[291], [292]. Altogether, these data make IL-4 a reasonable candidate contributing the schizophrenic phenotype of our $SCH^{Ik-:He-}$ model. Nonetheless, there is another plausible candidate underpinning the $SCH^{Ik-:He-}$ model phenotype, CXCL10. In that sense, previous studies have observed enhanced neural activity accompanied by increased firing rate and excitability and alterations in synaptic network activity in hippocampal cells after chronic treatment with CXCL10[293], [294]. These changes were associated with reduced levels of GABA receptors, reduced levels of GAD65/67, augmented levels of glutamate receptors and increased sensitivity of NMDA receptors Besides, another study[295] reported a microglia mediated reduction of GABA receptors through CXCL10 in hippocampal cultures after LPS

treatment, suggesting that the CXCL10 elevated levels were associated with the cognitive impairments caused by LPS. All these findings go in line with the enhanced hippocampal activity in our SCH$^{Ik-:He-}$ model, the basal hyperexcitability normally seen in schizophrenic patients and the reduced synchronized neural activity present in schizophrenia patients and in our SCH$^{Ik-:He-}$ model. Moreover, the joint action of all the possible effects of the augmented levels of CXCL10 could be also contributing to the cognitive decline in the context of schizophrenia. As a whole, this data raises IL-4 and CXCL10 as the most robust candidates mediating the phenotype of our SCH$^{Ik-:He-}$ model, particularly, the hippocampal-hyperactive state and cognitive deficits.

One way IL-4 could be implicated with the observed phenotypes is by regulating synaptic transmission. It has been shown that IL-4 acts directly on neurons, regulating synaptic vesicles release and, subsequently, participating in synaptic homeostasis[290]. Thus, IL-4 disruption could lead to network dynamics disfunction (e.g. network hyperactivity). Another possibility is that IL-4 is acting through a mediator. For instance, it has been shown that astrocytes of IL-4 KO mice do not release brain-derived neurotropic factor (BDNF) after a learning task in contrast to what occurs in WT mice[296]. BDNF is associated to neuronal growth and survival, increased arborization of dendrites and its presence promotes learning[297]. Therefore, the lack of IL-4 could hinder the astrocyte-mediated release of BDNF and ultimately affecting the cognitive performance. Noteworthy, the collective action of both is likely a possibility as well. On the other hand, the effects of CXCL10 could also be in both ways, by directly affecting neurons or through a mediator. The possibility that CXCL10 is directly affecting neurons could be mediated by CXCR3 receptors. It has been reported that hippocampal neurons exposed to CXCL10 display augmented intracellular Ca2+ leading to increased neuronal firing[294]. Besides inducing elevated intracellular Ca2+, activation of CXCR3s can also activate MAPK pathways that, in neurons, can affect synaptic plasticity[298]. In line with this, a study[299] found that hippocampal slices exposed to exogenous CXCL10 exhibited altered synaptic plasticity, revealed by augmented synaptic fatigue in a paired-pulse facilitation protocol, and decreased post-tetanic potentiation and long-term potentiation (LTP), in contrast to slices from CXCR3 KO mice that did not present alterations in synaptic plasticity. Moreover, in the same study[299], a transgenic line with chronic astrocytic production of CXCL10 also showed no considerable alterations. This, for one side, supports the idea that CXCL10 could be directly affecting neurons through CXCR3 and, for the other side, suggests that PNS-derived CXCL10 is may needed to elicit synaptic activity alterations as CNS-derived CXCL10 seems to be insufficient. Notwithstanding, other study[300], showed that in pathological conditions (i.e. excitotoxicity) WT hippocampal slice cultures exhibited neuronal death in the CA1-3 subfields while mice devoid of either CXCL10 or CXCR3 displayed considerable reduced neuronal death. Furthermore, they also found that in the absence of microglia the differences in neuronal vulnerability were totally abolished. Hence, this suggests that the CXCL10 deleterious effects can be mediated by microglia, particularly, in pathological conditions. Taken together, these data exhibit some ways by which IL-4 and CXCL10 could be playing a role in the phenotype of the SCH$^{Ik-:He-}$ model. The cooperative action of the different possibilities is also probable.

Regarding possibilities where, either of both, IL-4 or/and CXCL10 acts through a mediator, it is worth considering microglia as a plausible candidate for many reasons. First, as mentioned before, CXCL10 neuronal toxic effects can be microglia-mediated. Second, it has been shown that IL-4 can attenuate neuro-inflammatory states through microglia, placing also microglia as possible mediator of IL-4 effects[301]. Third, related to the former reason, microglia are one of the pivotal cell-populations orchestrating inflammation-related processes within the brain and schizophrenia is known to be a low-grade chronic inflammation condition[167], [178]. Forth, IL-4 and CXCL10 have been related to neuroinflammation processes[246], [289]. Last, microglia are myeloid-origine cells and, alike other macrophages, Ikaros is involved in their development process, thereby, it is not counter intuitive to think that Ikaros could be involved in the regulation of some microglia functions[4], [9].

5. Ikaros is implicated in the regulation of microglial responses in neuroinflammation conditions

Besides T cells alteration, central neuroinflammation is another way the immune system is proposed to be involved in the pathogenesis of schizophrenia[160], [172]. Although, the origine of the chronic neuroinflammation state in schizophrenia is still uncertain. Whether it is a secondary problem to a primary one or a primary problem itself is still yet to be determined. In any case, the implication of microglia seems to be undeniable[172], [178]. In that sense, Ikaros, that is known to regulate immune functions in other immune cells[10], [38], also participates in the regulation of microglia in neuroinflammation-associated conditions.

One of the important facts about Ikaros in the brain is where it is expressed. Ikaros has been largely studied in the immune system and in the developing CNS[8], [32]. We demonstrated, to our knowledge, for the first time that Ikaros is expressed in the adult brain and that its presence is exclusive, at least in the forebrain, within microglia population. Therefore, the alterations discussed in this section are microglia mediated. The first step to assess the involvement of Ikaros in microglia function was through an Ikaros total KO model (Ikaros null). We behaviorally characterized this model using different tests and, as we found deficiencies linked to a hippocampal-depended task, all our next experiments focused on the hippocampus.

The Ikaros null model presented a microglial ameboid morphological state normally associated to inflammation conditions[165]. This idea was confirmed by the elevated expression of some inflammatory markers, such as TNFα , Nuclear factor kappa β (NF-kβ) and MDK. Despite the fact we also observed astrogliosis and that TNFα and MDK can also be released by astrocytes during inflammation process[302], our results strongly suggest that the inflammation state in this animal is primary associated to microglia as the absence of Ikaros in the adult brain is affecting primordially microglia cells. Thus, if the enhanced levels TNFα and MDK are astrocytic-dependent, this is probably a secondary

outcome mediated by the primary microglia dysregulation. These results let us think that Ikaros was possibly regulating microglial response in neuroinflammatory conditions. Consistently, when we tested the level of Ikaros in many conditions with an associated neuroinflammatory state we found augmented levels of Ikaros in all of them. Hence, if Ikaros is upregulated during neuroinflammation conditions and the absence of Ikaros induced an inflammatory-like state, Ikaros is possibly regulating microglia homeostasis. One possibility is that Ikaros presence within microglia negatively regulates the expression of pro-inflammatory factors, similarly to its functions within T cells[21]. In the same way, Ikaros could also be involved in neuroprotective processes promoting the release of anti-inflammatory factors such as IL-10[303]. A deeper characterization of microglia under modulation of Ikaros could elucidate these ideas.

Besides releasing soluble factors, phagocytosis is another function of microglia[165]. We found that, by enhancing the expression of Ikaros within microglia, the phagocytic activity was reduced, suggesting that adequate levels of Ikaros are required within microglia to elicit normal phagocytic activity. Phagocytosis can be beneficial or have detrimental consequences in a context-dependent fashion[304]. Congruent with that idea, the Ikaros null model displayed reduced spine density and decreased PSD-95 positive clusters, possibly due to an exacerbated phagocytic state (i.e. synaptic engulfment) of microglia cells. Probably, these alterations were translated, physiologically, into the LTP defects and ultimately, behaviorally, into the impaired spatial memory deficits this model exhibited. However, we cannot rule out the possible implication of other processes such as neurotoxicity, secondary implication of astrocytes, and/or neuronal neurodevelopmental defects as Ikaros is expressed in some neuronal populations during neurodevelopment.
Regarding the mechanisms by which Ikaros could modulate microglia functions, when analyzing the Ikaros null model at the molecular level, we found upregulated levels of some inflammasome members, dysregulated levels at the acetylation-methylation axis and downregulated levels of the phosphorylated version of the protein SIRT1. In this line, a possibility is that the augmented expression of the inflammasome members is mediated by the altered epigenetic state of the cells. Consistently, the interaction SIRT1-Ikaros has been associated to the deacetylase activity in histones[305]. Thus, the alteration of these two pathways, regardless they are additive or synergistic, could be ending up by enhancing the inflammasome response that would be, then, contributing to the microgliosis this model displays. Nonetheless, why some members of the inflammasome are overexpressed whilst others are not, remains unclear. Another possibility is, as mentioned before, that Ikaros is participating, either as a positive or negative regulator, in the regulation of the cytokine expression profile of microglia. Microglia can synthesize a myriad of soluble factors[306], and dysregulations in this function could impact neuronal populations in different ways, such as altering synaptic function, network connectivity or even leading to neuronal death[307], [308].

In summary, we provided evidence showing that Ikaros play a role modulating microglia response in neuroinflammatory conditions. Notwithstanding, the functions through which microglia is acting and how Ikaros is modulating internal mechanisms that coordinate

these functions remain not fully described. These qualms could be the foundations of future research.

6. General discussion

Working on these projects over the last years has brought us many results and conclusions. On one side, we have seen dysregulations of Ikaros and Helios in circulating immune cells and that the secretome of these cells can induce several schizophrenia-like phenotypes. These results led me to think that Ikaros and Helios, and probably also other members of the Ikzf family, by influencing effector cell functions in peripheral immune cells, participate in the pathogenesis of schizophrenia. On the other side, we have seen that the absence of Ikaros induces inflammatory signatures in microglia and that Ikaros is over expressed in inflammatory-associated conditions in microglia. Besides, we have also observed that Ikaros can modulate microglia essential functions such as phagocytosis. These results let me think that the immune modulatory roles of Ikaros go beyond peripheral immune cells populations and that Ikaros, and maybe also other members of the Ikzf family, is/are playing an active immune modulatory role in the CNS. Altogether, these results and ideas are congruent with previous propositions of other researchers. Specifically, that dysregulation of T cells and neuroinflammation are two main ways through which the immune system contributes to the pathogenesis of schizophrenia[160], [162], [178]. Nevertheless, even if I consider we have contributed with an extensive new knowledge regarding the implication of the Ikaros family through the immune system in the context of schizophrenia, many gaps remain to be addressed to comprehensively understand the whole picture.

For instance, it has been proposed that the hyperexcitability of the hippocampus is a core feature of schizophrenia contributing to the three categories of symptoms [125], [309](See supplementary figure 8 of the first article). This prompts the inquiry of why the hippocampal region is hyperactive in schizophrenia. In line with our results, one of the most prominent findings in schizophrenia post-mortem brains is the loss of PV[310]. PV allows neurons to fire at high frequencies, which is one of the reasons why it is necessary for the generation of high-frequency evoked gamma rhythms, which are capital for complex cognitive functions. Notably, evoked gamma rhythms are shown to be altered in schizophrenia[311]. Thereby, as discussed in section 3, a possibility is that the reduction of PV+ interneurons is leading to a general reduction of pyramidal neurons inhibition and, consequently, to a disruption of the rhythmic activity along with an hyperactivation state. In the first article, we proposed that IL-4 and CXCL10 were possibly playing a role in the reduction of PV+ cells. However, the processes that could lead to this outcome were not included. Following the idea that Ikaros may be downregulated in Th1 and Th2 subpopulations, as explained in section 1, this would lead to over expression of IFN-γ by Th1 cells and, at the same time, less expression of IL-4 by Th2 cells. The elevated levels of IFN-γ and the reduced levels of IL-4 would synergistically lead to promotion of Th1 differentiation and repression of Th2 differentiation, acting as a constant positive feedback loop. IFN-γ is known to induce the production of, among other chemokines,

CXCL10, that in fact is a.k.a. interferon gamma-induced protein 10 (ip-10). This could initially underlie the altered levels of IL-4 and CXCL10. In addition, a downregulation of Helios on Treg cells would reduce the capacity of Treg cells to modulate inflammation and hindering the capacity of pTreg cells to maintain their phenotype. Wholly, these CD4+ T cells alterations could easily propitiate a pro-inflammatory state stemmed by the downregulations of Ikaros and Helios in those CD4+ T cells. However, how this peripheral-immune state could be translated to the brain, where schizophrenia mostly takes place, is unclear. A very strong candidate possibly mediating this peripheral-to-central connection in this context is microglia.

Microglia are a key cell population orchestrating inflammation within the brain parenchyma. They can sense a wide variety of soluble factors, such as cytokines, as well as to react to DAMPs and PAMPs, such as TLR-ligands[165]. Yet, how microglia react to these signals and how these reactions impact on neuronal function and survival can widely vary depending on the context. For instance, emerging evidence has shown that priming of microglia by the soluble factor IFN-γ can have many effects in microglia[312], [313], [314]. After *in-situ* exposure to IFN-γ, microglia can go through hypertrophy, reduction of ramification (ameboid shape) and enhanced proliferation[314]. Besides, IFN-γ also moderately elevates activation markers such as, inducible nitric oxide synthase (iNOS) and IL-6[314], [315]. Interestingly, some studies reported that neuronal gamma oscillations decreased in frequency after IFN-γ exposure[314], [316]. This dysregulation was not mirrored neither by IFN-α nor by IL-17, suggesting an unique function of IFN-γ in microglia[314]. In summary, IFN-γ priming can induce significant microglia proliferation, release of pro-inflammatory factors, and moderate activation that can affect neuronal networks. On the other hand, exposure of microglia to PAMPs, like LPS (a TLR4 ligand) also generates some effects. For instance, upon LPS exposure, microglia can exhibit morphological changes, release of pro-inflammatory cytokines and show moderate upregulation of iNOS[316], [317]. Noteworthy, this microglia phenotype is not associated with alterations in neuronal excitability, gamma oscillations and/or short-term synaptic plasticity[316], [318]. Wherefore, the individual effects of either IFN-γ or TLR4 ligands (e.g.LPS) on microglia seem not to elicit a critical inflammatory response. Nonetheless, a pivotal aspect of priming in macrophages is the over amplified cellular response to a secondary inflammatory stimulus such as viral of bacterial components[312], and IFN-γ priming followed by TLR4 stimulation in microglia is not the exception.

It has been shown that paired stimulation by IFN-γ and LPS results in a neurotoxic microglia phenotype[312], [314], [316]. This was displayed *in-situ* by amoeboid-like morphology, downregulated levels of “surveillance-associated” genes, and release of many pro-inflammatory factors (e.g.IL-6, IL-1, TNF-α) after paired IFN-γ +LPS stimulation[316], [318], [319]. Besides, the upregulation of iNOS expression was significantly intensified and correlated with the excessive generation of nitric oxide (NO) [316], [318], [319]. Substantial production of superoxide and enhanced aerobic glycolysis were also associated to this phenotype [320], [321]. Noticeably, the IFN-γ +LPS stimulation generated strong electrical activity dysfunction along with inflammatory neurodegeneration[316], [318]. IFN-γ priming on microglia seems to generate unique

effects, as other factors such as GM-CSF or IL-17 did not replicate its priming effects[286]. In the same line, paired exposure involving IFN-γ and TLR4 ligands seems to be a more aggressive phenotype when compared to other TLR ligands (e.i. TLR2-and TLR3)[322]. Finally, an *in-vivo* study reported that priming by IFN-γ generated impaired hippocampal neurogenesis that likely let to cognitive deficiencies[313]. Collectively, this suggests that IFN-γ priming is crucial to elicit TLR-sensed microglia into a neurotoxic phenotype driving to oxidative and energetic stress, strong neuronal network dysregulation and neurodegeneration, primarily due to release of oxidants.

Microglia priming by over-expressed IFN-γ followed by TLR stimulation is a plausible way the alterations of Ikaros and Helios in CD4+ cells are generating an inflammatory state within the brain. It has been shown that IFN-γ is able to pass the BBB in an intact form, similarly to other cytokines[323], [324]. Besides, BBB leakage have been shown to be enhanced during infectious and inflammatory states[325], [326]. These infiltrations account for soluble factors such as IFN-γ and immune cells such as T cells. Thereby, in the context of schizophrenia, the augmented levels of IFN-γ could be leading to elevated primed-microglia that upon an immune challenge during early life is driving to an over amplified immune response in the brain. Not surprisingly, infections by toxoplasma gondii are among the highest in risk of developing schizophrenia later[327], possibly, given that it is sensed by TLR4 (the more aggressive primed-microglia phenotype). With enhanced amounts of IFN-γ and decreased capacity of Treg cells to regulate inflammation states, the situation is probably affecting the person`s CNS progressively during years (see figure X) until the first psychotic period appears. After pharmacological treatment, besides remission of positive symptoms, the levels of IFN-γ are also generally downregulated, this is probably contributing to a less sensitive CNS immune reaction. Thereafter, the chronic low-grade inflammation state described in schizophrenia could be stemmed by the still deficient Treg cells. Consistently, the increased frequency of autoimmune diseases in patients could be also linked to that permanent Treg cells deficiencies.

During the inflammation states that involve the IFN-γ primed microglia, one possibility is that the hippocampus is one the most affected areas. As it has been proposed before, the oxidants from microglia in this context are probably generating alterations in neuronal energetic metabolism, synaptic transmission, inhibition-excitation equilibrium and neuronal survival[312], [320]. Besides, an increased body of evidence has reported that IFN-γ can negatively impact on hippocampal inhibition[316], [328], [329], [330]. Hence, the disbalances in excitation-inhibition could be driving to the reduction of activity of PV+ cells and ultimately also to their reduction[310], [331]. That possibility could explain the hyperactive hippocampus contributing to three kinds of symptoms of schizophrenia. However, it is equally possible that other brain areas are being affected along the hippocampus during IFN-γ+TLR4 ligand activated microglia inflammation and that these affectations are primarily contributing to the generation of the symptoms. Another important fact about microglia responses in neuroinflammation that could be worth taking into account in the context of schizophrenia is the involvement of Ikaros. Considering that microglia are immune cells that invade the brain during development[332], it would not be counter intuitive to ponder that Ikaros, and perhaps other Ikzf family members, are

dysregulated in microglia, similarly to its situation in PBMCs. Based on our results of the second article, downregulated levels of Ikaros could be provoking a more inflammatory-engaged microglia, likely with a more phagocytic phenotype and releasing pro-inflammatory cytokines that could be secondarily affecting other immune and glia cells. This tendency to a more inflammatory-engaged microglia generated by the dysregulation of Ikaros could drive to a more exacerbated microglia response in a IFN-γR+TLR stimulation context. Further, an Ikaros-downregulated microglia could also be implicated in the maintenance of the chronic low-grade inflammatory state of schizophrenia, as microglia would be constantly prone to exhibit an inflammatory profile. Certainly, the implication of Ikaros-downregulated microglia in both situations could be also taking place.

The dysregulated levels of IL-4 and CXCL10 could also play a role by directly acting within the brain parenchyma. For instance, as discussed in section 4, altered levels of both can have an impact in synaptic plasticity and in network function[290], [294], [298]. Furthermore, the presence of IL-4 has been related with decreased microglia-associated inflammation[301], thus, its reduced levels could also contribute to enhance microglia responses in inflammatory conditions. Similarly, high levels of CXCL10 have been shown to have neurotoxic effects likely mediated by microglia[299], [300]. Moreover, the presence of CXCL10 has been related to inhibition of angiogenesis during inflammation processes[333], [334], a reduction of vascularization could hinder the ability of the organism to manage severe inflammatory periods followed by chronic low-grade inflammation states.

Based on our results, the available literature about the topics and on my personal insights, my proposed model about the implication of the Ikaros family in the pathogenesis of schizophrenia could be summarized as follows(see Figure 9): The dysregulated levels of Ikaros acting in Th1 and Th2 cells generates elevated levels of IFN-γ and reduced levels of IL-4, the elevated levels of IFN-γ induce, in turn, augmented release of CXCL10. On the other hand, the downregulated levels of Helios in Treg cells produces, in the same cells, abridged inflammatory-modulation capacity, difficulties maintaining a regulatory phenotype and maybe expression of IFN-γ. IFN-γ is leaking into the brain parenchyma (equivalently possible that activated T cells are also leaking), driving to a general IFN-γ primed-microglia state. Upon immune challenges like Toxoplasma gondii infection, an over amplified immune response is generated affecting neuronal functions and ultimately leading to neuronal death. This circuit is repeated during life upon different immune insults and in between remains a constant tendency towards developing inflammatory states. Besides IFN-γ priming, inflammatory states are also underpinned by deficient Treg cells and perhaps by downregulation of Ikaros within microglia. As a result of the combination of these factors over years, the brain tissue is gradually affected until the manifestation of the first psychotic episode. A possibility is that some brain regions, such as the hippocampus, are more pronouncedly affected. After pharmacological treatment, IFN-γ is downregulated. However, the reduced levels of Helios in Treg cells and the possibly reduced levels of Ikaros in microglia are still contributing to the low-grade inflammatory state in the brain. Other soluble factors such as IL-4 and CXCL10 are

perhaps directly acting on neurons and/or on glia cells contributing to inflammation spreading and neuronal dysfunction.

The perspective presented is perhaps an oversimplification of the intricate neuroimmune interactions related to the pathogenesis of schizophrenia. Furthermore, many other variables implicated (e.g. genetic alterations) in schizophrenia pathogenesis should be taken in consideration to comprehensively understand such a complicated psychiatric condition. Nonetheless, I truly hope this work can contribute to and inspire the development of future research regarding this matter.

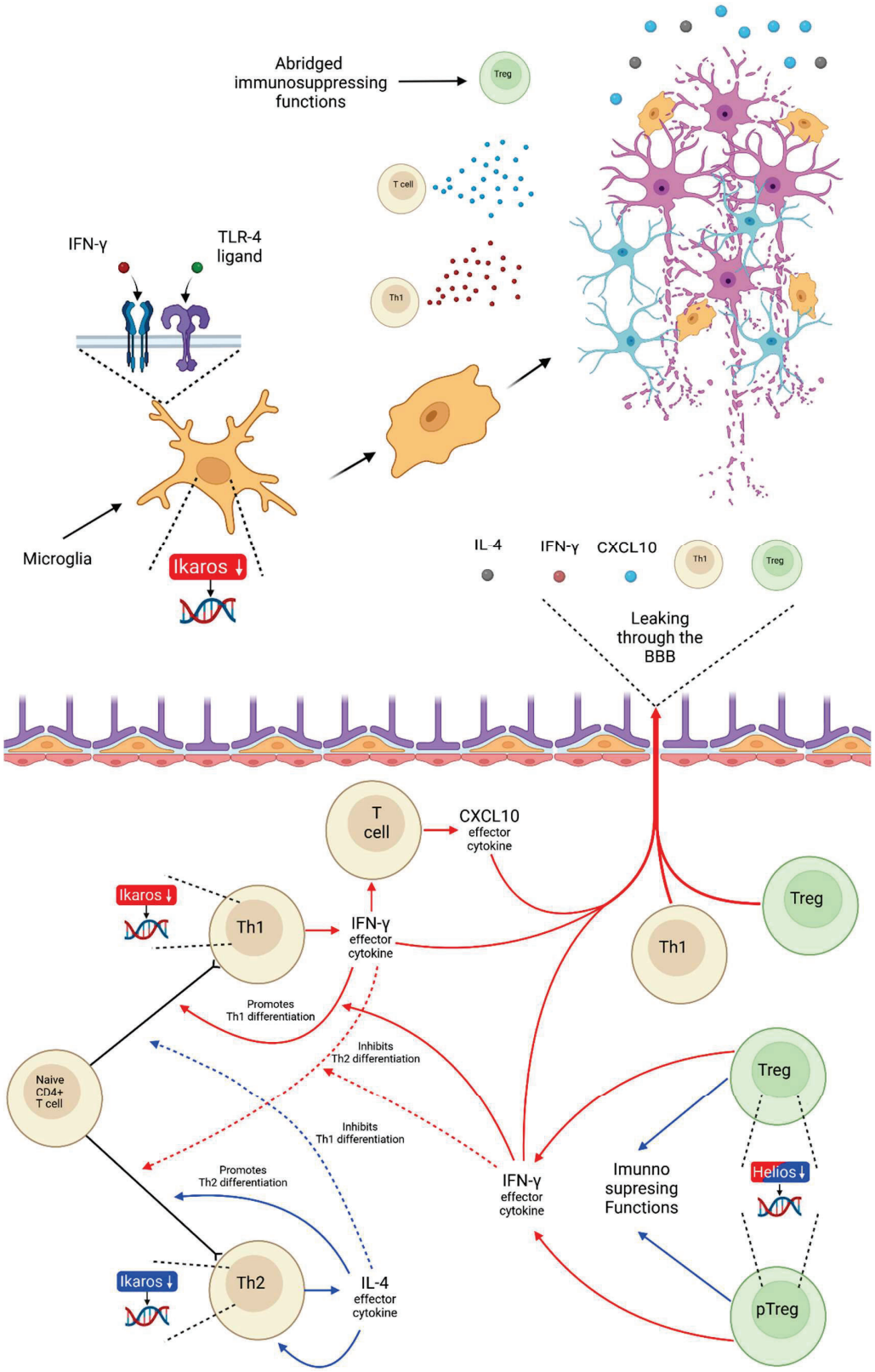

Figure 9. *Illustration of the proposed model of the possible implication of Ikaros and Helios in the pathogenesis of schizophrenia. Red arrows depict the outcomes that are promoted by the downregulation of Ikaros and Helios. Blue arrows depict the outcomes that are reduced or inhibited by the downregulation of Ikaros and Helios. Possible cell differentiation is depicted by* ⊣.

VI. Conclusions

- The transcription factors Ikaros and Helios are downregulated in PBMCs and in CD4+ cells of a cohort of patients diagnosed with schizophrenia.

- The animal model presenting a double downregulation of Ikaros and Helios (*Ikaros*$^{+/-}$: *Helios*$^{+/-)}$ presents schizophrenia-like behavior in the three categories of symptoms.

- PBMCs-derivate secretome from schizophrenia patients with downregulated levels of Ikaros and Helios can induce *in-vitro* and *in-vivo* schizophrenia-like phenotypes.

- Some cytokines levels like IL-4 and CXCL10 are specifically altered PBMCs-derivate secretome from schizophrenia patients with downregulated levels of Ikaros and Helios.

- The presence of Ikaros in adult mice is exclusive within microglia cells in the Forebrain.

- Ikaros regulates microglia homeostasis in inflammation and neurodegeneration and its alteration can impact memory-associated processes like LTP or synaptic plasticity.

VII. References

[1] K. Georgopoulos, D. D. Moore, y B. Derfler, «Ikaros, an Early Lymphoid-Specific Transcription Factor and a Putative Mediator for T Cell Commitment», *Science*, vol. 258, n.º 5083, pp. 808-812, oct. 1992, doi: 10.1126/science.1439790.
[2] P. Kastner, A. Aukenova, y S. Chan, «Evolution of the Ikaros family transcription factors: From a deuterostome ancestor to humans», *Biochem. Biophys. Res. Commun.*, vol. 694, p. 149399, ene. 2024, doi: 10.1016/j.bbrc.2023.149399.
[3] S. A. Lambert *et al.*, «The Human Transcription Factors», *Cell*, vol. 172, n.º 4, pp. 650-665, feb. 2018, doi: 10.1016/j.cell.2018.01.029.
[4] Y. Fan y D. Lu, «The Ikaros family of zinc-finger proteins», *Acta Pharm. Sin. B*, vol. 6, n.º 6, pp. 513-521, nov. 2016, doi: 10.1016/j.apsb.2016.06.002.
[5] K. J. Payne, J.-H. Nicolas, J. Y. Zhu, L. W. Barsky, y G. M. Crooks, «Cutting Edge: Predominant Expression of a Novel Ikaros Isoform in Normal Human Hemopoiesis1», *J. Immunol.*, vol. 167, n.º 4, pp. 1867-1870, ago. 2001, doi: 10.4049/jimmunol.167.4.1867.
[6] M. Affar *et al.*, «IKAROS: from chromatin organization to transcriptional elongation control», *Cell Death Differ.*, pp. 1-19, ago. 2023, doi: 10.1038/s41418-023-01212-2.
[7] F. Romero, C. Martínez-A, J. Camonis, y A. Rebollo, «Aiolos transcription factor controls cell death in T cells by regulating Bcl-2 expression and its cellular localization», *EMBO J.*, vol. 18, n.º 12, pp. 3419-3430, jun. 1999, doi: 10.1093/emboj/18.12.3419.
[8] B. Heizmann, P. Kastner, y S. Chan, «The Ikaros family in lymphocyte development», *Curr. Opin. Immunol.*, vol. 51, pp. 14-23, abr. 2018, doi: 10.1016/j.coi.2017.11.005.
[9] F. da Silva Lima, C. E. da Silva Gonçalves, y R. A. Fock, «A review of the role of zinc finger proteins on hematopoiesis», *J. Trace Elem. Med. Biol.*, vol. 80, p. 127290, dic. 2023, doi: 10.1016/j.jtemb.2023.127290.
[10] L. B. John y A. C. Ward, «The Ikaros gene family: Transcriptional regulators of hematopoiesis and immunity», *Mol. Immunol.*, vol. 48, n.º 9, pp. 1272-1278, may 2011, doi: 10.1016/j.molimm.2011.03.006.
[11] J.-H. Wang *et al.*, «Aiolos Regulates B Cell Activation and Maturation to Effector State», *Immunity*, vol. 9, n.º 4, pp. 543-553, oct. 1998, doi: 10.1016/S1074-7613(00)80637-8.
[12] J.-H. Wang *et al.*, «Selective Defects in the Development of the Fetal and Adult Lymphoid System in Mice with an Ikaros Null Mutation», *Immunity*, vol. 5, n.º 6, pp. 537-549, dic. 1996, doi: 10.1016/S1074-7613(00)80269-1.
[13] C. Schmitt, C. Tonnelle, A. Dalloul, C. Chabannon, P. Debré, y A. Rebollo, «Aiolos and Ikaros: Regulators of lymphocyte development, homeostasis and lymphoproliferation», *Apoptosis*, vol. 7, n.º 3, pp. 277-284, jun. 2002, doi: 10.1023/A:1015372322419.
[14] P. Agnihotri, N. M. Robertson, S. E. Umetsu, K. Arakcheeva, y S. Winandy, «Lack of Ikaros cripples expression of Foxo1 and its targets in naive T cells», *Immunology*, vol. 152, n.º 3, pp. 494-506, nov. 2017, doi: 10.1111/imm.12786.
[15] B. Boast *et al.*, «A Point Mutation in IKAROS ZF1 Causes a B Cell Deficiency in Mice», *J. Immunol.*, vol. 206, n.º 7, pp. 1505-1514, abr. 2021, doi: 10.4049/jimmunol.1901464.
[16] K. Georgopoulos *et al.*, «The ikaros gene is required for the development of all lymphoid lineages», *Cell*, vol. 79, n.º 1, pp. 143-156, oct. 1994, doi: 10.1016/0092-8674(94)90407-3.
[17] P. Kirstetter, M. Thomas, A. Dierich, P. Kastner, y S. Chan, «Ikaros is critical for B cell differentiation and function», *Eur. J. Immunol.*, vol. 32, n.º 3, pp. 720-730, 2002, doi: 10.1002/1521-4141(200203)32:3<720::AID-IMMU720>3.0.CO;2-P.
[18] P. Papathanasiou *et al.*, «Widespread failure of hematolymphoid differentiation caused by a recessive niche-filling allele of the Ikaros transcription factor», *Immunity*, vol. 19, n.º 1, pp. 131-144, jul. 2003, doi: 10.1016/s1074-7613(03)00168-7.

[19] T. Yoshida, S. Yao-Ming Ng, J. C. Zuniga-Pflucker, y K. Georgopoulos, «Early hematopoietic lineage restrictions directed by Ikaros», *Nat. Immunol.*, vol. 7, n.º 4, pp. 382-391, abr. 2006, doi: 10.1038/ni1314.

[20] W. Goh *et al.*, «IKAROS and AIOLOS directly regulate AP-1 transcriptional complexes and are essential for NK cell development», *Nat. Immunol.*, vol. 25, n.º 2, pp. 240-255, feb. 2024, doi: 10.1038/s41590-023-01718-4.

[21] M. D. Powell, K. A. Read, B. K. Sreekumar, y K. J. Oestreich, «Ikaros Zinc Finger Transcription Factors: Regulators of Cytokine Signaling Pathways and CD4+ T Helper Cell Differentiation», *Front. Immunol.*, vol. 10, jun. 2019, doi: 10.3389/fimmu.2019.01299.

[22] K. Hahm *et al.*, «Helios, a T cell-restricted Ikaros family member that quantitatively associates with Ikaros at centromeric heterochromatin», *Genes Dev.*, vol. 12, n.º 6, pp. 782-796, mar. 1998.

[23] Z. Zhang, C. S. Swindle, J. T. Bates, R. Ko, C. V. Cotta, y C. A. Klug, «Expression of a non–DNA-binding isoform of Helios induces T-cell lymphoma in mice», *Blood*, vol. 109, n.º 5, pp. 2190-2197, nov. 2006, doi: 10.1182/blood-2005-01-031930.

[24] Q. Cai, A. Dierich, M. Oulad-Abdelghani, S. Chan, y P. Kastner, «Helios Deficiency Has Minimal Impact on T Cell Development and Function1», *J. Immunol.*, vol. 183, n.º 4, pp. 2303-2311, ago. 2009, doi: 10.4049/jimmunol.0901407.

[25] A. M. Thornton *et al.*, «Expression of Helios, an Ikaros Transcription Factor Family Member, Differentiates Thymic-Derived from Peripherally Induced Foxp3+ T Regulatory Cells», *J. Immunol.*, vol. 184, n.º 7, pp. 3433-3441, abr. 2010, doi: 10.4049/jimmunol.0904028.

[26] A. M. Thornton y E. M. Shevach, «Helios: still behind the clouds», *Immunology*, vol. 158, n.º 3, pp. 161-170, 2019, doi: 10.1111/imm.13115.

[27] D. Getnet *et al.*, «A role for the transcription factor Helios in human CD4+CD25+ regulatory T cells», *Mol. Immunol.*, vol. 47, n.º 7, pp. 1595-1600, abr. 2010, doi: 10.1016/j.molimm.2010.02.001.

[28] H.-J. Kim *et al.*, «Stable inhibitory activity of regulatory T cells requires the transcription factor Helios», *Science*, vol. 350, n.º 6258, pp. 334-339, oct. 2015, doi: 10.1126/science.aad0616.

[29] I. Baine, S. Basu, R. Ames, R. S. Sellers, y F. Macian, «Helios Induces Epigenetic Silencing of Il2 Gene Expression in Regulatory T Cells», *J. Immunol.*, vol. 190, n.º 3, pp. 1008-1016, feb. 2013, doi: 10.4049/jimmunol.1200792.

[30] C. Raffin, P. Pignon, C. Celse, E. Debien, D. Valmori, y M. Ayyoub, «Human Memory Helios− FOXP3+ Regulatory T Cells (Tregs) Encompass Induced Tregs That Express Aiolos and Respond to IL-1β by Downregulating Their Suppressor Functions», *J. Immunol.*, vol. 191, n.º 9, pp. 4619-4627, nov. 2013, doi: 10.4049/jimmunol.1301378.

[31] D. V. Agoston *et al.*, «Ikaros is expressed in developing striatal neurons and involved in enkephalinergic differentiation», *J. Neurochem.*, vol. 102, n.º 6, pp. 1805-1816, 2007, doi: 10.1111/j.1471-4159.2007.04653.x.

[32] R. Martín-Ibáñez *et al.*, «Ikaros-1 couples cell cycle arrest of late striatal precursors with neurogenesis of enkephalinergic neurons», *J. Comp. Neurol.*, vol. 518, n.º 3, pp. 329-351, 2010, doi: 10.1002/cne.22215.

[33] J. M. Alsiö, B. Tarchini, M. Cayouette, y F. J. Livesey, «Ikaros promotes early-born neuronal fates in the cerebral cortex», *Proc. Natl. Acad. Sci.*, vol. 110, n.º 8, pp. E716-E725, feb. 2013, doi: 10.1073/pnas.1215707110.

[34] R. Martín-Ibáñez *et al.*, «Helios expression coordinates the development of a subset of striatopallidal medium spiny neurons», *Development*, vol. 144, n.º 8, pp. 1566-1577, abr. 2017, doi: 10.1242/dev.138248.

[35] R. Martín-Ibáñez *et al.*, «Helios Transcription Factor Expression Depends on Gsx2 and Dlx1&2 Function in Developing Striatal Matrix Neurons», https://home-liebertpub-

com.sire.ub.edu/scd. Accedido: 30 de abril de 2024. [En línea]. Disponible en: https://www-liebertpub-com.sire.ub.edu/doi/10.1089/scd.2011.0607
[36] A. Giralt *et al.*, «Helios modulates the maturation of a CA1 neuronal subpopulation required for spatial memory formation», *Exp. Neurol.*, vol. 323, p. 113095, ene. 2020, doi: 10.1016/j.expneurol.2019.113095.
[37] S. M. Chan, «The Making of a Leukemic Stem Cell: A Novel Role for IKZF2 in AML Stemness and Differentiation», *Cell Stem Cell*, vol. 24, n.º 1, pp. 5-6, ene. 2019, doi: 10.1016/j.stem.2018.12.007.
[38] M. Cippitelli *et al.*, «Role of Aiolos and Ikaros in the Antitumor and Immunomodulatory Activity of IMiDs in Multiple Myeloma: Better to Lose Than to Find Them», *Int. J. Mol. Sci.*, vol. 22, n.º 3, Art. n.º 3, ene. 2021, doi: 10.3390/ijms22031103.
[39] R. Xia, Y. Cheng, X. Han, Y. Wei, y X. Wei, «Ikaros Proteins in Tumor: Current Perspectives and New Developments», *Front. Mol. Biosci.*, vol. 8, dic. 2021, doi: 10.3389/fmolb.2021.788440.
[40] S. I. Tayel, S. M. El-Hefnway, W. M. M. Abo El-fotoh, y R. S. El-Zayat, «The Genetic Variants of IKZF1 Gene Linked with the Growing Risk of Childhood Acute Lymphoblastic Leukaemia», *Curr. Mol. Med.*, vol. 19, n.º 1, pp. 32-39, ene. 2019, doi: 10.2174/1566524019666190219123900.
[41] W. Zhao, T. Chen, y H. Wang, «Ikaros is heterogeneously expressed in lung adenocarcinoma and is involved in its progression», *J. Int. Med. Res.*, vol. 48, n.º 8, p. 0300060520945860, ago. 2020, doi: 10.1177/0300060520945860.
[42] H. Kose y S. S. Kilic, «Can Ikaros mutation lead to intellectual disability?», *Scand. J. Immunol.*, vol. 95, n.º 4, p. e13138, 2022, doi: 10.1111/sji.13138.
[43] A. Sancho-Balsells *et al.*, «Lack of Helios During Neural Development Induces Adult Schizophrenia-Like Behaviors Associated With Aberrant Levels of the TRIF-Recruiter Protein WDFY1», *Front. Cell. Neurosci.*, vol. 14, may 2020, doi: 10.3389/fncel.2020.00093.
[44] K. Jaeschke, F. Hanna, S. Ali, N. Chowdhary, T. Dua, y F. Charlson, «Global estimates of service coverage for severe mental disorders: findings from the WHO Mental Health Atlas 2017», *Glob. Ment. Health*, vol. 8, p. e27, ene. 2021, doi: 10.1017/gmh.2021.19.
[45] «Schizophrenia». Accedido: 3 de mayo de 2024. [En línea]. Disponible en: https://www.who.int/news-room/fact-sheets/detail/schizophrenia
[46] I. Calzavara Pinton *et al.*, «The economic burden of schizophrenia spectrum disorders: clinical and functional correlates and predictors of direct costs. A retrospective longitudinal study», *Psychiatry Res.*, vol. 342, p. 116240, dic. 2024, doi: 10.1016/j.psychres.2024.116240.
[47] R. A. McCutcheon, T. Reis Marques, y O. D. Howes, «Schizophrenia—An Overview», *JAMA Psychiatry*, vol. 77, n.º 2, pp. 201-210, feb. 2020, doi: 10.1001/jamapsychiatry.2019.3360.
[48] H. L. Provencher y K. T. Mueser, «Positive and negative symptom behaviors and caregiver burden in the relatives of persons with schizophrenia», *Schizophr. Res.*, vol. 26, n.º 1, pp. 71-80, jul. 1997, doi: 10.1016/S0920-9964(97)00043-1.
[49] D. De Berardis, S. De Filippis, G. Masi, S. Vicari, y A. Zuddas, «A Neurodevelopment Approach for a Transitional Model of Early Onset Schizophrenia», *Brain Sci.*, vol. 11, n.º 2, Art. n.º 2, feb. 2021, doi: 10.3390/brainsci11020275.
[50] C. Hjorthøj, A. E. Stürup, J. J. McGrath, y M. Nordentoft, «Years of potential life lost and life expectancy in schizophrenia: a systematic review and meta-analysis», *Lancet Psychiatry*, vol. 4, n.º 4, pp. 295-301, abr. 2017, doi: 10.1016/S2215-0366(17)30078-0.
[51] «Diagnostic and Statistical Manual of Mental Disorders», DSM Library. Accedido: 2 de mayo de 2024. [En línea]. Disponible en: https://dsm-psychiatryonline-org.sire.ub.edu/doi/book/10.1176/appi.books.9780890425787

[52] E. Kraepelin, «Dementia præcox and paraphrenia | CiNii Research», Accedido: 11 de julio de 2024. [En línea]. Disponible en: https://cir.nii.ac.jp/crid/1130000796358739200
[53] J. O. Haug, «Pneumoencephalographic studies in mental disease», *Acta Psychiatr. Neurol. KjøBenhavn*, vol. 38, n.º Suppl. No. 165, pp. 104-104, 1962.
[54] S. V. Haijma, N. Van Haren, W. Cahn, P. C. M. P. Koolschijn, H. E. Hulshoff Pol, y R. S. Kahn, «Brain Volumes in Schizophrenia: A Meta-Analysis in Over 18 000 Subjects», *Schizophr. Bull.*, vol. 39, n.º 5, pp. 1129-1138, sep. 2013, doi: 10.1093/schbul/sbs118.
[55] P. J. Harrison, N. Freemantle, y J. R. Geddes, «Meta-analysis of brain weight in schizophrenia», *Schizophr. Res.*, vol. 64, n.º 1, pp. 25-34, nov. 2003, doi: 10.1016/S0920-9964(02)00502-9.
[56] E. C. del Re *et al.*, «Enlarged lateral ventricles inversely correlate with reduced corpus callosum central volume in first episode schizophrenia: association with functional measures», *Brain Imaging Behav.*, vol. 10, n.º 4, Art. n.º 4, dic. 2015, doi: 10.1007/s11682-015-9493-2.
[57] M. E. Shenton, C. C. Dickey, M. Frumin, y R. W. McCarley, «A review of MRI findings in schizophrenia», *Schizophr. Res.*, vol. 49, n.º 1, pp. 1-52, abr. 2001, doi: 10.1016/S0920-9964(01)00163-3.
[58] M. R. Williams *et al.*, «Changes in cortical thickness in the frontal lobes in schizophrenia are a result of thinning of pyramidal cell layers», *Eur. Arch. Psychiatry Clin. Neurosci.*, vol. 263, n.º 1, Art. n.º 1, may 2012, doi: 10.1007/s00406-012-0325-8.
[59] K. O. Lim, E. V. Sullivan, R. B. Zipursky, y A. Pfefferbaum, «Cortical gray matter volume deficits in schizophrenia: a replication», *Schizophr. Res.*, vol. 20, n.º 1, pp. 157-164, may 1996, doi: 10.1016/0920-9964(95)00081-X.
[60] G. Rajkowska, A. Halaris, y L. D. Selemon, «Reductions in neuronal and glial density characterize the dorsolateral prefrontal cortex in bipolar disorder», *Biol. Psychiatry*, vol. 49, n.º 9, pp. 741-752, may 2001, doi: 10.1016/S0006-3223(01)01080-0.
[61] J. J. Thune, H. B. M. Uylings, y B. Pakkenberg, «No deficit in total number of neurons in the prefrontal cortex in schizophrenics», *J. Psychiatr. Res.*, vol. 35, n.º 1, pp. 15-21, ene. 2001, doi: 10.1016/S0022-3956(00)00043-1.
[62] J. N. Pierri, C. L. E. Volk, S. Auh, A. Sampson, y D. A. Lewis, «Somal size of prefrontal cortical pyramidal neurons in schizophrenia: differential effects across neuronal subpopulations», *Biol. Psychiatry*, vol. 54, n.º 2, pp. 111-120, jul. 2003, doi: 10.1016/S0006-3223(03)00294-4.
[63] S. A. Mauney *et al.*, «Developmental Pattern of Perineuronal Nets in the Human Prefrontal Cortex and Their Deficit in Schizophrenia», *Biol. Psychiatry*, vol. 74, n.º 6, pp. 427-435, sep. 2013, doi: 10.1016/j.biopsych.2013.05.007.
[64] L. A. Glantz y D. A. Lewis, «Decreased Dendritic Spine Density on Prefrontal Cortical Pyramidal Neurons in Schizophrenia», *Arch. Gen. Psychiatry*, vol. 57, n.º 1, pp. 65-73, ene. 2000, doi: 10.1001/archpsyc.57.1.65.
[65] N. Kolluri, Z. Sun, A. R. Sampson, y D. A. Lewis, «Lamina-Specific Reductions in Dendritic Spine Density in the Prefrontal Cortex of Subjects With Schizophrenia», *Am. J. Psychiatry*, vol. 162, n.º 6, pp. 1200-1202, jun. 2005, doi: 10.1176/appi.ajp.162.6.1200.
[66] N. A. Uranova, V. M. Vostrikov, D. D. Orlovskaya, y V. I. Rachmanova, «Oligodendroglial density in the prefrontal cortex in schizophrenia and mood disorders: a study from the Stanley Neuropathology Consortium», *Schizophr. Res.*, vol. 67, n.º 2, pp. 269-275, abr. 2004, doi: 10.1016/S0920-9964(03)00181-6.
[67] L. Garey, «When cortical development goes wrong: schizophrenia as a neurodevelopmental disease of microcircuits», *J. Anat.*, vol. 217, n.º 4, pp. 324-333, 2010, doi: 10.1111/j.1469-7580.2010.01231.x.

[68] F. M. Benes, S. L. Vincent, A. Marie, y Y. Khan, «Up-regulation of GABAA receptor binding on neurons of the prefrontal cortex in schizophrenic subjects», *Neuroscience*, vol. 75, n.º 4, pp. 1021-1031, nov. 1996, doi: 10.1016/0306-4522(96)00328-4.

[69] D. W. Volk, J. N. Pierri, J.-M. Fritschy, S. Auh, A. R. Sampson, y D. A. Lewis, «Reciprocal Alterations in Pre- and Postsynaptic Inhibitory Markers at Chandelier Cell Inputs to Pyramidal Neurons in Schizophrenia», *Cereb. Cortex*, vol. 12, n.º 10, pp. 1063-1070, oct. 2002, doi: 10.1093/cercor/12.10.1063.

[70] D. W. Volk, M. C. Austin, J. N. Pierri, A. R. Sampson, y D. A. Lewis, «Decreased Glutamic Acid Decarboxylase67 Messenger RNA Expression in a Subset of Prefrontal Cortical γ-Aminobutyric Acid Neurons in Subjects With Schizophrenia», *Arch. Gen. Psychiatry*, vol. 57, n.º 3, pp. 237-245, mar. 2000, doi: 10.1001/archpsyc.57.3.237.

[71] S. J. Dienel, K. N. Fish, y D. A. Lewis, «The Nature of Prefrontal Cortical GABA Neuron Alterations in Schizophrenia: Markedly Lower Somatostatin and Parvalbumin Gene Expression Without Missing Neurons», *Am. J. Psychiatry*, vol. 180, n.º 7, pp. 495-507, jul. 2023, doi: 10.1176/appi.ajp.20220676.

[72] D. W. Chung, K. N. Fish, y D. A. Lewis, «Pathological Basis for Deficient Excitatory Drive to Cortical Parvalbumin Interneurons in Schizophrenia», *Am. J. Psychiatry*, vol. 173, n.º 11, pp. 1131-1139, nov. 2016, doi: 10.1176/appi.ajp.2016.16010025.

[73] A. Marsman, M. P. van den Heuvel, D. W. J. Klomp, R. S. Kahn, P. R. Luijten, y H. E. Hulshoff Pol, «Glutamate in Schizophrenia: A Focused Review and Meta-Analysis of 1H-MRS Studies», *Schizophr. Bull.*, vol. 39, n.º 1, pp. 120-129, ene. 2013, doi: 10.1093/schbul/sbr069.

[74] A. Banerjee *et al.*, «Src kinase as a mediator of convergent molecular abnormalities leading to NMDAR hypoactivity in schizophrenia», *Mol. Psychiatry*, vol. 20, n.º 9, pp. 1091-1100, sep. 2015, doi: 10.1038/mp.2014.115.

[75] M. Williams, «Frontal Cortex», 2021. doi: 10.1007/978-3-030-68308-5_4.

[76] M. Nakamura *et al.*, «Orbitofrontal volume deficit in schizophrenia and thought disorder», *Brain*, vol. 131, n.º 1, pp. 180-195, ene. 2008, doi: 10.1093/brain/awm265.

[77] C. Zhao *et al.*, «Structural and functional brain abnormalities in schizophrenia: A cross-sectional study at different stages of the disease», *Prog. Neuropsychopharmacol. Biol. Psychiatry*, vol. 83, pp. 27-32, abr. 2018, doi: 10.1016/j.pnpbp.2017.12.017.

[78] D. Cotter, L. Hudson, y S. Landau, «Evidence for orbitofrontal pathology in bipolar disorder and major depression, but not in schizophrenia», *Bipolar Disord.*, vol. 7, n.º 4, pp. 358-369, 2005, doi: 10.1111/j.1399-5618.2005.00230.x.

[79] A. B. Whitworth *et al.*, «Hippocampal volume reduction in male schizophrenic patients», *Schizophr. Res.*, vol. 31, n.º 2, pp. 73-81, may 1998, doi: 10.1016/S0920-9964(98)00013-9.

[80] M. D. Nelson, A. J. Saykin, L. A. Flashman, y H. J. Riordan, «Hippocampal Volume Reduction in Schizophrenia as Assessed by Magnetic Resonance Imaging: A Meta-analytic Study», *Arch. Gen. Psychiatry*, vol. 55, n.º 5, pp. 433-440, may 1998, doi: 10.1001/archpsyc.55.5.433.

[81] F. Briend, E. A. Nelson, O. Maximo, W. P. Armstrong, N. V. Kraguljac, y A. C. Lahti, «Hippocampal glutamate and hippocampus subfield volumes in antipsychotic-naive first episode psychosis subjects and relationships to duration of untreated psychosis», *Transl. Psychiatry*, vol. 10, n.º 1, pp. 1-11, may 2020, doi: 10.1038/s41398-020-0812-z.

[82] J. A. Kovelman y A. B. Scheibel, «A neurohistological correlate of schizophrenia», *Biol. Psychiatry*, vol. 19, n.º 12, pp. 1601-1621, dic. 1984.

[83] B. Bogerts, «The Temporolimbic System Theory of Positive Schizophrenic Symptoms», *Schizophr. Bull.*, vol. 23, n.º 3, pp. 423-435, ene. 1997, doi: 10.1093/schbul/23.3.423.

[84] A. J. Dwork, «Postmortem Studies of the Hippocampal Formation in Schizophrenia», *Schizophr. Bull.*, vol. 23, n.º 3, pp. 385-402, ene. 1997, doi: 10.1093/schbul/23.3.385.
[85] A. J. Conrad, T. Abebe, R. Austin, S. Forsythe, y A. B. Scheibel, «Hippocampal Pyramidal Cell Disarray in Schizophrenia as a Bilateral Phenomenon», *Arch. Gen. Psychiatry*, vol. 48, n.º 5, pp. 413-417, may 1991, doi: 10.1001/archpsyc.1991.01810290025003.
[86] D. V. Jeste y J. B. Lohr, «Hippocampal Pathologic Findings in Schizophrenia: A Morphometric Study», *Arch. Gen. Psychiatry*, vol. 46, n.º 11, pp. 1019-1024, nov. 1989, doi: 10.1001/archpsyc.1989.01810110061009.
[87] C. Konradi *et al.*, «Hippocampal interneurons are abnormal in schizophrenia», *Schizophr. Res.*, vol. 131, n.º 1, pp. 165-173, sep. 2011, doi: 10.1016/j.schres.2011.06.007.
[88] S. E. Arnold *et al.*, «Smaller neuron size in schizophrenia in hippocampal subfields that mediate cortical-hippocampal interactions», *Am. J. Psychiatry*, vol. 152, n.º 5, pp. 738-748, may 1995, doi: 10.1176/ajp.152.5.738.
[89] F. M. Benes, I. Sorensen, y E. D. Bird, «Reduced Neuronal Size in Posterior Hippocampus of Schizophrenic Patients», *Schizophr. Bull.*, vol. 17, n.º 4, pp. 597-608, ene. 1991, doi: 10.1093/schbul/17.4.597.
[90] F. M. Benes, E. W. Kwok, S. L. Vincent, y M. S. Todtenkopf, «A reduction of nonpyramidal cells in sector CA2 of schizophrenics and manic depressives», *Biol. Psychiatry*, vol. 44, n.º 2, pp. 88-97, jul. 1998, doi: 10.1016/S0006-3223(98)00138-3.
[91] P. Falkai *et al.*, «Association between altered hippocampal oligodendrocyte number and neuronal circuit structures in schizophrenia: a postmortem analysis», *Eur. Arch. Psychiatry Clin. Neurosci.*, vol. 270, n.º 4, Art. n.º 4, sep. 2019, doi: 10.1007/s00406-019-01067-0.
[92] P. Falkai *et al.*, «Decreased Oligodendrocyte and Neuron Number in Anterior Hippocampal Areas and the Entire Hippocampus in Schizophrenia: A Stereological Postmortem Study», *Schizophr. Bull.*, vol. 42, n.º suppl_1, pp. S4-S12, jul. 2016, doi: 10.1093/schbul/sbv157.
[93] «No evidence for astrogliosis in brains of schizophrenic patients. A post-mortem study - Falkai - 1999 - Neuropathology and Applied Neurobiology - Wiley Online Library». Accedido: 16 de julio de 2024. [En línea]. Disponible en: https://onlinelibrary.wiley.com/doi/abs/10.1046/j.1365-2990.1999.00162.x
[94] C. F. M. G. van Kesteren *et al.*, «Immune involvement in the pathogenesis of schizophrenia: a meta-analysis on postmortem brain studies», *Transl. Psychiatry*, vol. 7, n.º 3, p. e1075, mar. 2017, doi: 10.1038/tp.2017.4.
[95] D. J. Lodge y A. A. Grace, «Hippocampal dysregulation of dopamine system function and the pathophysiology of schizophrenia», Accedido: 16 de julio de 2024. [En línea]. Disponible en: https://www.cell.com/trends/pharmacological-sciences/abstract/S0165-6147(11)00079-4
[96] S. Heckers, «Neuroimaging studies of the hippocampus in schizophrenia», *Hippocampus*, vol. 11, n.º 5, pp. 520-528, 2001, doi: 10.1002/hipo.1068.
[97] C. A. Tamminga, A. D. Stan, y A. D. Wagner, «The Hippocampal Formation in Schizophrenia», *Am. J. Psychiatry*, vol. 167, n.º 10, pp. 1178-1193, oct. 2010, doi: 10.1176/appi.ajp.2010.09081187.
[98] S. Heckers y C. Konradi, «Hippocampal Pathology in Schizophrenia», 2010. doi: 10.1007/7854_2010_43.
[99] N. S. Kolomeets, D. D. Orlovskaya, V. I. Rachmanova, y N. A. Uranova, «Ultrastructural alterations in hippocampal mossy fiber synapses in schizophrenia: A postmortem morphometric study», *Synapse*, vol. 57, n.º 1, pp. 47-55, 2005, doi: 10.1002/syn.20153.

[100] W. Li *et al.*, «Synaptic Proteins in the Hippocampus Indicative of Increased Neuronal Activity in CA3 in Schizophrenia», *Am. J. Psychiatry*, vol. 172, n.º 4, pp. 373-382, abr. 2015, doi: 10.1176/appi.ajp.2014.14010123.

[101] Y. Uno y J. T. Coyle, «Glutamate hypothesis in schizophrenia», *Psychiatry Clin. Neurosci.*, vol. 73, n.º 5, pp. 204-215, 2019, doi: 10.1111/pcn.12823.

[102] M. J. Millan *et al.*, «Altering the course of schizophrenia: progress and perspectives», *Nat. Rev. Drug Discov.*, vol. 15, n.º 7, pp. 485-515, jul. 2016, doi: 10.1038/nrd.2016.28.

[103] J. W. Olney y N. B. Farber, «Glutamate Receptor Dysfunction and Schizophrenia», *Arch. Gen. Psychiatry*, vol. 52, n.º 12, pp. 998-1007, dic. 1995, doi: 10.1001/archpsyc.1995.03950240016004.

[104] M. Williams, «The Amygdala, Hippocampus, Fornix and Nucleus Basalis», 2021. doi: 10.1007/978-3-030-68308-5_6.

[105] M. T. M. Park *et al.*, «Hippocampal neuroanatomy in first episode psychosis: A putative role for glutamate and serotonin receptors», *Prog. Neuropsychopharmacol. Biol. Psychiatry*, vol. 110, p. 110297, ago. 2021, doi: 10.1016/j.pnpbp.2021.110297.

[106] T. Nakahara *et al.*, «Glutamatergic and GABAergic metabolite levels in schizophrenia-spectrum disorders: a meta-analysis of 1H-magnetic resonance spectroscopy studies», *Mol. Psychiatry*, vol. 27, n.º 1, pp. 744-757, ene. 2022, doi: 10.1038/s41380-021-01297-6.

[107] A. O. Kruse y J. R. Bustillo, «Glutamatergic dysfunction in Schizophrenia», *Transl. Psychiatry*, vol. 12, n.º 1, pp. 1-13, dic. 2022, doi: 10.1038/s41398-022-02253-w.

[108] F. A. Provenzano *et al.*, «Hippocampal Pathology in Clinical High-Risk Patients and the Onset of Schizophrenia», *Biol. Psychiatry*, vol. 87, n.º 3, pp. 234-242, feb. 2020, doi: 10.1016/j.biopsych.2019.09.022.

[109] N. V. Kraguljac *et al.*, «A longitudinal magnetic resonance spectroscopy study investigating effects of risperidone in the anterior cingulate cortex and hippocampus in schizophrenia», *Schizophr. Res.*, vol. 210, pp. 239-244, ago. 2019, doi: 10.1016/j.schres.2018.12.028.

[110] C. C. Joyal *et al.*, «The amygdala and schizophrenia: a volumetric magnetic resonance imaging study in first-episode, neuroleptic-naive patients», *Biol. Psychiatry*, vol. 54, n.º 11, pp. 1302-1304, dic. 2003, doi: 10.1016/S0006-3223(03)00597-3.

[111] N. F. Ho, P. L. H. Chong, D. R. Lee, Q. H. Chew, G. Chen, y K. Sim, «The Amygdala in Schizophrenia and Bipolar Disorder: A... : Harvard Review of Psychiatry», Accedido: 19 de julio de 2024. [En línea]. Disponible en: https://journals.lww.com/hrpjournal/abstract/2019/05000/the_amygdala_in_schizophrenia_and_bipolar.3.aspx

[112] P. Kreczmanski *et al.*, «Volume, neuron density and total neuron number in five subcortical regions in schizophrenia», *Brain*, vol. 130, n.º 3, pp. 678-692, mar. 2007, doi: 10.1093/brain/awl386.

[113] H. Pantazopoulos, T.-U. W. Woo, M. P. Lim, N. Lange, y S. Berretta, «Extracellular Matrix-Glial Abnormalities in the Amygdala and Entorhinal Cortex of Subjects Diagnosed With Schizophrenia», *Arch. Gen. Psychiatry*, vol. 67, n.º 2, pp. 155-166, feb. 2010, doi: 10.1001/archgenpsychiatry.2009.196.

[114] A. M. Shepherd, S. L. Matheson, K. R. Laurens, V. J. Carr, y M. J. Green, «Systematic Meta-Analysis of Insula Volume in Schizophrenia», *Biol. Psychiatry*, vol. 72, n.º 9, pp. 775-784, nov. 2012, doi: 10.1016/j.biopsych.2012.04.020.

[115] R. E. Gur *et al.*, «An fMRI Study of Facial Emotion Processing in Patients With Schizophrenia», *Am. J. Psychiatry*, vol. 159, n.º 12, pp. 1992-1999, dic. 2002, doi: 10.1176/appi.ajp.159.12.1992.

[116] D. Mamah, L. Wang, D. Barch, G. A. de Erausquin, M. Gado, y J. G. Csernansky, «Structural analysis of the basal ganglia in schizophrenia», *Schizophr. Res.*, vol. 89, n.º 1, pp. 59-71, ene. 2007, doi: 10.1016/j.schres.2006.08.031.

[117] B. H. Ebdrup *et al.*, «Hippocampal and caudate volume reductions in antipsychotic-naive first-episode schizophrenia», mar. 2010, doi: 10.1503/jpn.090049.

[118] B. H. Ebdrup *et al.*, «Progressive striatal and hippocampal volume loss in initially antipsychotic-naive, first-episode schizophrenia patients treated with quetiapine: relationship to dose and symptoms», *Int. J. Neuropsychopharmacol.*, vol. 14, n.º 1, pp. 69-82, feb. 2011, doi: 10.1017/S1461145710000817.

[119] N. A. Uranova, N. S. Kolomeets, O. V. Vikhreva, I. S. Zimina, V. I. Rachmanova, y D. D. Orlovskaya, «[Ultrastructural pathology of myelinated fibers in schizophrenia]», *Zh. Nevrol. Psikhiatr. Im. S. S. Korsakova*, vol. 113, n.º 9, pp. 63-69, ene. 2013.

[120] M. Goldstein y A. Y. Deutch, «Dopaminergic mechanisms in the pathogenesis of schizophrenia», *FASEB J.*, vol. 6, n.º 7, pp. 2413-2421, 1992, doi: 10.1096/fasebj.6.7.1348713.

[121] A. Lesch y B. Bogerts, «The diencephalon in schizophrenia: Evidence for reduced thickness of the periventricular grey matter», *Eur. Arch. Psychiatry Neurol. Sci.*, vol. 234, n.º 4, Art. n.º 4, dic. 1984, doi: 10.1007/BF00381351.

[122] L. M. Rimol *et al.*, «Cortical Thickness and Subcortical Volumes in Schizophrenia and Bipolar Disorder», *Biol. Psychiatry*, vol. 68, n.º 1, pp. 41-50, jul. 2010, doi: 10.1016/j.biopsych.2010.03.036.

[123] M. Lauer, D. Senitz, y H. Beckmann, «Increased volume of the nucleus accumbens in schizophrenia», *J. Neural Transm.*, vol. 108, n.º 6, Art. n.º 6, jun. 2001, doi: 10.1007/s007020170042.

[124] L. A. McCollum, C. K. Walker, J. K. Roche, y R. C. Roberts, «Elevated Excitatory Input to the Nucleus Accumbens in Schizophrenia: A Postmortem Ultrastructural Study», *Schizophr. Bull.*, vol. 41, n.º 5, pp. 1123-1132, sep. 2015, doi: 10.1093/schbul/sbv030.

[125] A. A. Grace y F. V. Gomes, «The Circuitry of Dopamine System Regulation and its Disruption in Schizophrenia: Insights Into Treatment and Prevention», *Schizophr. Bull.*, vol. 45, n.º 1, pp. 148-157, ene. 2019, doi: 10.1093/schbul/sbx199.

[126] O. D. Howes y S. Kapur, «The Dopamine Hypothesis of Schizophrenia: Version III—The Final Common Pathway», *Schizophr. Bull.*, vol. 35, n.º 3, pp. 549-562, may 2009, doi: 10.1093/schbul/sbp006.

[127] O. D. Howes *et al.*, «Midbrain dopamine function in schizophrenia and depression: a post-mortem and positron emission tomographic imaging study», *Brain*, vol. 136, n.º 11, pp. 3242-3251, nov. 2013, doi: 10.1093/brain/awt264.

[128] M. R. Williams *et al.*, «Neuropathological changes in the substantia nigra in schizophrenia but not depression», *Eur. Arch. Psychiatry Clin. Neurosci.*, vol. 264, n.º 4, Art. n.º 4, dic. 2013, doi: 10.1007/s00406-013-0479-z.

[129] W. Byne *et al.*, «Postmortem Assessment of Thalamic Nuclear Volumes in Subjects With Schizophrenia», *Am. J. Psychiatry*, vol. 159, n.º 1, pp. 59-65, ene. 2002, doi: 10.1176/appi.ajp.159.1.59.

[130] K. A. Young, K. F. Manaye, C.-L. Liang, P. B. Hicks, y D. C. German, «Reduced number of mediodorsal and anterior thalamic neurons in schizophrenia», *Biol. Psychiatry*, vol. 47, n.º 11, pp. 944-953, jun. 2000, doi: 10.1016/S0006-3223(00)00826-X.

[131] P. Danos *et al.*, «Volume and neuron number of the mediodorsal thalamic nucleus in schizophrenia: A replication study», *Psychiatry Res. Neuroimaging*, vol. 140, n.º 3, pp. 281-289, dic. 2005, doi: 10.1016/j.pscychresns.2005.09.005.

[132] K.-A. Dorph-Petersen, J. N. Pierri, Z. Sun, A. R. Sampson, y D. A. Lewis, «Stereological analysis of the mediodorsal thalamic nucleus in schizophrenia:

Volume, neuron number, and cell types», *J. Comp. Neurol.*, vol. 472, n.º 4, pp. 449-462, 2004, doi: 10.1002/cne.20055.
[133] J. G. Csernansky *et al.*, «Abnormalities of Thalamic Volume and Shape in Schizophrenia», *Am. J. Psychiatry*, vol. 161, n.º 5, pp. 896-902, may 2004, doi: 10.1176/appi.ajp.161.5.896.
[134] V. Danivas, S. V. Kalmady, G. Venkatasubramanian, y B. N. Gangadhar, «Thalamic Shape Abnormalities in Antipsychotic Naïve Schizophrenia», *Indian J. Psychol. Med.*, vol. 35, n.º 1, pp. 34-38, ene. 2013, doi: 10.4103/0253-7176.112198.
[135] P. Danos *et al.*, «The ventral lateral posterior nucleus of the thalamus in schizophrenia: a post-mortem study», *Psychiatry Res. Neuroimaging*, vol. 114, n.º 1, pp. 1-9, feb. 2002, doi: 10.1016/S0925-4927(01)00131-7.
[136] P. Danos *et al.*, «Schizophrenia and anteroventral thalamic nucleus: selective decrease of parvalbumin-immunoreactive thalamocortical projection neurons», *Psychiatry Res. Neuroimaging*, vol. 82, n.º 1, pp. 1-10, abr. 1998, doi: 10.1016/S0925-4927(97)00071-1.
[137] L. D. Selemon y A. Begovic´, «Stereologic analysis of the lateral geniculate nucleus of the thalamus in normal and schizophrenic subjects», *Psychiatry Res.*, vol. 151, n.º 1, pp. 1-10, may 2007, doi: 10.1016/j.psychres.2006.11.003.
[138] M. J. Owen, A. Sawa, y P. B. Mortensen, «Schizophrenia», *The Lancet*, vol. 388, n.º 10039, pp. 86-97, jul. 2016, doi: 10.1016/S0140-6736(15)01121-6.
[139] R. E. Gur, «Considering alternatives to the schizophrenia construct», *Schizophr. Res.*, vol. 242, pp. 49-51, abr. 2022, doi: 10.1016/j.schres.2021.12.027.
[140] H. Kato, H. Kimura, I. Kushima, N. Takahashi, B. Aleksic, y N. Ozaki, «The genetic architecture of schizophrenia: review of large-scale genetic studies», *J. Hum. Genet.*, vol. 68, n.º 3, pp. 175-182, mar. 2023, doi: 10.1038/s10038-022-01059-4.
[141] V. Trubetskoy *et al.*, «Mapping genomic loci implicates genes and synaptic biology in schizophrenia», *Nature*, vol. 604, n.º 7906, pp. 502-508, abr. 2022, doi: 10.1038/s41586-022-04434-5.
[142] R. Tamouza, R. Krishnamoorthy, y M. Leboyer, «Understanding the genetic contribution of the human leukocyte antigen system to common major psychiatric disorders in a world pandemic context», *Brain. Behav. Immun.*, vol. 91, pp. 731-739, ene. 2021, doi: 10.1016/j.bbi.2020.09.033.
[143] A. S. Bassett y E. W. C. Chow, «Schizophrenia and 22q11.2 deletion syndrome», *Curr. Psychiatry Rep.*, vol. 10, n.º 2, pp. 148-157, abr. 2008, doi: 10.1007/s11920-008-0026-1.
[144] R. Falkovich *et al.*, «A synaptic molecular dependency network in knockdown of autism- and schizophrenia-associated genes revealed by multiplexed imaging», *Cell Rep.*, vol. 42, n.º 5, p. 112430, may 2023, doi: 10.1016/j.celrep.2023.112430.
[145] J. G. Pouget, «The Emerging Immunogenetic Architecture of Schizophrenia», *Schizophr. Bull.*, vol. 44, n.º 5, pp. 993-1004, ago. 2018, doi: 10.1093/schbul/sby038.
[146] R. Hilker *et al.*, «Heritability of Schizophrenia and Schizophrenia Spectrum Based on the Nationwide Danish Twin Register», *Biol. Psychiatry*, vol. 83, n.º 6, pp. 492-498, mar. 2018, doi: 10.1016/j.biopsych.2017.08.017.
[147] L. Orsolini, S. Pompili, y U. Volpe, «Schizophrenia: A Narrative Review of Etiopathogenetic, Diagnostic and Treatment Aspects», *J. Clin. Med.*, vol. 11, n.º 17, Art. n.º 17, ene. 2022, doi: 10.3390/jcm11175040.
[148] M. Large, K. Mullin, P. Gupta, A. Harris, y O. Nielssen, «Systematic meta-analysis of outcomes associated with psychosis and co-morbid substance use», *Aust. N. Z. J. Psychiatry*, vol. 48, n.º 5, pp. 418-432, may 2014, doi: 10.1177/0004867414525838.
[149] M. D. Forti *et al.*, «Proportion of patients in south London with first-episode psychosis attributable to use of high potency cannabis: a case-control study», *Lancet Psychiatry*, vol. 2, n.º 3, pp. 233-238, mar. 2015, doi: 10.1016/S2215-0366(14)00117-5.

[150] D. Quattrone *et al.*, «Transdiagnostic dimensions of psychopathology at first episode psychosis: findings from the multinational EU-GEI study», *Psychol. Med.*, vol. 49, n.º 8, pp. 1378-1391, jun. 2019, doi: 10.1017/S0033291718002131.
[151] G. Ursini *et al.*, «Convergence of placenta biology and genetic risk for schizophrenia», *Nat. Med.*, vol. 24, n.º 6, pp. 792-801, jun. 2018, doi: 10.1038/s41591-018-0021-y.
[152] M.-Q. Xu *et al.*, «Prenatal Malnutrition and Adult Schizophrenia: Further Evidence From the 1959-1961 Chinese Famine», *Schizophr. Bull.*, vol. 35, n.º 3, pp. 568-576, may 2009, doi: 10.1093/schbul/sbn168.
[153] N. Robinson, A. Ploner, M. Leone, P. Lichtenstein, K. S. Kendler, y S. E. Bergen, «Impact of Early-Life Factors on Risk for Schizophrenia and Bipolar Disorder», *Schizophr. Bull.*, vol. 49, n.º 3, pp. 768-777, may 2023, doi: 10.1093/schbul/sbac205.
[154] G. M. Khandaker, J. Zimbron, C. Dalman, G. Lewis, y P. B. Jones, «Childhood infection and adult schizophrenia: A meta-analysis of population-based studies», *Schizophr. Res.*, vol. 139, n.º 1, pp. 161-168, ago. 2012, doi: 10.1016/j.schres.2012.05.023.
[155] G. K. Ahmed, H. K.-A. Ramadan, K. Elbeh, y N. A. Haridy, «The role of infections and inflammation in schizophrenia: review of the evidence», *Middle East Curr. Psychiatry*, vol. 31, n.º 1, p. 9, feb. 2024, doi: 10.1186/s43045-024-00397-7.
[156] I. Mikocziova, V. Greiff, y L. M. Sollid, «Immunoglobulin germline gene variation and its impact on human disease», *Genes Immun.*, vol. 22, n.º 4, pp. 205-217, 2021, doi: 10.1038/s41435-021-00145-5.
[157] «Common polygenic variation contributes to risk of schizophrenia that overlaps with bipolar disorder», *Nature*, vol. 460, n.º 7256, pp. 748-752, ago. 2009, doi: 10.1038/nature08185.
[158] J. R. Bishop, L. Zhang, y P. Lizano, «Inflammation Subtypes and Translating Inflammation-Related Genetic Findings in Schizophrenia and Related Psychoses: A Perspective on Pathways for Treatment Stratification and Novel Therapies», *Harv. Rev. Psychiatry*, vol. 30, n.º 1, pp. 59-70, 2022, doi: 10.1097/HRP.0000000000000321.
[159] W. W. Eaton *et al.*, «Immunologic profiling in schizophrenia and rheumatoid arthritis», *Psychiatry Res.*, vol. 317, p. 114812, nov. 2022, doi: 10.1016/j.psychres.2022.114812.
[160] C. Chaves, S. M. Dursun, M. Tusconi, y J. E. C. Hallak, «Neuroinflammation and schizophrenia – is there a link?», *Front. Psychiatry*, vol. 15, feb. 2024, doi: 10.3389/fpsyt.2024.1356975.
[161] M. Yu. Plotnikova, S. S. Kunizheva, E. V. Rozhdestvenskikh, y T. V. Andreeva, «Immunogenetic Factors in the Pathogenesis of Schizophrenia», *Russ. J. Genet.*, vol. 59, n.º 10, pp. 975-982, oct. 2023, doi: 10.1134/S1022795423100101.
[162] M. Debnath, «Adaptive Immunity in Schizophrenia: Functional Implications of T Cells in the Etiology, Course and Treatment», *J. Neuroimmune Pharmacol.*, vol. 10, n.º 4, pp. 610-619, dic. 2015, doi: 10.1007/s11481-015-9626-9.
[163] M. J. Carson, J. Cameron Thrash, y B. Walter, «The cellular response in neuroinflammation: The role of leukocytes, microglia and astrocytes in neuronal death and survival», *Clin. Neurosci. Res.*, vol. 6, n.º 5, pp. 237-245, dic. 2006, doi: 10.1016/j.cnr.2006.09.004.
[164] W. J. Streit, M. B. Graeber, y G. W. Kreutzberg, «Functional plasticity of microglia: A review», *Glia*, vol. 1, n.º 5, pp. 301-307, 1988, doi: 10.1002/glia.440010502.
[165] R. C. Paolicelli *et al.*, «Microglia states and nomenclature: A field at its crossroads», *Neuron*, vol. 110, n.º 21, pp. 3458-3483, nov. 2022, doi: 10.1016/j.neuron.2022.10.020.

[166] R. Yamasaki *et al.*, «Differential roles of microglia and monocytes in the inflamed central nervous system», *J. Exp. Med.*, vol. 211, n.º 8, pp. 1533-1549, jul. 2014, doi: 10.1084/jem.20132477.

[167] K. Nakajima y S. Kohsaka, «Microglia: Activation and Their Significance in the Central Nervous System», *J. Biochem. (Tokyo)*, vol. 130, n.º 2, pp. 169-175, ago. 2001, doi: 10.1093/oxfordjournals.jbchem.a002969.

[168] R. M. Ransohoff, «Microgliosis: the questions shape the answers», *Nat. Neurosci.*, vol. 10, n.º 12, pp. 1507-1509, dic. 2007, doi: 10.1038/nn1207-1507.

[169] B. Cameron y G. E. Landreth, «Inflammation, microglia, and alzheimer's disease», *Neurobiol. Dis.*, vol. 37, n.º 3, pp. 503-509, mar. 2010, doi: 10.1016/j.nbd.2009.10.006.

[170] D. Mukhara, U. Oh, y G. N. Neigh, «Chapter 15 - Neuroinflammation», en *Handbook of Clinical Neurology*, vol. 175, R. Lanzenberger, G. S. Kranz, y I. Savic, Eds., en Sex Differences in Neurology and Psychiatry, vol. 175. , Elsevier, 2020, pp. 235-259. doi: 10.1016/B978-0-444-64123-6.00017-5.

[171] I. Yang, S. J. Han, G. Kaur, C. Crane, y A. T. Parsa, «The role of microglia in central nervous system immunity and glioma immunology», *J. Clin. Neurosci.*, vol. 17, n.º 1, pp. 6-10, ene. 2010, doi: 10.1016/j.jocn.2009.05.006.

[172] N. Shebl, «Neuroinflammation and Microglial Activation in Schizophrenia: An Overview», en *Handbook of Neurodegenerative Disorders*, E. Mohamed, Ed., Singapore: Springer Nature, 2023, pp. 1-16. doi: 10.1007/978-981-19-3949-5_5-1.

[173] I. K. Malashenkova *et al.*, «[A role of the immune system in the pathogenesis of schizophrenia]», *Zh. Nevrol. Psikhiatr. Im. S. S. Korsakova*, vol. 118, n.º 12, pp. 72-80, ene. 2018, doi: 10.17116/jnevro201811812172.

[174] M. O. Trépanier, K. E. Hopperton, R. Mizrahi, N. Mechawar, y R. P. Bazinet, «Postmortem evidence of cerebral inflammation in schizophrenia: a systematic review», *Mol. Psychiatry*, vol. 21, n.º 8, pp. 1009-1026, ago. 2016, doi: 10.1038/mp.2016.90.

[175] T. Wierzba-Bobrowicz, E. Lewandowska, W. Lechowicz, T. Stepień, y E. Pasennik, «Quantitative analysis of activated microglia, ramified and damage of processes in the frontal and temporal lobes of chronic schizophrenics», *Folia Neuropathol.*, vol. 43, n.º 2, pp. 81-89, 2005.

[176] O. Pasternak, C.-F. Westin, B. Dahlben, S. Bouix, y M. Kubicki, «The extent of diffusion MRI markers of neuroinflammation and white matter deterioration in chronic schizophrenia», *Schizophr. Res.*, vol. 161, n.º 1, pp. 113-118, ene. 2015, doi: 10.1016/j.schres.2014.07.031.

[177] C. M. Sellgren *et al.*, «Increased synapse elimination by microglia in schizophrenia patient-derived models of synaptic pruning», *Nat. Neurosci.*, vol. 22, n.º 3, pp. 374-385, mar. 2019, doi: 10.1038/s41593-018-0334-7.

[178] A. Monji *et al.*, «Neuroinflammation in schizophrenia especially focused on the role of microglia», *Prog. Neuropsychopharmacol. Biol. Psychiatry*, vol. 42, pp. 115-121, abr. 2013, doi: 10.1016/j.pnpbp.2011.12.002.

[179] Y. Zhang, V. S. Catts, D. Sheedy, T. McCrossin, J. J. Kril, y C. Shannon Weickert, «Cortical grey matter volume reduction in people with schizophrenia is associated with neuro-inflammation», *Transl. Psychiatry*, vol. 6, n.º 12, pp. e982-e982, dic. 2016, doi: 10.1038/tp.2016.238.

[180] M. Kose, C. M. Pariante, P. Dazzan, y V. Mondelli, «The Role of Peripheral Inflammation in Clinical Outcome and Brain Imaging Abnormalities in Psychosis: A Systematic Review», *Front. Psychiatry*, vol. 12, feb. 2021, doi: 10.3389/fpsyt.2021.612471.

[181] E. A. Ermakov, I. A. Mednova, A. S. Boiko, V. N. Buneva, y S. A. Ivanova, «Chemokine Dysregulation and Neuroinflammation in Schizophrenia: A Systematic Review», *Int. J. Mol. Sci.*, vol. 24, n.º 3, Art. n.º 3, ene. 2023, doi: 10.3390/ijms24032215.

[182] M. Cho, T. Y. Lee, Y. B. Kwak, Y. B. Yoon, M. Kim, y J. S. Kwon, «Adjunctive use of anti-inflammatory drugs for schizophrenia: A meta-analytic investigation of randomized controlled trials», *Aust. N. Z. J. Psychiatry*, vol. 53, n.º 8, pp. 742-759, ago. 2019, doi: 10.1177/0004867419835028.

[183] Delves Peter J. y Roitt Ivan M., «The Immune System», *N. Engl. J. Med.*, vol. 343, n.º 1, pp. 37-49, 2000, doi: 10.1056/NEJM200007063430107.

[184] J. Parkin y B. Cohen, «An overview of the immune system», *The Lancet*, vol. 357, n.º 9270, pp. 1777-1789, jun. 2001, doi: 10.1016/S0140-6736(00)04904-7.

[185] R. S. Sauls, C. McCausland, y B. N. Taylor, «Histology, T-Cell Lymphocyte», en *StatPearls*, Treasure Island (FL): StatPearls Publishing, 2024. Accedido: 15 de mayo de 2024. [En línea]. Disponible en: http://www.ncbi.nlm.nih.gov/books/NBK535433/

[186] W. Wang, N. Sung, A. Gilman-Sachs, y J. Kwak-Kim, «T Helper (Th) Cell Profiles in Pregnancy and Recurrent Pregnancy Losses: Th1/Th2/Th9/Th17/Th22/Tfh Cells», *Front. Immunol.*, vol. 11, p. 2025, ago. 2020, doi: 10.3389/fimmu.2020.02025.

[187] L. B. Nicholson, «The immune system», *Essays Biochem.*, vol. 60, n.º 3, pp. 275-301, oct. 2016, doi: 10.1042/EBC20160017.

[188] J. E. Craft, «Follicular helper T cells in immunity and systemic autoimmunity», *Nat. Rev. Rheumatol.*, vol. 8, n.º 6, pp. 337-347, jun. 2012, doi: 10.1038/nrrheum.2012.58.

[189] B. Zygmunt y M. Veldhoen, «Chapter 5 - T Helper Cell Differentiation: More than Just Cytokines», en *Advances in Immunology*, vol. 109, F. W. Alt, Ed., Academic Press, 2011, pp. 159-196. doi: 10.1016/B978-0-12-387664-5.00005-4.

[190] G. Del Prete, «The Concept of Type-1 and Type-2 Helper T Cells and Their Cytokines in Humans», *Int. Rev. Immunol.*, vol. 16, n.º 3-4, pp. 427-455, ene. 1998, doi: 10.3109/08830189809043004.

[191] C. Dong, «Cytokine Regulation and Function in T Cells», abr. 2021, doi: 10.1146/annurev-immunol-061020-053702.

[192] F. Lyu, T. Ozawa, H. Hamana, E. Kobayashi, A. Muraguchi, y H. Kishi, «A novel and simple method to produce large amounts of recombinant soluble peptide/major histocompatibility complex monomers for analysis of antigen-specific human T cell receptors», *New Biotechnol.*, vol. 49, pp. 169-177, mar. 2019, doi: 10.1016/j.nbt.2018.11.005.

[193] C. E. Coffey, J. L. Sullivan, y J. R. Rice, «T lymphocytes in schizophrenia», *Biol. Psychiatry*, vol. 18, n.º 1, pp. 113-119, ene. 1983.

[194] J. Steiner *et al.*, «Acute schizophrenia is accompanied by reduced T cell and increased B cell immunity», *Eur. Arch. Psychiatry Clin. Neurosci.*, vol. 260, n.º 7, pp. 509-518, oct. 2010, doi: 10.1007/s00406-010-0098-x.

[195] A. Henneberg, B. Riedl, H.-O. Dumke, y H. H. Kornhuber, «T-lymphocyte subpopulations in schizophrenic patients», *Eur. Arch. Psychiatry Neurol. Sci.*, vol. 239, n.º 5, pp. 283-284, sep. 1990, doi: 10.1007/BF01735051.

[196] K. Schlaaff *et al.*, «Increased densities of T and B lymphocytes indicate neuroinflammation in subgroups of schizophrenia and mood disorder patients», *Brain. Behav. Immun.*, vol. 88, pp. 497-506, ago. 2020, doi: 10.1016/j.bbi.2020.04.021.

[197] «Aberrant T cell-mediated immunity in untreated schizophrenic patients: deficient interleukin-2 production», *Am. J. Psychiatry*, vol. 146, n.º 5, pp. 609-616, may 1989, doi: 10.1176/ajp.146.5.609.

[198] S. Busse *et al.*, «Different distribution patterns of lymphocytes and microglia in the hippocampus of patients with residual versus paranoid schizophrenia: Further evidence for disease course-related immune alterations?», *Brain. Behav. Immun.*, vol. 26, n.º 8, pp. 1273-1279, nov. 2012, doi: 10.1016/j.bbi.2012.08.005.

[199] M. Mandal, A. C. Marzouk, R. Donnelly, y N. M. Ponzio, «Preferential development of Th17 cells in offspring of immunostimulated pregnant mice», *J. Reprod. Immunol.*, vol. 87, n.º 1, pp. 97-100, dic. 2010, doi: 10.1016/j.jri.2010.06.156.

[200] R. Luan *et al.*, «Maternal Lipopolysaccharide Exposure Promotes Immunological Functional Changes in Adult Offspring CD4+ T Cells», *Am. J. Reprod. Immunol.*, vol. 73, n.º 6, pp. 522-535, 2015, doi: 10.1111/aji.12364.

[201] Q. Li *et al.*, «Clonal Characteristics of T-Cell Receptor Repertoires in Violent and Non-violent Patients With Schizophrenia», *Front. Psychiatry*, vol. 9, ago. 2018, doi: 10.3389/fpsyt.2018.00403.

[202] M. Yu. Plotnikova, A. D. Patrikeev, A. Yu. Levchenko, O. Yu. Fedorenko, T. V. Andreeva, y E. I. Rogaev, «Pilot Study to Detect the Repertoires of T-Cell Receptor Gamma Chains in Patients with Juvenile Schizophrenia», *Russ. J. Genet.*, vol. 59, n.º 7, pp. 739-743, jul. 2023, doi: 10.1134/S1022795423070086.

[203] M. J. Besser, Y. Ganor, y M. Levite, «Dopamine by itself activates either D2, D3 or D1/D5 dopaminergic receptors in normal human T-cells and triggers the selective secretion of either IL-10, TNFα or both», *J. Neuroimmunol.*, vol. 169, n.º 1, pp. 161-171, dic. 2005, doi: 10.1016/j.jneuroim.2005.07.013.

[204] Y. Watanabe *et al.*, «Dopamine Selectively Induces Migration and Homing of Naive CD8+ T Cells via Dopamine Receptor D31», *J. Immunol.*, vol. 176, n.º 2, pp. 848-856, ene. 2006, doi: 10.4049/jimmunol.176.2.848.

[205] C. Prado, S. Bernales, y R. Pacheco, «Modulation of T-cell Mediated Immunity by Dopamine Receptor D5», *Endocr. Metab. Immune Disord. - Drug TargetsFormerly Curr. Drug Targets - Immune Endocr. Metab. Disord.*, vol. 13, n.º 2, pp. 184-194, jun. 2013.

[206] S. Thomas Broome, K. Louangaphay, K. A. Keay, G. M. Leggio, G. Musumeci, y A. Castorina, «Dopamine: an immune transmitter», *Neural Regen. Res.*, vol. 15, n.º 12, p. 2173, dic. 2020, doi: 10.4103/1673-5374.284976.

[207] M. Levite, «Dopamine and T cells: dopamine receptors and potent effects on T cells, dopamine production in T cells, and abnormalities in the dopaminergic system in T cells in autoimmune, neurological and psychiatric diseases», *Acta Physiol.*, vol. 216, n.º 1, pp. 42-89, 2016, doi: 10.1111/apha.12476.

[208] C. K. Glass, K. Saijo, B. Winner, M. C. Marchetto, y F. H. Gage, «Mechanisms Underlying Inflammation in Neurodegeneration», *Cell*, vol. 140, n.º 6, pp. 918-934, mar. 2010, doi: 10.1016/j.cell.2010.02.016.

[209] T. Ilani *et al.*, «A peripheral marker for schizophrenia: Increased levels of D3 dopamine receptor mRNA in blood lymphocytes», *Proc. Natl. Acad. Sci.*, vol. 98, n.º 2, pp. 625-628, ene. 2001, doi: 10.1073/pnas.98.2.625.

[210] Á. Zvara *et al.*, «Over-expression of dopamine D_2 receptor and inwardly rectifying potassium channel genes in drug-naive schizophrenic peripheral blood lymphocytes as potential diagnostic markers», *Dis. Markers*, vol. 21, n.º 2, pp. 61-69, ene. 2005.

[211] M. Vogel *et al.*, «Decreased Levels of Dopamine D3 Receptor mRNA in Schizophrenic and Bipolar Patients», *Neuropsychobiology*, vol. 50, n.º 4, pp. 305-310, nov. 2004, doi: 10.1159/000080958.

[212] G. E. A. Brito-Melo *et al.*, «Increase in dopaminergic, but not serotoninergic, receptors in T-cells as a marker for schizophrenia severity», *J. Psychiatr. Res.*, vol. 46, n.º 6, pp. 738-742, jun. 2012, doi: 10.1016/j.jpsychires.2012.03.004.

[213] M. Urhan-Kucuk, M. E. Erdal, M. E. Ozen, S. Kul, y H. Herken, «Is the dopamine D3 receptor mRNA on blood lymphocytes help to for identification and subtyping of schizophrenia?», *Mol. Biol. Rep.*, vol. 38, n.º 4, pp. 2569-2572, abr. 2011, doi: 10.1007/s11033-010-0396-4.

[214] S. K. Garg, R. Banerjee, y J. Kipnis, «Neuroprotective Immunity: T Cell-Derived Glutamate Endows Astrocytes with a Neuroprotective Phenotype», *J. Immunol.*, vol. 180, n.º 6, pp. 3866-3873, mar. 2008, doi: 10.4049/jimmunol.180.6.3866.

[215] X. Chen *et al.*, «Microglia-mediated T cell infiltration drives neurodegeneration in tauopathy», *Nature*, vol. 615, n.º 7953, pp. 668-677, mar. 2023, doi: 10.1038/s41586-023-05788-0.

[216] M. Gelderblom, P. Arunachalam, y T. Magnus, «γδ T cells as early sensors of tissue damage and mediators of secondary neurodegeneration», *Front. Cell. Neurosci.*, vol. 8, nov. 2014, doi: 10.3389/fncel.2014.00368.
[217] H. González y R. Pacheco, «T-cell-mediated regulation of neuroinflammation involved in neurodegenerative diseases», *J. Neuroinflammation*, vol. 11, n.º 1, p. 201, dic. 2014, doi: 10.1186/s12974-014-0201-8.
[218] K. Derkow, C. Krüger, P. Dembny, y S. Lehnardt, «Microglia Induce Neurotoxic IL-17+ γδ T Cells Dependent on TLR2, TLR4, and TLR9 Activation», *PLOS ONE*, vol. 10, n.º 8, p. e0135898, ago. 2015, doi: 10.1371/journal.pone.0135898.
[219] E. Parellada y P. Gassó, «Glutamate and microglia activation as a driver of dendritic apoptosis: a core pathophysiological mechanism to understand schizophrenia», *Transl. Psychiatry*, vol. 11, n.º 1, pp. 1-13, may 2021, doi: 10.1038/s41398-021-01385-9.
[220] R. J. L. Anney *et al.*, «Meta-analysis of GWAS of over 16,000 individuals with autism spectrum disorder highlights a novel locus at 10q24.32 and a significant overlap with schizophrenia», *Mol. Autism*, vol. 8, n.º 1, p. 21, may 2017, doi: 10.1186/s13229-017-0137-9.
[221] E. Sada-Fuente *et al.*, «Common genetic variants contribute to heritability of age at onset of schizophrenia», *Transl. Psychiatry*, vol. 13, n.º 1, pp. 1-9, jun. 2023, doi: 10.1038/s41398-023-02508-0.
[222] S. F. Ahmad, A. Nadeem, M. A. Ansari, S. A. Bakheet, L. Y. AL-Ayadhi, y S. M. Attia, «Downregulation in Helios transcription factor signaling is associated with immune dysfunction in blood leukocytes of autistic children», *Prog. Neuropsychopharmacol. Biol. Psychiatry*, vol. 85, pp. 98-104, jul. 2018, doi: 10.1016/j.pnpbp.2018.04.011.
[223] Z. Zheng, P. Zheng, y X. Zou, «Association between schizophrenia and autism spectrum disorder: A systematic review and meta-analysis», *Autism Res.*, vol. 11, n.º 8, pp. 1110-1119, 2018, doi: 10.1002/aur.1977.
[224] *The Neuropathology of Schizophrenia*. Accedido: 13 de agosto de 2024. [En línea]. Disponible en: https://link-springer-com.sire.ub.edu/book/10.1007/978-3-030-68308-5
[225] Y. Gao *et al.*, «Single-cell transcriptomic and chromatin accessibility analyses of dairy cattle peripheral blood mononuclear cells and their responses to lipopolysaccharide», *BMC Genomics*, vol. 23, n.º 1, Art. n.º 1, abr. 2022, doi: 10.1186/s12864-022-08562-0.
[226] W. Wu *et al.*, «Overcoming IMiD resistance in T-cell lymphomas through potent degradation of ZFP91 and IKZF1», *Blood*, vol. 139, n.º 13, pp. 2024-2037, mar. 2022, doi: 10.1182/blood.2021014701.
[227] J. Q. Wu *et al.*, «Altered neural signaling and immune pathways in peripheral blood mononuclear cells of schizophrenia patients with cognitive impairment: A transcriptome analysis», *Brain. Behav. Immun.*, vol. 53, pp. 194-206, mar. 2016, doi: 10.1016/j.bbi.2015.12.010.
[228] R. V. Luckheeram, R. Zhou, A. D. Verma, y B. Xia, «$CD4^+$T Cells: Differentiation and Functions», *J. Immunol. Res.*, vol. 2012, p. e925135, mar. 2012, doi: 10.1155/2012/925135.
[229] D. Artis y H. Spits, «The biology of innate lymphoid cells», *Nature*, vol. 517, n.º 7534, pp. 293-301, ene. 2015, doi: 10.1038/nature14189.
[230] S. Halstead *et al.*, «Alteration patterns of peripheral concentrations of cytokines and associated inflammatory proteins in acute and chronic stages of schizophrenia: a systematic review and network meta-analysis», doi: 10.1016/S2215-0366(23)00025-1.
[231] R. E. Kneeland y S. H. Fatemi, «Viral infection, inflammation and schizophrenia», *Prog. Neuropsychopharmacol. Biol. Psychiatry*, vol. 42, pp. 35-48, abr. 2013, doi: 10.1016/j.pnpbp.2012.02.001.

[232] P. Marcinowicz *et al.*, «A Meta-Analysis of the Influence of Antipsychotics on Cytokines Levels in First Episode Psychosis», *J. Clin. Med.*, vol. 10, n.º 11, Art. n.º 11, jun. 2021, doi: 10.3390/jcm10112488.

[233] V. Arolt, M. Rothermundt, K.-P. Wandinger, y H. Kirchner, «Decreased in vitro production of interferon-gamma and interleukin-2 in whole blood of patients with schizophrenia during treatment», *Mol. Psychiatry*, vol. 5, n.º 2, pp. 150-158, mar. 2000, doi: 10.1038/sj.mp.4000650.

[234] K. E. Wilson, H. Demyanovich, L. H. Rubin, H. J. Wehring, C. Kilday, y D. L. Kelly, «Relationship of Interferon-γ to Cognitive Function in Midlife Women with Schizophrenia», *Psychiatr. Q.*, vol. 89, n.º 4, Art. n.º 4, jul. 2018, doi: 10.1007/s11126-018-9591-6.

[235] M. Paul-Samojedny *et al.*, «Association Study of Interferon Gamma (IFN-γ) +874T/A Gene Polymorphism in Patients with Paranoid Schizophrenia», *J. Mol. Neurosci.*, vol. 43, n.º 3, Art. n.º 3, sep. 2010, doi: 10.1007/s12031-010-9442-x.

[236] M. Al-Amin, M. M. N. Uddin, y H. M. Reza, «Effects of Antipsychotics on the Inflammatory Response System of Patients with Schizophrenia in Peripheral Blood Mononuclear Cell Cultures», dic. 2013, doi: 10.9758/cpn.2013.11.3.144.

[237] M.-L. Chen *et al.*, «Clozapine inhibits Th1 cell differentiation and causes the suppression of IFN-γ production in peripheral blood mononuclear cells», ago. 2012, Accedido: 22 de agosto de 2024. [En línea]. Disponible en: https://www.tandfonline.com/doi/pdf/10.3109/08923973.2011.651535?needAccess=true

[238] K. T, M. A, H. S, y K. S, «Risperidone significantly inhibits interferon-gamma-induced microglial activation in vitro», *PubMed*, Accedido: 22 de agosto de 2024. [En línea]. Disponible en: https://pubmed.ncbi.nlm.nih.gov/17363222/

[239] D. Shevyrev y V. Tereshchenko, «Frontiers | Treg Heterogeneity, Function, and Homeostasis», doi: 10.3389/fimmu.2019.03100.

[240] D. L. Kelly *et al.*, «Increased circulating regulatory T cells in medicated people with schizophrenia», *Psychiatry Res.*, vol. 269, pp. 517-523, nov. 2018, doi: 10.1016/j.psychres.2018.09.006.

[241] T.-J. Jiang *et al.*, «Percentage and function of CD4+CD25+ regulatory T cells in patients with hyperthyroidism», *Mol. Med. Rep.*, vol. 17, n.º 2, pp. 2137-2144, feb. 2018, doi: 10.3892/mmr.2017.8154.

[242] M. A. Koch, G. Tucker-Heard, N. R. Perdue, J. R. Killebrew, K. B. Urdahl, y D. J. Campbell, «The transcription factor T-bet controls regulatory T cell homeostasis and function during type 1 inflammation», *Nat. Immunol.*, vol. 10, n.º 6, pp. 595-602, jun. 2009, doi: 10.1038/ni.1731.

[243] J. A. Burger, «Chemokines and chemokine receptors in chronic lymphocytic leukemia (CLL): From understanding the basics towards therapeutic targeting», *Semin. Cancer Biol.*, vol. 20, n.º 6, pp. 424-430, dic. 2010, doi: 10.1016/j.semcancer.2010.09.005.

[244] V. Nehra, E. V. Marietta, y J. A. Murray, «Chapter 12 - Celiac Disease and its Therapy: Current Approaches and New Advances», en *Wheat and Rice in Disease Prevention and Health*, R. R. Watson, V. R. Preedy, y S. Zibadi, Eds., San Diego: Academic Press, 2014, pp. 143-155. doi: 10.1016/B978-0-12-401716-0.00012-X.

[245] Y. Tsuchida y K. Fujio, «Chapter 15 - Cytokines and Chemokines», en *Mosaic of Autoimmunity*, C. Perricone y Y. Shoenfeld, Eds., Academic Press, 2019, pp. 127-141. doi: 10.1016/B978-0-12-814307-0.00015-3.

[246] E. Y. Lee, Z.-H. Lee, y Y. W. Song, «CXCL10 and autoimmune diseases», *Autoimmun. Rev.*, vol. 8, n.º 5, pp. 379-383, mar. 2009, doi: 10.1016/j.autrev.2008.12.002.

[247] A. D. Luster, J. C. Unkeless, y J. V. Ravetch, «γ-Interferon transcriptionally regulates an early-response gene containing homology to platelet proteins», *Nature*, vol. 315, n.º 6021, pp. 672-676, jun. 1985, doi: 10.1038/315672a0.
[248] D. Michlmayr y C. S. McKimmie, «Role of CXCL10 in central nervous system inflammation», *Int. J. Interferon Cytokine Mediat. Res.*, vol. 6, pp. 1-18, feb. 2014, doi: 10.2147/IJICMR.S35953.
[249] «Neuroimmune Signaling: Cytokines and the Central Nervous System | SpringerLink». Accedido: 13 de agosto de 2024. [En línea]. Disponible en: https://link-springer-com.sire.ub.edu/referenceworkentry/10.1007/978-3-030-88832-9_174#Sec5
[250] J. Kealy, C. Greene, y M. Campbell, «Blood-brain barrier regulation in psychiatric disorders», *Neurosci. Lett.*, vol. 726, p. 133664, may 2020, doi: 10.1016/j.neulet.2018.06.033.
[251] A. Liston, J. Dooley, y L. Yshii, «Brain-resident regulatory T cells and their role in health and disease», *Immunol. Lett.*, vol. 248, pp. 26-30, ago. 2022, doi: 10.1016/j.imlet.2022.06.005.
[252] S. Prasad y J. R. Lokensgard, «Brain-Resident T Cells Following Viral Infection», *Viral Immunol.*, vol. 32, n.º 1, pp. 48-54, feb. 2019, doi: 10.1089/vim.2018.0084.
[253] J. G. Bramness *et al.*, «Amphetamine-induced psychosis - a separate diagnostic entity or primary psychosis triggered in the vulnerable?», *BMC Psychiatry*, vol. 12, p. 221, dic. 2012, doi: 10.1186/1471-244X-12-221.
[254] Y. Li, B. Kolb, y T. E. Robinson, «The Location of Persistent Amphetamine-Induced Changes in the Density of Dendritic Spines on Medium Spiny Neurons in the Nucleus Accumbens and Caudate-Putamen», *Neuropsychopharmacology*, vol. 28, n.º 6, pp. 1082-1085, jun. 2003, doi: 10.1038/sj.npp.1300115.
[255] B. Zhang *et al.*, «Gender differences measured by the MATRICS consensus cognitive battery in chronic schizophrenia patients», *Sci. Rep.*, vol. 7, n.º 1, p. 11821, sep. 2017, doi: 10.1038/s41598-017-12027-w.
[256] M. A. Rabadan *et al.*, «An in vitro model of neuronal ensembles», *Nat. Commun.*, vol. 13, n.º 1, p. 3340, jun. 2022, doi: 10.1038/s41467-022-31073-1.
[257] A. C. Caznok Silveira *et al.*, «Frontiers | Between neurons and networks: investigating mesoscale brain connectivity in neurological and psychiatric disorders», doi: 10.3389/fnins.2024.1340345.
[258] G. Flores, J. C. Morales-Medina, y A. Diaz, «Neuronal and brain morphological changes in animal models of schizophrenia», *Behav. Brain Res.*, vol. 301, pp. 190-203, mar. 2016, doi: 10.1016/j.bbr.2015.12.034.
[259] E. Mısır y G. G. Akay, «Synaptic dysfunction in schizophrenia», *Synapse*, vol. 77, n.º 5, p. e22276, 2023, doi: 10.1002/syn.22276.
[260] K. M. Harris y R. J. Weinberg, «Ultrastructure of Synapses in the Mammalian Brain», may 2012, doi: 10.1101/cshperspect.a005587.
[261] N. Matosin *et al.*, «Molecular evidence of synaptic pathology in the CA1 region in schizophrenia», *Npj Schizophr.*, vol. 2, n.º 1, pp. 1-8, jun. 2016, doi: 10.1038/npjschz.2016.22.
[262] L. V. Moran y L. E. Hong, «High vs Low Frequency Neural Oscillations in Schizophrenia», *Schizophr. Bull.*, vol. 37, n.º 4, pp. 659-663, jul. 2011, doi: 10.1093/schbul/sbr056.
[263] P. J. Uhlhaas y W. Singer, «Abnormal neural oscillations and synchrony in schizophrenia», *Nat. Rev. Neurosci.*, vol. 11, n.º 2, pp. 100-113, feb. 2010, doi: 10.1038/nrn2774.
[264] J. M. Ford y D. H. Mathalon, «Neural Synchrony in Schizophrenia», *Schizophr. Bull.*, vol. 34, n.º 5, pp. 904-906, sep. 2008, doi: 10.1093/schbul/sbn090.
[265] R. Lencer, M. Nagel, A. Sprenger, W. Heide, y F. Binkofski, «Reduced neuronal activity in the V5 complex underlies smooth-pursuit deficit in schizophrenia: evidence

from an fMRI study», *NeuroImage*, vol. 24, n.º 4, pp. 1256-1259, feb. 2005, doi: 10.1016/j.neuroimage.2004.11.013.
[266] E. Fernandez-Egea *et al.*, «Peripheral Immune Cell Populations Associated with Cognitive Deficits and Negative Symptoms of Treatment-Resistant Schizophrenia», doi: 10.1371/journal.pone.0155631.
[267] A. Karahan, I. Manzak Saka, D. Sağlam Aykut, F. Civil Arslan, E. Selçuk Özmen, y E. Özkorumak Karagüzel, «The relationship between peripheral immune cell markers and cognitive functions in patients with schizophrenia», *Int. J. Psychiatry Med.*, p. 00912174241266059, jul. 2024, doi: 10.1177/00912174241266059.
[268] D. Wegrzyn, G. Juckel, y A. Faissner, «Structural and Functional Deviations of the Hippocampus in Schizophrenia and Schizophrenia Animal Models», *Int. J. Mol. Sci.*, vol. 23, n.º 10, Art. n.º 10, may 2022, doi: 10.3390/ijms23105482.
[269] A. A. Coley y W.-J. Gao, «PSD95: A synaptic protein implicated in schizophrenia or autism?», *Prog. Neuropsychopharmacol. Biol. Psychiatry*, vol. 82, pp. 187-194, mar. 2018, doi: 10.1016/j.pnpbp.2017.11.016.
[270] A. J. Funk *et al.*, «Postsynaptic Density-95 Isoform Abnormalities in Schizophrenia», *Schizophr. Bull.*, vol. 43, n.º 4, pp. 891-899, jul. 2017, doi: 10.1093/schbul/sbw173.
[271] S. Heckers y C. Konradi, «GABAergic mechanisms of hippocampal hyperactivity in schizophrenia», *Schizophr. Res.*, vol. 167, n.º 1, pp. 4-11, sep. 2015, doi: 10.1016/j.schres.2014.09.041.
[272] J. Wang, L. Tong, G. Lin, H. Wang, L. Zhang, y X. Yang, «Immunological and clinicopathological characteristics of C1RL in 2120 glioma patients», *BMC Cancer*, vol. 20, n.º 1, p. 931, sep. 2020, doi: 10.1186/s12885-020-07436-6.
[273] M. Föcking *et al.*, «Complement pathway changes at age 12 are associated with psychotic experiences at age 18 in a longitudinal population-based study: evidence for a role of stress», *Mol. Psychiatry*, vol. 26, n.º 2, pp. 524-533, feb. 2021, doi: 10.1038/s41380-018-0306-z.
[274] K. R. Mayilyan, D. R. Weinberger, y R. B. Sim, «The Complement System in Schizophrenia», *Drug News Perspect.*, vol. 21, n.º 4, pp. 200-210, may 2008, doi: 10.1358/dnp.2008.21.4.1213349.
[275] T. Vogl *et al.*, «Mrp8 and Mrp14 are endogenous activators of Toll-like receptor 4, promoting lethal, endotoxin-induced shock», *Nat. Med.*, vol. 13, n.º 9, pp. 1042-1049, sep. 2007, doi: 10.1038/nm1638.
[276] K. Croce *et al.*, «Myeloid-Related Protein-8/14 Is Critical for the Biological Response to Vascular Injury», *Circulation*, vol. 120, n.º 5, pp. 427-436, ago. 2009, doi: 10.1161/CIRCULATIONAHA.108.814582.
[277] Y. Hwang *et al.*, «Gene expression profiling by mRNA sequencing reveals increased expression of immune/inflammation-related genes in the hippocampus of individuals with schizophrenia», *Transl. Psychiatry*, vol. 3, n.º 10, pp. e321-e321, oct. 2013, doi: 10.1038/tp.2013.94.
[278] M. Oppermann, «Chemokine receptor CCR5: insights into structure, function, and regulation», *Cell. Signal.*, vol. 16, n.º 11, pp. 1201-1210, nov. 2004, doi: 10.1016/j.cellsig.2004.04.007.
[279] E. Domenici *et al.*, «Plasma Protein Biomarkers for Depression and Schizophrenia by Multi Analyte Profiling of Case-Control Collections», doi: 10.1371/journal.pone.0009166.
[280] Y. Huang, M. Peng, W. Yu, y H. Li, «Activation of Wnt/*β*-catenin signaling promotes immune evasion via the *β*-catenin/*IKZF1*/*CCL5* axis in hepatocellular carcinoma», *Int. Immunopharmacol.*, vol. 138, p. 112534, sep. 2024, doi: 10.1016/j.intimp.2024.112534.

[281] R. Ajoy *et al.*, «CCL5 promotion of bioenergy metabolism is crucial for hippocampal synapse complex and memory formation», *Mol. Psychiatry*, vol. 26, n.º 11, pp. 6451-6468, nov. 2021, doi: 10.1038/s41380-021-01103-3.

[282] M. Reale, M. A. Kamal, L. Velluto, D. Gambi, M. Di Nicola, y N. H. Greig, «Relationship between Inflammatory Mediators, Aβ Levels and ApoE Genotype in Alzheimer Disease», *Curr. Alzheimer Res.*, vol. 9, n.º 4, pp. 447-457, may 2012, doi: 10.2174/156720512800492549.

[283] A. Francisco-Cruz *et al.*, «Granulocyte–macrophage colony-stimulating factor: not just another haematopoietic growth factor», *Med. Oncol.*, vol. 31, n.º 1, Art. n.º 1, nov. 2013, doi: 10.1007/s12032-013-0774-6.

[284] E. A. Ermakov *et al.*, «Association of Peripheral Inflammatory Biomarkers and Growth Factors Levels with Sex, Therapy and Other Clinical Factors in Schizophrenia and Patient Stratification Based on These Data», *Brain Sci.*, vol. 13, n.º 5, Art. n.º 5, may 2023, doi: 10.3390/brainsci13050836.

[285] B. J. Miller *et al.*, «Longitudinal study of inflammation and relapse in schizophrenia», *Schizophr. Res.*, vol. 252, pp. 88-95, feb. 2023, doi: 10.1016/j.schres.2022.12.028.

[286] H. O. Dikmen, M. Hemmerich, A. Lewen, J.-O. Hollnagel, B. Chausse, y O. Kann, «GM-CSF induces noninflammatory proliferation of microglia and disturbs electrical neuronal network rhythms in situ», *J. Neuroinflammation*, vol. 17, n.º 1, Art. n.º 1, ago. 2020, doi: 10.1186/s12974-020-01903-4.

[287] S. Xie *et al.*, «Frontiers | Ikzf2 Regulates the Development of ICOS+ Th Cells to Mediate Immune Response in the Spleen of S. japonicum-Infected C57BL/6 Mice», doi: 10.3389/fimmu.2021.687919.

[288] M. J. Schwarz *et al.*, «IL-2 and IL-4 polymorphisms as candidate genes in schizophrenia», *Eur. Arch. Psychiatry Clin. Neurosci.*, vol. 256, n.º 2, Art. n.º 2, ago. 2005, doi: 10.1007/s00406-005-0603-9.

[289] S. P. Gadani, J. C. Cronk, G. T. Norris, y J. Kipnis, «IL-4 in the Brain: A Cytokine To Remember», *J. Immunol.*, vol. 189, n.º 9, pp. 4213-4219, nov. 2012, doi: 10.4049/jimmunol.1202246.

[290] N. Hanuscheck *et al.*, «Interleukin-4 receptor signaling modulates neuronal network activity», *J. Exp. Med.*, vol. 219, n.º 6, p. e20211887, jun. 2022, doi: 10.1084/jem.20211887.

[291] Ş. Şimşek, V. Yıldırım, A. Çim, y S. Kaya, «Serum IL-4 and IL-10 Levels Correlate with the Symptoms of the Drug-Naive Adolescents with First Episode, Early Onset Schizophrenia», *J. Child Adolesc. Psychopharmacol.*, vol. 26, n.º 8, pp. 721-726, oct. 2016, doi: 10.1089/cap.2015.0220.

[292] D. Wang *et al.*, «Frontiers | Differences in inflammatory marker profiles and cognitive functioning between deficit and nondeficit schizophrenia», doi: 10.3389/fimmu.2022.958972.

[293] J. Cho, T. E. Nelson, H. Bajova, y D. L. Gruol, «Chronic CXCL10 alters neuronal properties in rat hippocampal culture», Accedido: 19 de agosto de 2024. [En línea]. Disponible en: https://www.jni-journal.com/article/S0165-5728(08)00496-7/abstract

[294] T. E. Nelson y D. L. Gruol, «The chemokine CXCL10 modulates excitatory activity and intracellular calcium signaling in cultured hippocampal neurons», *J. Neuroimmunol.*, vol. 156, n.º 1, pp. 74-87, nov. 2004, doi: 10.1016/j.jneuroim.2004.07.009.

[295] X. Liu *et al.*, «Activated Microglia Mediate Downregulation of Surface GABAA Receptors Through CXCL10: A Mechanism for Cognitive Impairments Caused by Systemic Lipopolysaccharide», *Rochester, NY*: 3247852. Accedido: 19 de agosto de 2024. [En línea]. Disponible en: https://papers.ssrn.com/sol3/papers.cfm?abstract_id=3247852

[296] N. C. Derecki *et al.*, «Regulation of learning and memory by meningeal immunity: a key role for IL-4», *J. Exp. Med.*, vol. 207, n.º 5, pp. 1067-1080, may 2010, doi: 10.1084/jem.20091419.

[297] J. Hall, K. L. Thomas, y B. J. Everitt, «Rapid and selective induction of BDNF expression in the hippocampus during contextual learning», *Nat. Neurosci.*, vol. 3, n.º 6, pp. 533-535, jun. 2000, doi: 10.1038/75698.

[298] J. D. Sweatt, «The neuronal MAP kinase cascade: a biochemical signal integration system subserving synaptic plasticity and memory», *J. Neurochem.*, vol. 76, n.º 1, pp. 1-10, 2001, doi: 10.1046/j.1471-4159.2001.00054.x.

[299] R. Vlkolinský, G. R. Siggins, I. L. Campbell, y T. Krucker, «Acute exposure to CXC chemokine ligand 10, but not its chronic astroglial production, alters synaptic plasticity in mouse hippocampal slices», *J. Neuroimmunol.*, vol. 150, n.º 1, pp. 37-47, may 2004, doi: 10.1016/j.jneuroim.2004.01.011.

[300] H. R. J. van Weering *et al.*, «CXCL10/CXCR3 signaling in glia cells differentially affects NMDA-induced cell death in CA and DG neurons of the mouse hippocampus», *Hippocampus*, vol. 21, n.º 2, pp. 220-232, 2011, doi: 10.1002/hipo.20742.

[301] A. Lyons *et al.*, «Decreased neuronal CD200 expression in IL-4-deficient mice results in increased neuroinflammation in response to lipopolysaccharide», *Brain. Behav. Immun.*, vol. 23, n.º 7, pp. 1020-1027, oct. 2009, doi: 10.1016/j.bbi.2009.05.060.

[302] A. Kumar, I. C. Fontana, y A. Nordberg, «Reactive astrogliosis: A friend or foe in the pathogenesis of Alzheimer's disease», *J. Neurochem.*, vol. 164, n.º 3, pp. 309-324, 2023, doi: 10.1111/jnc.15565.

[303] C. Gao, J. Jiang, Y. Tan, y S. Chen, «Microglia in neurodegenerative diseases: mechanism and potential therapeutic targets», *Signal Transduct. Target. Ther.*, vol. 8, n.º 1, pp. 1-37, sep. 2023, doi: 10.1038/s41392-023-01588-0.

[304] C. A. Butler, A. S. Popescu, E. J. A. Kitchener, D. H. Allendorf, M. Puigdellívol, y G. C. Brown, «Microglial phagocytosis of neurons in neurodegeneration, and its regulation», *J. Neurochem.*, vol. 158, n.º 3, pp. 621-639, 2021, doi: 10.1111/jnc.15327.

[305] K. Kadono *et al.*, «Myeloid Ikaros–SIRT1 signaling axis regulates hepatic inflammation and pyroptosis in ischemia-stressed mouse and human liver», doi: 10.1016/j.jhep.2021.11.026.

[306] U.-K. Hanisch, «Microglia as a source and target of cytokines», *Glia*, vol. 40, n.º 2, pp. 140-155, 2002, doi: 10.1002/glia.10161.

[307] A. R. Saitgareeva, K. V. Bulygin, I. F. Gareev, O. A. Beylerli, y L. R. Akhmadeeva, «The role of microglia in the development of neurodegeneration», *Neurol. Sci.*, vol. 41, n.º 12, Art. n.º 12, may 2020, doi: 10.1007/s10072-020-04468-5.

[308] J. A. Rodríguez-Gómez *et al.*, «Microglia: Agents of the CNS Pro-Inflammatory Response», *Cells*, vol. 9, n.º 7, Art. n.º 7, jul. 2020, doi: 10.3390/cells9071717.

[309] S. F. Sonnenschein, F. V. Gomes, y A. A. Grace, «Frontiers | Dysregulation of Midbrain Dopamine System and the Pathophysiology of Schizophrenia», doi: 10.3389/fpsyt.2020.00613.

[310] O. Marín, «Parvalbumin interneuron deficits in schizophrenia», *Eur. Neuropsychopharmacol.*, vol. 82, pp. 44-52, may 2024, doi: 10.1016/j.euroneuro.2024.02.010.

[311] D. A. Lewis, T. Hashimoto, y D. W. Volk, «Cortical inhibitory neurons and schizophrenia», *Nat. Rev. Neurosci.*, vol. 6, n.º 4, pp. 312-324, abr. 2005, doi: 10.1038/nrn1648.

[312] O. Kann, F. Almouhanna, y B. Chausse, «Interferon γ: a master cytokine in microglia-mediated neural network dysfunction and neurodegeneration», doi: 10.1016/j.tins.2022.10.007.

[313] J. Zhang *et al.*, «Priming of microglia with IFN-γ impairs adult hippocampal neurogenesis and leads to depression-like behaviors and cognitive defects», *Glia*, vol. 68, n.º 12, pp. 2674-2692, 2020, doi: 10.1002/glia.23878.
[314] T.-T. Ta *et al.*, «Priming of microglia with IFN-γ slows neuronal gamma oscillations in situ», *Proc. Natl. Acad. Sci.*, vol. 116, n.º 10, pp. 4637-4642, mar. 2019, doi: 10.1073/pnas.1813562116.
[315] H. Neumann, T. Misgeld, K. Matsumuro, y H. Wekerle, «Neurotrophins inhibit major histocompatibility class II inducibility of microglia: Involvement of the p75 neurotrophin receptor», *Proc. Natl. Acad. Sci.*, vol. 95, n.º 10, pp. 5779-5784, may 1998, doi: 10.1073/pnas.95.10.5779.
[316] I. E. Papageorgiou *et al.*, «TLR4-activated microglia require IFN-γ to induce severe neuronal dysfunction and death in situ», *Proc. Natl. Acad. Sci.*, vol. 113, n.º 1, pp. 212-217, ene. 2016, doi: 10.1073/pnas.1513853113.
[317] M. Antonietta Ajmone-Cat, M. Mancini, R. De Simone, P. Cilli, y L. Minghetti, «Microglial polarization and plasticity: Evidence from organotypic hippocampal slice cultures», *Glia*, vol. 61, n.º 10, pp. 1698-1711, 2013, doi: 10.1002/glia.22550.
[318] B. Chausse, A. Lewen, G. Poschet, y O. Kann, «Selective inhibition of mitochondrial respiratory complexes controls the transition of microglia into a neurotoxic phenotype *in situ*», *Brain. Behav. Immun.*, vol. 88, pp. 802-814, ago. 2020, doi: 10.1016/j.bbi.2020.05.052.
[319] S. Duport y J. Garthwaite, «Pathological consequences of inducible nitric oxide synthase expression in hippocampal slice cultures», *Neuroscience*, vol. 135, n.º 4, pp. 1155-1166, ene. 2005, doi: 10.1016/j.neuroscience.2005.06.035.
[320] L.-P. Bernier, E. M. York, y B. A. MacVicar, «Immunometabolism in the Brain: How Metabolism Shapes Microglial Function», doi: 10.1016/j.tins.2020.08.008.
[321] S. Ghosh, E. Castillo, E. S. Frias, y R. A. Swanson, «Bioenergetic regulation of microglia», *Glia*, vol. 66, n.º 6, pp. 1200-1212, 2018, doi: 10.1002/glia.23271.
[322] T. Kawai y S. Akira, «Toll-like Receptors and Their Crosstalk with Other Innate Receptors in Infection and Immunity», Accedido: 24 de agosto de 2024. [En línea]. Disponible en: https://www.cell.com/immunity/abstract/S1074-7613(11)00190-7
[323] W. Pan, W. A. Banks, y A. J. Kastin, «Permeability of the blood–brain and blood–spinal cord barriers to interferons», *J. Neuroimmunol.*, vol. 76, n.º 1, pp. 105-111, jun. 1997, doi: 10.1016/S0165-5728(97)00034-9.
[324] W. Pan y A. J. Kastin, «TNFα Transport across the Blood–Brain Barrier Is Abolished in Receptor Knockout Mice», *Exp. Neurol.*, vol. 174, n.º 2, pp. 193-200, abr. 2002, doi: 10.1006/exnr.2002.7871.
[325] N. J. Abbott, A. A. K. Patabendige, D. E. M. Dolman, S. R. Yusof, y D. J. Begley, «Structure and function of the blood–brain barrier», *Neurobiol. Dis.*, vol. 37, n.º 1, pp. 13-25, ene. 2010, doi: 10.1016/j.nbd.2009.07.030.
[326] A. Varatharaj y I. Galea, «The blood-brain barrier in systemic inflammation», *Brain. Behav. Immun.*, vol. 60, pp. 1-12, feb. 2017, doi: 10.1016/j.bbi.2016.03.010.
[327] D. G. Contopoulos-Ioannidis, M. Gianniki, A. Ai-Nhi Truong, y J. G. Montoya, «Toxoplasmosis and Schizophrenia: A Systematic Review and Meta-Analysis of Prevalence and Associations and Future Directions», *Psychiatr. Res. Clin. Pract.*, vol. 4, n.º 2, pp. 48-60, jun. 2022, doi: 10.1176/appi.prcp.20210041.
[328] A. D. Pusic, H. M. Mitchell, P. E. Kunkler, N. Klauer, y R. P. Kraig, «Spreading depression transiently disrupts myelin via interferon-gamma signaling», *Exp. Neurol.*, vol. 264, pp. 43-54, feb. 2015, doi: 10.1016/j.expneurol.2014.12.001.
[329] D. N. Clark, L. R. Begg, y A. J. Filiano, «Unique aspects of IFN-γ/STAT1 signaling in neurons», *Immunol. Rev.*, vol. 311, n.º 1, pp. 187-204, 2022, doi: 10.1111/imr.13092.

[330] L. Flood, S. V. Korol, L. Ekselius, B. Birnir, y Z. Jin, «Interferon-γ potentiates GABAA receptor-mediated inhibitory currents in rat hippocampal CA1 pyramidal neurons», *J. Neuroimmunol.*, vol. 337, p. 577050, dic. 2019, doi: 10.1016/j.jneuroim.2019.577050.

[331] S. J. Dienel, K. E. Schoonover, y D. A. Lewis, «Cognitive Dysfunction and Prefrontal Cortical Circuit Alterations in Schizophrenia: Developmental Trajectories», *Biol. Psychiatry*, vol. 92, n.º 6, pp. 450-459, sep. 2022, doi: 10.1016/j.biopsych.2022.03.002.

[332] D. Nayak, T. L. Roth, y D. B. McGavern, «Microglia Development and Function*», mar. 2014, doi: 10.1146/annurev-immunol-032713-120240.

[333] A. L. Angiolillo *et al.*, «Human interferon-inducible protein 10 is a potent inhibitor of angiogenesis in vivo.», *J. Exp. Med.*, vol. 182, n.º 1, pp. 155-162, jul. 1995, doi: 10.1084/jem.182.1.155.

[334] R. M. Strieter, S. L. Kunkel, D. A. Arenberg, M. D. Burdick, y P. J. Polverini, «Interferon γ-Inducible Protein-10 (IP-10), a Member of the C-X-C Chemokine Family, Is an Inhibitor of Angiogenesis», *Biochem. Biophys. Res. Commun.*, vol. 210, n.º 1, pp. 51-57, may 1995, doi: 10.1006/bbrc.1995.1626.

VIII. Annex

1. Supplementary data of “Alterations of the *IKZF1-IKZF2* tandem in immune cells of schizophrenia patients regulate associated phenotypes”:

Supplementary figures and tables

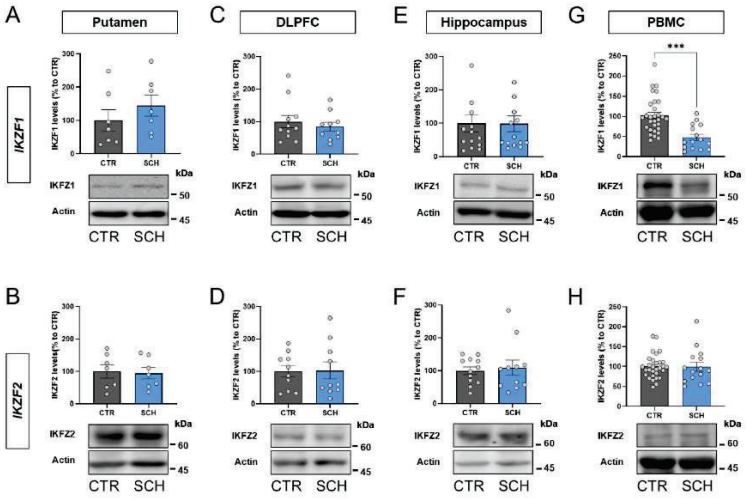

Supplementary figure 1. Determination of IKZF1 and IKZF2 protein levels in different brain regions and in circulating PBMCs. Results from western blot of total IKZF1 and IKZF2 protein levels in different brain regions namely putamen (**a** and **b** respectively), dorso-lateral prefrontal cortex (DLPFC, **c** and **d** respectively) and hippocampus (**e** and **f** respectively) from patients with schizophrenia (SCH) or matched controls (CTR). Demographics of the samples are displayed in supplementary table 1. Results from western blot of total IKZF1 and IKZF2 protein levels in peripheral blood mononuclear cells or PBMCs (**g** and **h** respectively) from patients with schizophrenia (SCH) or matched controls (CTR). Demographics of the samples are displayed in supplementary table 4. Data are means ± SEM and they were analyzed using the two-tailed Student t-test.

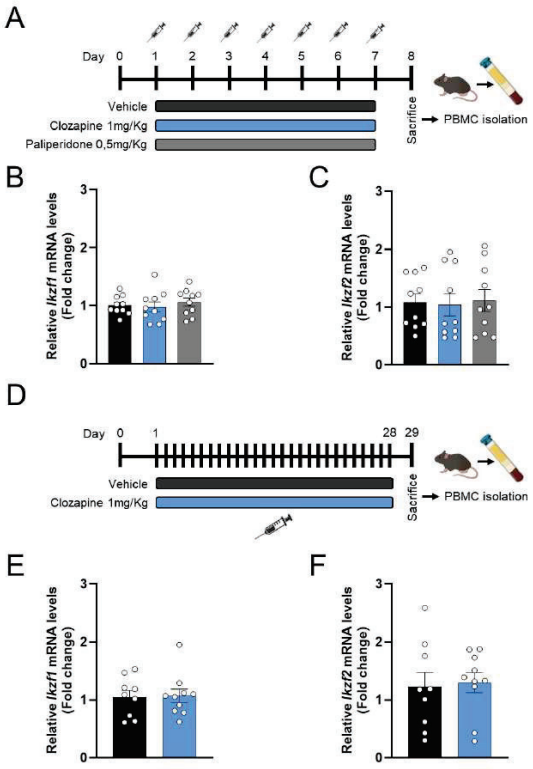

Supplementary figure 2. Effects of antipsychotics on *Ikzf1* and *Ikzf2* mRNA levels in mice PBMCs. Timeline of experimental design for sub-chronic treatments (**a**). Mice were treated with vehicle (n = 20), 1 mg/Kg Clozapine (n = 20) or 0.5 mg/Kg Paliperidone (n = 20) i.p. for 7 days. On day 8, all mice were sacrificed and blood samples were obtained by cardiac puncture. Mice were pooled in groups of two to obtain enough peripheral blood mononuclear cells (PBMCs). PBMC were obtained and *Ikzf1* (**b**) and *Ikzf2* (**c**) mRNA levels were determined for each sample. The final "n" was 10/group. Timeline of experimental design for chronic treaments (**d**). Mice were treated with vehicle (n = 20) or 1 mg/Kg Clozapine (n = 20) i.p. for 28 days. On day 29, all mice were sacrificed and blood samples were obtained by cardiac puncture. Mice were pooled in groups of two to obtain enough peripheral blood mononuclear cells (PBMCs). PBMC were obtained and *Ikzf1* (**e**) and Ikzf2 (**f**) mRNA levels were determined for each sample. The final "n" was 10/group. No differences were observed by 7-days treatments either in *Ikzf1* mRNA levels (one-way ANOVA, $F_{(2, 27)}$ = 0,3250, p=0.725) or *Ikzf2* mRNA levels (one-way ANOVA, $F_{(2, 27)}$ = 0,0471, p=0.954). Similarly, no differences were observed by 28-days treatment either in *Ikzf1* mRNA levels (T-test, t=0,1024, df=17; p = 0.91) or *Ikzf2* mRNA levels (T-test, t=0,2373, df=17; p = 0.81). Data are means ± SEM.

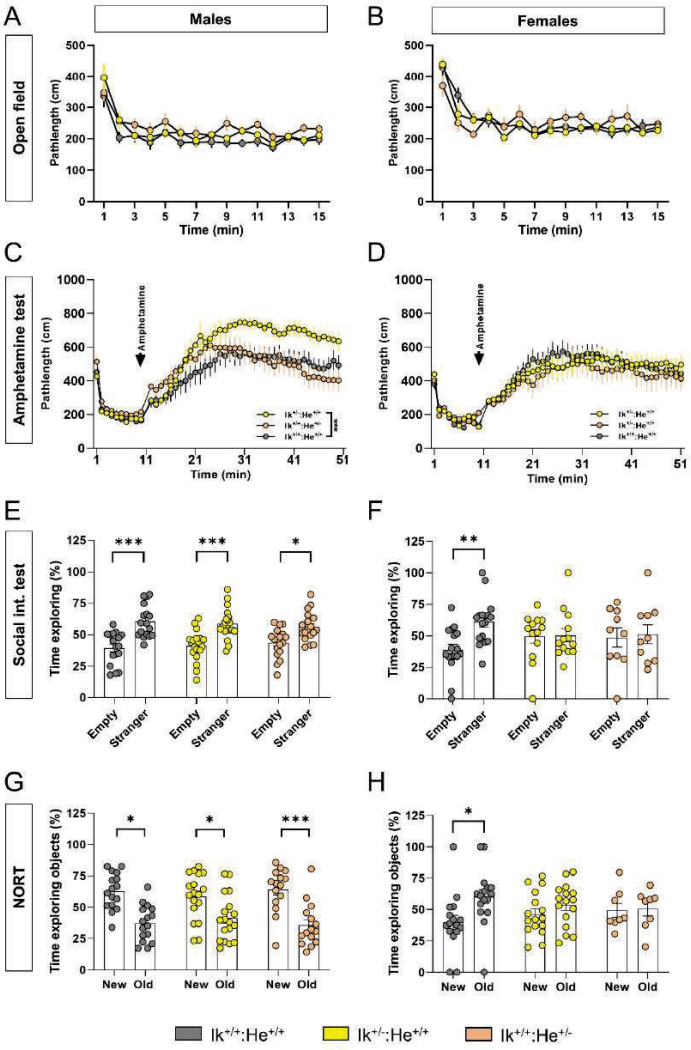

Supplementary figure 3. Generation and characterization of the Ik$^{+/-}$:He$^{+/+}$ and Ik$^{+/+}$:He$^{+/-}$ mutant mice. Basal locomotor activity was evaluated in the three groups of adult mice (Ik$^{+/+}$:He$^{+/+}$, Ik$^{+/-}$:He$^{+/+}$ and Ik$^{+/+}$:He$^{+/-}$ mice) separated in (**a**) males (Genotype effect: $F_{(2, 48)} = 2.574$, $p = 0.087$) and (**b**) females (Genotype effect: $F_{(2, 38)} = 0.1940$, $p = 0.8244$) in a 15 min testing session of free exploration in an open field. Induced agitation and sensitivity to the psychostimulant D-amphetamine was measured in a 45 min testing

session in an open field upon injection of 5 mg/Kg of D-amphetamine in (**c**) adult male (Genotype effect: $F_{(2, 45)} = 3.457$, $p = 0.0401$) and in (**d**) adult female (Genotype effect: $F_{(2, 38)} = 21{,}58$, $p = 0.8069$) mice. Sociability was evaluated in the three-chamber social interaction test (TCSIT). Mice from the three groups were subjected to the TCSIT and data were depicted for (**e**) males (Social preference effect: $F_{(1, 102)} = 53.58$, $p < 0.001$) and (**f**) females (Social preference effect: $F_{(1, 74)} = 3.482$, $p = 0.066$). Recognition memory was evaluated in the novel object recognition test (NORT). Mice from the three groups were subjected to the NORT and data were depicted for (**g**) males (Novel object preference effect: $F_{(1, 92)} = 48{,}68$, $p < 0.001$) and (**h**) females (Novel object preference effect: $F_{(1, 74)} = 4.296$, $p = 0.0417$). Data are means ± SEM. Results were analyzed using the two-way ANOVA with Bonferroni's *post hoc* test. ***p<0.001 vs $Ik^{+/+}$:$He^{+/+}$ mice in **c.** *p< 0.05, **p< 0.01 and ***p<0.001 vs time exploring the new object or vs time exploring the empty cage in **e**, **f,** and **g**. Male mice: $Ik^{+/+}$:$He^{+/+}$ (n = 16), $Ik^{+/-}$:$He^{+/+}$ (n = 19) and $Ik^{+/+}$:$He^{+/-}$ (n = 16). Female mice: $Ik^{+/+}$:$He^{+/+}$ (n = 16), $Ik^{+/-}$:$He^{+/+}$ (n = 8) and $Ik^{+/+}$:$He^{+/-}$ (n = 13).

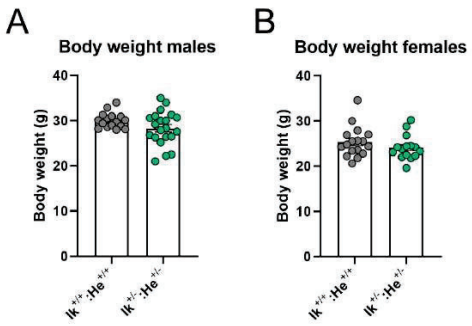

Supplementary figure 4. Body weight of $Ik^{+/+}$:$He^{+/+}$ and $Ik^{+/-}$:$He^{+/-}$ mice. (**a**) Body weight measured in adult males $Ik^{+/+}$:$He^{+/+}$ (n = 17) and $Ik^{+/-}$:$He^{+/-}$ (n = 21) mice. (**b**) Body weight measured in adult females $Ik^{+/+}$:$He^{+/+}$ (n = 17) and $Ik^{+/-}$:$He^{+/-}$ (n = 15) mice. Data are means ± SEM. Results were analyzed using the two-tailed Student t-test.

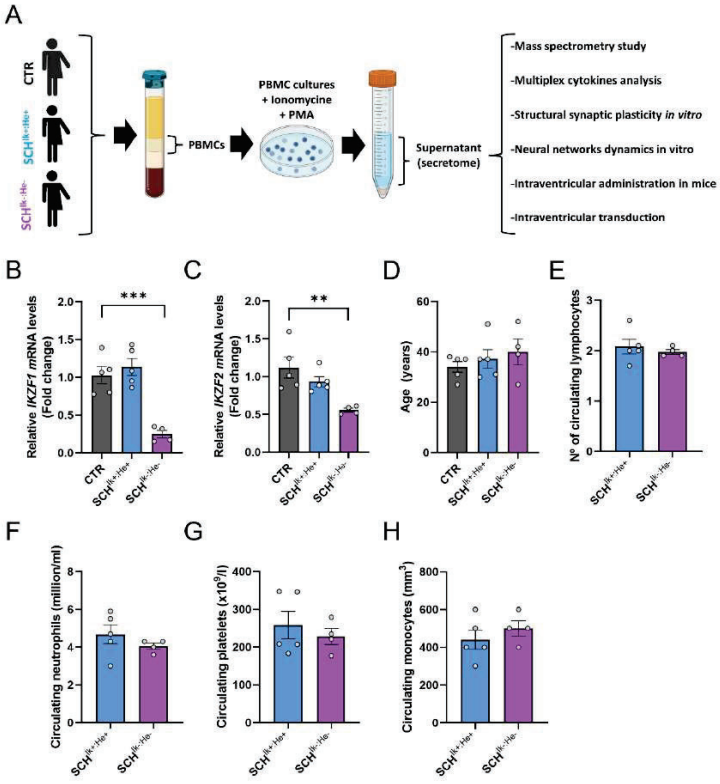

Supplementary figure 5. Characterization of CTR, SCH$^{Ik+:He+}$, and SCH$^{Ik-:He-}$ supernatants. (**a**) Schematic representation of the experimental design. First, patients were stratified according to whether they displayed significantly reduced (≥40% *IKZF1* and *IKZF2* mRNA levels (SCH$^{Ik-:He-}$) or not (SCH$^{Ik+:He+}$). These patients were matched with controls (CTR). Peripheral blood mononuclear cells (PBMCs) from the three groups of patients were isolated, cultured and stimulated (with Ionomycin and PMA) to obtain their secretomes (a.k.a. supernatants or conditioned media). Those supernatants were subjected to comprehensive characterization (Mass spectrometry, *in vitro* and *in vivo* studies, Multiplex cytokines analysis). As indicated, the three groups of patients were selected based on their psychiatric affectation (schizophrenia or not) and based on their (**b**) *IKZF1* and (**c**) *IKZF2* mRNA levels in PBMCs. Patients were matched by sex (**Suppl. Table 3**) and age (**d**). To determine that both groups, SCH$^{Ik+:He+}$ and SCH$^{Ik-:He-}$, are homogeneous and comparable, the number of circulating neutrophils (**f**), number of circulating platelets (**g**), and number of circulating monocytes (**h**) were proven to be similar. Data are means ± SEM. Results were analyzed using the one-way ANOVA with Dunnett's *post hoc* test in **b**, **c** and **d**. Results in **e**, **f**, **g**, and **h** were analyzed using the two-tailed Student t-test. **p< 0.01 and ***p<0.001 vs CTR group. CTR (n = 5), SCH$^{Ik+:He+}$ (n = 5) and SCH$^{Ik-:He-}$ (n = 4).

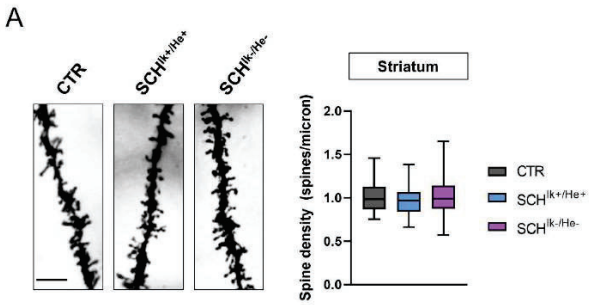

Supplementary figure 6. Characterization of striatal structural synaptic plasticity in mice intraventricularly administered with CTR, SCH$^{lk+:He+}$ and SCH$^{lk-:He-}$ supernatants. (**a**) Representative images (left panels) and quantification (right panels) of spine density in dendrites from medium spiny neurons (MSNs) of the dorsal striatum labeled with Golgi staining. Images were obtained in a bright-field microscope in adult male mice intraventricularly administered with CTR, SCH$^{lk+:He+}$ and SCH$^{lk-:He-}$ supernatants. Scale bar, 5 µm. Data are means ± SEM and they were analyzed using one-way ANOVA and Tukey's multiple comparisons test was used as a *post hoc*. N = 55–71 dendrites/genotype (from 7 mice/genotype).

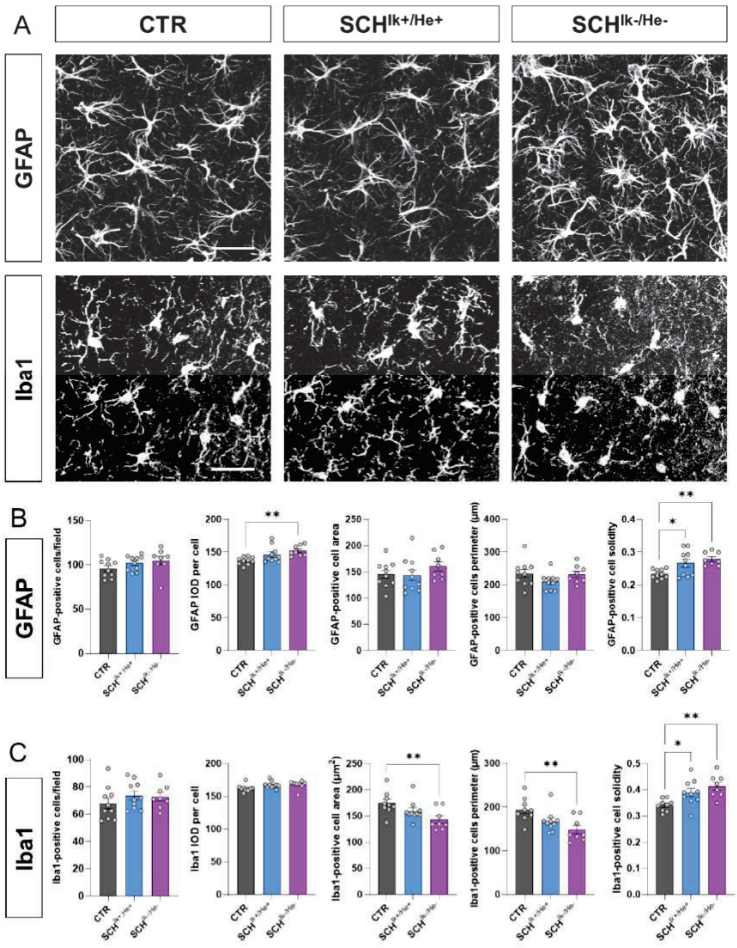

Supplementary figure 7. Morphometric changes in glial cells induced by the SCH$^{lk+:He+}$ and SCH$^{lk-:He-}$ supernatants intraventricularly administered in mice. (**a**) Representative images of GFAP staining (upper row) as an astrocyte's marker and Iba1 (lower row) as a microglia marker in the *stratum radiatum* of the hippocampal CA1 in each condition. (**b**) GFAP-positive cells morphometric parameters including in the following order; number of cells per field, integrated optical density of the cells, area of the cells, perimeter of the cells and solidity of the cells. (**c**) Iba1-positive cells morphometric parameters including in the following order; number of cells per field, integrated optical density of the cells, area of the cells, perimeter of the cells and solidity of the cells. One-way ANOVA was performed with the Dunnett's test as a post hoc test. All values are mean ± SEM. N = 8–10 mice per group. *P < 0.05 and **P < 0.01. Scale bar, 25 µm.

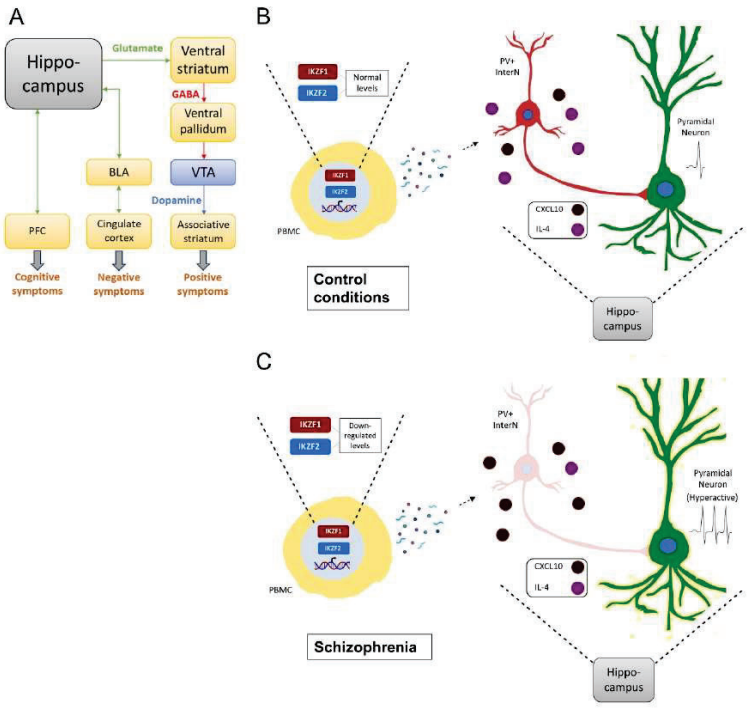

Supplementary figure 8. Proposed model. (**a**) In the context of schizophrenia, the hyperactive and dysrhythmic hippocampus is proposed to be associated with the appearance of the three categories of symptoms (positive, negative, and cognitive). The overdrive in the responsivity of dopaminergic neurons in the ventral tegmental area (VTA) that project to the associative striatum is proposed to underlie the positive symptoms. Besides, the hyperactive hippocampus can also be implicated in the dysfunction of other circuits. The hippocampus-basolateral amygdala (BLA) connection would interfere with the BLA-limbic cortical pathway implicated in the control of emotional responses, probably contributing to the appearance of negative symptoms. The hippocampus-PFC projection would possibly alter the PFC activity and rhythmicity, generating dysfunctions at the cognitive level. Taking in account our results, (**b-c**) the proposed model to explain the reduced quantity of parvalbumin-positive interneurons (PV+) in the context of schizophrenia would be through the altered secretome of the PBMCs with downregulated levels of both, *IKZF1* and *IKZF2*. The dysregulated levels of CXCL10 and Il-4 would be underlying the diminished number (or function) of PV+ interneurons. The reduced inhibition generated by the lack of these GABAergic PV+ interneurons would lead to the hyperactive and dysrhythmic state in the hippocampus and this in turn contributing to the appearance of all types of symptoms of schizophrenia.

Hippocampus

Patient	Age	PMT (h)	Sex	PANSS+	PANSS-	PANSS G	Antipsychotic	Psychiatric Affectation
CTR 1	64	3	M	n.a.	n.a.	n.a.	n.a.	n.a.
CTR 2	39	3	M	n.a.	n.a.	n.a.	n.a.	n.a.
CTR 3	81	23	F	n.a.	n.a.	n.a.	n.a.	n.a.
CTR 4	31	17	M	n.a.	n.a.	n.a.	n.a.	n.a.
CTR 5	86	7	M	n.a.	n.a.	n.a.	n.a.	n.a.
CTR 6	90	13	F	n.a.	n.a.	n.a.	n.a.	n.a.
CTR 7	58	5	M	n.a.	n.a.	n.a.	n.a.	n.a.
CTR 8	69	24	F	n.a.	n.a.	n.a.	n.a.	n.a.
CTR 9	78	5	M	n.a.	n.a.	n.a.	n.a.	n.a.
CTR 10	63	7	F	n.a.	n.a.	n.a.	n.a.	n.a.
CTR 11	97	7	F	n.a.	n.a.	n.a.	n.a.	n.a.
CTR 12	63	5	M	n.a.	n.a.	n.a.	n.a.	n.a.
CTR 13	83	7	F	n.a.	n.a.	n.a.	n.a.	n.a.
CTR 14	86	7	M	n.a.	n.a.	n.a.	n.a.	n.a.
SCH 1	34	2	M	...	...	...	No treatment	Schizophrenia
SCH 2	76	7	M	12	18	37	Quetiapine	Schizophrenia
SCH 3	80	4.5	M	12	28	34	Olanzapine	Schizophrenia
SCH 4	66	1	M	...	...	...	Levomepromacine	Schizophrenia
SCH 5	77	2	M	11	23	50	Risperidone and Quetiapine	Schizophrenia
SCH 6	82	6	M	...	...	...	Risperidone	Schizophrenia
SCH 7	79	7	M	...	...	...	Haloperidol	Schizophrenia
SCH 8	67	8.5	M	16	41	59	n.a.	Schizophrenia
SCH 9	83	4	M	11	26	47	Clorpromazine and Haloperidol	Schizophrenia
SCH 10	90	3	M	...	...	...	No treatment	Schizophrenia
SCH 11	86	6	M	...	...	...	n.a.	Schizophrenia
SCH 12	84	3	M	29	47	82	Amisulpride	Schizophrenia
SCH 13	82	7	M				n.a.	Schizophrenia
SCH 14	91	3	M	35	42	66	No treatment	Schizophrenia

PMT stats	MEAN	DesvT	t-test
CTR	9,5	7,0027469	0,0191
SCH	4,5714	2,3058176	

Age stats	MEAN	DesvT	t-test
CTR	73,5	20,10644749	0,517690503
SCH	73,78571429	2,230381492	

DLPFC

Patient	Age	PMT (h)	Sex	PANSS+	PANSS-	PANSS G	Antipsychotic	Psychiatric Affectation
CTR 1	59	5	M	n.a.	n.a.	n.a.	n.a.	n.a.
CTR 2	68	13	F	n.a.	n.a.	n.a.	n.a.	n.a.
CTR 3	81	23	F	n.a.	n.a.	n.a.	n.a.	n.a.
CTR 4	31	17	M	n.a.	n.a.	n.a.	n.a.	n.a.
CTR 5	83	13	M	n.a.	n.a.	n.a.	n.a.	n.a.
CTR 6	79	5	M	n.a.	n.a.	n.a.	n.a.	n.a.
CTR 7	86	4	F	n.a.	n.a.	n.a.	n.a.	n.a.
CTR 8	65	4	M	n.a.	n.a.	n.a.	n.a.	n.a.
CTR 9	90	13	F	n.a.	n.a.	n.a.	n.a.	n.a.
CTR 10	76	11	M	n.a.	n.a.	n.a.	n.a.	n.a.
CTR 11	74	5	F	n.a.	n.a.	n.a.	n.a.	n.a.
SCH 1	34	2	M	...	...	...	No treatment	Schizophrenia
SCH 2	80	0	M	25	48	44	No treatment	Schizophrenia
SCH 3	74	7	M	19	23	39	Levomepromacine and Haloperidol	Schizophrenia
SCH 4	76	7	M	13	18	37	Quetiapine	Schizophrenia
SCH 5	69	9	M	36	27	53	Quetiapine	Schizophrenia
SCH 6	79	5	M	18	15	32	Levopromacine and Quetiapine	Schizophrenia
SCH 7	65	4	M	56	58	70	Quetiapine and Amisulpride	Schizophrenia
SCH 8	82	4	M	31	18	43	Haloperidol and Olanzapine	Schizophrenia
SCH 9	79	9	M	12	31	34	Perfenazine, Sulpiride and Haloperidol	Schizophrenia
SCH 10	98	8	M	...	...	...	No treatment	Schizophrenia
SCH 11	77	5	M	...	...	...	Olanzapine	Schizophrenia

PMT stats	MEAN	DesvT	t-test
CTR	10,091	6,4568498	0,0458
SCH	5,3364	2,5405797	

Age stats	MEAN	DesvT	t-test
CTR	70,1818182	18,9465357	0,630330875
SCH	73,9090909	15,63625507	

Putamen

Patient	Age	PMT (h)	Sex	PANSS+	PANSS-	PANSS G	Antipsychotic	Psychiatric Affectation
CTR 1	60	15	F	n.a.	n.a.	n.a.	n.a.	n.a.
CTR 2	64	3	M	n.a.	n.a.	n.a.	n.a.	n.a.
CTR 3	56	3	M	n.a.	n.a.	n.a.	n.a.	n.a.
CTR 4	71	8	F	n.a.	n.a.	n.a.	n.a.	n.a.
CTR 5	68	13	F	n.a.	n.a.	n.a.	n.a.	n.a.
CTR 6	81	23	F	n.a.	n.a.	n.a.	n.a.	n.a.
CTR 7	65	4	M	n.a.	n.a.	n.a.	n.a.	n.a.
SCH 1	65	4	M	69	22	71	Quetiapine and Amisulpride	Schizophrenia
SCH 2	79	3	M	89	13	36	No treatment	Schizophrenia
SCH 3	89	1	M	0	0	0	No treatment	Schizophrenia
SCH 4	76	8	M	0	0	0	Olanzapine	Schizophrenia
SCH 5	84	3	M	0	0	0	Amisulpride	Schizophrenia
SCH 6	71	8	M	0	0	0	Quetiapine and Olanzapine	Schizophrenia
SCH 7	91	3	M	0	0	0	No treatment	Schizophrenia

PMT stats	MEAN	DesvT	t-test
CTR	9,8571	7,5372059	0,0900
SCH	4,2857	2,6903708	

Age stats	MEAN	DesvT	t-test
CTR	66,4285714	8,200598479	0,018245603
SCH	79,2857143	9,464218529	

Supplementary table 1. Demographic characteristics from the patients of whom we obtained the post-mortem tissue including the hippocampus, the dorsolateral prefrontal cortex (DLPFC) and Putamen. MPT: Post-mortem time. Scores from the positive (PANSS+), negative (PANSS-) and general (PANSS G) are depicted from PANSS scale. CTR: Control patients, SCH: Patients with schizophrenia. Data are mean ± DesvT and they were analyzed using the two-tailed Student t-test.

Patient	Age	Sex	PANSS+	PANSS-	PANS G	Antipsychotic	IKZF1 mRNA levels	IKZF2 mRNA levels	Psychiatric affection
CTR 1	27	F	n.a.	n.a.	n.a.	n.a.	0,99271069	1,07449258	n.a.
CTR 2	37	F	n.a.	n.a.	n.a.	n.a.	1,42329635	1,25758898	n.a.
CTR 3	39	M	n.a.	n.a.	n.a.	n.a.	0,800646	0,892336944	n.a.
CTR 4	37	M	n.a.	n.a.	n.a.	n.a.	0,49980777	0,63889711	n.a.
CTR 4	42	M	n.a.	n.a.	n.a.	n.a.	1,063961	1,595109558	n.a.
CTR 5	31	F	n.a.	n.a.	n.a.	n.a.	1,1053018	1,01403947	n.a.
CTR 6	40	F	n.a.	n.a.	n.a.	n.a.	0,776058	0,85007408	n.a.
CTR 7	24	M	n.a.	n.a.	n.a.	n.a.	0,800	0,8900	n.a.
CTR 8	26	M	n.a.	n.a.	n.a.	n.a.	0,7800	0,8500	n.a.
CTR 9	26	F	n.a.	n.a.	n.a.	n.a.	1,364207	1,242852869	n.a.
CTR 10	26	M	n.a.	n.a.	n.a.	n.a.	1,04931311	0,44864789	n.a.
CTR 11	24	F	n.a.	n.a.	n.a.	n.a.	1,39420745	1,24285287	n.a.
CTR 12	60	M	n.a.	n.a.	n.a.	n.a.	1,04930955	0,44910161	n.a.
CTR 13	55	F	n.a.	n.a.	n.a.	n.a.	0,76283363	0,50877998	n.a.
CTR 14	53	M	n.a.	n.a.	n.a.	n.a.	1,08255502	2,02807894	n.a.
CTR 15	52	M	n.a.	n.a.	n.a.	n.a.	1,105302	1,014039469	n.a.
SCH 1	35	M	12	19	31	Paliperidone	0,81758761	0,792046	Schizophrenia
SCH 2	43	M	14	22	29	Clozapine	0,426153545	1,251498	Schizophrenia
SCH 3	29	M	7	18	26	Clozapine	0,204396902	0,504755	Schizophrenia
SCH 4	27	M	9	24	36	Clozapine	0,177937839	1,268968	Schizophrenia
SCH 5	43	F	15	18	26	Paliperidone	0,864204853	0,9354	Schizophrenia
SCH 6	49	F	21	18	36	Olanzapine	0,34855068	0,611368	Schizophrenia
SCH 7	32	M	11	27	40	Clozapine	1,086313376	0,885837	Schizophrenia
SCH 8	22	F	10	33	34	Aripiprazol	0,472846964	0,866731	Schizophrenia
SCH 9	58	F	-	-	-	Paliperidone	0,789734897	0,450661	Schizophrenia
SCH 10	48	F	17	26	39	Clozapine	0,795227938	0,773844	Schizophrenia
SCH 11	28	F	14	28	34	Clozapine	0,318517653	0,617134	Schizophrenia
SCH 12	56	F	9	29	33	Clozapine	0,793678	0,652981	Schizophrenia
SCH 13	46	M	14	25	29	Clozapine	0,773482388	0,25439	Schizophrenia
SCH 14	54	F	10	21	27	Clozapine	0,788236	0,545504	Schizophrenia
SCH 15	50	M	19	25	32	Aripiprazol	1,433196157	0,804219	Schizophrenia
SCH 16	45	M	7	11	20	Clozapine	0,213076772	0,848894	Schizophrenia
SCH 17	50	M	18	36	49	Clozapine	1,355886183	1,185635	Schizophrenia
SCH 18	32	M	7	19	25	Clozapine	0,260516244	0,518946	Schizophrenia
SCH 19	39	M	-	-	-	Paliperidone	1,18446542	0,530587	Schizophrenia
SCH 20	48	F	-	-	-	Olanzapine	1,408774155	0,598787	Schizophrenia
SCH 21	33	M	10	16	27	Clozapine	0,515641522	0,790104	Schizophrenia
SCH 22	28	F	11	20	27	Clozapine	0,355875677	1,104701	Schizophrenia
SCH 23	37	F	12	14	27	Clozapine	0,952268521	0,858633	Schizophrenia
SCH 24	36	M	18	19	40	Paliperidone	0,152771278	0,687905	Schizophrenia
SCH 25	19	F	9	29	22	Clozapine	0,285081285	0,854798	Schizophrenia
SCH 26	37	F	32	11	49	Olanzapine	0,873234084	0,719524	Schizophrenia
SCH 27	51	F	12	34	38	Paliperidone	0,916648387	0,308879	Schizophrenia
SCH 28	25	M	14	14	28	Clozapine	0,709286477	0,611368	Schizophrenia
SCH 29	18	M	-	-	-	Olanzapine	1,197014267	0,489749	Schizophrenia
SCH 30	27	M	7	11	28	-	0,867202216	0,426351	Schizophrenia
SCH 31	35	F	7	14	24	Aripiprazol	0,174275931	0,625749	Schizophrenia
SCH 32	40	F	7	16	16	Olanzapine	0,58012687	0,452225	Schizophrenia
SCH 33	54	F	14	29	35	Aripiprazol	0,47613426	0,426351	Schizophrenia
SCH 34	23	M	13	13	19	Paliperidone	0,913477024	0,873642	Schizophrenia
SCH 35	57	M	7	27	19	Risperidone	0,515641522	0,566407	Schizophrenia

Age stats	MEAN	DesvT	t-test
CTR	37,5	12,2	0,71585
SCH	38,8	11,6	

Supplementary table 2. Demographic characteristics from the patients of whom we obtained the peripheral blood mononuclear cells (PBMCs) supernatants. CTR: Control patients; SCH:Ik-/He- Patients with schizophrenia. Colored cells (also highlighted in figure 1g-h) indicate the subgroups (Gray: CTR group; blue, $SCH^{Ik+/He+}$ group and violet, $SCH^{Ik-/He-}$ group) selected for the experimentation depicted in figure 4 onwards. Data are mean ± DesvT and they were analyzed using the two-tailed Student t-test

.

Patient/Immune cell	Neutrophils x10³/mm³(Mean/SEM)	Lymphocites x10³/mm³ (Mean/SEM)	Monocytes x10³/mm³(Mean/SEM)
CTR (n = 15)	3.850/0.36	2.10/0.174	0.509/0.045
SCH (n = 35)	4.569/0.32	2.194/0.176	0.773/0.248
Normal values in Spanish population	1.5 - 7.7	1.1 - 4.5	0.1 - 0.95
Tow-tailed t-test CNT vs SCH	t=1.350; p value = 0,1835	t=0.2933; p value = 0,7708	t=0.675; p value = 0,5035

Supplementary table 3. Descriptive statistics of immune circulating cells in blood samples from controls (CTR) and patients with schizophrenia (SCH) was conducted in the current study. Mean values of circulating neutrophils, lymphocytes, and monocytes densities from blood samples are depicted. No differences were observed between the groups in our cohort. Densities were found to be within normal distributions compared to the Spanish population. Data are mean ± SEM and they were analyzed using the two-tailed Student t-test.

Patient	Age	Sex	Antipsychotic	Psychiatric affection
CTR 1	28	M	n.a.	n.a.
CTR 2	42	M	n.a.	n.a.
CTR 3	43	F	n.a.	n.a.
CTR 4	30	M	n.a.	n.a.
CTR 5	24	M	n.a.	n.a.
CTR 6	25	F	n.a.	n.a.
CTR 7	23	F	n.a.	n.a.
CTR 8	55	F	n.a.	n.a.
CTR 9	31	F	n.a.	n.a.
CTR 10	25	F	n.a.	n.a.
CTR 11	26	F	n.a.	n.a.
CTR 12	34	M	n.a.	n.a.
CTR 13	49	F	n.a.	n.a.
CTR 14	56	M	n.a.	n.a.
CTR 15	30	F	n.a.	n.a.
CTR 16	30	F	n.a.	n.a.
CTR 17	50	M	n.a.	n.a.
CTR 18	45	F	n.a.	n.a.
CTR 19	48	M	n.a.	n.a.
CTR 20	59	F	n.a.	n.a.
CTR 21	52	F	n.a.	n.a.
CTR 22	48	F	n.a.	n.a.
CTR 23	30	M	n.a.	n.a.
CTR 24	61	F	n.a.	n.a.
CTR 25	55	F	n.a.	n.a.
CTR 26	21	F	n.a.	n.a.
CTR 27	21	F	n.a.	n.a.
CTR 28	26	F	n.a.	n.a.
CTR 29	28	F	n.a.	n.a.
CTR 30	21	M	n.a.	n.a.
SCH 1	51	M	Olanzapine	Schizophrenia
SCH 2	46	F	Clozapine	Schizophrenia
SCH 3	48	F	Clozapine	Schizophrenia
SCH 4	58	M	Clozapine	Schizophrenia
SCH 5	44	M	Clozapine	Schizophrenia
SCH 6	47	M	Clozapine	Schizophrenia
SCH 7	45	M	Olanzapine	Schizophrenia
SCH 8	54	F	Haloperidol	Schizophrenia
SCH 9	26	M	Clozapine	Schizophrenia
SCH 10	48	M	Clozapine	Schizophrenia
SCH 11	55	M	Clozapine	Schizophrenia
SCH 12	23	F	Clozapine	Schizophrenia
SCH 13	26	M	Clozapine	Schizophrenia
SCH 14	30	M	Amisulpride	Schizophrenia
SCH 15	18	M	Clozapine	Schizophrenia
SCH 16	55	F	Clozapine	Schizophrenia

Age stats	MEAN	DesvT
CTR	37,20	13,18
SCH	42,12	13,00

Supplementary table 4. Demographic characteristics from the patients of whom we obtained the peripheral blood mononuclear cells (PBMCs) for protein analysis of IKZF1 and IKZF2. CTR: Control patients; SCH: Patients with schizophrenia. Data are mean ± DesvT and they were analyzed using the two-tailed Student t-test.

Patient	Age	Sex	PANSS+	PANSS-	PANS G	Antipsychotic	Psychiatric affection
CTR 1	26	F	n.a.	n.a.	n.a.	n.a.	n.a.
CTR 2	40	F	n.a.	n.a.	n.a.	n.a.	n.a.
CTR 3	39	M	n.a.	n.a.	n.a.	n.a.	n.a.
CTR 4	40	M	n.a.	n.a.	n.a.	n.a.	n.a.
CTR 5	50	M	n.a.	n.a.	n.a.	n.a.	n.a.
SCH$^{IKZF1+/+IKZF2+/+}$ 1	43	F	15	18	26	Paliperidone	Schizophrenia
SCH$^{IKZF1+/+IKZF2+/+}$ 2	32	M	11	27	40	Clozapine	Schizophrenia
SCH$^{IKZF1+/+IKZF2+/+}$ 3	50	M	19	25	32	Aripiprazol	Schizophrenia
SCH$^{IKZF1+/+IKZF2+/+}$ 4	40	M	18	36	49	Clozapine	Schizophrenia
SCH$^{IKZF1+/+IKZF2+/+}$ 5	37	F	12	14	27	Clozapine	Schizophrenia
SCH$^{IKZF1-/-IKZF2-/-}$ 1	35	M	18	19	40	Paliperidone	Schizophrenia
SCH$^{IKZF1-/-IKZF2-/-}$ 2	29	M	7	18	26	Clozapina	Schizophrenia
SCH$^{IKZF1-/-IKZF2-/-}$ 3	49	F	21	18	36	Olanzapine	Schizophrenia
SCH$^{IKZF1-/-IKZF2-/-}$ 4	28	F	14	28	34	Clozapine	Schizophrenia

Supplementary table 5. Demographic characteristics from the patients of whom we obtained the peripheral blood mononuclear cells (PBMCs) supernatants. Black: Control patients (CTR). Blue: Patients with schizophrenia (SCH) but with no alterations in the expression of the *IKZF1* and *IKZF2* genes. Pink: Patients with schizophrenia (SCH) and with a double reduction in the expression of the *IKZF1* and *IKZF2* genes.

2. Supplementary data of “Ikzf1 as a novel regulator of microglial homeostasis in inflammation and neurodegeneration”:

Supplemental material

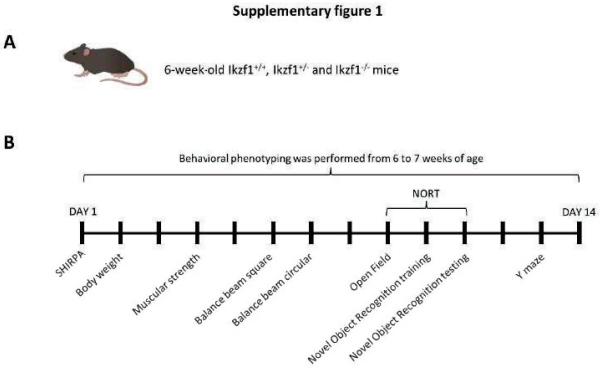

Supplementary Figure 1: Timeline of the behavioural phenotype in Ikzf1$^{+/+}$, Ikzf1$^{+/-}$ and Ikzf1$^{-/-}$ mice. (A) Schematic representation of the mice employed and at which age. (B) Scheme of the timeline used for the behavioural characterization of 6- to 7-week-old Ikzf1$^{+/+}$, Ikzf1$^{+/-}$ and Ikzf1$^{-/-}$ mice.

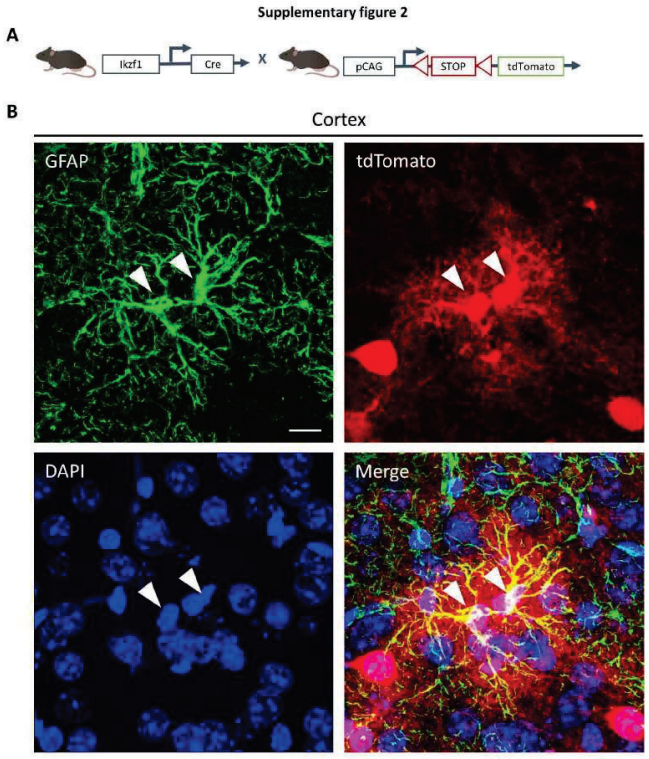

Supplementary Figure 2: The tdTomato signalling in Ikzf1-Cre:tdTomato^{Flox} mice colocalizes with punctual astrocytes in cortex. (A) Schematic representation of the adult Ikzf1-Cre:tdTomato^{Flox} mice employed. (B) Triple staining for astroglia (GFAP-positive cells, green), nuclei (DAPI-positive cells, blue) and cells that expressed Ikzf1 at some point of their (tdTomato-positive cells, red) in the mouse sensory cortex. White arrows are depicting double positive cells for GFAP and tdTomato. Scale bar, 10 µm.

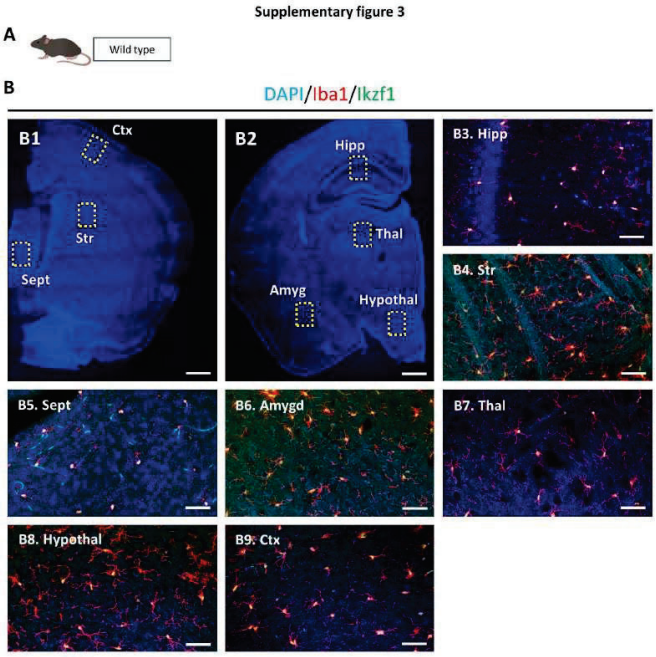

Supplementary Figure 3: Characterization of Iba1-Ikzf1 double positive cells in several brain regions of the adult mouse. (A) Schematic representation of the adult wild type (WT) adult mice employed. (B) Brain mosaic stained with DAPI (Blue) to depict the insets at two different coordinates (B1 at 0.6 mm from bregma and B2 at -2.0 mm from bregma). Scale bar, 800 µm. From B3 to B9 triple staining for microglia (Iba1-positive cells, Red), nuclei (DAPI-positive cells, blue) and Ikzf1 (Green) in insets from B1 and B2. Yellow color indicates colocalization (Iba1-Ikzf1). B3 is an inset from the dorsal hippocampal CA1; B4 is an inset from the dorsal striatum; B5 is an inset from the septum; B6 is an inset from the amygdala; B7 is an inset from the thalamus; B8 is an inset from the hypothalamus and B9 is an inset from the sensory cortical area 1. Scale bar in all insets, 30 µm.

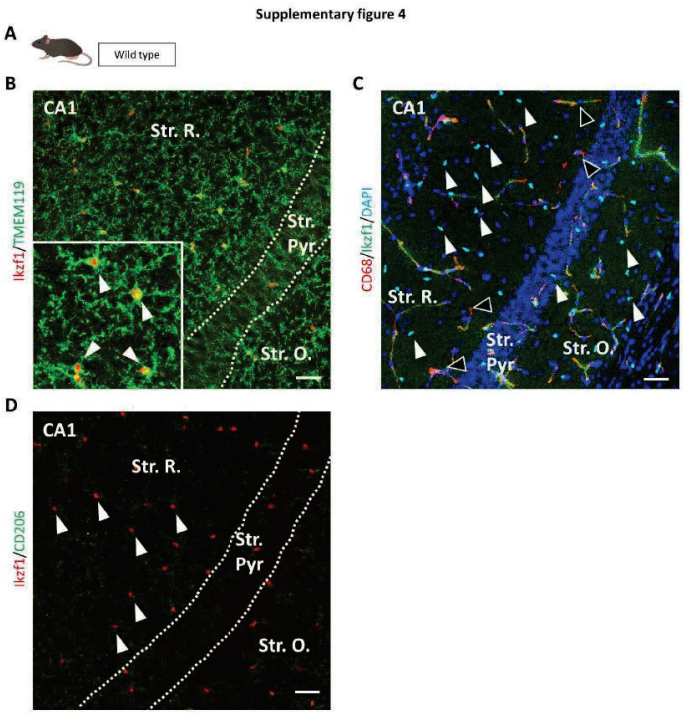

Supplementary Figure 4: Characterization of Ikzf1 expression in the hippocampus. (A) Schematic representation of the adult wild type (WT) employed. (B) Double staining in the hippocampal CA1 for microglia (TMEM119-positive cells, green) and cells that express Ikzf1. White arrows depict a clear TMEM119-Ikzf1 colocalization in the inset. (C) Double staining in the hippocampal CA1 for CD68 and Ikzf1. Note there is almost no colocalization. (C) Double staining in the hippocampal CA1 for CD206 and Ikzf1. Note there is no colocalization. Str. R.: Stratum Radiatum; Str. Pyr.: Stratum Pyramidale; Str. O.: Stratum oriens. Scale bar in all pictures, 50 µm.

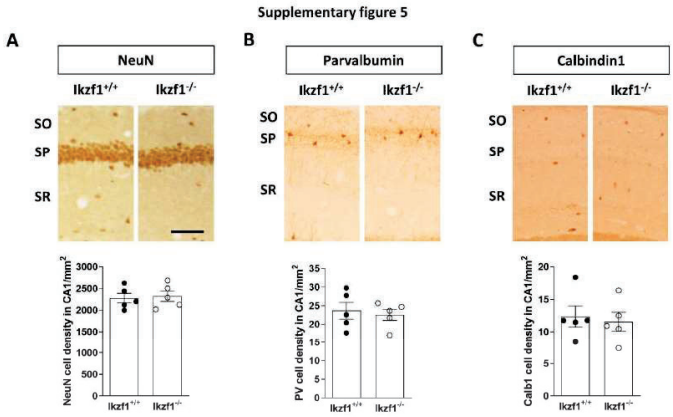

Supplementary Figure 5: Characterization of neuronal subpopulations in the hippocampus of adult Ikzf1$^{+/+}$ and Ikzf1$^{-/-}$ mice. (A) Upper panel: 3,3'-Diaminobenzidine(DAB)-based staining in the hippocampal CA1 for NeuN in adult Ikzf1$^{+/+}$ and Ikzf1$^{-/-}$ mice. Lower panel: Quantification of NeuN-positive cells density from upper panel was performed in adult Ikzf1$^{+/+}$ and Ikzf1$^{-/-}$ mice. Unpaired t-test: t=0,2943, df=8, p = 0.776. (B) Upper panel: DAB-based staining in the hippocampal CA1 for Parvalbumin (PV) in adult Ikzf1$^{+/+}$ and Ikzf1$^{-/-}$ mice. Lower panel: Quantification of PV-positive cells density from upper panel was performed in adult Ikzf1$^{+/+}$ and Ikzf1$^{-/-}$ mice. Unpaired t-test: t=0,3931, df=8, p = 0.7045. (C) Upper panel: DAB-based staining in the hippocampal CA1 for Calbindin1 (Calb1) in adult Ikzf1$^{+/+}$ and Ikzf1$^{-/-}$ mice. Lower panel: Quantification of Calb1-positive cells density from upper panel was performed in adult Ikzf1$^{+/+}$ and Ikzf1$^{-/-}$ mice. Unpaired t-test: t=0,3750, df=8, p = 0.7174. SR: Stratum Radiatum; SP.: Stratum Pyramidale; SO: Stratum oriens. Scale bar in all pictures, 70 µm.

Supplementary table 1

Patient	Clinical diagnosis	Braak stage	Thal stage	Sex	Age (years)	PMD (hh:mm)
1	Control	3	0	M	86	7:25
2	Control	3	3	F	90	13:40
3	Control	-	-	M	58	05:00
4	Control	2	3	F	88	24:00
5	Control	5	5	M	78	05:00
6	Control	2	0	F	83	07:30
7	Control	2	5	F	97	07:20
8	Control	2	4	F	93	05:30
9	Control	2	5	F	83	07:33
11	AD	6	5	F	85	12:00
12	AD	6	5	F	84	11:00
13	AD	6	4	F	80	15:00
14	AD	5	3	M	86	17:30
15	AD	6	5	M	85	15:35
16	AD	6	5	F	82	16:45
17	AD	6	5	F	78	11:30
18	AD	6	5	M	86	12:00
19	AD	6	5	M	78	07:20
20	AD	6	5	F	90	05:30
21	AD	5	5	F	95	14:30
22	AD	5	5	F	85	16:00

Supplementary table 1. Human postmortem hippocampal samples. PMD, postmortem delay; M, male; F, female; AD, Alzheimer's disease.